



Universiteit  
Leiden  
The Netherlands

## Enhancing epicardial EMT to repair the heart

Dronkers, E.

### Citation

Dronkers, E. (2023, February 2). *Enhancing epicardial EMT to repair the heart*. Retrieved from <https://hdl.handle.net/1887/3514309>

Version: Publisher's Version

License: [Licence agreement concerning inclusion of doctoral thesis in the Institutional Repository of the University of Leiden](#)

Downloaded from: <https://hdl.handle.net/1887/3514309>

**Note:** To cite this publication please use the final published version (if applicable).

# Enhancing epicardial EMT to repair the heart

ESTHER DRONKERS

THESIS



Enhancing epicardial EMT to repair the heart

**Esther Dronkers**

**Enhancing epicardial EMT to repair the heart**

© Esther Dronkers-van Zwet, Leiden, the Netherlands, 2022.

ISBN 978-94-6458-791-3

Provided by thesis specialist Ridderprint, [ridderprint.nl](http://ridderprint.nl)

Printing: Ridderprint

Layout and design: Erwin Timmerman, [persoonlijkproefschrift.nl](http://persoonlijkproefschrift.nl)

The work presented in this thesis was carried out at the Department of Cell and Chemical Biology of the Leiden University Medical Center.

Financial support by the Dutch Heart Foundation for the publication of this thesis is gratefully acknowledged.

# Enhancing epicardial EMT to repair the heart

## Proefschrift

ter verkrijging van  
de graad van doctor aan de Universiteit Leiden,  
op gezag van rector magnificus prof.dr.ir. H. Bijl,  
volgens besluit van het college voor promoties  
te verdedigen op donderdag 2 februari 2023

klokke 15:00 uur

door

**Esther Dronkers - van Zwet**

geboren te Wageningen

in 1992

**Promotor:**

Prof. Dr. M.J.T.H. Goumans

**Co-Promotor:**

Dr. A.M. Smits

**Promotiecommissie:**

Prof. dr. P. ten Dijke

Prof. dr. S.M. Chuva de Sousa Lopes

Prof. dr. P.Y.W. Dankers (Technische Universiteit Eindhoven)

Dr. M.J.B. van den Hoff (Universiteit van Amsterdam)

## TABLE OF CONTENTS

	Nederlandse Samenvatting	7
<b>Chapter 1</b>	Introduction	11
<b>Chapter 2</b>	The epicardium as a source of multipotent adult cardiac progenitor cells: Their origin role and fate (review)	23
<b>Chapter 3</b>	The Isolation and Culture of Primary Epicardial Cells Derived from Human Adult and Fetal Heart Specimens	59
<b>Chapter 4</b>	Small molecule screen identifies novel activators of epithelial to mesenchymal transition in human epicardial cells	77
<b>Chapter 5</b>	Epicardial TGF $\beta$ and BMP Signaling in Cardiac Regeneration: What Lesson Can We Learn from the Developing Heart? (review)	113
<b>Chapter 6</b>	Activin A and ALK4 Identified as Novel Regulators of Epithelial to Mesenchymal Transition (EMT) in Human Epicardial Cells	155
<b>Chapter 7</b>	Epicardial Prrx1b restricts fibrosis and promotes Nrg1-dependent cardiomyocyte proliferation during zebrafish heart regeneration	181
<b>Chapter 8</b>	Optimization of two self-adhering drug delivery patches to target the epicardium of the injured heart	221
<b>Chapter 9</b>	Discussion	239
	List of publications	261
	Curriculum Vitae	263
	Dankwoord	265



## NEDERLANDSE SAMENVATTING

Elk jaar worden in Nederland 34.000 patiënten opgenomen in het ziekenhuis vanwege een myocardinfarct. Bij dit infarct sterven duizenden cellen af als gevolg van een verstopping in één van de kransslagaders waardoor een deel van de hartspier geen zuurstof en voedingsstoffen ontvangt. Omdat hartweefsel slecht in staat is zichzelf te herstellen, wordt dit dode weefsel vervangen door littekens, die het hart belemmeren voldoende bloed rond te pompen. Patiënten kunnen daardoor na een myocardinfarct een verslechterde hartfunctie krijgen, wat leidt tot hartfalen. Op dit moment zijn er weinig therapieën beschikbaar die beschadigd hartweefsel herstellen en daarmee hartfalen kunnen voorkomen.

Door beschadigd hartweefsel te regenereren kan hartfalen tegengegaan worden. Voor dit proces van regenereren is het nodig om de spiercellen, de cardiomyocyten, te laten vermenigvuldigen en de doorbloeding te herstellen. Het ontwikkelende hart is een blauwdruk van een optimale werking van deze processen; de embryonale en foetale ontwikkeling tonen in optima forma hoe hartweefsel gevormd kan worden.

Een belangrijke bijdrage aan hartontwikkeling wordt geleverd door het epicard, een vlies dat het hart omgeeft. Het epicard stimuleert en reguleert de vorming van nieuw hartweefsel door middel van de afgifte van cellen en biochemische signalen. De epicardiale epitheliale-naar-mesenchymale transitie (epiMT) staat hierin centraal. Een epitheliale cel wordt gekenmerkt door een ronde vorm en de expressie van eiwitten die de cellen met elkaar verbinden waardoor ze een stevige buitenste laag van het hart vormen. Een mesenchymale cel daarentegen is langwerpiger en beweeglijker en kan daardoor het weefsel migreren. EpiMT is het proces waarin een epitheliale cel in het epicard verandert in een mesenchymale cel, een zogenoemde "epicardial derived cell (EPDC)". Doordat cellen epiMT ondergaan kunnen de gevormde mesenchymale

cellen het hartweefsel in migreren en daar bijdragen aan de vorming van bloedvaten en bindweefselcellen (fibroblasten). Daarnaast scheiden deze cellen stoffen af die de groei van hartweefsel en deling van cardiomyocyten stimuleren. Dit proces van epiMT is daarmee essentieel voor de bijdrage van het epicard aan de ontwikkeling van het hart.

Als de ontwikkeling van het hart is voltooid worden de epicard cellen inactief. Bij beschadiging van het hart worden de epicardcellen echter weer actief en zijn er cellen die epiMT ondergaan. Maar vergeleken met het foetale hart is dit proces suboptimaal: cellen ondergaan minder snel epiMT en er wordt minder migratie van EPDCs in het hartweefsel waargenomen. Studies hebben laten zien dat het optimaliseren van epiMT is gecorreleerd aan een verbeterde hartfunctie. Het doel van dit proefschrift is daarom om factoren te identificeren die epiMT kunnen stimuleren in het volwassen hart, met als uiteindelijke doel om hartweefsel te herstellen na een myocardinfarct (**Hoofdstuk 1**).

**Hoofdstuk 2** beschrijft de literatuur die bekend is over de bijdrage van het epicard aan hartontwikkeling en het beschadigde hart. Ook wordt beschreven welke modellen beschikbaar zijn om dit te onderzoeken.

Om de regulatie van epiMT goed te kunnen bestuderen hebben wij een celkweekmodel ontwikkeld, zoals beschreven in **hoofdstuk 3**. Hiervoor worden primaire epicardiale cellen geïsoleerd van humaan foetaal en adult hartweefsel en vervolgens in kweek gebracht. Deze cellen hebben een epitheliaal fenotype. Toevoeging van het signaalmolecuul TGF $\beta$  induceert epiMT in deze cellen. Opvallend is dat foetale cellen ook zonder toevoeging van TGF $\beta$  spontaan epiMT kunnen ondergaan, terwijl adulte cellen dit niet kunnen.

Adult epicardiale cellen kunnen daarom goed gebruikt worden voor het identificeren van nieuwe activatoren van epiMT. In **hoofdstuk 4** wordt een screening uitgevoerd met ruim 1.200 moleculen waarin wordt onderzocht of een van deze stoffen epiMT induceert in de cellen. We identificeren twee nieuwe epiMT-activatoren: Oltipraz metabolite M2 (M2) en TBBz. Vervolgens onderzoeken we welk signaleringspad deze stoffen aanzetten. Bij behandeling met TBBz zien we een sterk effect op epigenetica, specifiek op H3K27 methylering. Dit kan mogelijk de route zijn die epiMT drijft.

De TGF $\beta$  en bijbehorende BMP signaleringspaden zijn essentieel in epiMT tijdens de ontwikkeling van het hart. Daarom wordt in **hoofdstuk 5** beschreven wat hierover

reeds bekend is en welke lessen er geleerd kunnen worden om epiMT in het volwassen hart beter te begrijpen. Hieruit blijkt dat er veel bewijs is voor de rol van TGF $\beta$  in epiMT, maar dat er minder bekend is over de rol van TGF $\beta$  -gerelateerde paden zoals BMP en Activine.

Daarom wordt in **hoofdstuk 6** een vergelijking gemaakt tussen deze paden waarin het epicardiale celweekmodel wordt ingezet. De adulte cellen worden gebruikt om te kijken of stoffen als BMPs en Activine epiMT kunnen induceren in epicardiale cellen. Terwijl de foetale cellen worden ingezet om te kijken of spontane epiMT voorkomen kan worden door remmers van o.a. BMP en Activine. Hieruit concluderen we dat het Activine pad, via de receptor ALK4, betrokken is bij epiMT.

In **hoofdstuk 7** wordt gekeken naar de rol van PRRX1 in het epicard. Dit eiwit is belangrijk voor compleet herstel van beschadigd hartweefsel in zebravissen en komt met name tot expressie in het epicard. Daarom beschrijven we de rol van PRRX1 in humane epicardcellen. Hieruit blijkt dat PRRX1 essentieel is voor de expressie van NRG-1, een eiwit dat wordt uitgescheiden door mesenchymale epicardcellen, en cardiomyocyten aanzet om te vermenigvuldigen. We zien hoge PRRX1 expressie in het zebravis hart en in foetale humane epicardcellen, maar het is vrijwel afwezig in het humane geïnfarceerde hart.

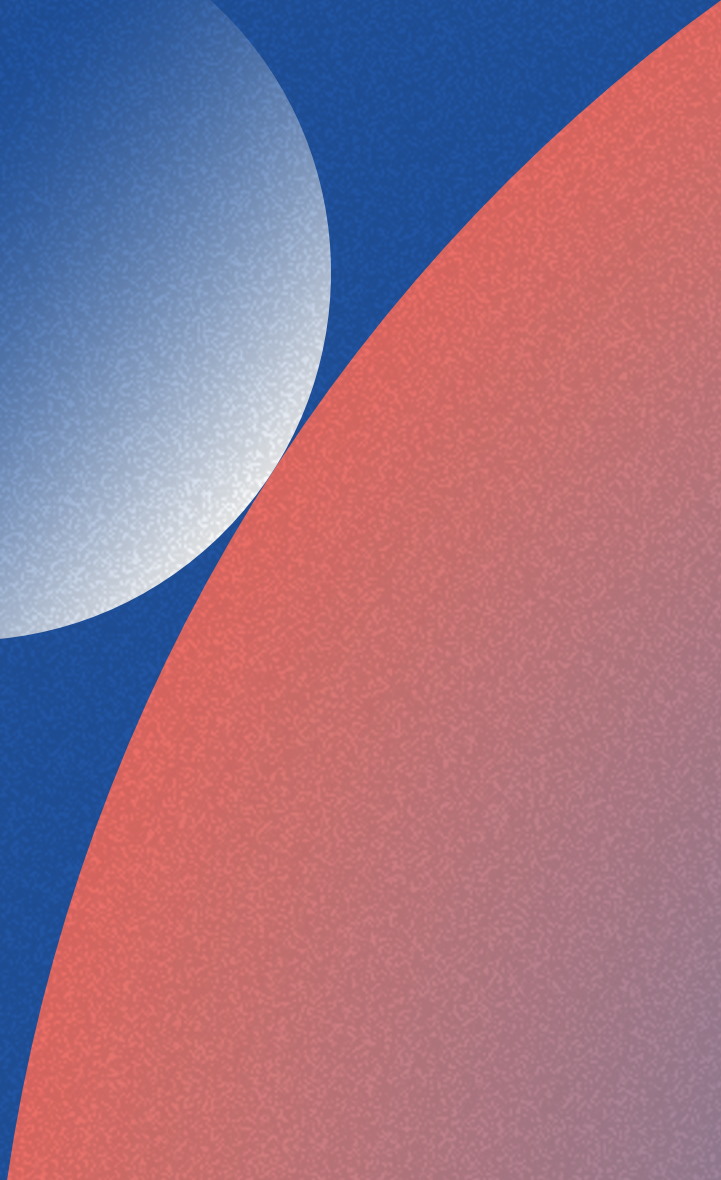
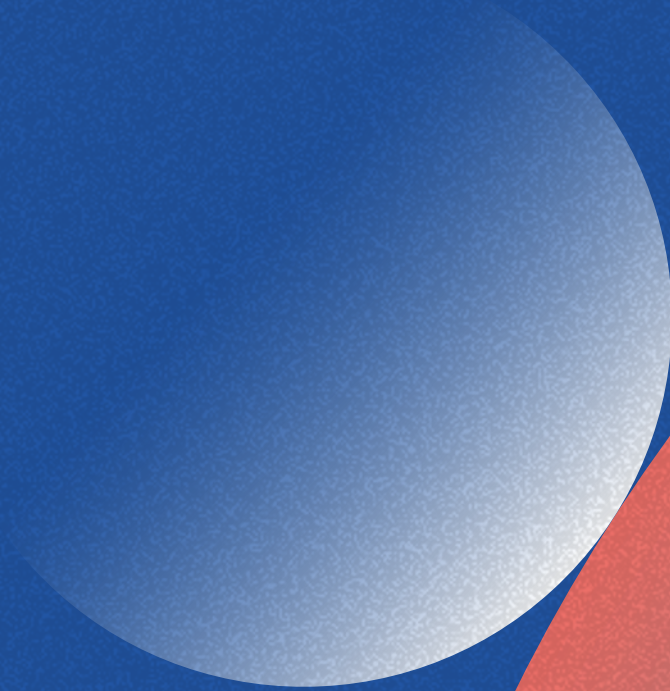
Na de identificatie van epiMT inducerende factoren, TBBz, M2 en Activin/ALK4, is de volgende stap om het beschadigde hart te behandelen. Hiervoor is het nodig om hartweefsel voor langere tijd bloot te stellen aan de deze factoren. Daarom worden in **hoofdstuk 8** twee epicardiale, zelfklevende patches beschreven waarin factoren gemengd kunnen worden en die toegediend kunnen worden op het hart.

In **hoofdstuk 9** worden de gevonden resultaten bediscussieerd.



1

Introduction





## THE LIMITED REGENERATIVE CAPACITY OF THE HEART

The human body is in a continuous process of losing and renewing cells. Some organs are successful tissue regenerators: the gut epithelium replenishes every 4-6 days, the liver can fully regrow itself when partially resected, and – most visible in day to day life – the skin can completely restore (small) wounds without leaving a scar. These regenerative processes can be divided into two types: physiological regeneration (maintenance, e.g. gut epithelium, blood cells) and reparative regeneration (e.g. liver and skin regeneration upon injury). Unfortunately, some tissues have very limited reparative abilities. One of the organs in the human body with the least effective reparative capacity is the heart. Although cardiac tissue can maintain itself during the first decades of life by an annual cell renewal of 1% of the cardiac muscle cells (cardiomyocytes)(1), it cannot cope with massive loss of tissue upon wounding. Such a loss of tissue can happen when people experience a myocardial infarction (MI), a phenomenon that occurred 70.000 times in the Netherlands in 2020 (2). During the course of an MI, one of the coronary arteries becomes obstructed, which prevents oxygen and nutrients to reach downstream tissue. As a consequence, the tissue dies and the heart, which cannot stop beating and therefore has no time for proper wound healing, replaces the dead cells within the injured area by a non-contractile fibrotic scar. Although the scar is initially supportive and prevents tissue rupture, the heart's decreased contractility results in insufficient output to provide the required amount of oxygen and nutrient rich blood to the body. Having to work harder, to maintain the body's demand, the cardiac muscle becomes exhausted, leading to stiffening of the cardiac wall and ultimately to a progressive loss of cardiac pump function. This progressive and incurable disease, characterized by fatigue and shortness of breath, is known as heart failure which can be fatal if left untreated. In the Netherlands, 1 out of 3 patients who experienced an MI develops heart failure within a few years (3). Due to adequate first aid policies, nowadays less people acutely die of MI (2).

However, this brings about an increasing number of patients with a scarred heart who are at risk of developing heart failure (4). Therapy includes life-style changes and medication to lower the demand on the heart and thereby slow the progression towards heart failure. Currently, the only resolving treatment for patients with heart failure is partial or full replacement of cardiac function, either by a Left-ventricular assist device (LVAD), heart transplantation or, recently added to this list of curative treatments in the Netherlands, the total artificial heart (TAH). Although highly promising, these solutions are not without risk or burden for the patient, necessitate life-long immunosuppressive drugs and require either scarce donor hearts or a cardiac device which is still considered less optimal than a biological heart (5). A much more elegant and effective solution would be to target the actual problem and restore the damaged heart tissue.

### **The development of the heart**

To repair an injured heart, the lost tissue needs to be replaced, meaning that cardiomyocytes must be substituted, and vasculature renewed. To achieve this, mechanisms need to be identified that support tissue repair. One way to study cardiac tissue renewal is to compare the mammalian adult heart with its counterpart that is perfectly able to form cardiac tissue: the embryonic heart.

The human embryonic heart is the first functional organ with a blood circulation already present after 4 weeks. The primitive heart initiates as a primitive tube, that starts to form a loop and to twist in such a way that it results in the structure of what will become a four chambered heart consisting of two ventricles and two atria. Progenitor cells migrate towards the heart to populate the heart, aiming to form a strong cardiac wall and to create a network of vessels and nerves. Cells that partake in the formation of the heart originate from three sources (reviewed in Tan 2020). The first one is the so-called cardiac mesoderm that gives rise to cardiac progenitors which provide cardiomyocytes and the endocardial cells that form the inner lining of the heart. The second source is the neural crest, which cells mainly contribute to cardiac innervation and valve formation. In this thesis, we focus on the third source of cells that populate the heart, which is the pro-epicardium, a transient structure at the base of the heart. Between week 4 and 6 of human development, pro-epicardial cells migrate towards the heart and start to populate the outside of the heart forming the epicardium (6,7). At that moment, the heart is still a thin-walled and poorly vascularized structure. However, when the epicardium has covered the heart, it starts to participate in cardiac development in several manners. First, epicardial cells undergo epithelial to mesenchymal transition (epiMT, see below), a process that transforms the

epicardial cell into a mesenchymal cell with the ability to migrate into the myocardium (8). Although there is debate about which cell types derive from the epicardium, it is generally accepted the epicardial-derived cells (EPDCs) differentiate into smooth muscle cells that cover developing vessels and thereby contribute to the maturation of the coronary system (9). Furthermore, EPDCs differentiate towards cardiac fibroblast securing the stability and organization of the heart. Second, the biochemical cross talk between epicardial cells and myocardial cells direct the cardiomyocytes in their growth (10,11). Altogether, the epicardial layer plays a crucial role in the formation of the heart (see Fig. 1). Most importantly, it comprises the endogenous capacity to contribute to cardiac tissue formation. Stimulating this endogenous capacity in the adult heart may be a way to repair injured tissue.

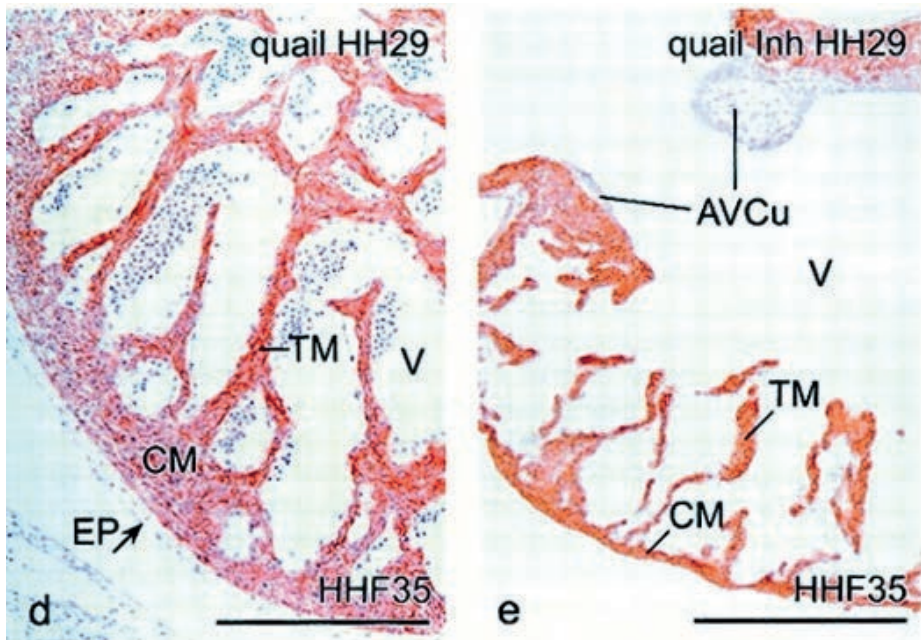


**Fig. 1 | Crucial role of the epicardium during cardiac development.** The left picture represents a normal quail heart, covered by the epicardium (EP) and properly developed compact myocardium (CM). The right picture shows a quail heart in which epicardial formation was blocked by preventing pro-epicardial outgrowth. The absence of the epicardium, as can be appreciated by the lack of an outer layer, prevents proper development of the myocardium, shown by the thin-walled compact myocardium (CM). Derived from (9).

### **Epicardial epithelial to mesenchymal transition (epiMT)**

As stated before, an essential step of epicardial behavior is epiMT, allowing the cells to migrate and to conduct a variety of tasks. We refer to epicardial EMT as epiMT to make a clear distinction with the general EMT process, a common overarching process that does not solely occur in the epicardium, but is involved in tissue development and wound healing, and when dysregulated, can lead to severe pathological diseases such as fibrosis and metastatic cancer. EpiMT generally involves the epicardium, an epithelial tissue lining which is characterized by firm cell-cell adhesions, such as E-cadherin (12), and strong attachment to a basal membrane. If epiMT is initiated, structural changes start to occur. These include losing cell-cell adhesions and changes in the actin skeleton that prepares the cell to migrate (13). Because the cell needs to pass the basal membrane before migrating into underlying tissue, the production of matrix metalloproteases (MMPs) is increased to free the way. Furthermore, mesenchymal markers such as  $\alpha$ SMA and Vimentin are upregulated (14,15). Phenotypically, epicardial cells undergo a major change from a squamous epithelial cell, defined by a clear apical and basal side and the nucleus centered in a web of the cytoskeleton, towards an elongated spindle-shaped cell that lacks polarization.

### **EpiMT and TGF $\beta$ signaling**

If we zoom in on the regulation of epiMT, it starts with an initiator. One of the best known initiators is Transforming Growth Factor  $\beta$  (TGF $\beta$ ), a pleiotropic factor involved in the regulation of critical cellular processes such as proliferation, apoptosis, and differentiation. TGF $\beta$  signaling starts by binding of one of the ligands (TGF $\beta$ 1,2 or 3) to the TGF $\beta$  type 2 receptor which initiates pairing with the TGF $\beta$  type I receptor ALK5. Upon activation of the ALK5 kinase, the intracellular SMAD2/3 proteins become phosphorylated and consequently bind SMAD4, translocate to the nucleus where the SMAD complex acts as a co-factor that regulates gene transcription. Inhibitory SMADs (SMAD6 and SMAD7) can prevent transmission of the signal by competing with SMAD4 (reviewed in (16)). Besides the SMAD-dependent signaling, TGF $\beta$  is also known to interact with other pathways, such as MAPK/JNK and PI3K/Akt (reviewed in (17)), independent of SMAD, which is referred to as 'SMAD-independent' or 'non-canonical' signaling. The intricacy of this pathway allows for regulation at multiple levels, e.g. availability of receptors, balance between inhibitory and phosphorylated SMADs, transcriptional environment in the nucleus, etc. Hence, this explains how it is possible that TGF $\beta$  regulates so many processes, dependent on cellular context. In the context of EMT, TGF $\beta$  is known to reduce cell adhesion protein E-cadherin and increase mesenchymal markers such as Smooth muscle actin. It is doing so via the induction of EMT-transcription factors (EMT-TFs), such as Snail (Reviewed in (18)).

TGF $\beta$  is essential for epicardial behavior during cardiac development. This was demonstrated by the observation that absence of ALK5 results in loose epicardium and an underdeveloped heart (19). Furthermore, TGF $\beta$  induces epiMT in epicardial cells in vitro (20). TGF $\beta$  signaling and its related pathways are therefore an interesting starting point to study the regulation of epiMT.

### **Epicardial reactivation in the injured heart**

A decade after the functional characterization of the embryonic epicardium at the end of the 20th century, it was discovered in 2006 that the epicardium does not solely play a role during development but also becomes active directly after ischemic injury in the adult heart. The initial study of Lepilina et al. demonstrated the contribution of the epicardium to cardiac regeneration in the partially resected zebrafish heart (21). Further research into the re-activation of the epicardium after injury showed that epicardial cells start to recapitulate developmental behavior, including upregulation of EpiMT genes (22). Studies in mice showed the relevance of embryonic recapitulation; mice with an epicardium-specific knockdown of  $\beta$ -catenin displayed diminished epicardial thickening and worsened cardiac function compared to wildtype mice (23). Although this response resembles fetal epicardial activities, there are also differences. For example, in the adult injured heart, the (sub-) epicardial layer thickens upon epicardial activation which barely occurs in the fetal heart. Furthermore, there appears to be less invasion of EPDCs into adult myocardial tissue compared to the fetal heart (24). Given that the epicardium has a proven record of contributing to tissue formation during development, optimizing the epicardial recapitulation may serve as an interesting target to increase cardiac repair. Therefore, studies were performed to exploit its potential to contribute to repair. Smart et al. showed that priming the epicardium with Thymosin  $\beta$ 4 increased the number of epicardial cells and improved cardiac repair in the injured mouse heart (25). Moreover, local epicardial treatment with mesenchymal stem cell-derived exosomes increased epiMT which was related to improved cardiac repair (26). To summarize, inhibition of epiMT hampers cardiac repair, while stimulation of epiMT corresponds to an improved reparative response, demonstrating a window of opportunity to enhance epicardium-driven repair via epiMT. Therefore, the aim of my thesis is to find ways to boost epiMT in the injured heart. In this thesis, we describe a cell culture model which allows us to study epiMT. Using this model, we identify novel epiMT regulators. Because EMT is also involved in pathological remodeling, application of an epiMT stimulator should be transient and local. Therefore, we describe a method to locally administer these factors to the injured mouse heart (see Fig.2).

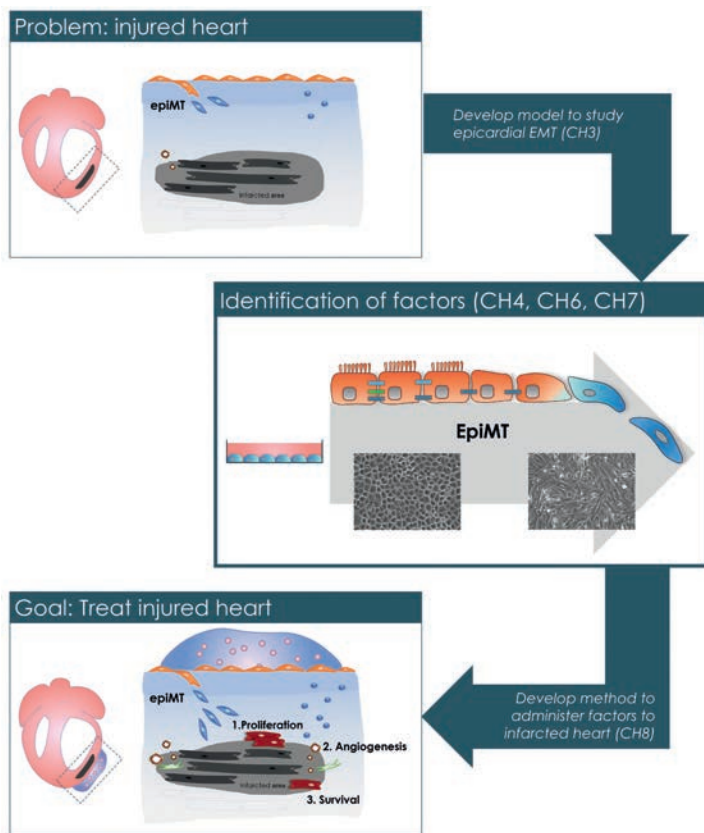


Fig. 2 | Overview of thesis

## Scope

The ultimate goal is to enhance epicardium-driven repair after myocardial infarction. In this thesis, we aim to identify approaches to enhance epicardial EMT (epiMT).

**Chapter 2** comprises a literature overview of epicardial behavior during development and disease. We describe that epiMT is an essential part of epicardial behavior. To study epiMT, we have developed an *in vitro* cell culture model of human primary epicardial cells, which is described in **chapter 3**. In **chapter 4**, we exploit these epicardial cells in a phenotypic compound screen resulting in the identification of novel inducers of epiMT.

One of the main regulators of EMT are members of the TGF $\beta$  family. In **chapter 5** we summarize what is already known about the role of TGF $\beta$  family signaling in epiMT.

Although the role of TGF $\beta$  in epicardial behaviour has been elaborately described, we conclude that other factors such as BMP and Activin may also be involved. Therefore, we used our cell culture model to study these pathways in epiMT in **chapter 6**, revealing that Activin and ALK4 signaling are regulators of epiMT.

Once cells have undergone EpiMT, they have the ability to invade underlying tissue and contribute to the generation of cardiac tissue. In **chapter 7** we describe how epicardial mesenchymal cells may contribute to cardiac repair by investigating the role of epicardial PRRX1 in fetal mesenchymal EPDCs and human tissue. We show that PRRX1 regulates NRG1 secretion, which is beneficial for cardiac regeneration. Furthermore, we demonstrate that PRRX1 is scarcely present in injured human cardiac tissue.

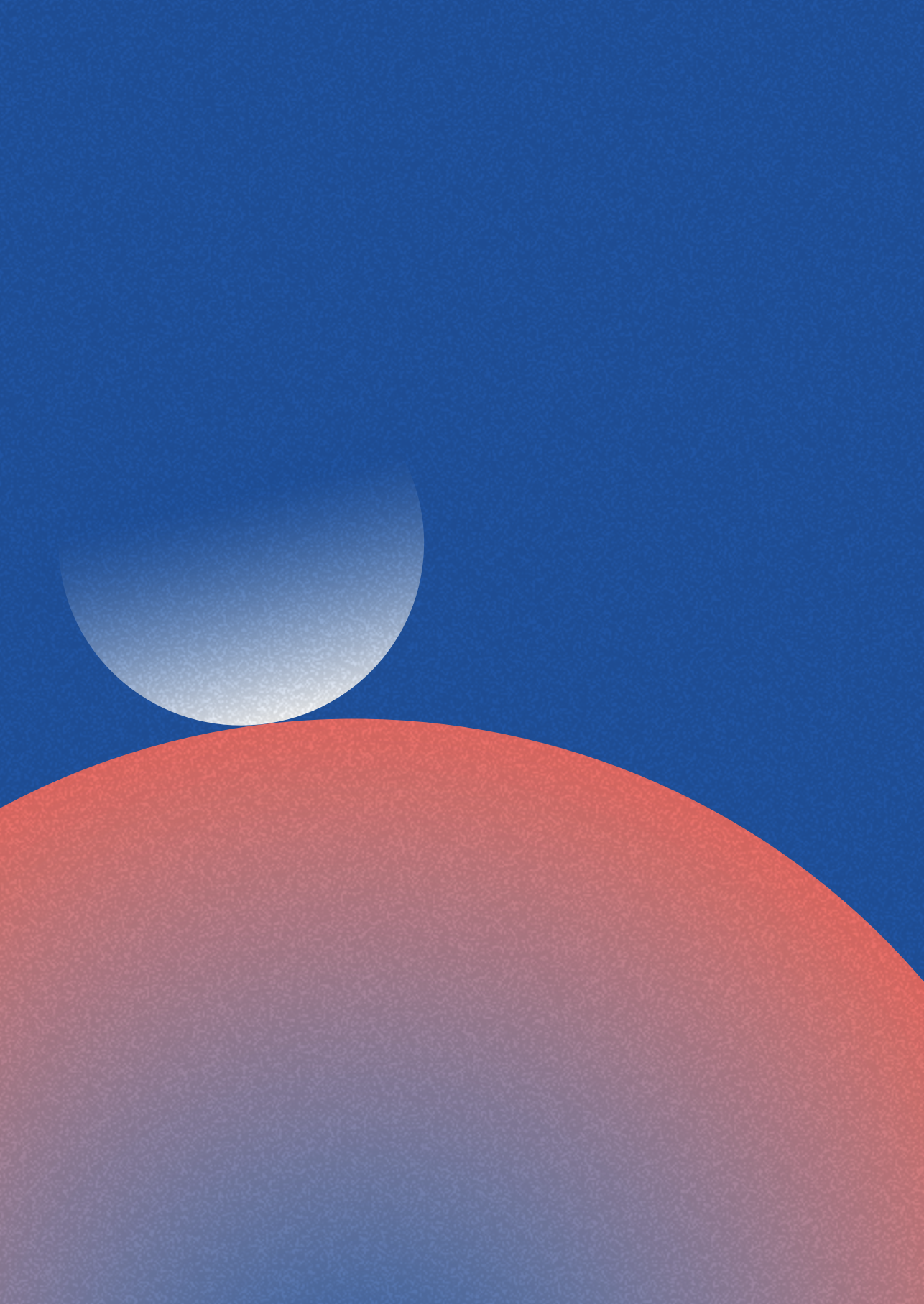
To be able to demonstrate the effectiveness of the identified factors on epiMT in the injured heart, a biomaterial needed to be developed that releases the factor locally to the epicardium in a timely manner. Therefore, in **chapter 8** we describe two types of self-adhering biomaterials that can be mixed with any compound and applied to the mouse heart.

Finally, in **chapter 9** the results and conclusions of this thesis are discussed.

## REFERENCES

1. Bergmann O, Bhardwaj RD, Bernard S, Zdunek S, Barnabé-Heider F, Walsh S, et al. Evidence for cardiomyocyte renewal in humans. *Science*. 2009 Apr 3;324(5923):98–102.
2. Koop Y, Wimmers RH, Vaartjes I, Bots ML. Hart- en vaatziekten in Nederland 2021. 2021.
3. Hartstichting. Hartfalen: Signalen en cijfers. Available from: <https://professionals.hartstichting.nl/getmedia/c495437f-f59f-47ee-95c0-34e0a06b7cee/factsheet-hartfalen-zvl.pdf>
4. Ezekowitz JA, Kaul P, Bakal JA, Armstrong PW, Welsh RC, McAlister FA. Declining In-Hospital Mortality and Increasing Heart Failure Incidence in Elderly Patients With First Myocardial Infarction. *J Am Coll Cardiol*. 2009;53(1):13–20.
5. Dal Sasso E, Bagno A, Scuri STG, Gerosa G, Iop L. The Biocompatibility Challenges in the Total Artificial Heart Evolution. *Annu Rev Biomed Eng*. 2019 Jun 4;21(1):85–110.
6. Viragh S, Challice CE. The origin of the epicardium and the embryonic myocardial circulation in the mouse. *Anat Rec*. 1981 Sep;201(1):157–68.
7. Hirakow R. Epicardial formation in staged human embryos. *Kaibogaku Zasshi*. 1992 Oct;67(5):616–22.
8. Gittenberger-de Groot AC, Vrancken Peeters MP, Mentink MM, Gourdie RG, Poelmann RE. Epicardium-derived cells contribute a novel population to the myocardial wall and the atrioventricular cushions. *Circ Res*. 1998 Jun 1;82(10):1043–52.
9. Gittenberger-de Groot AC, Vrancken Peeters M-PFM, Bergwerff M, Mentink MMT, Poelmann RE. Epicardial Outgrowth Inhibition Leads to Compensatory Mesothelial Outflow Tract Collar and Abnormal Cardiac Septation and Coronary Formation. *Circ Res*. 2000 Nov 24;87(11):969–71.
10. Chen THP, Chang T-C, Kang J-O, Choudhary B, Makita T, Tran CM, et al. Epicardial induction of fetal cardiomyocyte proliferation via a retinoic acid-inducible trophic factor. *Dev Biol*. 2002 Oct 1 ;250(1):198–207.
11. Weeke-Klimp A, Bax NAM, Bellu AR, Winter EM, Vrolijk J, Plantinga J, et al. Epicardium-derived cells enhance proliferation, cellular maturation and alignment of cardiomyocytes. *J Mol Cell Cardiol*. 2010 Oct;49(4):606–16.
12. Martínez-Estrada OM, Lettice LA, Essafi A, Guadix JA, Slight J, Velecela V, et al. Wt1 is required for cardiovascular progenitor cell formation through transcriptional control of Snail and E-cadherin. *Nat Genet*. 2010 Jan 20;42(1):89–93.
13. Wu M, Smith CL, Hall JA, Lee I, Luby-Phelps K, Tallquist MD. Epicardial Spindle Orientation Controls Cell Entry into the Myocardium. *Dev Cell*. 2010 Jul;19(1):114–25.
14. Witty AD, Mihic A, Tam RY, Fisher SA, Mikryukov A, Shoichet MS, et al. Generation of the epicardial lineage from human pluripotent stem cells. *Nat Biotechnol*. 2014 Oct 21;32(10):1026–35.
15. Moerkamp AT, Lodder K, van Herwaarden T, Dronkers E, Dingenouts CKE, Tengström FC, et al. Human fetal and adult epicardial-derived cells: a novel model to study their activation. *Stem Cell Res Ther*. 2016 Dec 29;7(1):174.

16. Massagué J. TGF-beta signal transduction. *Annu Rev Biochem.* 1998;
17. Zhang YE. Non-Smad Signaling Pathways of the TGF- $\beta$  Family. *Cold Spring Harb Perspect Biol.* 2017 Feb 1;9(2):a022129.
18. Xu J, Lamouille S, Derynck R. TGF-beta-induced epithelial to mesenchymal transition. *Cell Res.* 2009 Feb;19(2):156–72.
19. Sridurongrit S, Larsson J, Schwartz R, Ruiz-Lozano P, Kaartinen V. Signaling via the Tgf- $\beta$  type I receptor Alk5 in heart development. *Dev Biol.* 2008 Oct;322(1):208–18.
20. Bax NAM, Oorschot AAM, Maas S, Braun J, Tuyn J, Vries AAF, et al. In vitro epithelial-to-mesenchymal transformation in human adult epicardial cells is regulated by TGF $\beta$ -signaling and WT1. *Basic Res Cardiol.* 2011 Sep 24;106(5):829–47.
21. Lepilina A, Coon AN, Kikuchi K, Holdway JE, Roberts RW, Burns CG, et al. A Dynamic Epicardial Injury Response Supports Progenitor Cell Activity during Zebrafish Heart Regeneration. *Cell.* 2006;127(3):607–19.
22. van Wijk B, Gunst QD, Moorman AFM, van den Hoff MJB. Cardiac regeneration from activated epicardium. *PLoS One.* 2012;7(9):e44692.
23. Duan J, Gherghe C, Liu D, Hamlett E, Srikantha L, Rodgers L, et al. Wnt1/ $\beta$ catenin injury response activates the epicardium and cardiac fibroblasts to promote cardiac repair. *EMBO J.* 2012 Jan 18;31(2):429–42.
24. Zhou B, Honor LB, He H, Ma Q, Oh J-H, Butterfield C, et al. Adult mouse epicardium modulates myocardial injury by secreting paracrine factors. *J Clin Invest.* 2011 May 2;121(5):1894–904.
25. Smart N, Bollini S, Dubé KN, Vieira JM, Zhou B, Davidson S, et al. De novo cardiomyocytes from within the activated adult heart after injury. *Nature.* 2011;474(7353):640–4.
26. Balbi C, Lodder K, Costa A, Moimas S, Moccia F, van Herwaarden T, et al. Reactivating endogenous mechanisms of cardiac regeneration via paracrine boosting using the human amniotic fluid stem cell secretome. *Int J Cardiol.* 2019;287:87–95.



# 2

## The epicardium as a source of multipotent adult cardiac progenitor cells: Their origin, role and fate

Anke M Smits<sup>1</sup>, Esther Dronkers<sup>1</sup>, Marie-José Goumans<sup>1</sup>

<sup>1</sup>Department of Cell and Chemical Biology, Leiden University Medical Center, Leiden, The Netherlands.

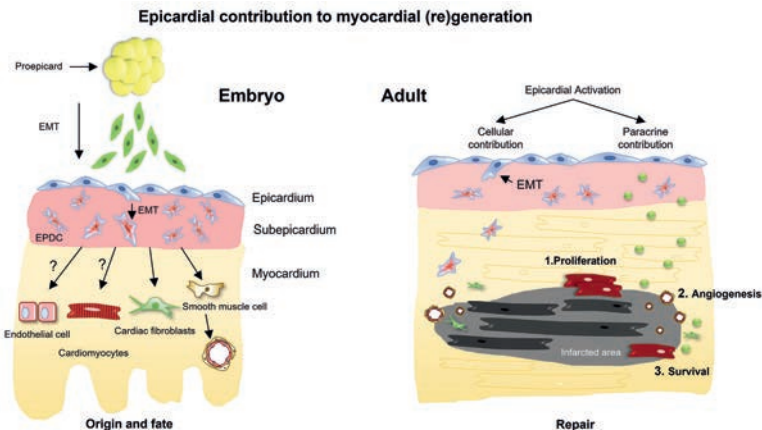
*Published in Pharmacological research (2018)*

*[doi.org/10.1016/j.phrs.2017.07.020](https://doi.org/10.1016/j.phrs.2017.07.020)*

## ABSTRACT

Since the regenerative capacity of the adult mammalian heart is limited, cardiac injury leads to the formation of scar tissue and thereby increases the risk of developing compensatory heart failure. Stem cell therapy is a promising therapeutic approach but is facing problems with engraftment and clinical feasibility. Targeting an endogenous stem cell population could circumvent these limitations. The epicardium, a membranous layer covering the outside of the myocardium, is an accessible cell population which plays a key role in the developing heart. Epicardial cells undergo epithelial to mesenchymal transition (EMT), thus providing epicardial derived cells (EPDCs) that migrate into the myocardium and cooperate in myocardial vascularisation and compaction. In the adult heart, injury activates the epicardium, and an embryonic-like response is observed which includes EMT and differentiation of the EPDCs into cardiac cell types. Furthermore, paracrine communication between the epicardium and myocardium improves the regenerative response. The significant role of the epicardium has been shown in both the developing and the regenerating heart. Interestingly, the epicardial contribution to cardiac repair can be improved in several ways. In this review, an overview of the epicardial origin and fate will be given and potential therapeutic approaches will be discussed.

## Graphical abstract



## Keywords

Cardiac progenitor cell, Epicardium, Myocardial infarction, Cardiac development, Cardiac repair

## 1. INTRODUCTION

Myocardial infarction (MI) is one of the most frequently occurring consequences of coronary heart disease. It has been the leading cause of death in the western world for many decades, and it is expected to remain so for years to come [1]. The obstruction of blood flow in a coronary artery and the ensuing sudden cessation of oxygen supply to regions of the muscle results in massive cell death, followed by an influx of inflammatory cells and collagen producing myofibroblasts [2]. Although adult cardiomyocytes may still possess some residual proliferative ability [3], it is evident that their contribution is insufficient to repair the heart. As a result, injured tissue is replaced by a rigid non-contractile scar. This scar tissue provides tensile strength that potentially prevents the rupture of the damaged myocardial wall. Importantly, scar tissue also severely impairs cardiac contraction which will result in cardiac dysfunction because of pathological compensatory remodelling. Eventually, this combination of factors will progress into heart failure.

Current therapies for MI mainly aim at reopening the culprit blood vessel, thereby reinstating perfusion of the damaged area. These approaches are very effective, and have greatly reduced the number of patients that acutely die after MI. Conversely, it has resulted in an increase in the number of people prone to developing heart failure, for which a heart transplant is the only option for treatment. To repair the heart, it is necessary to find other ways to increase the number of cardiac myocytes after damage.

Over the last two decades, extensive research has been invested in identifying cells with the ability to generate new cardiac tissue (reviewed in [4], [5]). Several of these cell sources, which include the bone marrow, blood, and adipose tissue, have been tested in clinical trials but the influence on cardiac function has been lower than was anticipated [6]. However, one of the most important observations in this era of cell-based therapy is the fact that the adult heart itself harbours cardiac progenitor cells. These cells bear stem cell-like features and have the ability to differentiate into new cardiac cells *in vitro* and *in vivo* [7], [8], [9], [10], [11]. The direct transplantation of cultured human cardiac progenitor cells into the ischemic mouse heart positively influenced cardiac function [12], but only resulted in a marginal increase in newly formed cardiac tissue [7]. Nevertheless it has opened new avenues to explore for treating cardiac damage. The current cell-based therapy approach would require the isolation of progenitor cells from biopsies of cardiac tissue, and a subsequent lengthy culture protocol to increase the number of these rare cells to obtain sufficient

material to transplant. If it is possible to locally stimulate progenitor cells, this could be a valuable addition to current therapies. As such, the epicardium is an intriguing cell population to study since it is an easily accessible source of cells as it is located on the outside of the heart. In this review we will highlight the origin and fate of the epicardium, and why it can potentially be used in therapeutic approaches to cure the damaged heart.

## 2. THE EPICARDIUM

Anatomically the epicardium is part of the pericardium, which is a double layered membranous sac covering the heart and the root of the large vessels. The outer, most superficial layer of the pericardium is known as the fibrous pericardium and consists of connective tissue. It anchors the heart to the diaphragm, the pleura, and the sternum. The inner fibrous pericardium is lined with a serous membrane that folds and covers the heart, thereby forming the pericardial sac. The serous layer lining the fibrous pericardium is called the parietal pericardium, while the layer lining the heart is known as the visceral pericardium or epicardium.

### 2.1. The proepicardium: developmental origin of the epicardium

Early in development, the embryonic heart consists of only two layers: the myocardium and the endocardium. The epicardium, which is not yet present at this tubular heart stage, derives from an extra-cardiac mesothelial cell cluster known as the proepicardium (PE, Fig. 1).

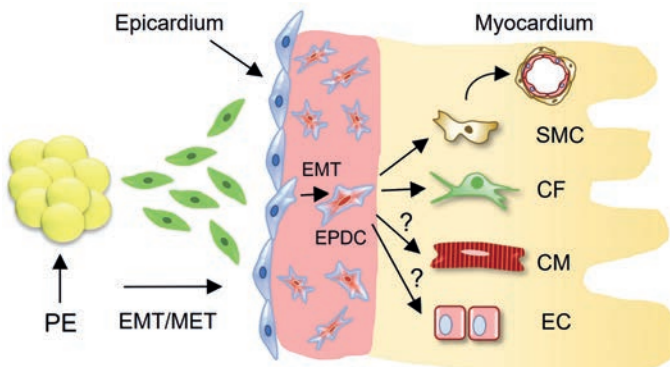


**Fig. 1 | Development of the epicardium and epicardial lineages.** The epicardium originates from the proepicardium (PE). Proepicardial cells go through epithelial to mesenchymal transition (EMT) and translocate to the myocardial surface of the looping heart where they adhere, migrate,

proliferate and undergo mesenchymal to epithelial transition (MET) to form a squamous epithelial layer; the epicardium. While the epicardium remains an intact layer, some of the epithelial cells will undergo a second round of EMT and migrate into the matrix rich sub-epicardial layer (pink). Fate mapping and genetic lineage tracing has demonstrated the multi-lineage potential of these epicardium derived cells (EPDCs). EPDCs differentiate into smooth muscle cells (SMCs), contributing to the coronary vasculature and cardiac fibroblasts (CF) of the mature heart. The contribution of EPDCs to cardiac endothelial cells (ECs) and cardiomyocytes (CMs) has been described but is matter of an ongoing debate.

This structure arises from the pericardial coelomic mesothelium in close proximity of the heart and the liver (Reviewed in [13]). The liver provides additional inductive signals that aid the development of the PE [14]. In mouse, the PE becomes visible from embryonic day 8.5 (E8.5) as a transient cauliflower-like cluster of cells located at the base of the venous inflow tract of the developing heart. The cells of the PE are located adjacent to the primitive heart tube, but do not directly interact with the cardiogenic mesoderm that will form the future myocardium [15], [16].

The PE is composed of different cell populations, with an outer layer of cuboidal epithelial cells expressing Wilms' tumour 1 (WT1) that overlies an inner core of extracellular matrix harbouring several mesenchymal cell types, as well as endothelial cells [17]. The WT1 positive cells within the PE originate from the early cardiac progenitor fields that express Nkx2.5 and Isl-1 [18]. Together with the T-box transcription factor Tbx18 and the basic helix-loop-helix transcription factor Tcf21, WT1 is used to identify PE and (later in development) epicardial (-derived) cells [19], [20]. A distinct subset of PE cells express Scleraxis (Scx) and Semaphorin 3D (Sema3D) and both proteins only partially overlap with WT1 and Tbx18 [21], thereby emphasising the heterogeneity of the cell cluster.

Once the embryonic heart has looped, the bare heart tube will be covered with an epicardial layer of cells derived from the PE that translocate to the heart via different mechanisms. For instance in chick, villous protrusions of the PE extend and directly attach to the myocardial surface, generating a "bridge" for cells to cross [22], while in mice islands of PE cells are formed as they are either pulled off from the villi [23] or are released as free-floating vesicles [24]. Recently, another mechanism was reported where PE cells reach the ventricle by migrating along the surface of the inflow tract [25]. Next, the adhering clusters of PE cells start to proliferate and spread to cover the developing myocardium with a squamous epithelial layer. Epicardial coverage occurs in the mouse between E9.5 and E10.5 in a dorsal to ventral pattern. In

addition, the left ventricle is covered first, and with a more dense layer as compared to the right ventricle [26].

To unravel the role of the PE in the formation of the epicardium and myocardial wall, studies were conducted where the PE was prevented from outgrowth. Both microsurgical and genetic inhibition of the PE cells' migration and adhesion reduced the proliferation of cardiomyocytes, resulting in a thin-walled compact myocardium [20], [27], [28]. Moreover, genetic mouse models causing disturbed epicardial development are associated with defects in endocardial valve development and heart looping [29], cardiomyocyte proliferation and alignment [30], development of the coronary vasculature [27], [31], [32], and the cardiac conduction system [33]. Given the crucial role of the (pro)epicardium in the formation of a fully functioning heart, it is important to understand its contribution in development and disease.

## **2.2. The heterogeneous composition of the epicardium**

When the epicardium completely covers the heart around E11.5 in mouse [26], and week 5 during human cardiac development [34], it has established a multi-cellular epithelium lining the ventricles [35]. The detailed composition of the epicardium is not fully known, but several epicardial cell specific proteins have been suggested, although not necessarily expressed in the same cell. These include WT1 [36], Tbx18 [37], Tcf21 [38], Gata5 [39] and cytokeratin [40]. Additionally, Semad3D, and Scx are expressed in a subset of cells [21]. Furthermore, within the epicardium, clusters with bone marrow-derived CD45+ cells are present, demonstrating that the epicardium is not solely composed of PE-derived cells [41]. Whether the cell populations within the PE are related, i.e. if they represent distinct stages of a continuum of differentiation, or if they are distinct populations with specific abilities, remains to be investigated.

## **2.3. The epicardium in the formation of the myocardium**

### ***2.3.1. Epithelial to mesenchymal transition and migration of epicardial (-derived) cells***

Once the epicardium is established, epicardial cells will directly start to participate in the formation of the cellular composition of the myocardium. A subset of the epicardial cells will undergo a process known as epithelial-to-mesenchymal transition (EMT) (reviewed in [42]; Fig. 1). EMT starts with epicardial cells losing epithelial characteristics like their apical-basal polarity, and their cell-cell contacts, by reducing the expression of the transmembrane adhesion proteins E-cadherin and zonula occludens-1 (ZO-1). Subsequently the epicardial cells acquire mesenchymal cell characteristics; they gain a spindle shape morphology and upregulate the expression of fibronectin,

N-cadherin and matrix metalloproteases (MMPs). This endows the EPDCs with the ability to migrate and populate the subepicardial space: an amorphous matrix-rich layer which is present between the epicardium and the myocardium (Fig. 1). From the subepicardium, EPDCs migrate into the myocardial interstitium where they can differentiate into different cell types and contribute to the development and maturation of the myocardium [43] (Fig. 1).

Epicardial EMT and migration are controlled via various myocardial- and epicardial-derived growth factors like TGF $\beta$  [44], PDGF [45], and FGF [46] (reviewed in [42]). EMT is regulated by transcription factors such as WT1, TCF21, as well as the snail family members Snail1 and Snail2 [42]. For instance, WT1 stimulates EMT via downregulation of E-cadherin expression [47], by increasing the expression of Snail, by enhancing Wnt signalling, and via upregulation of Raldh2 resulting in enhanced retinoic acid signalling [48]. Furthermore, loss of neurofibromin (encoded by *Nf1*) resulted in increased EMT and EPDC proliferation [49]. Interestingly, when TCF21 is specifically deleted from the epicardium, migration of epicardial cells into the myocardium is hampered due to a defect in EMT [50].

Migration of epicardial cells into the myocardium is important for proper myocardial development and it is controlled by a set of transcription factors like Nfatc1 and MRTFs. Nfatc1 is expressed in a subset of epicardial cells and when deleted it resulted in reduced levels of matrix degrading enzymes and a subsequent impaired migration of EPDCs into the myocardium [51]. The myocardium related transcription factors (MRTF)-A and -B are induced when EPDCs are treated with TGF $\beta$  *in vitro*, resulting in enhanced migration. *In vivo*, when MRTF-A/B are knocked out specifically in the epicardium, migration of EPDCs into the sub epicardial layer is impaired [52].

The involvement of all these factors in a temporal and spatial controlled manner to regulate epicardial EMT and migration of EPDCs into the myocardium is crucial for proper development of the myocardial wall.

### **2.3.2. Differentiation of EPDCs into cardiac cell types**

Once EPDCs have invaded the myocardium, they will start to differentiate into several cardiac cell types (Fig. 1). The predominant cell types are interstitial fibroblasts that produce the cardiac extracellular matrix, smooth muscle cells (SMCs), and adventitial fibroblasts that sustain the coronary vasculature [36], [53], [54]. In contrast, contribution to endothelial cells and cardiomyocytes is subject to debate [55], [56] (Fig. 1).

To explore the differentiation capacity of EPDCs, *in vitro* models have been developed to culture EPDCs from mouse embryonic heart explants. These culture systems have confirmed differentiation of EPDCs into fibroblasts and SMCs after addition of TGF $\beta$  [44], [57], [58]. Furthermore, addition of thymosin  $\beta$ 4, combined with VEGF/FGF7, resulted in a highly significant increase in Tie2-positive endothelial cells [59]. Additionally, cardiomyocyte differentiation *in vitro* was observed using embryonic WT1<sup>+</sup> cells [36]. While these *in vitro* models may predict the ability of epicardial cells to differentiate into many cell types that compose the heart, it is important to realise that these conditions are artificial and may not represent the actual *in vivo* situation where interaction with other cells and signals occurs.

*In vivo*, the first studies investigating the differentiation potential of epicardium were performed using retroviral labelling in quail-chick chimera experiments. These experiments indicated an ability of EPDCs to contribute to fibroblast, SMC and coronary endothelial lineages [60], [61], [62]. Subsequent genetic fate-mapping experiments in mice where the expression of Cre-recombinase (Cre) is driven by epicardial-cell specific promoters (e.g. WT1, Tbx18, Tcf21, Gata5, Sema3d and Scx) generally confirmed the epicardial origin of fibroblasts and SMCs (see Table 1, and Tian et al. [63])

Concerning the origin of endothelial cells, lineage tracing studies have demonstrated different results depending on the promoter that was used to follow the cells. Tcf21 and Tbx18 lineage tracing studies were unable to establish epicardial derived endothelial cells [37], [50], [64], while WT1, GATA4, SEMA3D and Scx fate-mapping studies have shown co-localization of genetically labelled cells with EC proteins (Table 1) [21], [32], [36], [65]. Controversy between these studies could be explained by the fact that the PE and epicardium contain heterogeneous cell populations that could reflect distinct populations with a diverse differentiation potential (see Section 2.2). This was further demonstrated by Katz et al., showing that a TBX18/WT1 negative and SEMA3D/Scleraxis positive cell population in the PE gives rise to endothelial cells [21]. Furthermore, some results should be interpreted cautiously. Chick-quail chimeras can be contaminated with cells of the sinus venosus; a structure known to contribute to the coronary vasculature [66].

**Table 1 | Overview of *in vivo* epicardial lineage tracing in mouse embryos.** Only studies aiming to use the mouse model for epicardial lineage tracing were included. \*Did not investigate other cell types, \$ Sporadic, # investigated CMs only in right ventricle

Mouse model	Reporter gene	EPDC differentiation	Identified markers	Reference
<b>SEMA3D<sup>GFPcre/+</sup></b>	R26R <sup>lacZ</sup>	EC SMC CM <sup>\$</sup> Fibro	cTnT, SM22 $\alpha$ , Vimentin, Flk-1, PECAM	[21]
<b>SCX<sup>GFPcre</sup></b>	R26R <sup>lacZ</sup>	EC SMC <sup>\$</sup> CM Fibro Endocardial <sup>#</sup>	cTnT, Cx43, SMM, FSP, Flk-1, PECAM, Nfatc1, NRP-1, Ephrin B2	[21]
<b>G2-Gata4<sup>Cre</sup></b>	Rosa26 <sup>YFP</sup>	EC SMC *	PECAM, IB4, $\alpha$ SMA, NOTCH1	[32]
<b>Wt1<sup>CreYFP+</sup></b>	Rosa26 <sup>YFP</sup>	EC SMC *	PECAM, $\alpha$ SMA	[32]
<b>Wt1<sup>CreERT2</sup></b>	Rosa26 <sup>YFP</sup>	EC *	PECAM	[32]
<b>Wt1<sup>GFPcre</sup></b>	Rosa26 <sup>SLZ</sup> and Z/Red	SMC EC CM	PDGFRB, SM22, SM-MHC, Flk-1, PECAM, Tnnt2, Actn1, GATA4, Nkx2.5, Cx43, functional coupling	[36]
<b>Wt1<sup>CreERT2</sup></b>	Rosa26 <sup>SLZ</sup> and Z/Red	SMC EC CM	Actn1, PECAM, PDGFR, Tnnt	[36]

Table 1 (Continued)

Mouse model	Reporter gene	EPDC differentiation	Identified markers	Reference
<b>Tbx18<sup>Cre</sup></b>	R26 <sup>R<sup>lacZ</sup></sup>	CM SMC Fibro	Tnnt, cTnI, MF20, GATA4, Nkx2.5, SM-MHC, NRP-1, PDGFR $\beta$ , Col1a2	[37]
<b>Tcf21<sup>Cre/+</sup></b>	R26 <sup>R<sup>YFP</sup></sup> and R26 <sup>R<sup>tdT</sup></sup>	Fibro	PDGFR $\alpha$ , Col1	[50]
<b>Wt1<sup>Cre</sup></b>	R26 <sup>R<sup>mTmG</sup></sup>	Fibro CM*	FlnA, Vimentin, Col1a1, MF20	[54]
<b>Tbx18<sup>cre/+</sup></b>	Rosa26 <sup>mTmG</sup>	Fibro SMC #	Nos3, Emcn, SMAActin, Notch3, Postn, Tnni3, Myhc	[64]
<b>Wt1<sup>CreER</sup></b>	Rosa26 <sup>RFP</sup>	SMC Pericyte EC *	SM22, SM-MHC, SMA, PECAM	[65]
<b>Tbx18<sup>Cre</sup></b>	Rosa26 <sup>RFP</sup>	SMC *	SMA	[65]
<b>Wt1<sup>CreERT2</sup></b>	Rosa <sup>mTmG</sup>	Pericyte *	CSPG4, PDGFR $\beta$	[115]

Abbreviations: Actn1: Alpha-actinin-1, CM: Cardiomyocyte, Col: Collagen, CSPG4: Chondroitin Sulfate Proteoglycan 4, cTnI: cardiac Troponin I, cTnT: cardiac muscle troponin T, Cx43: Connexin 43, EC: Endothelial Cell, Emcn: Endomucin, Fibro: Fibroblast, Flk-1: Fetal liver kinase 1, FlnA: FilaminA, FSP: Fibroblast-specific Protein, IB4: Isolectin B4, MF20: Myosin Heavy Chain, Myhc: Myosin heavy chain cardiac muscle, Nfatc1: Nuclear factor of activated T-cells, cytoplasmic 1, Nkx2.5: NK2 Homeobox 5, Nos3: Nitric oxide synthase 3, Notch: Neurogenic locus notch homolog protein, NRP-1: Neuropilin-1, Pdgfr: Platelet-derived growth factor receptor, PECAM: Platelet Endothelial Cell Adhesion Molecule, Postn: Periostin, SM22: Smooth Muscle Protein 22, SMAActin: Actin  $\alpha$ 2 Smooth Muscle aorta, SMC: Smooth Muscle Cell, SMM: Smooth muscle myosin, SM-MHC: Smooth Muscle-Myosin Heavy Chain, Tnni3: Troponin I cardiac 3, Tnnt: Troponin T,  $\alpha$ SMA:  $\alpha$  Smooth Muscle Actin

Additionally, WT1 was shown to be expressed in cardiac endothelial cells [34], [56], [67], which may obscure the results from lineage tracing experiments. Therefore, although some studies conclude that endothelial cells can derive from the epicardium, it remains an ongoing debate to what extent the PE/epicardium contributes to the coronary vasculature in the developing heart. Overall the direct contribution of epicardial cells, if any, appears to be low and both the sinus venosus and endocardium [21], [68] are considered the major contributors (reviewed in [63]).

With respect to epicardial-derived cardiomyocytes, lineage tracing studies using Scleraxis, WT1 and TBX18 to trace cells have demonstrated epicardial-derived functionally active cardiomyocytes (Table 1). However it must be noted that these findings are controversial, since some of the genes driving the expression of Cre recombinase in these studies, e.g. *Tbx18* [37], and *WT1* [36], have been shown to be present within cardiomyocytes at certain stages during development [55], [67].

Although the full differentiation potential *in vivo* is yet to be confirmed, it is however clear that embryonic EPDCs have an essential impact on cardiac development via direct contribution of cells to the myocardium (Fig. 1).

### **2.3.3. Contribution of epicardial paracrine signalling to the formation of the myocardium**

Another process that occurs once the epicardium has covered the developing heart is that epicardial cells will start to produce paracrine factors that support myocardial growth [69], [70], [71]. These factors provide an essential exchange of signals between the myocardium and the epicardium that are crucially important for the development of the coronary vessels (reviewed in [72]), as well as the growth and differentiation of the heart muscle [73]. For instance, Kolander et al. showed that disrupting GATA4 and GATA6 signalling specifically in the epicardium results in defective coronary vascular development by regulation of the number of subepicardial endothelial cells via secreted factors [74]. Another example of epicardial-myocardial signalling is retinoic acid (RA), a known contributor to cardiomyocyte proliferation. Retinoid X receptor  $\alpha$  (RXR $\alpha$ ) knock out mice are lethal as a result of hypoplastic myocardium, and demonstrate a poorly attached epicardium [75]. Interestingly, this phenotype was demonstrated to be epicardial-related since deletion of RXR $\alpha$  in GATA5 expressing cells also demonstrated impaired cardiac compaction, as a consequence of a decreased cycling of cardiomyocytes [76]. Furthermore, multiple Fibroblast Growth Factors (FGFs) are expressed in the epicardium and are shown to be essential for proper myocardial formation [46], [77], [78]. For example, depletion of the epicardially expressed Fibroblast

Growth Factor 9 (FGF9), or depletion of the concomitant FGF receptors present on premature cardiac myoblasts, results in embryonic lethality and reduced cardiomyocyte proliferation in the developing heart [77]. Also other produced factors, such as Hedgehog [78], [79] and CXCL12 [80] were shown to be involved in myocardial morphogenesis and coronary development. This emphasises the importance of the epicardium in cardiac development, by contributing cells as well as essential cytokines and growth factors to induce the myocardial development.

### 3. THE EPICARDIUM IN THE ADULT MAMMALIAN HEART

#### 3.1. *The quiescent epicardium in the adult intact heart*

Contrary to development, the postnatal mammalian epicardium is a dormant single-cell layer. This was shown via the analysis of genes involved in epicardial activation such as *WT1*, *Tbx18* and *Raldh2*. These genes are abundantly present in the embryonic heart, but are rapidly downregulated postnatally, only to be barely detectable at 3 months of age in the mouse [81]. The same conclusion on the dormancy of the epicardium was drawn by using a mouse model where the Green Fluorescent Protein (GFP) gene was knocked-in into the *WT1* locus (*WT1<sup>GFP<sup>Cre</sup></sup>*). When investigating the *WT1*-driven expression of GFP in different stages of heart development, Zhou et al. observed that in the embryo, its expression was restricted to the epicardium and labelled approximately 90% of the epicardial cells [82]. In contrast, in the adult heart, GFP expression was observed in fewer than 25% of the cells within the epicardium; thereby revealing that *WT1* is present at stages where the epicardium actively plays a role in heart development. This lack of activation in the adult heart was further underscored by using a tamoxifen inducible *WT1<sup>CreERT2</sup>* mice crossed onto a Cre reporter line (*Rosa<sup>mTmG</sup>*). In this model, the activation of *WT1* only results in translocation of Cre recombinase to the nucleus when tamoxifen is administered. By crossing these mice onto the *Rosa<sup>mTmG</sup>* reporter line, nuclear translocation of Cre results in the irreversible exchange of expression of red fluorescent Tomato into the indefinite expression of green fluorescent GFP. This model, which is extensively used in the field of epicardial research, thereby provides the opportunity to label *WT1*<sup>+</sup> cells at any given time point, and to track their fate based on the continuous expression of GFP. Investigating uninjured adult hearts using this model up to eight weeks after tamoxifen injection revealed no migration of *WT1*/GFP expressing cells into the myocardium [82]. Together, these data show that in the adult uninjured heart, the epicardium is a quiescent cell layer, as shown by the downregulation of epicardial specific genes and the lack of migration of cells after the formation of the heart is completed.

### **3.2. The activated epicardium in the infarcted adult heart**

#### **3.2.1. Activation of the embryonic gene programme in the epicardium post-MI**

In the adult heart, the epicardium can be awakened from its dormant state. Several studies have shown that MI or ischemia/reperfusion can result in reactivation of the epicardial layer, including its proliferation and expansion, EMT, and migration of epicardial derived cells (reviewed in [42], [83]).

Within the first days after MI, the epicardial layer displays a partial recapitulation of the embryonic gene programme, which is evident by the upregulation of the epicardial genes *Wt1*, *Raldh2* and *Tbx18* [82], [84], [85]. At five days post-MI, the expression of these genes peak, and they remain present in approximately 75% of the epicardial cells at 14 days after injury, after which the expression decreases gradually [82]. Interestingly, the upregulation of genes is observed not only at the site of injury, but throughout the epicardium. One theory is that this occurs via factors secreted into the pericardial fluid. Studies inducing MI with an intact pericardium have shown an attenuated cardiac function post-MI compared to MI where the pericardium was opened prior to ligation [84], [86].

How the activation of the epicardium is regulated on a transcriptional level is not fully understood, however it appears to be partially controlled via the C/EBP transcription factor family [85]. Interestingly, in contrast to MI, mice undergoing transverse aortic constriction (TAC) to induce hypertrophy and fibrosis display no activation of WT1<sup>+</sup> cells within the epicardium [87], suggesting that cardiac damage through ischemia is likely a potent activator of this layer.

#### **3.2.2. Proliferation and EMT of epicardial cells post-MI**

Following MI, the epicardium covering the injured area is initially completely lost and is rebuilt from the surviving epicardium within three days post-injury [88]. The tamoxifen inducible WT1<sup>CreERT2</sup>Rosa26<sup>mTmG</sup> lineage tracing model was able to confirm that this is due to proliferation of pre-existing epicardial cells. At two days post-MI, phospho-histone H3 and BrdU staining revealed many proliferating WT1<sup>+</sup>/GFP<sup>+</sup> epicardial cells [82]. This resulted in a transition from a single cell epithelium into a multi-layered sheet, in an organ wide fashion, but most pronounced near the injured area [82], [88]. This process is specific to acute ischemic injuries like MI and ischemia reperfusion, as thickening of the epicardium is absent in models for hypertrophy like TAC [89].

Further recapitulation of the embryonic activation process in the ischemic heart is shown by the upregulation of several EMT-related transcription factors including *Smad1*, *Snail*, *Slug* and *Twist* in EPDCs [82], [88]. Interestingly, BrdU incorporation experiments revealed that the epicardial cells positive for EMT-markers are responsible for the newly generated subepicardial mesenchyme [88].

The activation and expansion of the epicardial layer is crucial for the post-injury response, as was illustrated by Duan and colleagues [90]. The specific disruption of Wnt signalling within epicardial cells in a mouse model of cardiac ischemia reperfusion injury revealed less epicardial EMT, and a reduced subepicardial collagen deposition. As a result, ventricular dilatation and a decreased fractional shortening were observed [90]. Equally, in a study where the epicardium was primed by systemic injection of thymosin  $\beta$ 4 prior to MI, a thicker layer of activated epicardium, and more migration was observed and resulted in a subsequent positive effect on cardiac function [81]. These studies emphasize the importance of understanding and optimizing the epicardial activation and EMT to enhance the post-injury response [42]. Our recent *in vitro* data show that both human adult and foetal epicardial cells undergo activation and EMT [91]. Interestingly, foetal cells were activated more efficiently, and underwent EMT spontaneously. This potentially reflects the differences in efficiency of activation *in vivo* during development and in the adult heart. As such the foetal processes may serve as a blueprint for an optimal adult post-injury response.

### **3.2.3. Migration of EPDCs into the injured adult heart**

Whether adult EPDCs retain the ability to migrate into the damaged area is subject to debate. Two studies using the  $WT1^{CreERT2}Rosa26^{mTmG}$  injected with tamoxifen to trace the epicardium with GFP indeed confirmed the expansion of this layer after MI, but labelled  $WT1^+$  cells appeared to be retained subepicardially showing no indication of migrating into the damaged myocardium [82], [92]. However, in a later study using the same mouse model, the injection of modified-RNA encoding for VEGF-A protein (modRNA VEGF-A) after injury did reveal migration of cells into the heart [93].

Several alternative methods to mark cells within the epicardial layer have been applied. The first one is to inject fluorescent protein-producing lentiviruses into the pericardial fluid, which is in direct contact with the epicardial layer, allowing infection and labelling of the epicardium [53], [94]. A second approach is to apply a biocompatible gel containing a modified RNA for Cre on the epicardium of the  $Rosa^{mTmG}$  reporter mouse [93]. The patch was applied two weeks prior to MI to prevent labelling of non-epicardial cells in the complicated injured environment. Both methods revealed

that epicardial-derived cells were found within the infarcted myocardium at 7 and 21 days post-MI [93], [94]. Although these studies rely on epicardial labelling based on location rather than using epicardial specific markers, they coincide with the results of a genetic labelling study where in the Bacterial Artificial Chromosome (BAC)-WT-1<sup>Cre</sup>; R26R mice, beta-galactosidase expressing cells were observed in the infarcted area after 1 month [88].

It is challenging to correlate these different findings in mouse lineage trace models. In the non-inducible BAC model, background labelling can occur if cells within the myocardial wall start to express WT1 [56], which is less likely to happen in the inducible lineage trace model since the labelling occurs during a short period of time. However, a downside of the tamoxifen labelling is that the short duration of labelling may result in missing of many cells and therefore an underestimation of the epicardial contribution.

Although these different conclusions regarding migration may be the result of technical issues, it appears that, at least partially, migration is a component of the adult reactivating response to injury.

### ***3.3. Differentiation of adult epicardial cells into cardiac cell types in vivo***

#### **3.3.1. Fibroblasts**

As mentioned above, the most prominent contribution of epicardial cells to the formation of the embryonic myocardium is via differentiation into coronary SMCs, and interstitial and adventitial fibroblasts. In the adult injured heart, a similar differentiation profile is observed (Table 2). Lineage tracing models using WT1 as a Cre driver, showed that a majority of traced cells transition into fibroblasts [82], [88], [92]. Additionally, after ischemic injury, the epicardium thickness increases up to 6-fold, and the deposition of collagen in the subepicardial space is also dramatically increased [89] indicating a rise in fibroblast activity.

**Table 2 | Overview of *in vivo* epicardial lineage tracing following myocardial infarction in mice.** Only studies aiming to use the mouse model for epicardial lineage tracing were included. \* Other cell types not reported, \$ Sporadic, ^ Displayed no mature characteristics, remained rounded.

Mouse model	Reporter gene	EPDC differentiation	Identified markers	Treatment	Reference
WT1 <sup>CreERT2/+</sup>	R26R <sup>EYFP</sup>	CM *	cTnT, αActin, Cx43, N-Cad, Ca <sup>2+</sup> transients, Functional coupling	TB4	[81]
WT1 <sup>CreERT2/+</sup>	R26R <sup>mTmG</sup>	SMC Fibro EC <sup>\$</sup>	SM-MHC, αSMA, SM22α, FN1, ColIII, FSP1, ProCol1, PECAM	-	[82]
Ad:MsIn-Cre	R26R <sup>mTmG</sup>	Fibro	FSP1	-	[82]
(BAC)WT1 <sup>EGFPcre</sup>	R26R	SMC EC CM <sup>\$</sup> Fibro	αSMA, PECAM + location in vessel wall, cTnI, SERCA2, via exclusion of other markers	-	[88]
WT1 <sup>CreERT2/+</sup>	R26R <sup>mTmG</sup>	SMC Fibro	αSMA, DDR2, ProCol1, desmin, FSP1, ColIII	TB4	[92]
WT1 <sup>CreERT2</sup>	R26R <sup>mTmG</sup>	EC CM *	PECAM1, Kdr, Tnnt2, TNNI3	VEGF-A modRNA	[93]

Table 2 (Continued)

Mouse model	Reporter gene	EPDC differentiation	Identified markers	Treatment	Reference
<b>Cre modRNA gel</b>	R26R <sup>mTmG</sup>	SMC EC CM	SM-MHC, PECAM1, TNIN13	VEGF-A modRNA	[93]
<b>LV-CMVGFP</b>	-	CM *	αActin, morphology	-	[94]
<b>Gata5-Cre</b>	R26R <sup>EYFP</sup>	SMC <sup>Δ</sup> EC <sup>Δ</sup> Fibro	αSMA, PECAM, ProCol1	TB4	[97]

Abbreviations: Ad: Adenovirus, CM: Cardiomyocyte, ColIII: Collagen type III, cTnI: cardiac TroponinI, cTnT: cardiac muscle TroponinT, Cx43: Connexin 43, DDR2: Discoidin Domain Receptor2, EC: Endothelial Cell, Fibro: Fibroblast, FN1: Fibronectin 1, FSP1: Fibroblast-specific protein 1, Kdr: Kinase insert domain receptor, Msln: Mesothelin, N-Cad: N-Cadherin, PECAM: Platelet Endothelial Cell Adhesion Molecule, proCol1: procollagen1, SERCA2: Sarcoplasmic Reticulum Ca<sup>2+</sup> ATPase 2, SM22: Smooth Muscle Protein 22, SMC: Smooth Muscle Cell, SM-MHC: Smooth Muscle-Myosin Heavy Chain, saActin: sarcomeric α Actin, Tnni3: Troponin I cardiac 3, Tnnt: Troponin T, Tβ4: Thymosinβ4, αSMA: α Smooth Muscle Actin

Russell et al. [95] used a Notch reporter mouse line which revealed significant activation of the reporter in the epicardium. Notch reporter positive epicardial cells were isolated and subjected to microarray analysis which showed that these cells have a fibroblast signature with high expression of collagen-I, elastin and fibronectin. Therefore, fibroblasts likely represent the default programme in the activated epicardial layer [95]. Although too much activity of cardiac fibroblasts could result in excessive scar formation, they represent a vital cellular component in cardiac homeostasis and wound healing [96]. Reducing Wnt/ $\beta$ catenin specifically in cardiac fibroblasts resulted in reduced collagen deposition and a worse cardiac function post-injury revealing a beneficial role of cardiac fibroblasts in cardiac repair [90].

### 3.3.2. Endothelial and smooth muscle cells

With respect to neovascularisation post-injury, many studies have identified lineage-traced EPDCs that differentiate into smooth muscle cells post-MI [82], [88], [92], [93], [97], [98] (Table 2), which was anticipated based on the described embryonic fate of EPDCs. In contrast, most analyses failed to identify EPDCs that differentiated into endothelial cells [81], [82], [92] (Table 2). However, a study using the BAC WT1<sup>Cre</sup>;R26R mouse line to determine the fate of epicardial cells based on  $\beta$ -galactosidase ( $\beta$ -gal) expression revealed  $\beta$ -gal<sup>+</sup> cells co-expressing PECAM were found to line vessels within the infarcted area [88]. Although intriguing, this is likely due to the fact that WT1 can be re-expressed in endothelial cells post-injury [56] and could therefore represent an artefact, making it unlikely that there is a direct contribution to endothelial cells in the normal response of the heart to MI.

Interestingly, injection of modRNA VEGF-A into the mouse myocardium after MI resulted in an increased capillary density and a smaller infarct size. This coincided with an enhanced activation of epicardial cells, which showed an upregulation of the VEGF receptor KDR in WT1-GFP expressing cells in the WT1<sup>GFP<sup>Cre</sup></sup> mouse line. After isolation and sorting of epicardial cells post-MI, cultured WT1<sup>+</sup> cells responded to VEGF-A by increasing their proliferation. Moreover, VEGF-A was able to shift the differentiation of epicardial progenitor cells towards the endothelial lineage as shown by an increase of VE-Cadherin, KDR and PECAM1 expression. This was further corroborated by *in vitro* clonal assays and lineage trace experiments using either the WT-1<sup>CreRT2x</sup> ROSA<sup>mTmG</sup> and or a modRNA Cre expressing patch on the epicardium [93]. This study emphasises the plasticity of epicardial cells, provided the right cues are delivered at the right time (Table 2).

### 3.3.3. Cardiomyocytes

The differentiation of EPDCs into cardiomyocytes in the embryo is controversial, and the same holds true in the adult (Table 2). In a study by Limana et al., the epicardium was labelled via injection of a GFP producing lentivirus 3 days before experimentally induced MI, which revealed that some cells that migrated into the infarcted myocardium expressed  $\alpha$ -sarcomeric actin, albeit in very low numbers [94]. The observation that EPDCs have the ability to differentiate into cardiomyocytes was confirmed in the BAC-WT1<sup>Cre</sup>;R26R mouse line. Epicardial derived  $\beta$ -gal<sup>+</sup> cells co-expressing troponin I were found within the myocardium but only after one and three months post-MI. These EPDC-derived cardiomyocytes maintained an immature phenotype, being small round cells lacking sarcomeric organisation, and numbers were still very low [88].

An enhanced post-injury activation of the epicardium was observed when animals were treated with thymosin  $\beta$ 4 prior to myocardial infarction. Interestingly, in this study using the WT1<sup>CreERT2</sup>;R26R<sup>EYFP</sup> line, differentiation of epicardial derived cells into troponin T and  $\alpha$ -sarcomeric actin expressing YFP<sup>+</sup> cells that coupled to the surrounding myocardial tissue was observed. To counter that these results are due to extra-epicardial expression of WT1, YFP<sup>+</sup> epicardial derived cells were isolated from thymosin  $\beta$ 4 treated mice 4 days after myocardial infarction and transplanted into the infarcted myocardium of a recipient wildtype mouse; a small number of the YFP<sup>+</sup> donor cells differentiated into  $\alpha$ -sarcomeric actin expressing cells. A similar effect was observed when modRNA encoding VEGF-A was injected into the *peri*-infarct zone to enhance the epicardial response; besides endothelial cells, a slight increase in cardiomyocytes was found based on TNN3 expression in lineage traced epicardial cells [93]. Although the occurrence of cardiomyocyte differentiation is still extremely low in these two studies [81], [93], it provides a proof-of-concept that cardiomyocyte formation from EPDCs could be a possibility.

In contrast, there are several studies using a similar lineage tracing approach (WT-1<sup>CreERT2</sup>; R26<sup>mTmG</sup>) that did not observe differentiation into cardiomyocytes [82], [98]. Of note is that these studies also did not observe migration of EPDCs from the subepicardial to the myocardium after injury, whether this is due to technical issues needs to be addressed.

The data argue that in the adult, the epicardial potential for cardiomyocyte formation is comparable to the embryonic heart: its ability to deliver cardiomyocytes directly is low to non-existent but can be enhanced by priming the epicardium using specific factors.

### **3.4. Paracrine contribution of epicardial cells to cardiac repair**

Besides contributing directly to the formation of cardiac cell types, epicardial cells can participate in repair of the heart via paracrine processes.

Zhou et al. observed many blood vessels within the thickened subepicardium after MI. These newly formed vessels were often located in close proximity to EPDCs. *In vitro* experiments with the GFP<sup>+</sup> lineage-traced EPDCs confirmed that these cells indeed have proangiogenic properties [82]. Interestingly, the injection of conditioned medium from cultured EPDCs into the infarcted heart resulted in an increase in vessel density and reduced the adverse remodelling of the heart post-MI in short and long-term follow-up [82]. A similar finding was observed when injecting human EPDCs into the infarcted heart of NOD-SCID mice. Although human cell survival was minimal at 6 weeks post-MI, a significant effect on vascularisation was apparent, again emphasising an angiogenic effect of EPDCs [99] (and our own unpublished observations). Interestingly, EPDCs may also influence cardiomyocytes within the myocardium via paracrine mechanisms. Co-culture experiments of EPDCs and cardiomyocytes resulted in increased myocyte proliferation and enhanced levels of cardiomyocyte differentiation [30], [100].

Besides using conditioned medium or cells, a single factor excreted by epicardial cells was identified that significantly aids in cardiac repair. Follistatin-like 1 was identified as a highly enriched factor produced by epicardial cells with the ability to induce cardiomyocyte proliferation [101] and to increase cardiomyocyte survival [102], [103]. By delivering this factor directly to the infarcted myocardium via an epicardially applied patch Wei et al. showed an increase in proliferation of local cardiomyocytes resulting in an increased survival, a reduction of fibrosis and prevented deterioration of cardiac function [101]. Follistatin-like 1 did not have an effect on the epicardium itself.

Conversely, epicardial cells can be influenced to partake in cardiac repair by addition of a single factor. Foglio et al. identified clusterin as highly enriched protein within the pericardial fluid of MI patients [86]. *In vitro*, clusterin was shown to induce proliferation and EMT of epicardial cells. *In vivo*, the injection of this single protein into the pericardial fluid of the infarcted mouse heart was sufficient to enhance epicardial EMT, and induce cell survival, arteriole density, and resulted in an ameliorated cardiac function [86].

These studies stress that epicardial cells do not only participate in cardiac repair by providing cells, but have a major contribution to the repair mechanisms within the

heart via production of essential proteins. Moreover, since epicardial cells themselves are sensitive to induction via cytokines and growth factors, one can imagine a feedforward loop where single proteins enhance the number of epicardial cells that produce paracrine factors, thereby further stimulating cardiac repair after injury.

#### 4. THE EPICARDIUM AS A SOURCE OF MULTIPOTENT PROGENITOR CELLS?

From the data described above, the question arises whether EPDCs should be considered cardiac progenitor cells. It becomes clear that the adult epicardium in the infarcted heart is activated, undergoes EMT and contributes to several cardiac cell types. Epicardial EMT has been postulated to be involved in the formation of resident cardiac progenitor cells [104]. The adult epicardium may therefore function as a reservoir of mesenchymal progenitor cells [94].

Classically, stem or progenitor cells can be defined as a self-maintaining population of relatively undifferentiated, proliferative cells that can produce a variety of differentiated progeny with the ability to regenerate tissue of parts thereof [105]. Based on the expression of an embryonic gene programme, their ability to display proliferation upon damage, and their differentiation into several lineages, EPDCs partially fulfil these criteria. However, if they fulfil all criteria to be true *cardiac* progenitor cells remains to be established. To this end it is important to define which progenitors are necessary to deliver the cells of the developing heart [106].

Within the adult heart, cells have been discovered expressing stem cell markers like the tyrosine kinase receptor c-Kit [11], and stem cell antigen (Sca)-1 [10] on their cell surface. These c-Kit and Sca-1 expressing cells are considered to be stem- or progenitor cells based on their ability to form colonies, to display telomerase activity and to show long-term label retention. These cellular abilities are generally linked to stem-cell features. Moreover, these cells have been shown to differentiate into cardiomyocytes, endothelial cells, smooth muscle cells and fibroblasts, thereby indicating their ability to differentiate into all cell types required to generate cardiac tissue and participate in cardiac regeneration (please refer to the reviews included in this special edition of *Pharmacological Research*, Volume 127).

The human foetal and adult (sub)epicardium is highly heterogeneous [107] and was shown to harbour a minor population of c-Kit and CD34 expressing cells [84], [94].

In vitro, these c-Kit expressing epicardial cells differentiated into the endothelial and smooth muscle cell lineage [94]. A similar population was observed in the adult mouse heart. Interestingly, the percentage of proliferative c-Kit<sup>+</sup> cells increased after induction of MI and these cells appeared to participate in the formation of subepicardial blood vessels [94]. Bollini and colleagues [108] performed a direct comparison between the expression profiles of mouse embryonic EPDCs, and adult EPDCs isolated after thymosin  $\beta$ 4 stimulation and MI [108]. They observed a low expression of Sca-1 in the WT1<sup>+</sup> embryonic cells, while in the adult, Sca-1 was present on approximately 60% of the WT1<sup>+</sup> EPDCs. Moreover, the mesenchymal markers endoglin (CD105), the hyaluronan receptor CD44, major T-cell antigen 1 (Thy-1 or CD90) and Platelet Derived Growth Factor Receptor (PDGFR) $\beta$  were observed in the activated adult EPDCs. They continued to show that within the adult epicardium post-MI, the WT1<sup>+</sup>, Sca-1<sup>+</sup>, CD90<sup>hi</sup>, CD44<sup>hi</sup> populations retain cardiovascular multipotency, as based on the expression of cardiac progenitor markers in this population [108]. These data indicate that thymosin  $\beta$ 4 in combination with MI can stimulate a cardiac progenitor cell type within the epicardium.

Cells with mesenchymal-like properties have been isolated and cultured from the adult mouse [109] and adult human heart [110], [111]. These cells, termed cardiac colony-forming units fibroblast (cCFU-F), originated from the epicardium, and were defined as mesenchymal stem cells because they showed clonogenic propagation, long-term growth for over 40 passages without senescence, and multi-lineage differentiation. Furthermore, these mesenchymal progenitors express mesenchymal cell markers including CD105, CD44, CD90, and the stem cell markers Oct4 and c-Myc. Additionally, they are MSC-like in their transcriptome profile [112]. Although cCFU-Fs express Sca-1 and PDGFR $\alpha$ , lineage tracing using the Nkx2.5<sup>Cre</sup> fate mapping mouse line suggested that they do not arise from the Nkx2.5 cardiac progenitor lineage [109].

A comparable cell culture population of mesenchymal-like EPDCs was isolated from the human epicardium. These spindle EPDCs (sEPDCs) are abundantly decorated with the mesenchymal stem cell markers CD44, CD90 and CD105, express the early cardiac transcription factor GATA-4 and show multi-lineage differentiation. When stimulated *in vitro* with TGF- $\beta$ , sEPDCs express proteins of the smooth muscle cell lineage and calcify when cultured in osteogenic medium [58]. Interestingly, while sEPDCs only express GATA-4, freshly isolated cCFU-Fs are also reported to express the early cardiac marker Nkx2.5. Furthermore, sEPDCs differentiate into the mesenchymal lineage, but cCFU-Fs have the additional ability to acquire an endothelial phenotype, which has not been convincingly established for EPDCs. sEPDCs and cCFU-Fs are therefore

very alike, but whether they are similar is not clear to date. Russell et al. isolated a population of notch-reporter positive cells, that were related to the epicardium. These cells were not only able to differentiate into fibroblasts, but under the right culture conditions formed cardiomyocytes [95]. Additionally, in vitro studies using VEGF-A on WT-1 positive isolated cells showed that these cell could be instructed to proliferate and become cardiovascular cell types [93].

Overall, epicardial cells and EPDCs appear to behave like multipotent progenitor cells in the embryo proper. However in the adult, it appears that this potential is not fully exploited yet, but can be enhanced by providing the right cues.

2

## 5. FUTURE PERSPECTIVES

In the embryo, the contribution of the epicardium to the formation of the heart is essential *via* the contribution of cardiac cell types as well as the production of growth factors and cytokines that influence myocardial growth [113] (Fig. 1). As we have described in this review, many of these abilities are retained in the adult injured heart but appear to occur less efficient compared to the embryo. Therefore, the question arises whether the epicardial response can be optimised to more efficiently partake in the repair of the injured heart.

Possible approaches include inducing proliferation and subsequent EMT of the epicardium. This would provide a larger pool of cells that has the ability to migrate into the heart (Fig. 2, left). This method appears to be feasible based on the finding that thymosin  $\beta$ 4 treatment prior to MI increases the number of activated epicardial cells, and enhances cardiac function and differentiation into cardiac cell types [81]. Unfortunately, this treatment is only successful when applied prior to injury [92], making it difficult to imagine thymosin  $\beta$ 4 treatment as a clinical approach. Promising results came from applying modRNA for VEGF-A which resulted in an increase in the proliferation and migration of epicardial cells and direct their differentiation capacity into endothelial as well as cardiomyocytes. Importantly, this approach increased cardiac function post-injury [93]. Identifying the most potent activators of the epicardium will therefore be an important goal to pursue.

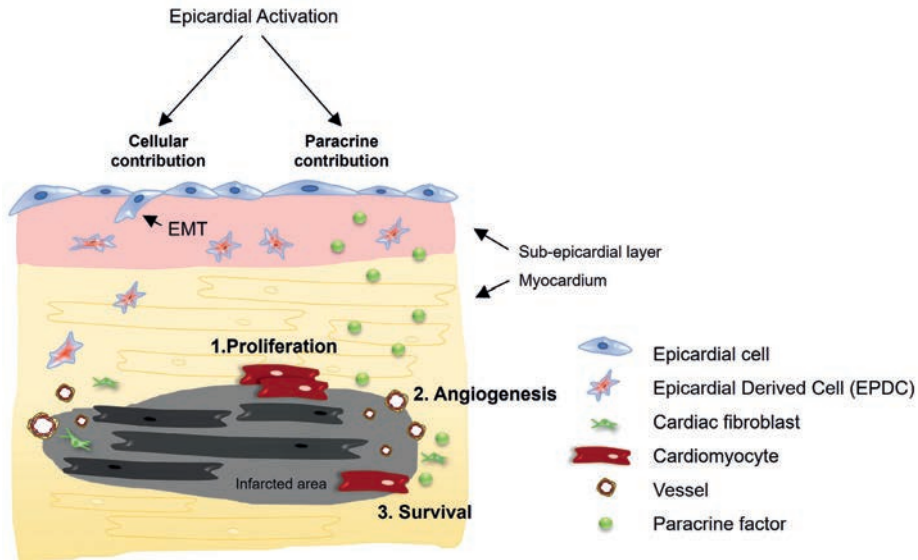


**Fig. 2 | Potential mechanisms of epicardial-derived contribution to cardiac repair.** Activated epicardial cells can have a direct cellular contribution to cardiac regeneration as epicardial cells undergo EMT, migrate into the myocardium and differentiate towards cardiac cells, such as cardiac fibroblasts, smooth muscle cells and potentially other cell types. A second epicardial contribution to cardiac repair acts via paracrine signalling, inducing (1) proliferation of cardiomyocytes, (2) angiogenesis and (3) survival of cardiomyocytes in the infarcted area.

Since the contribution of the epicardium is optimal during cardiac development, a potentially interesting method is to explore the embryonic or foetal epicardium as a paradigm to optimise the adult post-injury response. We have recently developed a cell culture system to efficiently isolate human foetal as well as adult epicardial cells, and culture them in their epithelial-like state [91]. This culture model allows direct comparison between these two cell sources. We have observed that EMT occurs spontaneously in foetal EPDCs, while adult cells require stimulation by TGF $\beta$  [91]. Identifying the differences in signalling pathways and receptor levels between foetal and adult EPDCs may help us understand how to unlock the full potential of the adult epicardial post-injury response.

Furthermore, it is important to explore the paracrine properties of the epicardial cells in more detail (Fig. 2, right). Zhou et al. showed that the epicardium can produce pro-angiogenic factors which positively influence the functional outcome post-MI [82]. A similar effect was observed by Winter et al. [99] where the transplantation of human EPDCs into the infarcted mouse heart resulted in increased vascularisation without

direct differentiation of the donor cells [99]. A more specific approach was used by Wei and colleagues [101], where the epicardial derived cytokine follistatin-like 1 was identified as a potent stimulator of cardiomyocyte proliferation [101]. A patch containing cells or growth factors can also be used to stimulate the epicardial layer directly. When loading a PCL/gelatine patch with MSCs, a beneficial effect was observed on the myocardium, but also induced proliferation and migration of the endogenous epicardial cells, thereby achieving a double effect on cardiac repair [114]. We envision that the foetal epicardium can again serve as a template to understand the optimal cocktail of growth factors and cytokines to achieve a maximal effect on the adult injured heart.

To summarize, several strategies are available to unlock the full potential of the epicardium as an endogenous cardiac progenitor cell source (Fig. 2). To which extend this will impact cardiac function after injury is part of future investigations.

## REFERENCES

- [1] E.J. Benjamin, F.J. Michael Blaha, M.E. Stephanie Chiuve, S. Mary Cushman, F.R. Sandeep Das, F. Rajat Deo, M.D. Sarah de Ferranti, M. James Floyd, M. Myriam Fornage, F. Cathleen Gillespie, M.R. Carmen Isasi, F.C. Monik Jiménez, S. Lori Chaffin Jordan, S.E. Judd, D. Lackland, F.H. Judith Lichtman, F. Lynda Lisabeth, F. Simin Liu, F.T. Chris Longenecker, R.H. Mackey, F. Kunihiro Matsushita, F. Dariush Mozaffarian, F.E. Michael Mussolino, F. Khurram Nasir, F.W. Robert Neumar, F. Latha Palaniappan, F.K. Dilip Pandey, F.R. Ravi Thiagarajan, M.J. Mathew Reeves, M. Ritchey, M.J. Carlos Rodriguez, F.A. Gregory Roth, M.D. Wayne Rosamond, F. Comilla Sasson, F. Amytis Towfighi, C.W. Tsao, M.B. Melanie Turner, M.S. Salim Virani, F.H. Jenifer Voeks, J.Z. Willey, M.T. John Wilkins, J.H. Wu, F.M. Heather Alger, S.S. Wong, F. Paul Muntner, AHA STATISTICAL UPDATE WRITING GROUP MEMBERS Heart Disease and Stroke Statistics—2017 Update A Report From the American Heart Association, *Circulation*. (2017). doi:10.1161/CIR.0000000000000485.
- [2] D. Vanhoutte, M. Schellings, Y. Pinto, S. Heymans, Relevance of matrix metalloproteinases and their inhibitors after myocardial infarction: A temporal and spatial window, *Cardiovasc. Res.* 69 (2006) 604–613. doi:10.1016/j.cardiores.2005.10.002.
- [3] S.E. Senyo, M.L. Steinhauser, C.L. Pizzimenti, V.K. Yang, L. Cai, M. Wang, T. Wu, C.P. Lechene, R.T. Lee, Mammalian heart renewal by pre-existing cardiomyocytes, *Nature*. 493 (2013) 433–436. doi:10.1038/nature11682.
- [4] R. Madonna, L.W. Van Laake, S.M. Davidson, F.B. Engel, D.J. Hausenloy, S. Lecour, J. Leor, C. Perrino, R. Schulz, K. Ytrehus, U. Landmesser, C.L. Mummery, S. Janssens, J. Willerson, T. Eschenhagen, P. Ferdinandy, J.P.G. Sluijter, Position Paper of the European Society of Cardiology Working Group Cellular Biology of the Heart: cell-based therapies for myocardial repair and regeneration in ischemic heart disease and heart failure., *Eur. Heart J.* 37 (2016) 1789–98. doi:10.1093/eurheartj/ehw113.
- [5] P.K. Nguyen, J.-W. Rhee, J.C. Wu, Adult Stem Cell Therapy and Heart Failure, 2000 to 2016: A Systematic Review., *JAMA Cardiol.* 1 (2016) 831–841. doi:10.1001/jamacardio.2016.2225.
- [6] M.-J. Goumans, J.A. Maring, A.M. Smits, A straightforward guide to the basic science behind cardiovascular cell-based therapies, *Heart*. 100 (2014) 1153–1157. doi:10.1136/heartjnl-2014-305646.
- [7] A.M. Smits, L.W. Van Laake, K. Den Ouden, C. Schreurs, K. Szuhai, C.J. Van Echteld, C.L. Mummery, P.A. Doevendans, M.-J. Goumans, Human cardiomyocyte progenitor cell transplantation preserves long-term function of the infarcted mouse myocardium, *Cardiovasc. Res.* 83 (2009). doi:10.1093/cvr/cvp146.
- [8] C. Bearzi, M. Rota, T. Hosoda, J. Tillmanns, A. Nascimbene, A. De Angelis, S. Yasuzawa-Amano, I. Trofimova, R.W. Siggins, N. Lecapitaine, S. Cascapera, A.P. Beltrami, D. a D'Alessandro, E. Zias, F. Quaini, K. Urbanek, R.E. Michler, R. Bolli, J. Kajstura, A. Leri, P. Anversa, Human cardiac stem cells., *Proc. Natl. Acad. Sci. U. S. A.* 104 (2007) 14068–14073. doi:10.1073/pnas.0706760104.

- [9] R.R. Smith, L. Barile, H.C. Cho, M.K. Leppo, J.M. Hare, E. Messina, A. Giacomello, M.R. Abraham, E. Marbán, Regenerative potential of cardiosphere-derived cells expanded from percutaneous endomyocardial biopsy specimens, *Circulation*. 115 (2007) 896–908. doi:10.1161/CIRCULATIONAHA.106.655209.
- [10] H. Oh, S.B. Bradfute, T.D. Gallardo, T. Nakamura, V. Gaussin, Y. Mishina, J. Pocius, L.H. Michael, R.R. Behringer, D.J. Garry, M.L. Entman, M.D. Schneider, Cardiac progenitor cells from adult myocardium: homing, differentiation, and fusion after infarction., *Proc. Natl. Acad. Sci. U. S. A.* 100 (2003) 12313–8. doi:10.1073/pnas.2132126100.
- [11] A.P. Beltrami, L. Barlucchi, D. Torella, M. Baker, F. Limana, S. Chimenti, H. Kasahara, M. Rota, E. Musso, K. Urbanek, A. Leri, J. Kajstura, B. Nadal-Ginard, P. Anversa, Adult cardiac stem cells are multipotent and support myocardial regeneration, *Cell*. 114 (2003) 763–776. doi:10.1016/S0092-8674(03)00687-1.
- [12] P.P. Zwetsloot, A. Maria, D. Végh, S. Johanna, G.P.J. Van Hout, G.L. Currie, E.S. Sena, H. Gremmels, J.W. Buikema, M. Goumans, M.R. Macleod, P.A. Doevendans, S.A.J. Chamuleau, J.P.G. Sluijter, Integrative Physiology Cardiac Stem Cell Treatment in Myocardial Infarction A Systematic Review and Meta-Analysis of Preclinical Studies, (2016). doi:10.1161/CIRCRESAHA.115.307676.
- [13] J. Schlueter, T. Brand, Origin and fates of the proepicardium, *Aswan Hear. Cent. Sci. Pract. Ser.* 2011 (2011) 11. doi:10.5339/ahcsp.2011.11.
- [14] Y. Ishii, J.D. Langberg, R. Hurtado, S. Lee, T. Mikawa, Induction of proepicardial marker gene expression by the liver bud., *Development*. 134 (2007) 3627–37. doi:10.1242/dev.005280.
- [15] L. Maya-Ramos, J. Cleland, M. Bressan, T. Mikawa, Induction of the Proepicardium., *J. Dev. Biol.* 1 (2013) 82–91. doi:10.3390/jdb1020082.
- [16] M. Bressan, G. Liu, T. Mikawa, Early Mesodermal Cues Assign Avian Cardiac Pacemaker Fate Potential in a Tertiary Heart Field, *Science (80-. )*. 340 (2013) 744–748. doi:10.1126/science.1232877.
- [17] S. Cossette, R. Misra, The identification of different endothelial cell populations within the mouse proepicardium., *Dev. Dyn.* 240 (2011) 2344–2353. doi:10.1002/dvdy.22724.
- [18] B. Zhou, A. von Gise, Q. Ma, J. Rivera-Feliciano, W.T. Pu, Nkx2-5- and Isl1-expressing cardiac progenitors contribute to proepicardium, *Biochem. Biophys. Res. Commun.* 375 (2008) 450–453. doi:10.1016/j.bbrc.2008.08.044.
- [19] S.N. Duim, M.-J. Goumans, B.P.T. Kruithof, WT1 in Cardiac Development and Disease, 2016. doi:10.15586/codon.wt.2016.ch13.
- [20] J. Manner, J. Schlueter, T. Brand, Experimental analyses of the function of the proepicardium using a new microsurgical procedure to induce loss-of-proepicardial-function in chick embryos, *Dev. Dyn.* 233 (2005) 1454–1463. doi:10.1002/dvdy.20487.
- [21] T.C. Katz, M.K. Singh, K. Degenhardt, J. Rivera-Feliciano, R.L. Johnson, J.A. Epstein, C.J. Tabin, Distinct Compartments of the Proepicardial Organ Give Rise to Coronary Vascular Endothelial Cells, *Dev. Cell*. 22 (2012) 639–650. doi:10.1016/j.devcel.2012.01.012.

- [22] P.C. Nahirney, T. Mikawa, D.A. Fischman, Evidence for an extracellular matrix bridge guiding proepicardial cell migration to the myocardium of chick embryos, *Dev. Dyn.* 227 (2003) 511–523. doi:10.1002/dvdy.10335.
- [23] L.S. Rodgers, S. Lalani, R.B. Runyan, T.D. Camenisch, Differential growth and multicellular villi direct proepicardial translocation to the developing mouse heart, *Dev. Dyn.* 237 (2008) 145–152. doi:10.1002/dvdy.21378.
- [24] T. Hirose, M. Karasawa, Y. Sugitani, M. Fujisawa, K. Akimoto, S. Ohni, T. Noda, PAR3 is essential for cyst-mediated epicardial development by establishing apical cortical domains, *Development.* 133 (2006) 1389–1398. doi:10.1242/dev.02294.
- [25] J. Li, Y. Liu, Y. Jin, R. Wang, J. Wang, S. Lu, V. VanBuren, D.E. Dostal, S.L. Zhang, X. Peng, Essential role of Cdc42 in cardiomyocyte proliferation and cell-cell adhesion during heart development, *Dev. Biol.* 421 (2017) 271–283. doi:10.1016/j.ydbio.2016.12.012.
- [26] R. Vicente-Steijn, R.W.C. Scherptong, B.P.T. Kruithof, S.N. Duim, M.J.T.H. Goumans, L.J. Wisse, B. Zhou, W.T. Pu, R.E. Poelmann, M.J. Schalij, M.D. Tallquist, A.C. Gittenberger-de Groot, M.R. Jongbloed, Regional differences in WT-1 and Tcf21 expression during ventricular development: implications for myocardial compaction, *PLoS One.* 10 (2015) e0136025. doi:10.1371/journal.pone.0136025.
- [27] A.C. Gittenberger-de Groot, M.P. Vrancken Peeters, M. Bergwerff, M.M. Mentink, R.E. Poelmann, Epicardial outgrowth inhibition leads to compensatory mesothelial outflow tract collar and abnormal cardiac septation and coronary formation., *Circ. Res.* 87 (2000) 969–971. doi:10.1161/01.RES.87.11.969.
- [28] N.A.M. Bax, H. Lie-Venema, R. Vicente-Steijn, S.B. Bleyl, N.M.S. Van Den Akker, S. Maas, R.E. Poelmann, A.C. Gittenberger-de Groot, Platelet-derived growth factor is involved in the differentiation of second heart field-derived cardiac structures in chicken embryos, *Dev. Dyn.* 238 (2009) 2658–2669. doi:10.1002/dvdy.22073.
- [29] E.A.F. Mahtab, M.C.E.F. Wijffels, N.M.S. Van Den Akker, N.D. Hahurij, H. Lie-Venema, L.J. Wisse, M.C. DeRuiter, P. Uhrin, J. Zaujec, B.R. Binder, M.J. Schalij, R.E. Poelmann, A.C. Gittenberger-De Groot, Cardiac malformations and myocardial abnormalities in Podoplanin knockout mouse embryos: Correlation with abnormal epicardial development, *Dev. Dyn.* 237 (2008) 847–857. doi:10.1002/dvdy.21463.
- [30] A. Weeke-Klump, N.A.M. Bax, A.R. Bellu, E.M. Winter, J. Vrolijk, J. Plantinga, S. Maas, M. Brinker, E.A.F. Mahtab, A.C. Gittenberger-de Groot, M.J.A. van Luyn, M.C. Harmsen, H. Lie-Venema, Epicardium-derived cells enhance proliferation, cellular maturation and alignment of cardiomyocytes, *J. Mol. Cell. Cardiol.* 49 (2010) 606–616. doi:10.1016/j.yjmcc.2010.07.007.
- [31] I. Eralp, H. Lie-Venema, M.C. DeRuiter, N.M.S. van den Akker, A.J.J.C. Bogers, M.M.T. Mentink, R.E. Poelmann, A.C. Gittenberger-de Groot, Coronary artery and orifice development is associated with proper timing of epicardial outgrowth and correlated Fas-ligand-associated apoptosis patterns., *Circ. Res.* 96 (2005) 526–34. doi:10.1161/01.RES.0000158965.34647.4e.
- [32] E. Cano, R. Carmona, A. Ruiz-Villalba, A. Rojas, Y.-Y. Chau, K.D. Wagner, N. Wagner, N.D. Hastie, R. Muñoz-Chápuli, J.M. Pérez-Pomares, Extracardiac septum transversum/proepicardial endothelial cells pattern embryonic coronary arterio-venous connections, *Proc. Natl. Acad. Sci.* 113 (2016) 656–661. doi:10.1073/pnas.1509834113.

- [33] T.P. Kelder, S.N. Duim, R. Vicente-Steijn, A.M.D. V?gh, B.P.T. Kruihof, A.M. Smits, T.C. van Bavel, N.A.M. Bax, M.J. Schalij, A.C. Gittenberger-de Groot, M.C. DeRuiter, M.-J. Goumans, M.R.M. Jongbloed, The epicardium as modulator of the cardiac autonomic response during early development, *J. Mol. Cell. Cardiol.* 89 (2015). doi:10.1016/j.yjmcc.2015.10.025.
- [34] S.N. Duim, A.M. Smits, B.P.T. Kruihof, M. Goumans, The roadmap of WT1 protein expression in the human fetal heart, *J. Mol. Cell. Cardiol.* 90 (2016) 139–145. doi:10.1016/j.yjmcc.2015.12.008.
- [35] C.A. Risebro, J.M. Vieira, L. Klotz, P.R. Riley, Characterisation of the human embryonic and foetal epicardium during heart development, *Development.* 142 (2015) 3630–3636. doi:10.1242/dev.127621.
- [36] B. Zhou, Q. Ma, S. Rajagopal, S.M. Wu, I. Domian, J. Rivera-Feliciano, D. Jiang, A. von Gise, S. Ikeda, K.R. Chien, W.T. Pu, Epicardial progenitors contribute to the cardiomyocyte lineage in the developing heart., *Nature.* 454 (2008) 109–13. doi:10.1038/nature07060.
- [37] C.-L. Cai, J.C. Martin, Y. Sun, L. Cui, L. Wang, K. Ouyang, L. Yang, L. Bu, X. Liang, X. Zhang, W.B. Stallcup, C.P. Denton, A. McCulloch, J. Chen, S.M. Evans, A myocardial lineage derives from Tbx18 epicardial cells., *Nature.* 454 (2008) 104–108. doi:10.1038/nature06969.
- [38] K. Kikuchi, V. Gupta, J. Wang, J.E. Holdway, A.A. Wills, Y. Fang, K.D. Poss, tcf21+ epicardial cells adopt non-myocardial fates during zebrafish heart development and regeneration., *Development.* 138 (2011) 2895–2902. doi:10.1242/dev.067041.
- [39] C. MacNeill, R. French, T. Evans, A. Wessels, J.B. Burch, Modular regulation of cGATA-5 gene expression in the developing heart and gut, *Dev. Biol.* 217 (2000) 62–76. doi:10.1006/dbio.2000.9806.
- [40] M.P.F.M. Vrancken Peeters, M.M.T. Mentink, R.E. Poelmann, A.C. Gittenberger-de Groot, Cytokeratins as a marker for epicardial formation in the quail embryo, *Anat. Embryol. (Berl.)* 191 (1995) 503–508. doi:10.1007/BF00186740.
- [41] G.M. Balmer, S. Bollini, K.N. Dubé, J.P. Martinez-Barbera, O. Williams, P.R. Riley, Dynamic haematopoietic cell contribution to the developing and adult epicardium., *Nat. Commun.* 5 (2014) 4054. doi:10.1038/ncomms5054.
- [42] A. Von Gise, W.T. Pu, Endocardial and epicardial epithelial to mesenchymal transitions in heart development and disease, *Circ. Res.* 110 (2012) 1628–1645. doi:10.1161/CIRCRESAHA.111.259960.
- [43] R. Carmona, M. González-Iriarte, J.M. Pérez-Pomares, R. Muñoz-Chápuli, Localization of the Wilms' tumour protein WT1 in avian embryos, *Cell Tissue Res.* 303 (2001) 173–186. doi:10.1007/s004410000307.
- [44] A.F. Austin, L.A. Compton, J.D. Love, C.B. Brown, J. V Barnett, Primary and immortalized mouse epicardial cells undergo differentiation in response to TGFbeta., *Dev. Dyn.* 237 (2008) 366–376. doi:10.1002/dvdy.21421.
- [45] A.M. Mellgren, C.L. Smith, G.S. Olsen, B. Eskiocak, B. Zhou, M.N. Kazi, F.R. Ruiz, W.T. Pu, M.D. Tallquist, Platelet-derived growth factor receptor beta signaling is required for efficient epicardial cell migration and development of two distinct coronary vascular smooth muscle cell populations, *Circ Res.* 103 (2008) 1393–1401. doi:10.1161/CIRCRESAHA.108.176768.

- [46] D.J. Pennisi, T. Mikawa, FGFR-1 is required by epicardium-derived cells for myocardial invasion and correct coronary vascular lineage differentiation., *Dev. Biol.* 328 (2009) 148–159. doi:10.1016/j.ydbio.2009.01.023.
- [47] O.M. Martínez-Estrada, L. a Lettice, A. Essafi, J.A. Guadix, J. Slight, V. Velecela, E. Hall, J. Reichmann, P.S. Devenney, P. Hohenstein, N. Hosen, R.E. Hill, R. Muñoz-Chapuli, N.D. Hastie, Wt1 is required for cardiovascular progenitor cell formation through transcriptional control of Snail and E-cadherin., *Nat. Genet.* 42 (2010) 89–93. doi:10.1038/ng.494.
- [48] A. von Gise, B. Zhou, L.B. Honor, Q. Ma, A. Petryk, W.T. Pu, WT1 regulates epicardial epithelial to mesenchymal transition through beta-catenin and retinoic acid signaling pathways, *Dev Biol.* 356 (2011) 421–431. doi:S0012-1606(11)00983-3 [pii]10.1016/j.ydbio.2011.05.668.
- [49] S.T. Baek, M.D. Tallquist, Nf1 limits epicardial derivative expansion by regulating epithelial to mesenchymal transition and proliferation., *Development.* 139 (2012) 2040–2049. doi:10.1242/dev.074054.
- [50] A. Acharya, S.T. Baek, G. Huang, B. Eskiocak, S. Goetsch, C.Y. Sung, S. Banfi, M.F. Sauer, G.S. Olsen, J.S. Duffield, E.N. Olson, M.D. Tallquist, The bHLH transcription factor Tcf21 is required for lineage-specific EMT of cardiac fibroblast progenitors, *Development.* 139 (2012) 2139–2149. doi:10.1242/dev.079970.
- [51] M.D. Combs, C.M. Braitsch, A.W. Lange, J.F. James, K.E. Yutzey, NFATC1 promotes epicardium-derived cell invasion into myocardium., *Development.* 138 (2011) 1747–1757. doi:10.1242/dev.060996.
- [52] M. a Trembley, L.S. Velasquez, K.L. de Mesy Bentley, E.M. Small, Myocardin-related transcription factors control the motility of epicardium-derived cells and the maturation of coronary vessels., *Development.* 142 (2015) 21–30. doi:10.1242/dev.116418.
- [53] A.C.G. Gittenberger-de Groot, E.M. Winter, R.E. Poelmann, Epicardium-derived cells (EPDCs) in development, cardiac disease and repair of ischemia, *J. Cell. Mol. Med.* 14 (2010) 1056–1060. doi:10.1111/j.1582-4934.2010.01077.x.
- [54] A. Wessels, M.J.B. van den Hoff, R.F. Adamo, A.L. Phelps, M.M. Lockhart, K. Sauls, L.E. Briggs, R.A. Norris, B. van Wijk, J.M. Pérez-Pomares, R.W. Dettman, J.B.E. Burch, Epicardially derived fibroblasts preferentially contribute to the parietal leaflets of the atrioventricular valves in the murine heart., *Dev. Biol.* 366 (2012) 111–124. doi:10.1016/j.ydbio.2012.04.020.
- [55] V.M. Christoffels, T. Grieskamp, J. Norden, M.T.M. Mommersteeg, C. Rudat, A. Kispert, Tbx18 and the fate of epicardial progenitors., *Nature.* 458 (2009) E8–9–10. doi:10.1038/nature07916.
- [56] S.N. Duim, K. Kurakula, M.J. Goumans, B.P.T. Kruithof, Cardiac endothelial cells express Wilms' tumor-1. Wt1 expression in the developing, adult and infarcted heart., *J. Mol. Cell. Cardiol.* 81 (2015) 127–135. doi:10.1016/j.yjmcc.2015.02.007.
- [57] N.A.M. Bax, A.A.M. van Oorschot, S. Maas, J. Braun, J. van Tuyn, A.A.F. de Vries, A.C.. Gittenberger-de Groot, M.-J. Goumans, In vitro epithelial-to-mesenchymal transformation in human adult epicardial cells is regulated by TGF $\beta$ -signaling and WT1., *Basic Res. Cardiol.* 106 (2011) 829–47. doi:10.1007/s00395-011-0181-0.

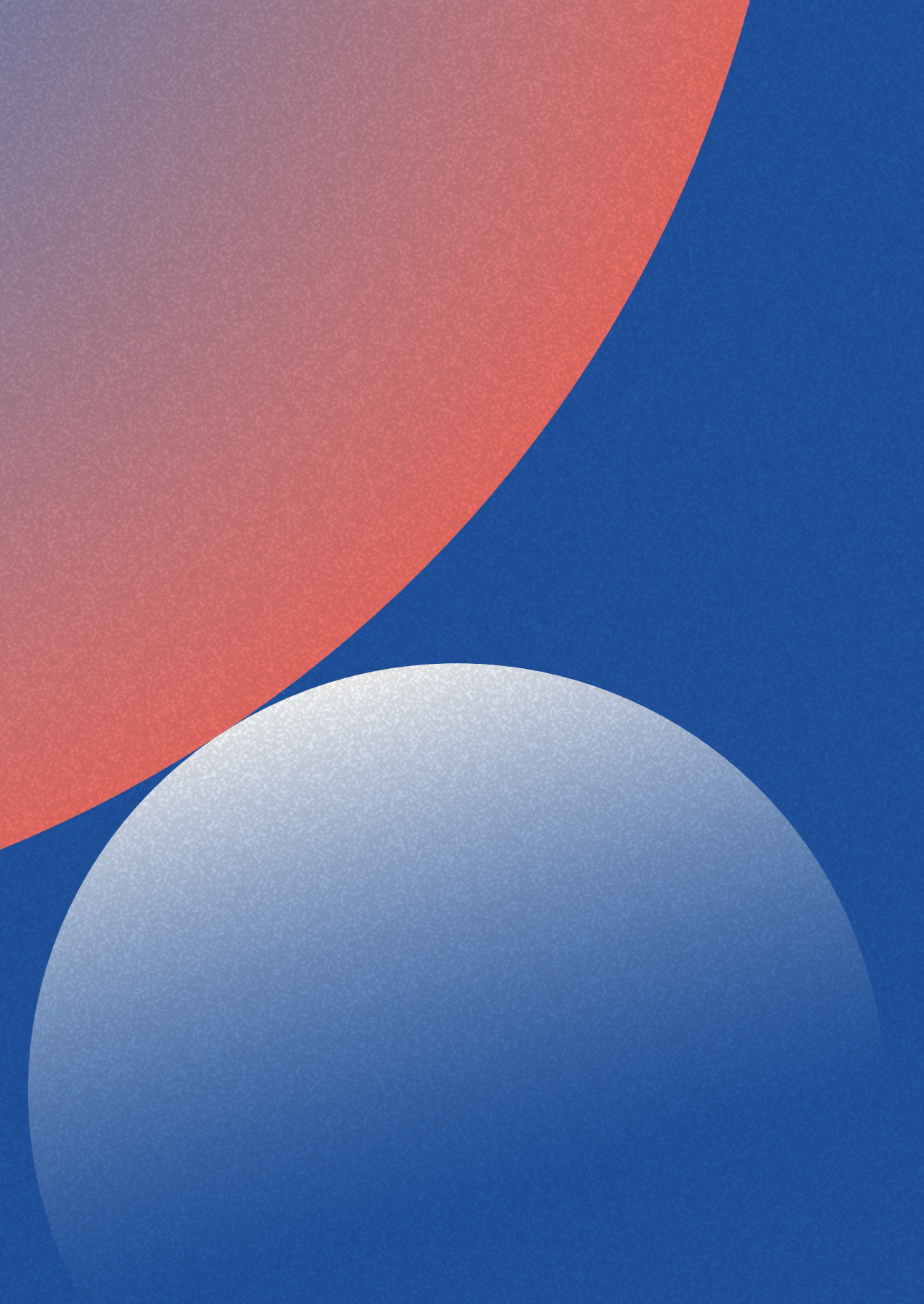
- [58] J. van Tuyn, D.E. Atsma, E.M. Winter, I. van der Velde-van Dijke, D.A. Pijnappels, N.A.M. Bax, S. Knaän-Shanzer, A.C. Gittenberger-de Groot, R.E. Poelmann, A. van der Laarse, E.E. van der Wall, M.J. Schalij, A.A.F. de Vries, Epicardial cells of human adults can undergo an epithelial-to-mesenchymal transition and obtain characteristics of smooth muscle cells in vitro., *Stem Cells*. 25 (2007) 271–278. doi:10.1634/stemcells.2006-0366.
- [59] N. Smart, C. a Risebro, A. a D. Melville, K. Moses, R.J. Schwartz, K.R. Chien, P.R. Riley, Thy-mosin beta4 induces adult epicardial progenitor mobilization and neovascularization., *Nature*. 445 (2007) 177–182. doi:10.1038/nature05383.
- [60] A.C. Gittenberger-de Groot, M.P. Vrancken Peeters, M.M. Mentink, R.G. Gourdie, R.E. Poelmann, Epicardium-derived cells contribute a novel population to the myocardial wall and the atrioventricular cushions., *Circ. Res.* 82 (1998) 1043–1052. doi:10.1161/01.RES.82.10.1043.
- [61] T. Mikawa, R.G. Gourdie, Pericardial Mesoderm Generates a Population of Coronary Smooth Muscle Cells Migrating into the Heart along with Ingrowth of the Epicardial Organ, *Dev. Biol.* 174 (1996) 221–232. doi:10.1006/dbio.1996.0068.
- [62] J.-M. Pérez-Pomares, R. Carmona, M. González-Iriarte, G. Atencia, A. Wessels, R. Muñoz-Chá-puli, Origin of coronary endothelial cells from epicardial mesothelium in avian embryos., *Int. J. Dev. Biol.* 46 (2002) 1005–13. doi:10.1387/IJDB.12533024.
- [63] X. Tian, W.T. Pu, B. Zhou, Cellular Origin and Developmental Program of Coronary Angiogenesis, *Circ. Res.* 116 (2015). <http://circres.ahajournals.org/content/116/3/515.long> (accessed June 2, 2017).
- [64] T. Grieskamp, C. Rudat, T.H.-W. Ludtke, J. Norden, A. Kispert, Notch Signaling Regulates Smooth Muscle Differentiation of Epicardium-Derived Cells, *Circ. Res.* 108 (2011) 813–823. doi:10.1161/CIRCRESAHA.110.228809.
- [65] Q. Liu, H. Zhang, X. Tian, L. He, X. Huang, Z. Tan, Y. Yan, S.M. Evans, J.D. Wythe, B. Zhou, Smooth muscle origin of postnatal 2nd CVP is pre-determined in early embryo, *Biochem. Biophys. Res. Commun.* 471 (2016) 430–436. doi:10.1016/j.bbrc.2016.02.062.
- [66] R.E. Poelmann, A.C. Gittenberger-de Groot, M.M. Mentink, R. Bökenkamp, B. Hogers, Development of the cardiac coronary vascular endothelium, studied with antiendothelial antibodies, in chicken-quail chimeras., *Circ. Res.* 73 (1993) 559–68. doi:10.1161/01.RES.73.3.559.
- [67] C. Rudat, A. Kispert, Wt1 and epicardial fate mapping, *Circ. Res.* 111 (2012) 165–169. doi:10.1161/CIRCRESAHA.112.273946.
- [68] K. Red-Horse, H. Ueno, I.L. Weissman, M. a Krasnow, Coronary arteries form by developmental reprogramming of venous cells., *Nature*. 464 (2010) 549–553. doi:10.1038/nature08873.
- [69] T.H.P. Chen, T.-C. Chang, J.-O. Kang, B. Choudhary, T. Makita, C.M. Tran, J.B.E. Burch, H. Eid, H.M. Sucov, Epicardial induction of fetal cardiomyocyte proliferation via a retinoic acid-inducible trophic factor., *Dev. Biol.* 250 (2002) 198–207. <http://www.ncbi.nlm.nih.gov/pubmed/12297106> (accessed March 22, 2017).

- [70] D.J. Pennisi, V.L.T. Ballard, T. Mikawa, Epicardium is required for the full rate of myocyte proliferation and levels of expression of myocyte mitogenic factors FGF2 and its receptor, FGFR-1, but not for transmural myocardial patterning in the embryonic chick heart, *Dev. Dyn.* 228 (2003) 161–172. doi:10.1002/dvdy.10360.
- [71] I. Stuckmann, S. Evans, A.B. Lassar, Erythropoietin and retinoic acid, secreted from the epicardium, are required for cardiac myocyte proliferation., *Dev. Biol.* 255 (2003) 334–49. <http://www.ncbi.nlm.nih.gov/pubmed/12648494> (accessed March 22, 2017).
- [72] H.E. Olivey, E.C. Svensson, Epicardial-myocardial signaling directing coronary vasculogenesis., *Circ. Res.* 106 (2010) 818–832. doi:10.1161/CIRCRESAHA.109.209197.
- [73] A. Wessels, J.M. Pérez-Pomares, The epicardium and epicardially derived cells (EPDCs) as cardiac stem cells, *Anat. Rec. Part A Discov. Mol. Cell. Evol. Biol.* 276A (2004) 43–57. doi:10.1002/ar.a.10129.
- [74] K.D. Kolander, M.L. Holtz, S.M. Cossette, S.A. Duncan, R.P. Misra, Epicardial GATA factors regulate early coronary vascular plexus formation., *Dev. Biol.* 386 (2014) 204–215. doi:10.1016/j.ydbio.2013.12.033.
- [75] H.M. Sucov, E. Dyson, C.L. Gumeringer, J. Price, K.R. Chien, R.M. Evans, RXR $\alpha$  mutant mice establish a genetic basis for vitamin A signaling in heart morphogenesis, *Genes Dev.* (1994). doi:10.1101/gad.8.9.1007.
- [76] E. Merki, M. Zamora, A. Raya, Y. Kawakami, J. Wang, X. Zhang, J. Burch, S.W. Kubalak, P. Kaliman, J.C. Izpisua Belmonte, K.R. Chien, P. Ruiz-Lozano, Epicardial retinoid X receptor alpha is required for myocardial growth and coronary artery formation., *Proc. Natl. Acad. Sci. U. S. A.* 102 (2005) 18455–18460. doi:10.1073/pnas.0504343102.
- [77] K.J. Lavine, K. Yu, A.C. White, X. Zhang, C. Smith, J. Partanen, D.M. Ornitz, Endocardial and epicardial derived FGF signals regulate myocardial proliferation and differentiation in vivo., *Dev. Cell.* 8 (2005) 85–95. doi:10.1016/j.devcel.2004.12.002.
- [78] K.J. Lavine, A.C. White, C. Park, C.S. Smith, K. Choi, F. Long, C.C. Hui, D.M. Ornitz, Fibroblast growth factor signals regulate a wave of Hedgehog activation that is essential for coronary vascular development, *Genes Dev.* (2006). doi:10.1101/gad.1411406.
- [79] K.J. Lavine, D.M. Ornitz, Fibroblast growth factors and Hedgehogs: at the heart of the epicardial signaling center, *Trends Genet.* 24 (2008) 33–40. doi:10.1016/j.tig.2007.10.007.
- [80] S. Cavallero, H. Shen, C. Yi, C.-L. Lien, S.R. Kumar, H.M. Sucov, CXCL12 Signaling Is Essential for Maturation of the Ventricular Coronary Endothelial Plexus and Establishment of Functional Coronary Circulation., *Dev. Cell.* 33 (2015) 469–77. doi:10.1016/j.devcel.2015.03.018.
- [81] N. Smart, S. Bollini, K.N. Dubé, J.M. Vieira, B. Zhou, S. Davidson, D. Yellon, J. Riegler, A.N. Price, M.F. Lythgoe, W.T. Pu, P.R. Riley, De novo cardiomyocytes from within the activated adult heart after injury., *Nature.* 474 (2011) 640–644. doi:10.1038/nature10188.
- [82] B. Zhou, L.B. Honor, H. He, Q. Ma, J. Oh, C. Butterfield, R. Lin, J.M. Melero-martin, E. Dumatova, H.S. Duffy, A. Von Gise, P. Zhou, Y.W. Hu, G. Wang, B. Zhang, L. Wang, J.L. Hall, M. a Moses, F.X. McGowan, W.T. Pu, Adult mouse epicardium modulates myocardial injury by secreting paracrine factors, *J. Clin. Invest.* 121 (2011). doi:10.1172/JCI45529DS1.

- [83] A. Smits, P. Riley, Epicardium-Derived Heart Repair, *J. Dev. Biol.* 2 (2014) 84–100. doi:10.3390/jdb2020084.
- [84] F. Limana, C. Bertolami, A. Mangoni, A. Di Carlo, D. Avitabile, D. Mocini, P. Iannelli, R. De Mori, C. Marchetti, O. Pozzoli, C. Gentili, A. Zacheo, A. Germani, M.C. Capogrossi, Myocardial infarction induces embryonic reprogramming of epicardial c-kit<sup>+</sup> cells: Role of the pericardial fluid, *J. Mol. Cell. Cardiol.* 48 (2010) 609–618. doi:10.1016/j.yjmcc.2009.11.008.
- [85] G.N. Huang, J.E. Thatcher, J. McAnally, Y. Kong, X. Qi, W. Tan, J.M. DiMaio, J.F. Amatruda, R.D. Gerard, J.A. Hill, R. Bassel-Duby, E.N. Olson, C/EBP Transcription Factors Mediate Epicardial Activation During Heart Development and Injury, *Science*. 338 (2012) 1599–1603. doi:10.1126/science.1229765.
- [86] E. Foglio, G. Puddighinu, P. Fasanaro, D. D'Arcangelo, G.A. Perrone, D. Mocini, C. Campanella, L. Coppola, M. Logozzi, T. Azzarito, F. Marzoli, S. Fais, L. Pieroni, V. Marzano, A. Germani, M.C. Capogrossi, M.A. Russo, F. Limana, Exosomal clusterin, identified in the pericardial fluid, improves myocardial performance following MI through epicardial activation, enhanced arteriogenesis and reduced apoptosis, *Int. J. Cardiol.* 197 (2015) 333–347. doi:10.1016/j.ijcard.2015.06.008.
- [87] T. Moore-morris, N. Guimarães-camboa, I. Banerjee, A.C. Zambon, T. Kisseleva, A. Ve-layoudon, W.B. Stallcup, Y. Gu, N.D. Dalton, M. Cedenilla, R. Gomez-amaro, B. Zhou, D. a Brenner, K.L. Peterson, J. Chen, S.M. Evans, Resident fibroblast lineages mediate pressure overload – induced cardiac fibrosis, 124 (2014) 1–14. doi:10.1172/JCI74783.types.
- [88] B. van Wijk, Q.D. Gunst, A.F.M. Moorman, M.J.B. van den Hoff, Cardiac Regeneration from Activated Epicardium, *PLoS One*. 7 (2012). doi:10.1371/journal.pone.0044692.
- [89] C.M. Braitsch, O. Kanisicak, J.H. van Berlo, J.D. Molkentin, K.E. Yutzey, Differential expression of embryonic epicardial progenitor markers and localization of cardiac fibrosis in adult ischemic injury and hypertensive heart disease, *J. Mol. Cell. Cardiol.* 65 (2013) 108–119. doi:10.1016/j.yjmcc.2013.10.005.
- [90] J. Duan, C. Gherghe, D. Liu, E. Hamlett, L. Srikantha, L. Rodgers, J.N. Regan, M. Rojas, M. Willis, A. Leask, M. Majesky, A. Deb, Wnt1/ $\beta$ catenin injury response activates the epicardium and cardiac fibroblasts to promote cardiac repair, *EMBO J.* 31 (2011) 429–442. doi:10.1038/emboj.2011.418.
- [91] A.T. Moerkamp, K. Lodder, T. van Herwaarden, E. Dronkers, C.K.E. Dingenouts, F.C. Tengström, T.J. van Brakel, M.-J. Goumans, A.M. Smits, Human fetal and adult epicardial-derived cells: a novel model to study their activation, *Stem Cell Res. Ther.* 7 (2016) 1–12. doi:10.1186/s13287-016-0434-9.
- [92] B. Zhou, L.B. Honor, Q. Ma, J.H. Oh, R.Z. Lin, J.M. Melero-Martin, A. von Gise, P. Zhou, T. Hu, L. He, K.H. Wu, H. Zhang, Y. Zhang, W.T. Pu, Thymosin beta 4 treatment after myocardial infarction does not reprogram epicardial cells into cardiomyocytes, *J. Mol. Cell. Cardiol.* 52 (2012) 43–47. doi:10.1016/j.yjmcc.2011.08.020.
- [93] L. Zangi, K.O. Lui, A. von Gise, Q. Ma, W. Ebina, L.M. Ptaszek, D. Später, H. Xu, M. Taborbbar, R. Gorbato, B. Sena, M. Nahrendorf, D.M. Briscoe, R.A. Li, A.J. Wagers, D.J. Rossi, W.T. Pu, K.R. Chien, Modified mRNA directs the fate of heart progenitor cells and induces vascular regeneration after myocardial infarction, *Nat. Biotechnol.* 31 (2013) 898–907. doi:10.1038/nbt.2682.

- [94] F. Limana, A. Zacheo, D. Mocini, A. Mangoni, G. Borsellino, A. Diamantini, R. De Mori, L. Battistini, E. Vigna, M. Santini, V. Loiaconi, G. Pompilio, A. Germani, M.C. Capogrossi, Identification of myocardial and vascular precursor cells in human and mouse epicardium, *Circ. Res.* 101 (2007) 1255–1265. doi:10.1161/CIRCRESAHA.107.150755.
- [95] J.L. Russell, S.C. Goetsch, N.R. Gaiano, J.A. Hill, E.N. Olson, J.W. Schneider, A dynamic notch injury response activates epicardium and contributes to fibrosis repair, *Circ. Res.* 108 (2011) 51–59. doi:10.1161/CIRCRESAHA.110.233262.
- [96] C.A. Souders, S.L.K. Bowers, T.A. Baudino, Cardiac fibroblast: The renaissance cell, *Circ. Res.* (2009). doi:10.1161/CIRCRESAHA.109.209809.
- [97] N. Smart, C.A. Risebro, J.E. Clark, E. Ehler, L. Miquerol, A. Rossdeutsch, M.S. Marber, P.R. Riley, Thymosin beta4 facilitates epicardial neovascularization of the injured adult heart, in: *Ann. N. Y. Acad. Sci.*, 2010. doi:10.1111/j.1749-6632.2010.05478.x.
- [98] B. Zhou, W.T. Pu, Epicardial epithelial-to-mesenchymal transition in injured heart, *J. Cell. Mol. Med.* 15 (2011) 2781–2783. doi:10.1111/j.1582-4934.2011.01450.x.
- [99] E.M. Winter, R.W. Grauss, B. Hogers, J. Van Tuyn, R. Van Der Geest, H. Lie-Venema, R.V. Steijn, S. Maas, M.C. Deruiter, a. a F. Devries, P. Steendijk, P. a. Doevendans, a. Van Der Laarse, R.E. Poelmann, M.J. Schalij, D.E. Atsma, a. C. Gittenberger-De Groot, Preservation of left ventricular function and attenuation of remodeling after transplantation of human epicardium-derived cells into the infarcted mouse heart, *Circulation.* 116 (2007) 917–927. doi:10.1161/CIRCULATIONAHA.106.668178.
- [100] H. Eid, D.M. Larson, J.P. Springhorn, M.A. Attawia, R.C. Nayak, T.W. Smith, R.A. Kelly, Role of epicardial mesothelial cells in the modification of phenotype and function of adult rat ventricular myocytes in primary coculture., *Circ. Res.* 71 (1992) 40–50. <http://www.ncbi.nlm.nih.gov/pubmed/1606667> (accessed March 22, 2017).
- [101] K. Wei, V. Serpooshan, C. Hurtado, M. Diez-Cunado, M. Zhao, S. Maruyama, W. Zhu, G. Fajardo, M. Nosedá, K. Nakamura, X. Tian, Q. Liu, A. Wang, Y. Matsuura, P. Bushway, W. Cai, A. Savchenko, M. Mahmoudi, M.D. Schneider, M.J.B. van den Hoff, M.J. Butte, P.C. Yang, K. Walsh, B. Zhou, D. Bernstein, M. Mercola, P. Ruiz-Lozano, Epicardial FSTL1 reconstitution regenerates the adult mammalian heart., *Nature.* 525 (2015) 479–485. doi:10.1038/nature15372.
- [102] Y. Oshima, N. Ouchi, K. Sato, Y. Izumiya, D.R. Pimentel, K. Walsh, Follistatin-like 1 is an Akt-regulated cardioprotective factor that is secreted by the heart, *Circulation.* 117 (2008) 3099–3108. doi:10.1161/CIRCULATIONAHA.108.767673.
- [103] Y. Ogura, N. Ouchi, K. Ohashi, R. Shibata, Y. Kataoka, T. Kambara, T. Kito, S. Maruyama, D. Yuasa, K. Matsuo, T. Enomoto, Y. Uemura, M. Miyabe, M. Ishii, T. Yamamoto, Y. Shimizu, K. Walsh, T. Murohara, Therapeutic impact of follistatin-like 1 on myocardial ischemic injury in preclinical models, *Circulation.* 126 (2012) 1728–1738. doi:10.1161/CIRCULATIONAHA.112.115089.
- [104] A. Germani, E. Foglio, M.C. Capogrossi, M.A. Russo, F. Limana, Generation of cardiac progenitor cells through epicardial to mesenchymal transition, *J. Mol. Med.* (2015). doi:10.1007/s00109-015-1290-2.

- [105] C.S. Potten, M. Loeffler, Stem cells: attributes, cycles, spirals, pitfalls and uncertainties. Lessons for and from the crypt., *Development*. 110 (1990) 1001–20. <http://www.ncbi.nlm.nih.gov/pubmed/2100251> (accessed March 22, 2017).
- [106] S.D. Vincent, M.E. Buckingham, How to make a heart. The origin and regulation of cardiac progenitor cells, *Curr. Top. Dev. Biol.* 90 (2010) 1–41. doi:10.1016/S0070-2153(10)90001-X.
- [107] M. Gherghiceanu, L.M. Popescu, Human epicardium: Ultrastructural ancestry of mesothelium and mesenchymal cells, *J. Cell. Mol. Med.* 13 (2009) 2949–2951. doi:10.1111/j.1582-4934.2009.00869.x.
- [108] S. Bollini, J.M.N. Vieira, S. Howard, K.N. Dubè, G.M. Balmer, N. Smart, P.R. Riley, Re-activated adult epicardial progenitor cells are a heterogeneous population molecularly distinct from their embryonic counterparts., *Stem Cells Dev.* 23 (2014) 1719–30. doi:10.1089/scd.2014.0019.
- [109] J.J.H. Chong, V. Chandrakanthan, M. Xaymardan, N.S. Asli, J. Li, I. Ahmed, C. Heffernan, M.K. Menon, C.J. Scarlett, A. Rashidianfar, C. Biben, H. Zoellner, E.K. Colvin, J.E. Pimanda, A. V. Biankin, B. Zhou, W.T. Pu, O.W.J. Prall, R.P. Harvey, Adult Cardiac-Resident MSC-like Stem Cells with a Proepicardial Origin, *Cell Stem Cell*. 9 (2011) 527–540. doi:10.1016/j.stem.2011.10.002.
- [110] J.J.H. Chong, H. Reinecke, M. Iwata, B. Torok-Storb, A. Stempien-Otero, C.E. Murry, Progenitor Cells Identified by PDGFR-Alpha Expression in the Developing and Diseased Human Heart, *Stem Cells Dev.* 22 (2013) 1932–1943. doi:10.1089/scd.2012.0542.
- [111] R. Koninckx, A. Daniels, S. Windmolders, U. Mees, R. Macianskiene, K. Mubagwa, P. Steels, L. Jamaer, J. Dubois, B. Robic, M. Hendriks, J.-L. Rummens, K. Hensen, The cardiac atrial appendage stem cell: a new and promising candidate for myocardial repair, *Cardiovasc. Res.* 97 (2013) 413–423. doi:10.1093/cvr/cvs427.
- [112] R.A. Pelekanos, J. Li, M. Gongora, V. Chandrakanthan, J. Scown, N. Suhaimi, G. Brooke, M.E. Christensen, T. Doan, A.M. Rice, G.W. Osborne, S.M. Grimmond, R.P. Harvey, K. Atkinson, M.H. Little, Comprehensive transcriptome and immunophenotype analysis of renal and cardiac MSC-like populations supports strong congruence with bone marrow MSC despite maintenance of distinct identities, *Stem Cell Res.* 8 (2012) 58–73. doi:10.1016/j.scr.2011.08.003.
- [113] R. Carmona, J.A. Guadix, E. Cano, A. Ruiz-Villalba, V. Portillo-Sánchez, J.M. Pérez-Pomares, R. Muñoz-Chápuli, The embryonic epicardium: an essential element of cardiac development., *J. Cell. Mol. Med.* 14 (2010) 2066–2072. doi:10.1111/j.1582-4934.2010.01088.x.
- [114] Q. Wang, H. Wang, Z. Li, Y. Wang, X. Wu, Y. Tan, Mesenchymal stem cell-loaded cardiac patch promotes epicardial activation and repair of the infarcted myocardium, *J. Cell. Mol. Med.* (2017). doi:10.1111/jcmm.13097.
- [115] M.A. Trembley, L.S. Velasquez, K.L. de Mesy Bentley, E.M. Small, Myocardin-related transcription factors control the motility of epicardium-derived cells and the maturation of coronary vessels, *Development*. 142 (2015) 21–30. doi:10.1242/dev.116418.



# 3

## The Isolation and Culture of Primary Epicardial Cells Derived from Human Adult and Fetal Heart Specimens

Esther Dronkers<sup>1</sup>, Asja T. Moerkamp<sup>1</sup>, Tessa van Herwaarden<sup>1</sup>,  
Marie-José Goumans<sup>1</sup>, Anke M. Smits<sup>1</sup>

<sup>1</sup> Department of Cell and Chemical Biology, Leiden University Medical Center, Leiden,  
The Netherlands.

*Published in Journal of Visualized Experiments (2018)*

*The video component of this article can be found at [www.jove.com/video/57370/](http://www.jove.com/video/57370/)*

## ABSTRACT

The epicardium, an epithelial cell layer covering the myocardium, has an essential role during cardiac development, as well as in the repair response of the heart after ischemic injury. When activated, epicardial cells undergo a process known as epithelial to mesenchymal transition (EMT) to provide cells to the regenerating myocardium. Furthermore, the epicardium contributes via secretion of essential paracrine factors. To fully appreciate the regenerative potential of the epicardium, a human cell model is required. Here we outline a novel cell culture model to derive primary epicardial derived cells (EPDCs) from human adult and fetal cardiac tissue. To isolate EPDCs, the epicardium is dissected from the outside of the heart specimen and processed into a single cell suspension. Next, EPDCs are plated and cultured in EPDC medium containing the ALK 5-kinase inhibitor SB431542 to maintain their epithelial phenotype. EMT is induced by stimulation with TGF $\beta$ . This method enables, for the first time, the study of the process of human epicardial EMT in a controlled setting, and facilitates gaining more insight in the secretome of EPDCs that may aid heart regeneration. Furthermore, this uniform approach allows for direct comparison of human adult and fetal epicardial behavior.

### Keywords

Developmental Biology, Human, Epicardium, EPDC, Primary Cell Culture, Cardiac Development, Cardiac Regeneration, Epithelial to Mesenchymal Transition, EMT

## INTRODUCTION

The epicardium, a single-cell epithelial layer that envelopes the heart, is of vital importance for cardiac development and repair (reviewed in Smits *et al.*<sup>1</sup>). Developmentally, the epicardium arises from the proepicardial organ, a small structure located at the base of the developing heart. Around developmental day E9.5 in mouse, and 4 weeks post-conception in human, cells start to migrate from this cauliflower structure and cover the developing myocardium<sup>2</sup>. Once a single epithelial cell layer is formed, a portion of the epicardial cells undergoes epithelial to mesenchymal transition (EMT). During EMT, cells lose their epithelial characteristics, such as cell-cell adhesions, and obtain a mesenchymal phenotype which gives them the capacity to migrate into the developing myocardium. The formed epicardial derived cells (EPDCs) can differentiate into several cardiac cell types including fibroblasts, smooth muscle cells, and potentially cardiomyocytes and endothelial cells<sup>3</sup>, although differentiation of the latter two cell populations remains subject to debate (reviewed in Smits *et al.*<sup>4</sup>). Furthermore, the epicardium provides instructive paracrine signals to the myocardium to regulate its growth and vascularization<sup>5,6,7,8</sup>. Multiple studies have demonstrated that impaired epicardial formation leads to developmental defects in cardiac muscle<sup>9,10</sup>, vasculature<sup>11</sup>, and conduction system<sup>12</sup>, emphasizing the essential contribution of the epicardium to the formation of the heart.

Although in the adult heart the epicardium is present as a dormant layer, it becomes reactivated upon ischemia<sup>13</sup>. Epicardial reactivation post-injury recapitulates several of the processes described for cardiac development, including proliferation and EMT<sup>14</sup>, albeit less efficiently. Interestingly, although the exact mechanism is not fully understood, the epicardial contribution to repair can be improved by treatment with, *e.g.*, Thymosin  $\beta$ 4<sup>15</sup> or modified VEGF-A mRNA<sup>16</sup>, resulting in ameliorated cardiac function after myocardial infarction. The epicardium is therefore considered an interesting cell source to enhance endogenous repair of the injured heart.

Mechanisms of cardiac development are often recapitulated during injury, although in a less efficient manner. In search of epicardial activators, it is paramount that we can determine and compare the full capacity of the fetal and adult epicardium. Moreover, from a therapeutic point of view, it is important that, in addition to animal experiments, we extend knowledge regarding the response of the human epicardium. Here, we describe a method to isolate and culture human adult and fetal epicardial derived cells (EPDCs) in an epithelial-cell-like morphology and to induce EMT. With this model, we aim to explore and compare adult and fetal epicardial cell behavior.

The main advantage of this protocol is the use of human epicardial material, which has not been thoroughly studied. Importantly, the described isolation and cell culture protocol provides a single uniform method to derive both fetal and adult cobble EPDCs, enabling a direct comparison between these two cell sources. Additionally, since the epicardium is isolated based on its location, it is ensured that the cells are actually epicardially derived<sup>17</sup>.

While human EPDC isolation methods have been established previously, these mostly rely on outgrowth protocols where pieces of cardiac or epicardial tissue are plated onto a cell culture dish<sup>18,19</sup>. This approach thereby selects specifically for cells that partially lose their epithelial phenotype in order to migrate, and that are more prone to undergo spontaneous EMT. In the current protocol, the epicardium is first processed into a single cell solution which allows the isolated EPDCs to maintain their epithelial state. This method therefore provides a solid *in vitro* model to study epicardial EMT.

## PROTOCOL

All experiments with human tissue specimens were approved by the ethics committee of the Leiden University Medical Center and conforms to the Declaration of Helsinki. All steps are performed with sterile equipment in a cell culture flow cabinet.

### 1. Preparations

1. Prepare EPDC medium by mixing Dulbecco's modified Eagle's medium (DMEM low- glucose) and Medium 199 (M199) in a 1:1 ratio. Add 10% heat inactivated fetal bovine serum (FBS, heat inactivated for 25 min at 56 °C) and supplement with 100 U/mL penicillin and 100 mg/mL streptomycin. Pre-warm the EPDC medium in a 37 °C water bath.
2. Pre-warm Trypsin 0.25%/EDTA (1:1) in a 37 °C water bath.
3. Coat wells with gelatin. Add 0.1% gelatin/PBS to each well and incubate the plates for at least 15 min at 37 °C. Guidelines for the required cell culture plate are summarized in **Table 1**. Carefully remove all fluid before plating cells.
4. Prepare a stock solution of 10 mM SB431542 (SB), diluted in DMSO (CAUTION). Make 50 µL aliquots in conical bottom polypropylene centrifuge tubes, like Eppendorf tubes, and store them at -20 °C. Note that SB aliquots can be thawed only once.

**Table 1: Guideline for selecting the appropriate cell culture plate.** The required well size depends on the amount of epicardial cells isolated. These guidelines can be used as a rule of thumb to select the appropriate cell culture plate.

Tissue	Well type	Cell Growth Area (cm <sup>2</sup> )	Volume of medium (mL)	Addition of SB
Fetal	24	1.9	0.5	Directly
Adult small (<4 cm)	12	3.8	1	After 1 <sup>st</sup> passage
Adult large (>4 cm)	6	9.6	2	After 1 <sup>st</sup> passage

## 2. Retrieval and Storage of Adult and Fetal Heart Specimens

1. Store human adult auricles directly upon removal during surgery in a 50-mL tube with 15 mL high-glucose DMEM containing 10% FBS, 100 U/mL penicillin, and 100 mg/mL streptomycin at 4 °C. Samples are generally 3 - 5 cm in size and can be stored up to 48 h after dissection.
2. Store fetal hearts obtained from elective abortion material in EPDC medium at 4 °C up to 24 h after isolation. For this protocol, use samples with a gestational age between 12 - 22 weeks. Note that the whole heart can be used for isolation of the epicardium.

## 3. Isolation of the Epicardial Layer

1. In the laminar flow cabinet, prepare a 100-mm cell-culture dish with PBS and place a separate droplet (~200 µL) of PBS in the lid. Fill a 15-mL tube with 5 mL pre-warmed EPDC medium.
2. Place the tissue in the cell-culture dish filled with PBS. Make sure that the tissue is moistened frequently during the procedure.
3. Using a stereomicroscope, remove as much of the epicardial layer from the tissue sample as possible by peeling it off using forceps. Note: The epicardium can be recognized as a very thin, transparent layer tightly adhered to the outside of the heart (**Figure 1A**). Try to avoid contamination with epicardial adipose tissue and blood vessels since this will hamper the isolation.
4. Collect pieces of epicardial tissue in the droplet of PBS on the lid.
5. Cut the epicardial tissue into small pieces (0.5 mm<sup>3</sup>) using a scalpel (**Figure 1B**), or using the sharp tips of small forceps. Note that the pieces should be able to pass a P1,000 pipet tip (step 3.6).
6. Add 1 mL of trypsin to the epicardial tissue and collect the pieces and trypsin with a P1,000 pipet tip. Transfer the tissue into a 1.5-mL conical centrifuge tube (**Figure 1C**).

7. Incubate the tube in a 37 °C water bath for 10 min, while shaking at ~60 rpm.
8. Remove the tube from the water bath, and clean the outside of the tube with 70% ethanol.
9. Allow the tissue to sink to the bottom of the tube (**Figure 1D**) and carefully transfer the supernatant containing epicardial cells to the 15-mL tube containing 5 mL EPDC medium to inactivate the trypsin.
10. Replenish the remaining tissue in the conical centrifuge tube with 1 mL trypsin, and mix by gently pipetting up and down.
11. Repeat step 3.7 to 3.10 two times. At the final step, after a total of 30 min of trypsin incubation, transfer both the supernatant and the remaining epicardial tissue into the tube containing EPDC medium.
12. When all cells are collected in EPDC medium, gently pass the suspension through a 10-mL syringe with a 19-gauge needle into a new 15-mL tube to mechanically dissociate the cells (**Figure 1E**). Note: Make sure to homogenize the suspension by pipetting up and down before passing the solution through the needle to prevent the needle getting obstructed.
13. To further dissociate the cells, repeat step 3.12 with a 21-gauge needle.
14. Place a 100- $\mu$ m cell strainer on top of a 50-mL tube and transfer the medium containing the epicardial cells onto the strainer using a 10-mL pipette to remove all remaining clumps (**Figure 1F**).
15. Wash the strainer to collect residual cells by pipetting 5 mL EPDC medium onto the strainer.
16. Pipet the cell suspension from the 50-mL tube into a 15-mL tube. Since cells sink to the bottom of the tube, shake the solution gently before pipetting. Note: While this step is not necessary, a smaller tube aids visualization of the pellet after centrifugation.
17. Centrifuge at 200 x g for 5 min at room temperature (**Figure 1G**).
18. Remove the supernatant and resuspend the cell pellet (**Figure 1H**) in the required volume of EPDC medium (**Table 1**). Note: For fetal EPDCs, directly use EPDC medium containing 10  $\mu$ M of the ALK5 kinase inhibitor (EPDC+SB). Adult cells can be plated without SB during the first passage.
19. Plate the cell suspension on the gelatin coated culture plates (**Figure 1I**). The size of the well depends on the size of the epicardial tissue sample (**Table 1**). Note that low confluency will induce the occurrence of EMT.
20. Place the cells in the incubator for at least 48 h at 37 °C, 5% CO<sub>2</sub> to allow the cells to attach to the culture plate.

#### 4. Culture of EPDCs

1. Replenish the EPDC+SB medium at least every 3 days.
2. Inspect the cells at least every 3 days using the microscope. When the cells reach confluency, *i.e.*, when the culture plate is fully covered with cells, passage the cells in a 1:2 surface ratio. Note that reaching confluency can take ~5 - 10 days.
1. Aspirate the medium using a pipet or an aspiration system with, *e.g.*, a glass pipet.
2. Wash the cells carefully by adding PBS to the cells. Gently swirl the plate and aspirate the PBS.
3. Add trypsin to the plate. Gently rotate the plate to cover all cells with trypsin and incubate the plate for 1 min at 37 °C. NOTE: Use as little trypsin as possible (indication: 200 µL per well of a 6 well plate)
4. Tap the plate to mechanically detach the cells from the bottom of the plate. Use the microscope to visually check if cells have detached. If not, incubate the cell culture plate for an extra minute.
5. Add the required volume of EPDC+SB medium to the cells, resuspend by pipetting up and down, and transfer the cell suspension to a new gelatin coated culture plate. NOTE: In general, cells can be kept in a cobblestone morphology up to passage 8.

#### 5. Induction of EMT in EPDCs

1. To induce EMT, dissociate the cells with trypsin and transfer the cells to new gelatin coated wells in a 1:2 surface ratio in EPDC+SB medium, as described in 4, and incubate for at least 24 h at 37 °C, 5% CO<sub>2</sub>.
2. Check if confluency is 50 - 70% and if EPDCs have a cobblestone morphology. NOTE: Confluency affects the ability of EPDCs to undergo EMT.
3. Aspirate the medium from the cells and wash the cells carefully with PBS (see step 4.2.1 - 4.2.2).
4. Stimulate cells with 1 ng/mL TGFβ<sub>3</sub> in EPDC medium and place them in an incubator at 37 °C, 5% CO<sub>2</sub> for 5 days. Note that during stimulation, the EPDC medium containing TGFβ<sub>3</sub> does not have to be replenished.
5. Monitor the cells daily. After 5 days, cells that underwent EMT are recognized by a spindle-shaped morphology (**Figure 2A**).
6. Culture spindle-shaped EPDCs according to the method described in 4 without addition of SB or TGFβ to the EPDC medium. Note that in general, spindle-shaped EPDCs can be cultured up to passage 20.
7. Validate the occurrence of EMT with immunofluorescent staining using antibodies against the mesenchymal markers αSMA or Vimentin or by phalloidin

to detect the formation of F-actin stress fibers (**Figure 2B**), or using qRT-PCR for EMT-related genes (*e.g.*, WT1, Periostin, Col1A1,  $\alpha$ SMA, N-Cadherin, MMP3, Snail, Slug) (**Figure 2C** and **Table 2**).

**Table 2: Primer sequences used for validation of EMT in EPDCs.** Sequences of forward and reverse primers used for qRT-PCR to determine the expression of several EMT related genes in adult EPDCs.

Gene	Sequence
WT1 Forward	CAG CTT GAA TGC ATG ACC TG
WT1 Reverse	TAT TCT GTA TTG GGC TCC GC
N-Cadherin Forward	CAG ACC GAC CCA AAC AGC AAC
N-Cadherin Reverse	GCA GCA ACA GTA AGG ACA AAC ATC
POSTN Forward	GGA GGC AAA CAG CTC AGA GT
POSTN Reverse	GGC TGA GGA AGG TGC TAA AG
SMA Forward	CCG GGA GAA AAT GAC TCA AA
SMA Reverse	GAA GGA ATA GCC ACG CTC AG
MMP3 Forward	TGG ATG CCG CAT ATG AAG
MMP3 Reverse	CAG AAA TGG CTG CAT CGA
COL1A1 Forward	CCA GAA GAA CTG GTA CAT CAG CA
COL1A1 Reverse	CGC CAT ACT CGA AAT GGG AAT
GAPDH Forward	AGC CAC ATC GCT CAG ACA C
GAPDH Reverse	GCC CAA TAC GAC CAA ATC C
B2M Forward	ACA CTG AAT TCA CCC CCA CT
B2M Reverse	GCT TAC ATG TCT CGA TCC CAC T

## REPRESENTATIVE RESULTS

Here, we outline a straightforward protocol to isolate EPDCs from human adult and fetal cardiac tissue (**Figure 1**). This protocol takes advantage of the easily accessible location of the epicardium on the outside of the heart (**Figure 1A**). Staining of the heart auricle after dissection demonstrates that the WT1+ epicardium is removed while the underlying subepicardial extracellular matrix and myocardial tissue remain intact (**Figure 1J**). Extensive characterization has been performed before, demonstrating that EPDCs express epicardial markers, *e.g.*, ALDH1A2, TBX18, KRT8, KRT19 and lack expression of other heart-resident cell types, *e.g.*, PECAM1, ISL1, CD34, and TNNT2.<sup>17</sup>

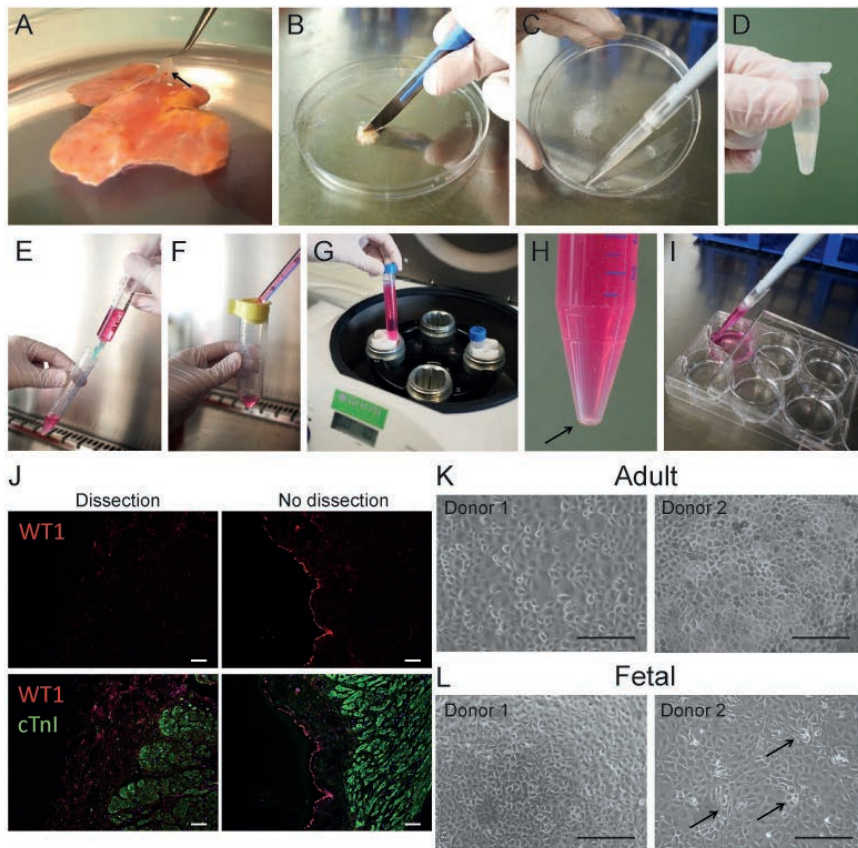


**Figure 1 | Isolation of Epicardial Derived Cells (EPDCs).** (A) Depicted is an adult auricle removed from the human heart with a thin outer membranous layer, the epicardium, which is removed. The black arrow points to the epicardium. (B-I) Visual representation of the isolation method of EPDCs. The black arrow points to the cell pellet. (J) Immunofluorescent staining of a heart auricle with and without dissection of the epicardium. Scale bar: 50  $\mu\text{m}$ . (K) Representative pictures of two different adult EPDC isolations cultured with SB. (L) Representative pictures of two different fetal EPDC isolations cultured with SB. Black arrows indicate mesenchymal-like cells in fetal EPDC culture. Scale bar: 200  $\mu\text{m}$ .

Both adult (**Figure 1K**) and fetal (**Figure 1L**) EPDCs cultured in the presence of ALK5 kinase inhibitor SB431542 show a cobblestone morphology. However, depending on the donor and culture conditions, fetal EPDCs can undergo EMT despite the presence of SB. This can result in spindle-shaped cells within the population of cobblestone cells (see arrows in **Figure 1L**). Please be aware that the isolation of cobblestone-shaped cells from fetal tissue is not always feasible, and may result in the derivation of mostly

spindle-shaped cells. Since these cells grow faster, they will rapidly overgrow other cell types.

EMT can be induced by incubating with TGF $\beta$ 3<sup>20</sup> for 5 days in both adult and fetal cells, as demonstrated by a clear morphological transition to spindle-shaped cells (Figure 2A). As demonstrated with the untreated control (“Empty”), fetal EPDCs will undergo spontaneous EMT upon removal of SB, while adult EPDCs will only undergo EMT upon stimulation with TGF $\beta$ 3. To validate EMT, EPDCs were immunostained with alpha-smooth muscle actin ( $\alpha$ SMA), a mesenchymal marker (Figure 2B). Furthermore, EMT was confirmed in adult EPDCs using qRT-PCR showing downregulation of the epicardial marker WT1 and upregulation of the mesenchymal markers POSTN,  $\alpha$ SMA, Collagen 1A1, MMP3, and N-Cadherin (Figure 2C). Comprehensive experiments regarding adult and fetal epicardial EMT are published before<sup>17</sup>.

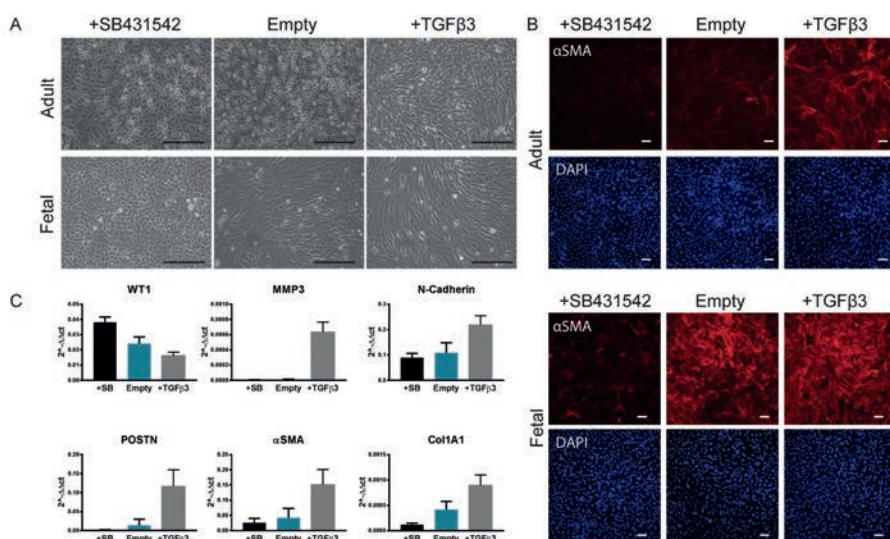


**Figure 2 | Validation of EMT in human adult and fetal Epicardial Derived Cells (EPDCs).** Adult and fetal EPDCs were cultured with SB, not treated (Empty) or stimulated with TGF $\beta$ 3 for 5 days. (A) Representative bright field pictures. Scale bar: 200  $\mu$ m. (B) Immunostaining for DAPI and  $\alpha$ SMA. Scale bar: 100  $\mu$ m. (C) mRNA levels of EMT-related genes, determined in adult EPDCs using qRT-PCR. Measured values were normalized to GAPDH and B2M expression. Values are depicted as mean + SD  $2^{-\Delta\Delta Ct}$  (n = 2). Abbreviations: WT1:Wilms' tumor 1, MMP3:Matrix Metalloproteinase 3, POSTN:Periostin,  $\alpha$ SMA: alpha Smooth Muscle Actin, Col1A1:Collagen 1A1.

## DISCUSSION

Here we describe a detailed protocol to isolate and culture primary epicardial cells derived from human adult and fetal hearts. Extensive characterization of these cells has been previously published<sup>17</sup>. We have shown that both cell types can be maintained as epithelial cobblestone-like cells when cultured with the ALK5 kinase inhibitor SB431542. EMT is an integral part of epicardial activation *in vivo* during both development and the post-injury response. EMT can be studied using this method by addition of TGF $\beta$ . Importantly, we previously observed that fetal EPDCs rapidly undergo spontaneous EMT when SB is removed, while adult EPDCs only undergo EMT upon stimulation<sup>17</sup>. Studying these processes in fetal EPDCs may aid in understanding how to optimally activate the adult epicardium after damage.

The presented method relies on patient material, which is obtained during surgery. Therefore, one can expect several variations in the state of the material isolated, which are either due to patient variability or the speed at which the material is collected in the operating theater. This variation may explain differences in the procedure: 1) how easily the epicardium can be dissected from the myocardium, 2) adherence of isolated cells to the plate, 3) the ability to prevent or undergo EMT, and 4) proliferation speed. In general, a quick isolation is preferable for cell survival. The main critical point is peeling the epicardium from the myocardium. If the epicardium is strongly adhered to the underlying tissue, a 15-min pre-treatment of the cardiac tissue with trypsin can help to remove the epicardium more easily. Furthermore, the efficacy of the trypsin treatment depends on several factors, including the trypsin activity and the composition of the tissue. Therefore, if a low yield is observed, the incubation time with trypsin can be adjusted. Additionally, if no cell pellet is visible after spinning down, the solution might not have been completely dissociated before running through the filter. Mixing the solution before passing the solution through the syringe or using an extra, smaller syringe could be useful to dissociate the cells. The well size for seeding EPDCs should be considered carefully to enable cells to maintain their epithelial state. **Table 1** gives an indication, but one can deviate from this guideline when, for example, only a small part of fetal heart can be used and plating in a smaller well is more convenient.

Since fetal cells will undergo EMT immediately without SB<sup>17</sup>, fetal EPDCs should always be plated with SB. However, adult EPDCs tend to maintain their epithelial morphology and therefore can be plated without SB during the first 48 h of the first passage, to promote cell adherence. After the first passage, both adult and fetal EPDCs are

continuously cultured with SB to prevent spontaneous EMT. In addition, low cell density is an important trigger for EMT. EPDCs should therefore never be cultured below 50% confluency. On the other hand, if EMT is desired, make sure that EPDCs are not seeded too densely, and stay below 70% confluency. Though this protocol utilizes TGF $\beta$ 3, stimulation with TGF $\beta$ 1 and 2 can induce EMT in EPDCs as well (observations unpublished).

In this protocol, cells are split directly without spinning down, since we observe a lower cell survival when using the centrifuge. Therefore, it is vital to use low volumes of trypsin to ensure its deactivation when serum containing medium is added.

After ~6 - 8 passages, EPDCs with an epithelial morphology will either stop growing or will undergo EMT spontaneously. Therefore, for experiments, we use cobble EPDCs between passage 3 and passage 6. In contrast, EPDCs with a mesenchymal morphology are less vulnerable and can be cultured up to passage 20. In experiments, however, we have never used spindle EPDCs after the 10th passage.

Since the epicardium is located at the outside of the heart and is easy to separate from underlying tissue, the authenticity of the cells is evident, and the chance of significant contamination is low. Although adipose tissue or blood vessels sometimes stick to the isolated epicardial layer, the majority of those cells will not pass the strainer during the isolation, and otherwise cannot survive in EPDC cell culture. Furthermore, as mentioned before, using human material provides a unique model to investigate human epicardial cell behavior. It is known that, for instance, epicardial adipose tissue is different between species, emphasizing the necessity of human epicardial cell models<sup>21</sup>.

It should be noted that the heart auricles were obtained during surgery on diseased hearts, and therefore the differences in disease, used medication, age, and gender of the donor may influence the reproducibility of the experiments. Experiments should therefore be performed on several isolations to obtain valid results and allow solid conclusions to be drawn. Furthermore, depending on the research question, one could choose specifically to only use epicardium from patients with ischemic disease or patients with non-ischemic valvular disease, which are expected to behave differently.

It has been suggested that atrial epicardium may have distinct characteristics from ventricle epicardium<sup>2</sup>, thereby questioning if epicardium derived from the atrial heart

auricle provides a valid model for epicardial behavior. In this context, it is important to point out that we could not find differences between fetal atrial and ventricular derived EPDCs (unpublished data). However, using epicardium from the human adult ventricle would be the ultimate cell source to verify this. Yet, collecting large specimens of human adult ventricles for EPDC isolation is highly invasive for the patient, and is therefore currently not feasible in this hospital.

We observed that SB is not always sufficient to prevent EMT, mainly in fetal EPDCs. When fetal EPDCs undergo EMT in the presence of SB, we exclude them from experiments. As a consequence, cells used for experiments are selected for their ability to maintain an epithelial phenotype in response to SB. We hypothesize that fetal cells can already be beyond a certain threshold in the process of EMT, and that inhibition with SB is not able to stop this.

This epicardial cell model has several applications, since both the developing and the adult epicardium can be investigated. In our lab, we focus on improvement of the epicardial regenerative response after cardiac damage. Adult EPDCs can be used to test compounds which induce EMT, aiming to find a potential therapeutic drug for an ameliorated regenerative response of the epicardium. In addition, it is possible to measure factors secreted by EPDCs to comprehend the paracrine signaling to the (re)generating myocardium. Furthermore, since we observed that fetal EPDCs are more prone to undergo EMT spontaneously compared to adult EPDCs, we investigate the differences between the fetal and adult EPDCs. Determining the underlying mechanism of increased fetal activation could provide a cue to improve epicardial activation in the adult heart.

## REFERENCES

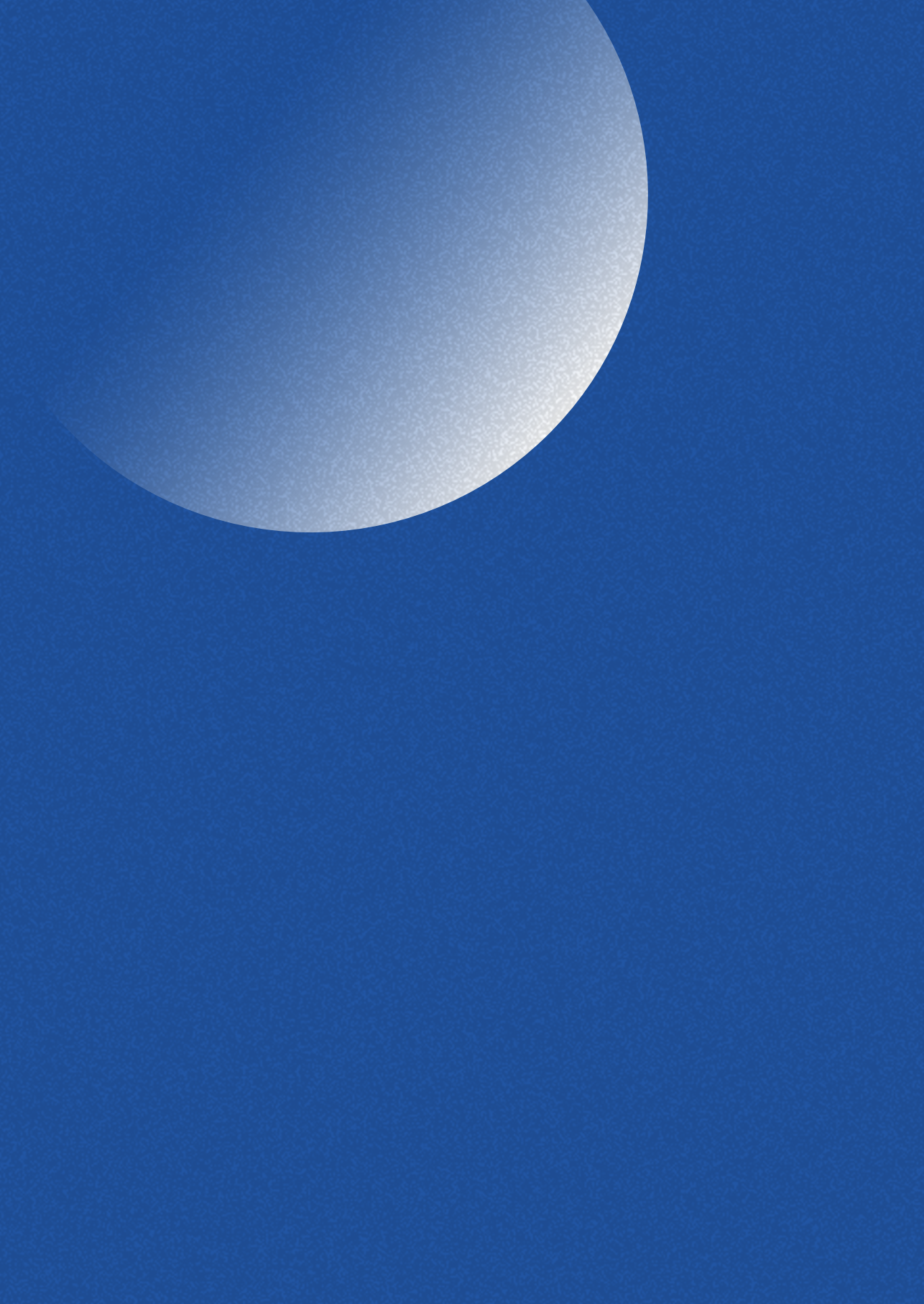
1. Smits, A. M., Dronkers, E., & Goumans, M.J. The epicardium as a source of multipotent adult cardiac progenitor cells: Their origin, role and fate. *Pharmacological research*. **127**, 129-140 (2017).
2. Risebro, C. A., Vieira, J. M., Klotz, L., & Riley, P. R. Characterisation of the human embryonic and foetal epicardium during heart development. *Development*. **142**(21), 3630-3636 (2015).
3. Zhou, B., Ma, Q., *et al.* Epicardial progenitors contribute to the cardiomyocyte lineage in the developing heart. *Nature*. **454**(7200), 109-113(2008).
4. Smits, A., & Riley, P. Epicardium-Derived Heart Repair. *Journal of Developmental Biology*. **2**(2), 84-100 (2014).
5. Chen, T.H.P., Chang, T.C., *et al.* Epicardial Induction of Fetal Cardiomyocyte Proliferation via a Retinoic Acid-Inducible Trophic Factor. *Developmental Biology*. **250**(1), 198-207 (2002).
6. Pennisi, D. J., Ballard, V. L. T., & Mikawa, T. Epicardium is required for the full rate of myocyte proliferation and levels of expression of myocyte mitogenic factors FGF2 and its receptor, FGFR-1, but not for transmural myocardial patterning in the embryonic chick heart. *Developmental Dynamics*. **228**(2), 161-172 (2003).
7. Lavine, K.J., Yu, K., *et al.* Endocardial and epicardial derived FGF signals regulate myocardial proliferation and differentiation in vivo. *Developmental Cell*. **8**(1), 85-95 (2005).
8. Stuckmann, I., Evans, S., & Lassar, A. B. Erythropoietin and retinoic acid, secreted from the epicardium, are required for cardiac myocyte proliferation. *Developmental biology*. **255**(2), 334-49 (2003).
9. Männer, J., Schlueter, J., & Brand, T. Experimental analyses of the function of the proepicardium using a new microsurgical procedure to induce loss-of-proepicardial-function in chick embryos. *Developmental Dynamics*. **233**(4), 1454-1463 (2005).
10. Weeke-Klump, A., Bax, N. A. M., *et al.* Epicardium-derived cells enhance proliferation, cellular maturation and alignment of cardiomyocytes. *Journal of Molecular and Cellular Cardiology*. **49**(4), 606-616 (2010).
11. Erarp, I., Lie-Venema, H., *et al.* Coronary Artery and Orifice Development Is Associated With Proper Timing of Epicardial Outgrowth and Correlated Fas Ligand Associated Apoptosis Patterns. *Circulation Research*. **96**(5) (2005).
12. Kelder, T. P., Duim, S. N., *et al.* The epicardium as modulator of the cardiac autonomic response during early development. *Journal of Molecular and Cellular Cardiology*. **89**, 251-259 (2015).
13. van Wijk, B., Gunst, Q. D., Moorman, A. F. M., & van den Hoff, M. J. B. Cardiac regeneration from activated epicardium. *PloS one*. **7**(9), e44692 (2012).
14. Zhou, B., Honor, L. B., *et al.* Adult mouse epicardium modulates myocardial injury by secreting paracrine factors. *The Journal of clinical investigation*. **121**(5), 1894-904 (2011).
15. Smart, N., Bollini, S., *et al.* De novo cardiomyocytes from within the activated adult heart after injury. *Nature*. **474**(7353), 640-644 (2011).

16. Zangi, L., Lui, K. O., *et al.* Modified mRNA directs the fate of heart progenitor cells and induces vascular regeneration after myocardial infarction. *Nature Biotechnology*. **31**(10), 898-907 (2013).
17. Moerkamp, A. T., Lodder, K., *et al.* Human fetal and adult epicardial-derived cells: a novel model to study their activation. *Stem Cell Research & Therapy*. **7**(1), 1-12 (2016).
18. Clunie-O'Connor, C., Smits, A. M., *et al.* The Derivation of Primary Human Epicardium-Derived Cells. *Current Protocols in Stem Cell Biology*. **35**, 2C.5.1-2C.5.12 (2015).
19. Van Tuyn, J., Atsma, D. E., *et al.* Epicardial Cells of Human Adults Can Undergo an Epithelial-to-Mesenchymal Transition and Obtain Characteristics of Smooth Muscle Cells In Vitro. *Stem Cells*. **25**(2), 271-278 (2007).
20. Bax, N. A. M., van Oorschot, A. A. M., *et al.* In vitro epithelial-to-mesenchymal transformation in human adult epicardial cells is regulated by TGF $\beta$ -signaling and WT1. *Basic research in cardiology*. **106**(5), 829-847 (2011).
21. Chechi, K., & Richard, D. Thermogenic potential and physiological relevance of human epicardial adipose tissue. *International Journal of Obesity Supplements*. **5**(Suppl 1), S28-S34 (2015).

## MATERIALS

Name of Material	Company	Catalog Number	Comments/Description
Dulbecco's modified Eagle's medium + GlutaMAX™	Gibco™	21885-025	
Medium 199	Gibco™	31150-022	
Fetal Bovine Serum	Gibco™	10270-106	
Penicillin G sodium salt	Roth	HP48	
Streptomycin sulphate	Roth	HP66	
Trypsin 1:250 from bovine pancreas	Serva	37289	
EDTA	Sigma	E4884	
Gelatin	Sigma-Aldrich	G1393	
Culture plates 6 well	Greiner-bio-one	657160	
Culture plates 12 well	Corning	3512	
Culture plates 24 well	Greiner bio-one	662160	
SB 431542	Tocris	1614	
Dimethyl Sulfoxide (DMSO)	Merck	102931	
100-1000µL Filtered Pipet Tips	Corning	4809	
10-ml pipet	Greiner-bio-one	607180	
5-ml pipet	Greiner bio-one	606180	
Cell culture dish 100/20 mm	Greiner bio-one	664160	
PBS	Gibco™	10010056	Or home-made and sterilized
Eppendorf tubes 1.5 mL	Eppendorf	0030120086	
15-ml centrifuge tubes	Greiner bio-one	188271	
50-ml centrifuge tubes	Greiner bio-one	227261	
10 mL Syringe	Becton Dickinson	305959	

Needles 19 Gauge	Becton Dickinson	301700
Needles 21 Gauge	Becton Dickinson	304432
EASystrainer™ Cell Sieves, 100 µm	Greiner-bio-one	542000
TGFB3	R&D systems	243-B3
Monoclonal Anti-Actin, $\alpha$ -Smooth Muscle	Sigma	A2547
Anti-Mouse Alexa Fluor 555	Invitrogen	A31570
Alexa Fluor™ 488 Phalloidin	Invitrogen	A12379



# 4

## Small molecule screen identifies novel activators of epithelial to mesenchymal transition in human epicardial cells

Esther Dronkers<sup>1</sup>, Tessa van Herwaarden<sup>1</sup>, Esmee J Groeneveld<sup>1</sup>,  
Jesper Hjortnaes<sup>2</sup>, Marie Jose Goumans<sup>1</sup>, Anke M Smits<sup>1</sup>

<sup>1</sup>Department of Cell and Chemical Biology, Leiden University Medical Center,  
Leiden, The Netherlands.

<sup>2</sup>Department of Cardiothoracic Surgery, Leiden University Medical Center,  
Leiden, The Netherlands.

## ABSTRACT

Since the adult heart has minimal capacity to repair itself, myocardial infarction often leads to pathological remodeling and ultimately to the development of fatal heart failure. Upon ischemic injury, the epicardium, the outer layer of the heart which is essential for cardiac development, becomes re-activated and displays reparative potential. In this process, epicardial epithelial-to-mesenchymal transition (epiMT) is an essential step. We hypothesize that the reparative capacity of the heart can be improved by enhancing the participation of the epicardium to cardiac repair, particularly by stimulating the occurrence of epiMT. Therefore the aim of this study is to identify novel epiMT-inducing compounds by performing a small molecule screen.

Primary epicardial cells were derived from human heart auricles and cultured as epithelial-like cells with a cobblestone morphology. Using these cells, a phenotypic screen was performed utilizing the LOPAC1280 small molecule library to identify epiMT-inducing compounds. EpiMT was defined using  $\alpha$ SMA positive immunostaining as a hallmark for a phenotypic switch to a mesenchymal cell. After validation of the positive hits, five compounds were selected that reproducibly induced epiMT, as shown by: 1) a phenotypic switch towards mesenchymal spindle-shaped cells, 2) a decrease in CHD1 and 3) an increase in mesenchymal markers, such as Periostin. The selected compounds displayed low or absent toxicity to cultured cardiomyocytes and fibroblasts, indicating that the compounds can safely be applied to the heart. To identify a potential mechanism of epiMT induction, cells were treated for 3 hours with the two most promising compounds: TBBz and Oltipraz Metabolite M2 (M2), and subjected to RNA sequencing. This approach revealed that TBBz induced histone modifications and that M2 increased the transcription factor FOXQ1.

In conclusion, high-throughput experiments using human primary epicardial derived cells to identify novel epiMT-inducing compounds is feasible. Using this model, we have identified TBBz and Oltipraz Metabolite M2 as novel inducers of epiMT.

### Keywords

Epicardium, EPDC, Primary Cell Culture, Cardiac Regeneration, Epithelial to Mesenchymal Transition, EMT, Small Molecule Screen

## INTRODUCTION

After a myocardial infarction, the injured heart lacks the potential to repair itself resulting in the generation of a fibrotic scar. Because of this, cardiac function decreases causing the remaining viable tissue to be subjected to pathological remodeling. This compensatory remodeling ultimately progresses into heart failure. To date, no therapy is available to restore injured cardiac tissue. Identifying therapeutic targets to improve vascularization and cardiomyocyte proliferation after infarction are therefore ultimate goals in the field of cardiac research.

The epicardium, a mesothelial layer covering the entire surface of the heart, plays a vital role during development of the heart by providing cells and biochemical factors to the growing cardiac tissue (reviewed in (1)). By doing so, the epicardium contributes to key developmental processes, such as vascularization and myocardial compaction (2). These features of the epicardium are reactivated in the injured hearts of lower vertebrates, such as the zebrafish (3). Here, epicardial re-activation is essential for fully restoring lost cardiac tissue (4). Also in mammals, the recapitulation of embryonic epicardial processes aids in the repair process in the injured heart (5). Moreover, research has shown that the epicardial contribution to repair can be improved, e.g. by stimulating the epicardium with Thymosin  $\beta$ 4 (6). Given the potential of epicardial cells in the context of the developing heart and in regenerative species, the epicardium emerges as an appealing target to enhance cardiac repair.

To partake in cardiac tissue generation, epicardial cells undergo epithelial to mesenchymal transition (epiMT) (7). In this process, epicardial cells lose their epithelial phenotype and delaminate from the epicardium to transform into motile mesenchymal cells. Typically, cells lose their epithelial proteins, such as E-cadherin (8), and gain mesenchymal markers, such as  $\alpha$ SMA (9,10). These mesenchymal epicardial derived cells differentiate into fibroblasts, smooth muscle cells and pericytes (1) and secrete factors that promote vessel maturation (11) and cardiomyocyte proliferation (12,13). Trajectory analysis of the epicardium using RNA single cell sequencing suggested that epiMT occurs prior to fate specification (Mantri et al. and Lupu et al.), indicating that epiMT is an essential first step for the epicardial contribution to tissue formation and therefore a potential therapeutic target for the injured heart.

Given the importance of epiMT in epicardial behavior, the aim of this study is to identify novel inducers of epiMT. We exploited our previously developed cell culture model of human primary epicardial cells where epiMT can be induced in a controlled

fashion, (14) and subjected it to an array of pharmacologically active compounds. Our goal was to identify molecules that robustly induce epiMT on a phenotypic and molecular level. For future application in vivo, these factors should not be toxic to other cardiac cell types including cardiomyocytes, nor induce excessive proliferation of fibroblasts. Here, we demonstrate that a phenotypic high-throughput screen using primary human epicardial cells is feasible and effective. Using this screen, we identified two novel epiMT inducing compounds: TBBz and Oltipraz Metabolite M2. In addition, we may have identified alternative routes of epiMT induction.

## MATERIAL AND METHODS

### *Cell culture*

Human primary epicardial cells were isolated and cultured as described (15). Briefly, the epicardium was peeled of human heart auricles which are considered surgical waste and obtained anonymously under general consent. The epicardium was processed into a single cell suspension and cultured on gelatin coated plates in epicardial cell medium consisting of Dulbecco's modified Eagle's medium (DMEM low-glucose, Gibco) and Medium 199 (M199, Gibco) mixed in a 1:1 ratio, supplemented with 10% fetal bovine serum (heat inactivated for 25 minutes at 56 °C, Biowest), 100 U/mL penicillin (Roth) and 100 mg/mL streptomycin (Roth). Cells were cultured in the presence of 10 µM SB431542 (SB, Tocris) at 37 °C in 5% CO<sub>2</sub>. Experiments were performed in cell culture medium without SB.

Human cardiac fibroblasts were derived from fetal hearts which were collected anonymously with informed consent. Three cell lines, derived from three individual fetal hearts, were cultured in Dulbecco's modified Eagle's medium (DMEM high-glucose, Gibco), supplemented with 10% fetal bovine serum, 100 U/mL penicillin (Roth) and 100 mg/mL streptomycin (Roth).

Induced pluripotent stem cells derived cardiomyocytes (iPSC-CM) were a kind gift of Dr. Buikema. The iPSC-CM were differentiated and matured for 30 days as previously described (16).

This research was carried out according to the official guidelines of the Leiden University Medical Center and approved by the local Medical Ethics Committee. This research conforms to the Declaration of Helsinki.

**LOPAC1280 small molecule screen**

Confluent epicardial cells were seeded in a 1:1 ratio in 50 µl epicardial cell medium in 8x384 wells plates per screen and incubated at 37 °C in 5% CO<sub>2</sub>. The next day, 1280 biologically active small molecules derived from the LOPAC1280 library (Sigma) were diluted in 50 µl epicardial cell medium and added to the cells in a final concentration of 5 (screen A) or 10 µM (screen B and C) in such a way that the dimethylsulfoxide (DMSO) concentration was 0.5%. All conditions were performed in duplicate. In every culture plate, the following controls were included: SB (10 µM), control epicardial cell medium, DMSO (0.5%), and TGFβ3 (1 ng/mL, R&D systems). After 5 days, cells were fixed in 4% PFA. The total procedure has been executed 3 times. For screen A, epicardial cells isolated from two patients were mixed, for screen B and C individual patient isolations were used.

After fixation, cells were stained with mouse anti-h-αSMA conjugated 488 antibody as described below. To increase the fluorescent signal, cells were incubated with a secondary antibody (Alexa Fluor Ms-488, Thermo Scientific). Automatic imaging was performed using BDPathway™ Bioimager (BD Biosciences) for screen A and EVOS FL Auto 2 Imaging System (Thermo Fisher Scientific) for screen B and C, taking 4 images per well (2x2 at the center of the well, 10x magnification). For every picture, the number of DAPI+ nuclei and αSMA surface area was quantified using Cell Profiler software. Data analysis was performed using R. Measurements containing a divergent (either exceptionally high or low) number of DAPI+ nuclei were excluded, as they represent failed imaging. αSMA surface area was normalized for the controls present in its own plate to reduce inter-plate variability, using the following formula:  $(SMA_{\text{Compound}} - SMA_{\text{DMSO.mean}}) / (SMA_{\text{TGFb.mean}} - SMA_{\text{DMSO.mean}}) * 100\%$ . For every screen the top 30 hits were selected, based on the αSMA value and taking into account the values of both duplicates. In addition, compounds present in the top 50 of more than 1 screen were also selected. These hits were confirmed by eyeballing the images to correct for artefacts. Compounds of interest were further validated in two additional individual cell isolations in a 96 well format.

**Cell stimulations**

The following compounds were used to stimulate cells: Phenamil methanesulfonate (10 µM, dissolved in DMSO, Sigma, p203), 3-deazaadenosine (20 µM, dissolved in mq, Biovision, 2771), H-8 dihydrochloride (10 µM, dissolved in DMSO, Sigma, M9656), TBBz (5 µM, dissolved in DMSO, Sigma, T6951), Oltipraz metabolite M2 (10 µM, dissolved in DMSO, SML0777, Sigma), SB431542 (10 µM, dissolved in DMSO, Tocris), DMSO, TGFβ3 (1 ng/mL, 4mM HCL/0.1%BSA, R&D systems). For the induction of epiMT, cells

were stimulated followed by isolation of RNA and protein after 5 days. To determine expression of epiMT-related transcription factors, RNA was isolated after 1.5, 3 and 24 hours of stimulation. To determine H3k27me3 levels, cells were stimulated for 3 hours. To determine cellular toxicity, iPSC-CM and cardiac fibroblast were stimulated for 48 hours whereafter an MTT assay was performed.

### ***Immunocytochemistry***

Cells were fixed in 4% PFA for 20 minutes at 4 °C followed by incubation with 1%BSA/PBS/Tw blocking buffer and overnight incubation with mouse anti-h- $\alpha$ SMA conjugated 488 antibody (R&D Ic1420g, 1:100), Vimentin (1:1000. ab195877, Abcam), Collagen 1 (1:200, 1310, Southern Biotech), Fibronectin (1:100, ab198933, Abcam), Phalloidin (1:1000, R415, Life Technologies) or Casein Kinase 2 alpha (MAB7957, 1  $\mu$ g/mL, R&D systems). After washing, cells were incubated with the corresponding secondary antibodies (Alexa Fluor 488, 555 or 647, Thermo Scientific) and nuclei were stained using DAPI (Thermo Scientific). Imaging was conducted using the Leica AF6000.

### ***qPCR***

To determine gene expression profiles, RNA was isolated using ReliaPrep™ RNA Mini-prep Systems (Promega). Concentration and purity of the RNA were determined using NanoDrop 1000 Spectrophotometer (Thermo Fisher Scientific). Next, cDNA synthesis was performed using the RevertAid H Minus First Strand cDNA Synthesis Kit (Thermo Fisher Scientific). Quantitative real time PCR was performed using SYBR Green (Promega) and run in 384 wells plates in technical triplicates on a CFX384 Touch™ Real-Time PCR Detection System (Bio-Rad). For every experiment and every primer set, mq and a cDNA sample without reverse transcriptase was taken along as negative controls. Expression levels were corrected for primer efficiency (Hellemans (2007)) determined by serial dilutions of three independent samples. For normalization, two reference genes (HPRT1 and TBP) were designed based on stable and robust expression in both epithelial and mesenchymal epicardial cells using geNORM (vandesompele 2002). Statistics were performed on the log transformed values.

**Table 1 Primer sequences for qPCR**

	Forward	Reverse
CDH1	CCC GGT ATC TTC CCC GC	CAG CCG CTT TCA GAT TTT CAT
CDH2	CAGACCGACCCAAACAGCAAC	GCAGCAACAGTAAGGACAAACATC
POSTN	GGAGGCAAACAGCTCAGAGT	GGCTGAGGAAGGTGCTAAAG
ACTA2	CCGGGAGAAAATGACTCAAA	GAAGGAATAGCCACGCTCAG
NR1H3	ATCCCCATGACCGACTGATG	CTCCCAGGAATGTTGCCCT
SNAI1	CCAGTGCCTCGACCACTATG	CTGCTGGAAGGTAAACTCTGGA
SNAI2	CGGACCCACACATTACCTTGT	TTCTCCCCGTGTGAGTTCTA
HPRT1	CTCATGGACTGATTATGGACAGGAC	GCAGGTCAGCAAAGAACTTATAGCC
TBP	TGGAAAAGTTGTATTAACAGGTGCT	GCAAGGGTACATGAGAGCCA

***MTT assay***

Fibroblasts were seeded in 96 wells and stimulated with indicated compounds for 48 hours after which DMEM containing MTT (0.5 mg/mL, Sigma) was added for 3 hours. Solubilization was performed by adding DMSO to the well whereafter absorbance was measured at 595 nm.

***TUNEL staining***

IPSC-CM were stimulated for 48 hours and fixed in 4% PFA. Cells were permeabilized in 0.25% TX100/PBS for 15 minutes and subsequently blocked in 1% BSA/PBS. TUNEL solution (ratio enzyme and label solution 1:25) was applied for 60 minutes. Next, cells were washed, blocked in 2% BSA/0.1% TX100/PBS/ and incubated for 2 hours with goat anti-cTnl (Hytest, 4T21, 1:200) antibody followed by one hour incubation with secondary antibody (Alexa Fluor 488, Thermo Scientific). DAPI was used as counter-staining (Thermo Scientific). Imaging was executed by EVOS FL Auto 2 Imaging System (Thermo Fisher Scientific).

***Western Blot***

Cells were lysed in radio immunoprecipitation assay (RIPA) buffer supplemented with protease inhibitors (Complete protease inhibitor cocktail tablets, Roche Diagnostics) and phosphatase inhibitors (1M NaF, 10% NaPi, 0.1M NaVan). Protein concentration was determined using a BCA assay (Pierce BCA Protein Assay Kit, 23225, Thermo Scientific). Samples were diluted to equal concentrations and loaded onto a 10% SDS-polyacrylamide gel followed by transfer to an Immobilon-P transfer membrane (# IPVH00010, PVDF membrane, Millipore) at 4°C. Blots were blocked in 5%BSA/TBST for 30 minutes at room temperature. Immunodetection was performed by overnight incubation at 4 °C with anti-E-cadherin (1:5000, ab40772, Abcam), anti-SMA

(1:500, A2547, Sigma-Aldrich), anti-Vinculin (1:5000, V9131, Sigma-Aldrich), anti-Phospho-CK2-Substrate Rabbit mAb mix (1:1000, #8738, Cell Signaling), anti-H3K27me3 (1:2500, 17622, Millipore) and subsequent incubation with Sheep anti-mouse HRP (NA931, GE Healthcare) or donkey anti-Rabbit HRP (ab98493, Abcam) for 30 minutes at room temperature, followed by chemiluminescent imaging using WesternBright ECL HRP substrate. Blots were imaged using ChemiDoc (Bio-rad).

### ***RNA sequencing***

Epicardial cells isolated from three patients (n=3) were incubated for 3 hours in epicardial cell medium supplemented with 0.1% DMSO, TGF $\beta$ 3 (1 ng/mL, R&D systems) plus DMSO, TBBz (5  $\mu$ M), or M2 (10  $\mu$ M). Total RNA was isolated as described above; and quality and integrity were assessed using an Agilent bioanalyzer. Library preparation, mRNA sequencing and data analysis was executed by Novogene Co., Ltd using the Illumina platform with a sequencing depth of 15G per sample. Reads containing adapters, reads with N > 10%, and low-quality reads were removed. The Q20, Q30 and GC content were established for quality control. The clean reads were mapped against the human reference genome (ensembl\_homo\_sapiens\_grch38\_p12\_gca\_000001405\_27) using STAR software. Gene expression levels were estimated as expected number of Fragments Per Kilobase of transcript sequence per Millions base pairs sequenced (FPKM). Clustering was determined using the  $\log_2(\text{FPKM}+1)$  value and differentially expressed genes (DEGs) were calculated using the DESeq2 R-package. Genes with an adjusted p-value <0.05 were considered as DEGs.

### **Statistics**

For every experiment, the n number is denoted in the legend, indicating biological repeats: the number of individual cell isolations that have been used. Displayed pictures are representative for multiple observations. Statistics were performed using Graphpad Prism 9 software. For every experiment, the performed statistical test is indicated in the figure legend. Only relevant comparisons were statistically tested. Significance was considered when  $P < 0.05$ .

## **RESULTS**

Human primary epicardial cells were isolated from human heart auricles. The epicardial cells were expanded in the presence of ALK4/5/7 kinase inhibitor SB431542 (SB) to maintain their epithelial phenotype which was evident by their cobblestone morphology. EpiMT was induced by TGF $\beta$  stimulation, which elicited a drastic phenotypical

transformation towards spindle-shaped cells, as previously described (14). To identify novel inducers of epiMT, we established an in vitro model for a high throughput phenotypal assay. First, we selected a proper and robust read out for epiMT by testing multiple antibodies for immunofluorescent analysis. The monoclonal mouse IgG2a clone #1A4 against human  $\alpha$ SMA from R&D (IC1420G) conveyed the highest discrimination between untreated cobblestone and spindle-shaped cells and was therefore selected for the screen read-out (Fig. S1). To screen for epiMT inducers, cobblestone epicardial cells were seeded in 384-wells plates and were incubated with small molecules derived from the Library of Pharmacologically Active Compounds (LOPAC1280). This library consists of small molecules dissolved in DMSO targeting a wide range of cell signaling processes. For every cell culture plate, DMSO-treated cells were included as a negative control, and TGF $\beta$ -treated cells as a positive control. Furthermore, SB treated cells and untreated cells were taken along as additional controls for the  $\alpha$ SMA staining (Fig. 1A).

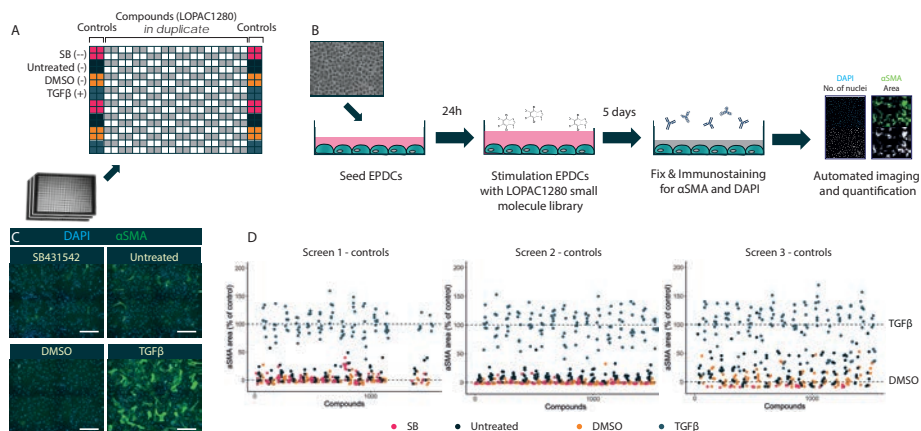


**Figure 1 | Design of phenotypic LOPAC1280 compound screen.** (A) Plate design of phenotypic LOPAC1280 compound screen. Eight 384 wells plates were used, each plate included control conditions SB, Untreated, DMSO and TGF $\beta$ . Compounds were added in duplicate. (B) Design of experiment. Cobblestone human primary epicardial derived cells were seeded and after 24 hours stimulated with compounds derived from the LOPAC1280 library. After 5 days of stimulation, cells were fixed and stained for  $\alpha$ SMA and DAPI which were subsequently automatically imaged and quantified. (C) Representative images of controls. Scale bar: 50  $\mu$ m. (D) Quantification of control conditions of the three individual screens displayed as  $\alpha$ SMA area relative to DMSO and TGF $\beta$  treated cells. The X-axis shows the number of the condition (first plate is 1-192, second plate is 193-384, etc). Every dot represents one well.

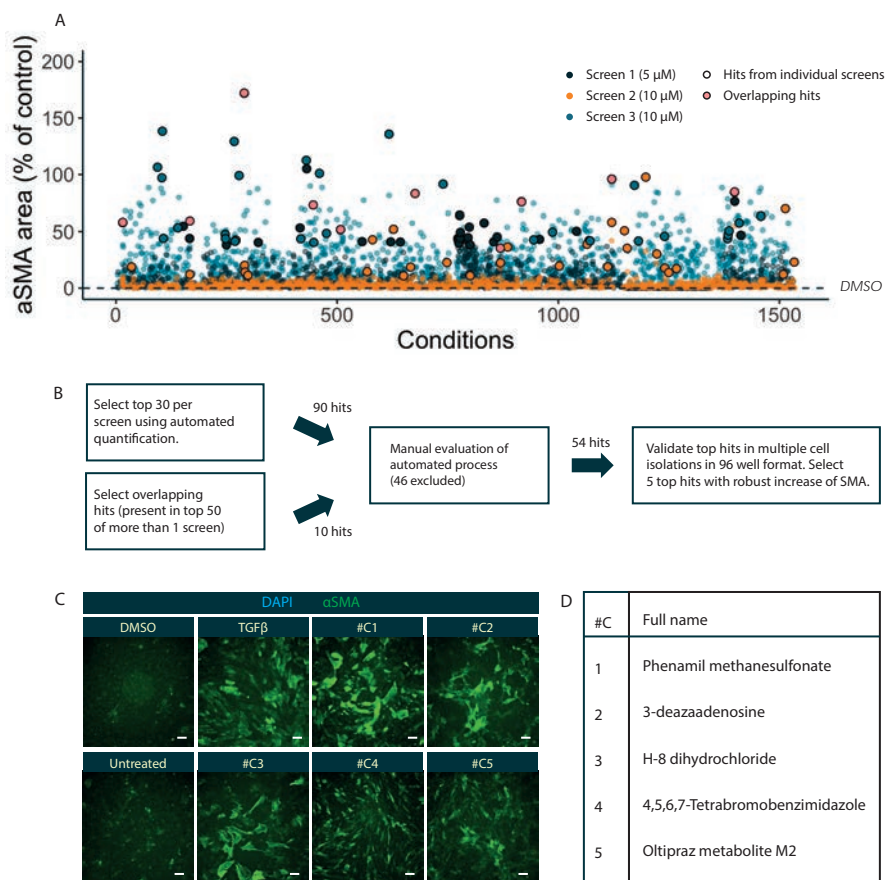


**Figure 2 | Phenotypic compound screen identifies five potential epiMT inducers.** (A) Results of the compound screen displayed as aSMA area relative to DMSO and TGFβ treated cells. The X-axis shows the number of the condition (first plate is 1-192, second plate is 193-384, etc). Every dot represents one well. (B) Schematic overview of the selection process leading to the final five hits. (C) Immunofluorescent staining of aSMA and DAPI of the five identified compounds and their controls after 5 days of stimulation (n=2-3). Scale bar: 100 μm. (D) List of the five selected molecules.

All conditions were tested in duplicate. We performed the screen three times, in epicardial cells isolated from different patients to account for patient variability, and in two concentrations (5 μM and 10 μM). After 5 days of incubation, the cells were fixed and stained for aSMA (Fig. 1B, C). aSMA-staining was automatically imaged and quantified as total area of positive aSMA immunostaining normalized against positive staining in control cells. The controls of the three individual screens are depicted in Fig.1D. In the first screen, we encountered technical difficulties with one cell culture

plate which is displayed as a gap in the figure. Screen 3 shows higher variation within each control condition compared to screen 1 and 2, shown by the spread of the dots. As expected, the percentage  $\alpha$ SMA area is lower in all three negative control conditions. Interestingly, DMSO treatment seemed to lower  $\alpha$ SMA expression compared to untreated cells. Overall, there is a clear distinction between the negative controls and the positive control TGF $\beta$ , indicating that this set-up is effective to identify novel epiMT inducers.

The results of all three screens are combined in Fig. 2A, where every dot represents one well. To select compounds for further analysis, we started by evaluating the compounds that induced  $\alpha$ SMA expression in more than one screen. Compounds that scored within the top 50 in more than one screen were listed (10 compounds, Fig. 2B and supplementary table 4). In addition, to ensure we did not miss any potential epiMT inducer, we also selected the top 30 hits from every screen (see supplementary table 1, 2 and 3). The pictures taken of these hits were evaluated manually and images containing artefacts were excluded, which resulted in a list of 54 compounds of interest. This selection was subjected to another round of testing in epicardial cells after which five small molecules were selected based on their capacity to robustly increase  $\alpha$ SMA expression, and to elicit morphological changes towards spindle-shaped cells in cells isolated from multiple patients (Fig. 2C-D).

We continued with five selected compounds and validated their effect on epiMT in more detail. First, we optimized the working concentration for all five compounds, defined as the lowest concentration that elicited  $\alpha$ SMA induction (data not shown). Next, we evaluated the morphology of the epicardial cells after compound stimulation. All small molecules induced a clear transition towards spindle-shaped mesenchymal cells compared to DMSO and untreated (Fig. 3A). Interestingly, there were morphological differences between the different stimulations, e.g. #C4' induced spindles displayed long dendritic-like tails while #C1' induced spindles have a thick and round body, with short tapered protrusions (Fig. 3A). Such variations were also observed in the  $\alpha$ SMA immunostaining pattern (Fig. 2C), e.g. #C3' induced spindles demonstrated a smooth muscle cell like striated pattern in large dissimilar cells, while #C5' induced spindles displayed a gradient of staining intensity and smaller, more rectangular-shaped cells. The variety in morphology between the compounds indicates that the five small molecules may not induce mesenchymal differentiation via the same mechanism or pathway. To confirm the morphological observed epiMT, gene profiling was performed to establish regulation of epiMT related genes. For all small molecules, the expression of CDH1 (encoding E-cadherin) decreased massively (Fig. 3B), demonstrating the loss

of epithelial morphology. This was corroborated by the loss of E-cadherin protein (Fig. 3D). Furthermore, almost all molecules, except for #C2, showed a trend towards an increase of CDH2 (encoding N-cadherin), which is a hallmark of a mesenchymal phenotype. For #C1, #C2 and #C3, the transition of E-cadherin to N-cadherin was not apparent in all tested epicardial cell isolations, which can be appreciated from the spread of the individual dots, suggesting that epiMT induction is less robust. We continued by determining the presence of the mesenchymal marker Periostin (POSTN) which was 10-fold increased in almost all stimulations (Fig. 3C).

Although we could not detect massive changes in ACTA2 gene regulation (Fig. 3C),  $\alpha$ SMA protein levels were upregulated in cell cultures stimulated with #C3, #C4 and #C5 (Fig. 3D). To conclude, while not to the same extent, the identified five small molecules all induce epiMT both phenotypically, and at a molecular and protein level.

For compounds to be used for *in vivo* stimulation of the epicardium, it is essential that they do not harm other cardiac cell types at concentrations required for the induction of epiMT. Therefore, we determined the toxicity of the compounds in cardiomyocytes and fibroblasts. Toxicity of the compounds in iPSC-CM (Fig. 4A) was determined by TUNEL staining and cell numbers, which was quantified by counting DAPI+ nuclei. Only at very high concentrations (>4x the working concentration), a small effect on cell death was observed for #C1 and #C4 (Fig. 4B). Furthermore, the identified small molecules did not induce the proliferation of cardiac fibroblasts, nor did they exert any harmful effects on these cells when stimulated with the working concentration, although 4x the working concentration of #C1 and #C4 was toxic for the cells, while #C2 was able to induce slight fibroblast proliferation (Fig. 4C). To conclude, at the working concentration, all compounds appear safe for cardiomyocytes and fibroblasts.

Based on their ability to induce epiMT and their robustness in doing so, we decided to continue with the two most promising compounds namely 4,5,6,7-Tetrabromobenzimidazole (TBBz, #C4) and Oltipraz metabolite M2 (M2, #C5), and studied the underlying mechanism of their epiMT induction. An essential step in the process of epiMT is the upregulation of EMT regulating transcription factors. In our epicardial cell culture model, TGF $\beta$  mainly induces epiMT via the upregulation of SNAI1 (encoding SNAIL)(Fig. 5A). Interestingly, TBBz and M2 mainly induced the expression of SNAI2 (encoding SLUG) (Fig. 5A) suggesting that both compounds follow a different pathway than TGF $\beta$  to induce epiMT. Noteworthy, M2 induced SNAI2 within 90 minutes, while upon TBBz stimulation this transcription factor is mainly upregulated after 24 hours, suggesting an indirect epiMT-induction.

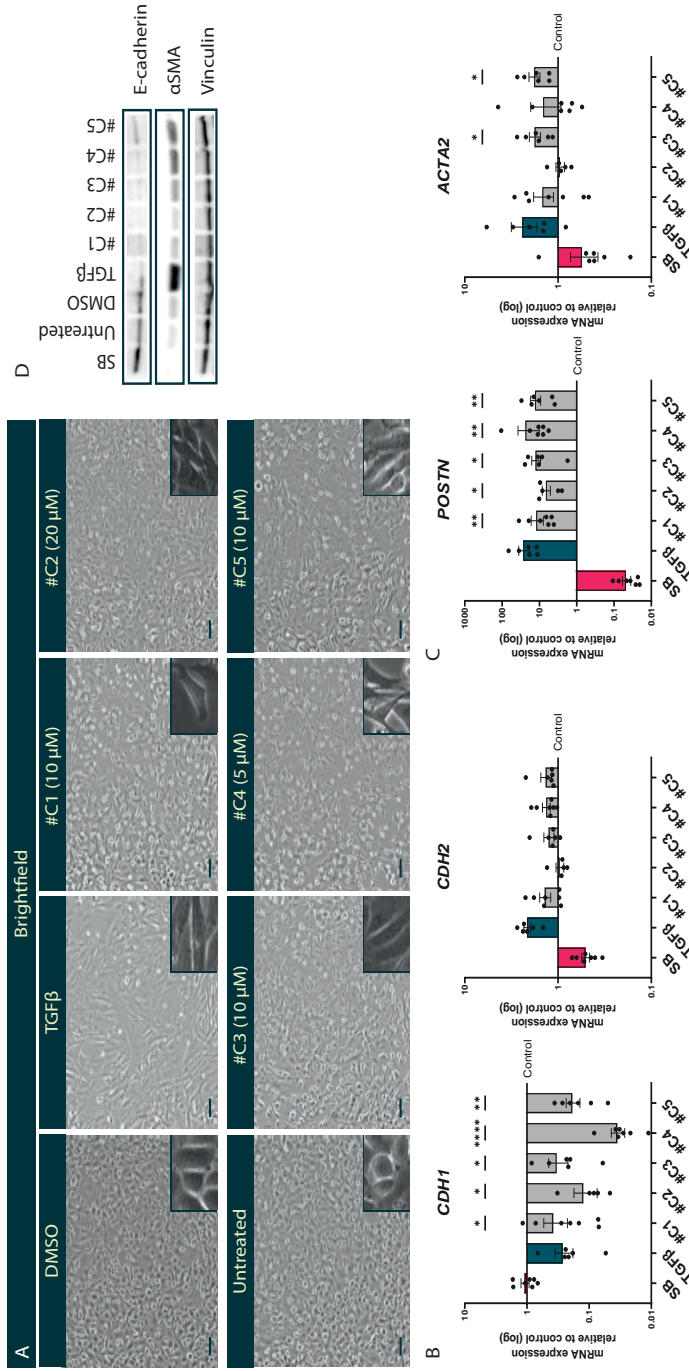


**Figure 3 | Identified hits induce EMT on molecular and protein level**

(A) Representative brightfield images of the five identified hits and their control conditions (n=7). Working concentration of each compound is displayed in the title. Scale bar: 100 μm. (B) mRNA expression levels for CDH1 and CDH2 relative to control (DMSO or mQ) determined in the five identified compounds after 5 days of stimulation (n=7, mixed-effects analysis, Sidak's multiple comparisons test, \* = p < 0.05, \*\* = p < 0.01, \*\*\* = p < 0.001, \*\*\*\* = p < 0.0001) (C) Representative western blot of protein expression levels for E-cadherin, αSMA and loading control Vinculin for the five identified compounds (n=3).

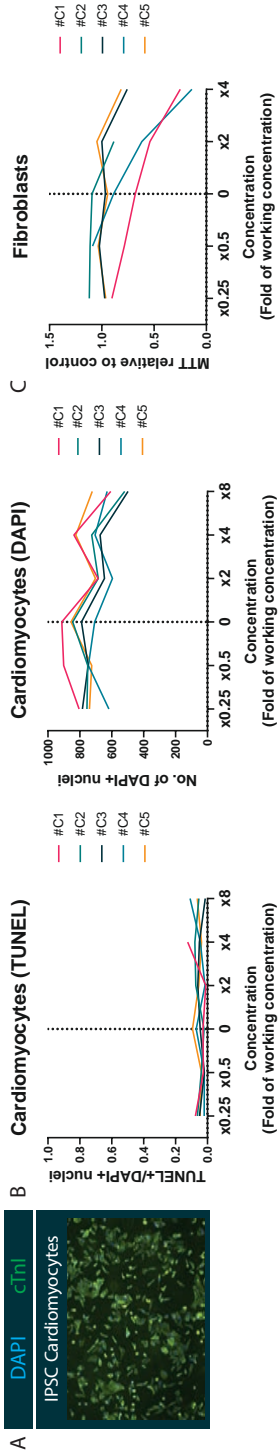


**Figure 4 | Identified compounds do not harm cardiomyocytes and fibroblasts in vitro**

(A) Representative picture of immunofluorescent staining for cTnI and DAPI of induced pluripotent stem cell (iPSC) derived cardiomyocytes. (B) Quantification of TUNEL staining of iPSCs-CMs exposed to increasing concentrations of the five identified compounds, displayed as the number of TUNEL+ nuclei divided by the number of DAPI+ nuclei (n=1). The number of DAPI+ nuclei are also separately displayed. Concentration is shown as fold of the working concentration. (C) Quantification of MTT assay on fetal cardiac fibroblasts exposed to increasing concentrations of the five identified compounds, displayed relative to their control (DMSO or mQ treated cells) (n=3). Concentration is displayed as fold of the working concentration.

To understand the underlying mechanism of epiMT induction, we focused on the known function of the identified compounds. TBBz is mostly described as an inhibitor of casein kinase 2 (CK2), which is present in many cell types including epicardial cells (Fig. S2) and has been related to EMT via FOXC2 (17). Interestingly, using an antibody against phosphorylated CK2 substrate, we did not observe an effect of TBBz on CK2 activity in epicardial cells (Fig. S2). The LOPAC1280 library includes a highly similar CK2 inhibitor, TBB, which did not induce  $\alpha$ SMA expression in any of our screens. Furthermore, another CK2 inhibitor, CX4945 did not induce epiMT to the same extent as TBBz. Altogether, our data indicates that TBBz elicits epiMT in a CK2 independent manner (Fig. S2).

M2 has been implicated in several processes, including liver X receptor  $\alpha$  (LXR $\alpha$ ) transcriptional activity, which has been associated with EMT (18). However, no effect of M2 on mRNA expression of LXR $\alpha$  was found in epicardial cells after 5 days of stimulation (Fig. S3).

In search of a epiMT inducing mechanism, we used an unbiased approach to investigate the direct effect of TBBz and M2 on three independent epicardial cell isolations by stimulating the cells for 3 hours and profiling all cell signaling processes using RNA sequencing (Fig. 5B). As controls, DMSO and TGF $\beta$  treated cells were included. The heatmap in Fig. 5C shows that both TGF $\beta$  and TBBz induce a strong and distinct response, displayed by a large number of differentially expressed genes compared to the DMSO treated samples and between these two conditions. TBBz induces a large set of DEGs (Fig. 5D), which are mainly involved in histone modification and histone lysine methylation (Fig. 5G). Zooming in on the specific genes that are involved in this reveals that genes encoding methyltransferases are downregulated by TBBz.

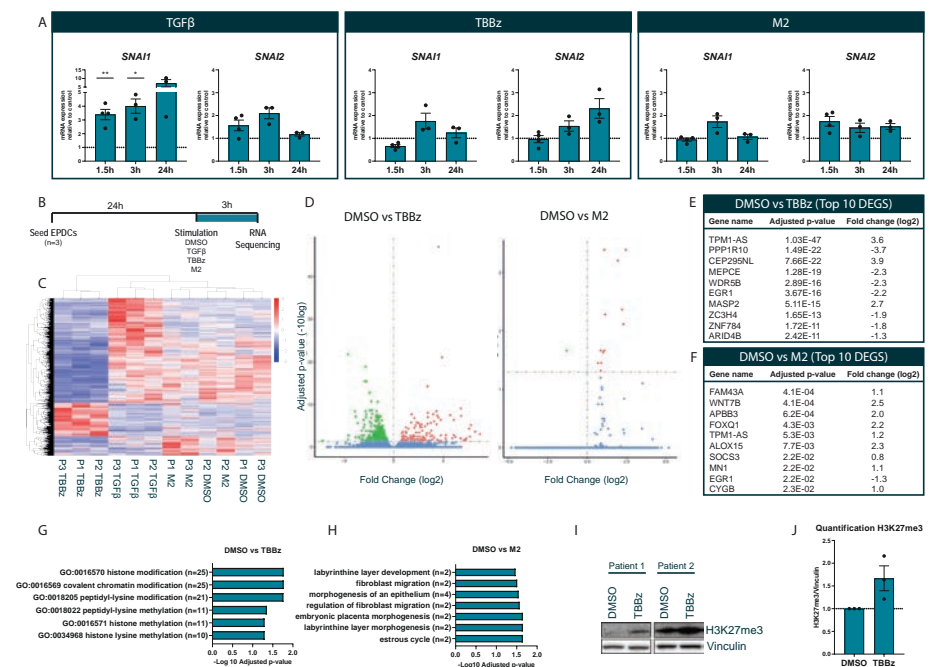


**Figure 5 | RNA sequencing reveals direct targets of TBBz and M2 in epicardial cells**

(A) mRNA expression levels for SNAI1 and SNAI2 in epicardial cells stimulated for 1.5, 3 or 24 hours with TGFβ, TBBz or M2 relative to control (n=3-4, mixed-effects analysis, Sidak's multiple comparisons test). (B) Schematic overview of experimental design. (C) Heatmap derived from RNA sequencing of three epicardial cell isolations (P1-P3) stimulated with DMSO, TGFβ+DMSO, TBBz or M2 for 3 hours. Samples and genes were clustered using the log2(FPKM+1) values. Red and blue indicate respectively high and low expression levels. (D) Volcano plot of differentially expressed genes (DEGs) of DMSO versus TBBz treated epicardial cells, and DMSO versus M2 stimulated epicardial cells. Green and red dots respectively indicate DEGs that are significantly downregulated or upregulated. (E) List of ten most significant DEGs of DMSO versus TBBz treated epicardial cells and their fold change difference. (F) List of ten most significant DEGs of DMSO versus M2 treated epicardial cells and their fold change difference. (G) Adjusted p-value of the significantly enriched GO terms in DMSO versus TBBz treated epicardial cells. Counts (n) indicate the number of differentially expressed genes concerning this GO term. (H) Adjusted p-value of the significantly enriched GO terms in DMSO versus M2 treated epicardial cells. Counts (n) indicate the number of differentially expressed genes concerning this GO term. (I) Representative western blot for protein expression levels of H3K27me3 and loading control Vinculin for epicardial cells derived from 2 patients treated with DMSO (n=3), TBBz (n=3) for 3 hours. (J) Quantification of the western blot in H for DMSO and TBBz conditions (n=3).

This suggests that TBBz may induce epiMT via epigenetic regulation. To further investigate this, we determined the effect of TBBz on H3K27 trimethylation (H3K27me3), a post-translational modification that has been related to EMT regulation (19). Although not significant, in three cell lines we observed an increase in H3K27me3 upon stimulation with TBBz (Fig. 5I and J). This was not observed by other epiMT-inducing stimulations, such as TGF $\beta$  (Fig. 54). In contrast to TBBz, M2 stimulations elicited only 14 DEGs (Fig. 5D). One gene that seemed particularly interesting in this setting was the upregulation of FOXQ1 (Fig. 5F), a known regulator of EMT but yet undescribed in epiMT. In summary, TBBz and M2 induce epiMT in a different manner than TGF $\beta$  does as they do not induce the same EMT-TF, nor do they exhibit a similar genetic profile 3h after stimulation. TBBz induces a large shift in the epigenetic landscape by increasing H3K27me3 causing a delayed upregulation of SNAI2 and induction of epiMT. M2 likely induces epiMT via upregulation of FOXQ1 and SNAI2.

4

## DISCUSSION

In this study, we developed a high throughput in vitro screening protocol using human primary epicardial cells and identified two novel inducers of epicardial epithelial to mesenchymal transition (epiMT).

To be able to perform a phenotypic screen, we exploited our previously described in vitro model in which human epicardial cells display a clear phenotypical switch between their epithelial and mesenchymal phenotype (14,15). The use of primary cells serves the benefit of representing the biological variability within the human epicardium and therefore is highly translational. This benefits over the difficulties that come with using human primary cells, such as the availability of cardiac tissue, and the challenge to achieve a sufficiently high number of cells to execute such a screen. As read-out, we selected a marker that provides a high contrast between the negative control (untreated) and the positive control (TGF $\beta$ ). The mesenchymal marker  $\alpha$ SMA turned out to be most distinctive, specifically the antibody offered by R&D (1c1420g).  $\alpha$ SMA is a marker for mesenchymal cells and more specifically for pericytes, myofibroblasts and smooth muscle cells. As with every antibody-based read-out, using  $\alpha$ SMA likely biased our results and consequently we may have missed epiMT inducing compounds which did not induce  $\alpha$ SMA. For example, basic fibroblast growth factor (BFGF) induces epiMT without the upregulation of  $\alpha$ SMA (20) and would not be picked up by our screening. Our list is therefore not exhaustive but nevertheless provided sufficient hits. To conclude, we provided a relatively easy and effective

model to study epicardial behavior which may pave the way for basic research or drug discovery in epiMT, and other epicardial read-outs such as proliferation, differentiation, and toxicity.

Using automated imaging, quantification of  $\alpha$ SMA expression, and subsequent validation, we initially selected five hits. Based on the description of these compounds provided by the LOPAC1280 library, we could not discover one common signaling pathway among these hits. In addition, the compound-induced mesenchymal cells displayed distinct morphologies. This suggests that the identified compounds do not directly or only indirectly activate the same pathway resulting in epiMT. Since epiMT is an intricate process, defined as plastic transition between two extremes with several intermediate stages (21), we found it essential to determine if the compounds induce full epiMT. Therefore, we used a variety of tests; we reported cell morphology, a decrease in epithelial markers and an increase in mesenchymal markers, both at the level of mRNA and protein and we show the presence of EMT transcription factors. This broad approach provided two reliable and robust epiMT inducers.

Research into epiMT has already established that TGF $\beta$ , Wnt and PDGF are its main regulators, mostly via WT1 but also other transcription factors such as TCF21 and SOX9 (reviewed in (22)). In our study, we identified two novel regulators. TBBz is a CK2 inhibitor and off target effects are barely described for this molecule. However, in our hands, we could not find an effect of TBBz on CK2 activity, and conversely other CK2 inhibitors did not elicit the same epiMT induction as TBBz. Although it is possible that this is due to technical issues, we consider that TBBz does not act on epiMT via CK2. Interestingly, RNA sequencing revealed that TBBz signals via downregulation of histone methyltransferases. The fact that EMT-TF SLUG is upregulated after 24 hours suggests that the changes in the epigenetic landscape lead to the upregulation of SLUG and consequently the induction of epiMT. Epigenetic regulation of epiMT has been described before (23–25). In addition to this, it has been shown that injury induces major changes in chromatin accessibility of epicardial cells in zebrafish which also points to a significant role for epigenetic regulation in injury-induced epicardial behavior (26). Interestingly, increased levels of KDM6A were shown to prevent epiMT *in vitro* by repressing H3K27Me3(24). This is in line with our data, showing that TBBz increases levels of H3K27Me3 and induces epiMT. Furthermore, protein arginine methyltransferase 1 (PRMT1) was shown to induce epiMT in the developing heart, most likely via SLUG (25). This demonstrates that histone modification, especially methyltransferases, are of relevance in epiMT regulation and can be exploited to target epiMT. For this, TBBz is a good starting point.

Oltipraz Metabolite M2 induces only a few genes and therefore seems to hit a more specific target. Within 1.5 hours, SLUG is upregulated and maintained over at least 24 hours. One of the differentially expressed genes in the first 3 hours is FOXQ1, a transcription factor that has been related to EMT (27) but not to the epicardium. Further experiments are required to determine which role FOXQ1 plays in M2-induced epiMT.

To conclude, it is feasible and effective to conduct a phenotypic high throughput compound screen using primary epicardial cells. Using this approach, we have identified two novel inducers of epiMT: TBBz, that induces histone modifications, and Oltipraz Metabolite M2 which increases FOXQ1.

## ACKNOWLEDGEMENT

We thank Lucia Clemens-Daxinger and Maja Vukic for their help with the H3K27me3 western blot.

## REFERENCES

1. Smits AM, Dronkers E, Goumans M-JJ. The epicardium as a source of multipotent adult cardiac progenitor cells: Their origin, role and fate. *Pharmacol Res.* 2018 Jan 24;127:129–40.
2. Gittenberger-de Groot AC, Vrancken Peeters M-PFM, Bergwerff M, Mentink MMT, Poelmann RE. Epicardial Outgrowth Inhibition Leads to Compensatory Mesothelial Outflow Tract Collar and Abnormal Cardiac Septation and Coronary Formation. *Circ Res.* 2000 Nov 24;87(11):969–71.
3. Lepilina A, Coon AN, Kikuchi K, Holdway JE, Roberts RW, Burns CG, et al. A Dynamic Epicardial Injury Response Supports Progenitor Cell Activity during Zebrafish Heart Regeneration. *Cell.* 2006;127(3):607–19.
4. Wang J, Cao J, Dickson AL, Poss KD. Epicardial regeneration is guided by cardiac outflow tract and Hedgehog signalling. *Nature.* 2015 Jun 4;522(7555):226–30.
5. Duan J, Gherghe C, Liu D, Hamlett E, Srikantha L, Rodgers L, et al. Wnt1/ $\beta$ catenin injury response activates the epicardium and cardiac fibroblasts to promote cardiac repair. *EMBO J.* 2012 Jan 18;31(2):429–42.
6. Smart N, Bollini S, Dubé KN, Vieira JM, Zhou B, Davidson S, et al. De novo cardiomyocytes from within the activated adult heart after injury. *Nature.* 2011;474(7353):640–4.
7. Pérez-Pomares JM, Macías D, García-Garrido L, Muñoz-Chápuli R. Contribution of the primitive epicardium to the subepicardial mesenchyme in hamster and chick embryos. *Dev Dyn.* 1997 Oct;210(2):96–105.
8. Martínez-Estrada OM, Lettice LA, Essafi A, Guadix JA, Slight J, Velecela V, et al. Wt1 is required for cardiovascular progenitor cell formation through transcriptional control of Snail and E-cadherin. *Nat Genet.* 2010 Jan 20;42(1):89–93.
9. Cano E, Carmona R, Ruiz-Villalba A, Rojas A, Chau Y-Y, Wagner KD, et al. Extracardiac septum transversum/proepicardial endothelial cells pattern embryonic coronary artery-venous connections. *Proc Natl Acad Sci.* 2016 Jan 19;113(3):656–61.
10. Liu Q, Zhang H, Tian X, He L, Huang X, Tan Z, et al. Smooth muscle origin of postnatal 2nd CVP is pre-determined in early embryo. *Biochem Biophys Res Commun.* 2016 Mar;471(4):430–6.
11. Quijada P, Trembley MA, Misra A, Myers JA, Baker CD, Pérez-Hernández M, et al. Coordination of endothelial cell positioning and fate specification by the epicardium. *Nat Commun.* 2021 Dec 6;12(1):4155.
12. Lavine KJ, Yu K, White AC, Zhang X, Smith C, Partanen J, et al. Endocardial and epicardial derived FGF signals regulate myocardial proliferation and differentiation in vivo. *Dev Cell.* 2005 Jan;8(1):85–95.
13. de Bakker DEM, Bouwman M, Dronkers E, Simões FC, Riley PR, Goumans M-J, et al. Prrx1b restricts fibrosis and promotes Nrg1-dependent cardiomyocyte proliferation during zebrafish heart regeneration. *Development.* 2021 Oct 1;148(19).

14. Moerkamp AT, Lodder K, van Herwaarden T, Dronkers E, Dingenouts CKE, Tengström FC, et al. Human fetal and adult epicardial-derived cells: a novel model to study their activation. *Stem Cell Res Ther.* 2016 Dec 29;7(1):174. A
15. Dronkers E, Moerkamp AT, van Herwaarden T, Goumans M-J, Smits AM. The Isolation and Culture of Primary Epicardial Cells Derived from Human Adult and Fetal Heart Specimens. *J Vis Exp.* 2018 Apr 24;134:e57370.
16. Maas RGC, Lee S, Harakalova M, Snijders Blok CJB, Goodyer WR, Hjortnaes J, et al. Massive expansion and cryopreservation of functional human induced pluripotent stem cell-derived cardiomyocytes. *STAR Protoc.* 2021 Mar;2(1):100334.
17. Golden D, Cantley LG. Casein Kinase 2 prevents mesenchymal transformation by maintaining Foxc2 in the cytoplasm HHS Public Access. *Oncogene.* 2015;34(36):4702–12.
18. Ji L, Zhang B, Zhao G. Liver X receptor  $\alpha$  (LXR $\alpha$ ) promoted invasion and EMT of gastric cancer cells by regulation of NF- $\kappa$ B activity. *Hum Cell.* 2017 Apr 16;30(2):124–32.
19. Segelle A, Núñez-Álvarez Y, Oldfield AJ, Webb KM, Voigt P, Luco RF. Histone marks regulate the epithelial-to-mesenchymal transition via alternative splicing. *Cell Rep.* 2022 Feb;38(7):110357.
20. Witty AD, Mihic A, Tam RY, Fisher SA, Mikryukov A, Shoichet MS, et al. Generation of the epicardial lineage from human pluripotent stem cells. *Nat Biotechnol.* 2014 Oct 21;32(10):1026–35.
21. Nieto MA, Huang RY-J, Jackson RA, Thiery JP. Emt: 2016. *Cell.* 2016;166(1):21–45.
22. Quijada P, Trembley MA, Small EM. The Role of the Epicardium During Heart Development and Repair. *Circ Res.* 2020 Jan;126(3):377–94.
23. Vieira JM, Howard S, Villa del Campo C, Bollini S, Dubé KN, Masters M, et al. BRG1-SWI/SNF-dependent regulation of the Wt1 transcriptional landscape mediates epicardial activity during heart development and disease. *Nat Commun.* 2017 Dec 24;8(1):16034.
24. Qureshi R, Kindo M, Boulberdaa M, von Hunolstein J-J, Steenman M, Nebigil CG. A prokineticin-driven epigenetic switch regulates human epicardial cell stemness and fate. *Stem Cells.* 2018 Jun 6;(Umr 7242).
25. Jackson-Weaver O, Ungvijanpunya N, Yuan Y, Qian J, Gou Y, Wu J, et al. PRMT1-p53 Pathway Controls Epicardial EMT and Invasion. *Cell Rep.* 2020 Jun 9;31(10).
26. Cao Y, Xia Y, Balowski JJ, Ou J, Song L, Safi A, et al. Identification of enhancer regulatory elements that direct epicardial gene expression during zebrafish heart regeneration. *Development.* 2022 Feb 15;149(4).
27. Qiao Y, Jiang X, Lee ST, Karuturi RKM, Hooi SC, Yu Q. FOXQ1 Regulates Epithelial-Mesenchymal Transition in Human Cancers. *Cancer Res.* 2011 Apr 15;71(8):3076–86.

## SUPPLEMENTARY FIGURES & TABLES

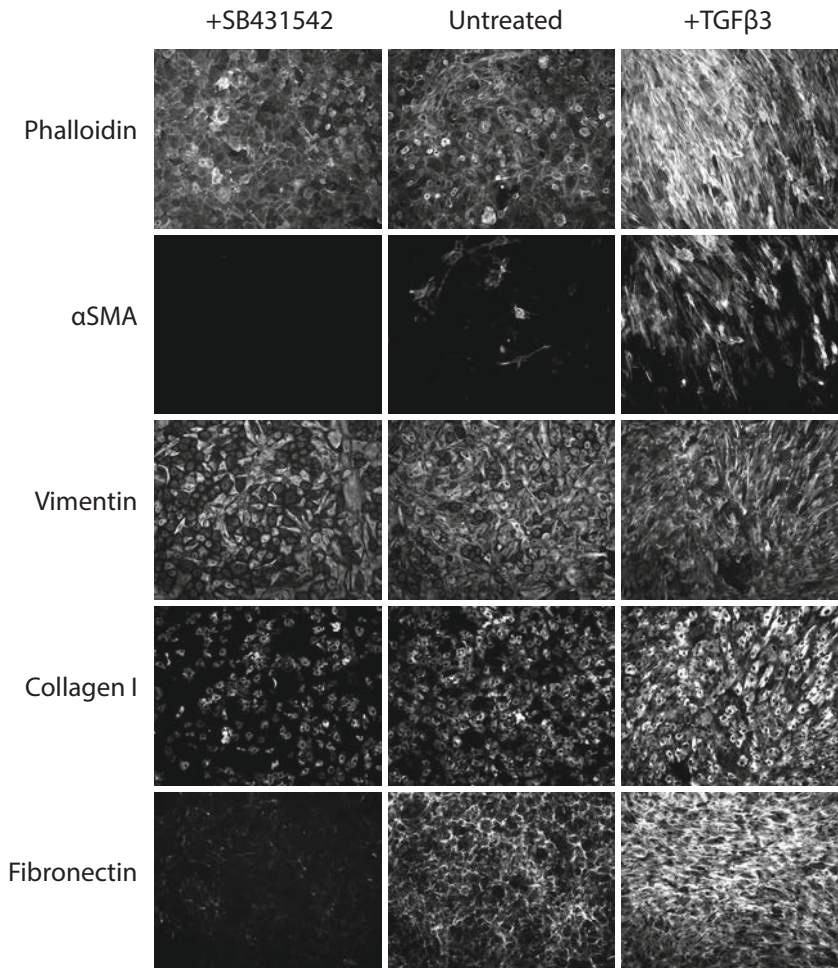


**Fig. S1 | αSMA immunostaining can be used as a read out for epiMT**

Representative immunostainings of epicardial cells that were treated with SB431542 (SB), TGFβ or with epicardial cell medium for 5 days.

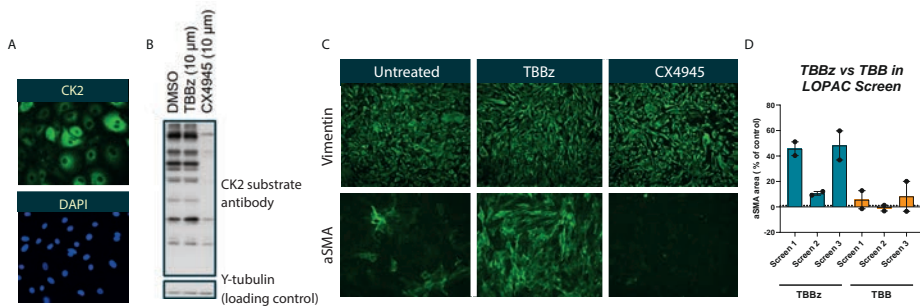


**Fig S2 | TBBz may not induce epiMT via CK2**

(A) Representative immunostaining for CK2 $\alpha$  in epicardial cells. (B) Representative image of western blot of epicardial cells treated with DMSO, TBBz, or CX4945 for 3 hours. The antibody against CK2 substrate phosphorylation indicates activity of CK2. Y-tubulin was used as loading control (n=3). (C) Representative immunostaining of epicardial cells which were treated for 5 days with TBBz or CX4945 or epicardial cell medium as control (n=3). (D) Results from LOPAC1280 screen in the three individual screens for TBBz and TBB.

4

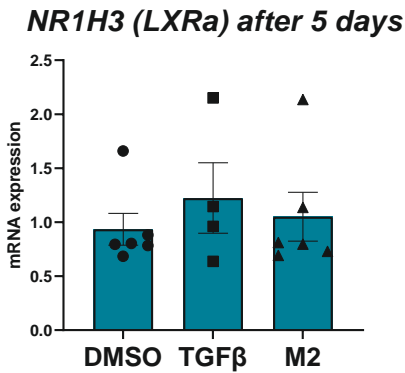


**Fig. S3 | M2 may not induce epiMT via LXR $\alpha$**

mRNA expression levels for NR1H3 in epicardial cells that were treated for 5 days with DMSO, TGF $\beta$  or M2 (n=3).

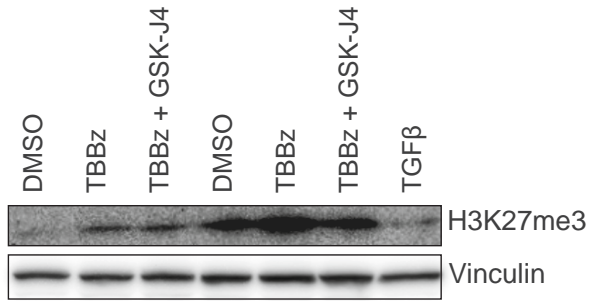


Fig. S4 | Effect of TBBz on H3K27me3 levels. Controls corresponding to Figure 5I. Western blot of protein expression levels for H3K27me3 and loading control Vinculin for epicardial cells treated with DMSO (n=3), TBBz (n=3), TBBz+GSK-J4 (n=2), or TGFβ (n=1) for 3 hours.

Supplementary Table 1 | Selection Screen 1

Screen	Compound ID	SMA (Relative to Control %)	Compound Name	Description
1	431	105,1	2',3'-dideoxycytidine	Nucleoside analog; reverse transcriptase inhibitor; antiviral
1	1399	76,2	Oltipraz metabolite M2	Oltipraz metabolite M2 acts as a potent inhibitor of LXRa transcriptional activity, and also AMPK activator inducing the phosphorylation of AMPK.
1	917	76,0	8-Methoxymethyl-3-isobutyl-1-methylxanthine	Selective inhibitor of Ca <sup>2+</sup> -calmodulin-dependent phosphodiesterase (PDE I)
1	777	64,2	LY-367,265	Inhibits serotonin reuptake; 5-HT <sub>2A</sub> serotonin receptor antagonist
1	15	57,8	PD 0325901	PD 0325901 is a potent MKK1 (MEK1) and MKK2 (MEK2) inhibitor
1	832	57,6	Ivermectin	Positive allosteric modulator of alpha7 neuronal nicotinic acetylcholine receptor; also modulates glutamate-GABA-activated chloride channels
1	152	54,7	Alaproclate hydrochloride	Potent and selective serotonin reuptake inhibitor
1	799	54,0	Ketoconazole	Potent inhibitor of cytochrome P450c17 enzyme; antifungal agent
1	416	53,2	Carvedilol	Antihypertensive; cardioprotective
1	508	51,7	3-deazaadenosine	Antiviral
1	1041	50,3	Nortriptyline hydrochloride	Tricyclic antidepressant
1	779	49,3	CP-154526 hydrochloride	CP-154526 is a selective, non-peptide antagonist of corticotropin releasing factor receptors (CRF1).

Supplementary Table 1 (Continued)

Screen	Compound ID	SMA (Relative to Control %)	Compound Name	Description
1	1413	46,8	PD-166866	PD-166866 is a selective inhibitor of the FGF-1 receptor tyrosine kinase (FGFR1) with IC50 = 55 nM, and no effect on c-Src, PDGFR- $\beta$ , EGFR or insulin receptor tyrosine kinases or MEK, PKC, and CDK4.
1	862	45,3	L-687,384 hydrochloride	Putative sigma-1 receptor agonist
1	796	44,7	L-N6-(1-Iminoethyl)lysine hydrochloride	Selective inducible nitric oxide synthase (iNOS) inhibitor.
1	778	44,2	Leflunomide	Immunosuppressive; its metabolite, a malonitrile derivative, inhibits dihydroorotate dehydrogenase (in the de novo pyrimidine synthesis pathway) and several protein tyrosine kinases
1	773	44,0	m-Iodobenzylguanidine hemisulfate	Antitumor agent which inhibits ADP ribosylation; induces changes in the mitochondrial membrane potential, activation of caspase-3 and DNA fragmentation
1	167	43,9	TBBz	Cell-permeable casein kinase 2 (CK2) inhibitor.
1	958	43,1	Eupatorin	Eupatorin acts as an antiproliferative in cells expressing the CYP1A- family. It induces G2/M block follow by apoptosis in cells expressing the CYP1A- family
1	1070	42,2	Nimodipine	Potent L-type Ca <sup>2+</sup> channel antagonist
1	774	42,1	Imetit dihydrobromide	Potent and selective H3 histamine receptor agonist

Supplementary Table 1 (Continued)

Screen	Compound ID	SMA (Relative to Control %)	Compound Name	Description
1	795	41,8	Rizatriptan benzoate salt	Rizatriptan is a serotonin 5HT-1B/1D-receptor agonist used to treat migraine
1	557	41,1	Dipyridamole	Coronary vasodilator; adenosine transport inhibitor
1	854	40,9	(±)-Isoproterenol hydrochloride	Sympathomimetic amine acting almost exclusively on beta adrenoceptors; bronchodilator
1	621	40,9	Fluspirilene	Dopamine receptor antagonist; antipsychotic
1	643	40,8	5-Fluorouracil	Thymidylate synthetase inhibitor; leads to accumulation of cells in S phase
1	322	40,4	Caffeic acid phenethyl ester	NFKB inhibitor
1	775	39,7	Agomelatine	Agomelatine is an extremely potent agonist at both melatonin receptors (MT1 and MT2), with additional antagonism at 5HT2C
1	801	38,3	Olvanil	Vanilloid receptor agonist
1	250	38,2	ML-9	Myosin light chain kinase (MLCK) inhibitor

Supplementary Table 2 | Selection Screen 2

Screen	Compound ID	SMA (Relative to Control %)	Compound Name	Description
2	1197	97,7	Phenamyl methanesulfonate	Irreversible inhibitor of amiloride-sensitive Na <sup>+</sup> channels; derivative of amiloride
2	1399	84,3	Oltipraz metabolite M2	Oltipraz metabolite M2 acts as a potent inhibitor of LXRα transcriptional activity, and also AMPK activator inducing the phosphorylation of AMPK.
2	1514	69,8	Tyrphostin AG 538	Insulin growth factor 1 (IGF-1) receptor protein tyrosine kinase inhibitor
2	1121	58,2	SB 216763	Potent, selective, cell permeable inhibitor of glycogen synthetase kinase-3 (GSK-3).
2	628	52,1	Phenserine	Selective, non-competitive acetylcholinesterase (AChE) inhibitor.
2	1149	50,8	R(-)-N6-(2-Phenylisopropyl) adenosine	A1 Adenosine receptor agonist
2	580	42,8	(-)-Physostigmine	Cholinesterase inhibitor
2	271	42,4	BTCP hydrochloride	Selective blocker of dopamine reuptake
2	1065	38,8	CID 11210285 hydrochloride	CID 11210285 is a cell-permeable, potent and selective activator of Wnt signaling without inhibiting GSK-3β.
2	885	36,3	6-Methyl-2-(phenylethynyl)pyridine hydrochloride	Highly selective, non-competitive mGluR5 metabotropic glutamate receptor antagonist
2	1156	35,3	PD-184161	PD-184161 is a MEK inhibitor.
2	1222	30,2	SMER28	Small molecule modulator of mammalian autophagy.
2	1533	23,0	CP-135807	CP-135807 is a selective 5-HT1D agonist

Supplementary Table 2 (Continued)

Screen	Compound ID	SMA (Relative to Control %)	Compound Name	Description
2	748	22,6	Bendamustine hydrochloride	DNA-alkylator with a distinct pattern of activity. Bendamustine activates DNA-damage stress response and apoptosis; inhibits mitotic checkpoints; and induces mitotic catastrophe.
2	869	22,4	PF-429242 dihydrochloride	PF-429242 is a potent inhibitor of S1P (cellular proprotein convertase sterol regulatory element-binding protein (SREBP) site 1 protease).
2	290	20,1	Icaritin	Enhances osteoblastic differentiation of mesenchymal stem cells (MSCs) while it inhibits adipogenic differentiation of MSCs by inhibiting PPAR-gamma pathway.
2	1002	19,6	Levetiracetam	Anticonvulsant; antiepileptic; exact mechanism of action is unclear but may be related to a synaptic vesicle protein.
2	1111	18,9	LP44	A high affinity 5-HT7 receptor agonist.
2	35	18,8	Atropine methyl bromide	Competitive muscarinic acetylcholine receptor antagonist
2	666	18,6	Fluphenazine dihydrochloride	Dopamine receptor antagonist; antipsychotic
2	1241	17,7	Prochlorperazine dimaleate	Antipsychotic agent; used in the treatment of spastic gastrointestinal disorders
2	1267	17,2	(+)-CP-99994 dihydrochloride	(+)-CP-99994 is a selective neurokinin (NK)-1 tachykinin antagonist.
2	568	14,6	SP600125	Selective c-Jun N-terminal kinase (c-JNK) inhibitor.
2	292	14,2	Carbachol	Acetylcholine receptor agonist

Supplementary Table 2 (Continued)

Screen	Compound ID	SMA (Relative to Control %)	Compound Name	Description
2	1250	13,7	Ritodrine hydrochloride	beta2-Adrenoceptor agonist; relaxes uterine muscle contractions
2	1509	12,1	EMPA	EMPA is a potent, selective OX2R antagonist
2	167	12,1	TBBz	Cell-permeable casein kinase 2 (CK2) inhibitor.
2	298	11,4	Chlorpromazine hydrochloride	Dopamine receptor antagonist; anti-emetic; antipsychotic
2	800	11,0	L-701,324	Selective antagonist at the glycine site of the NMDA glutamate receptor
2	650	10,9	RepSox	RepSox Inhibits TGF-beta receptor signaling. Retroviral transduction of Sox2, Oct4, and Klf4 genes results in direct reprogramming of somatic cells into induced pluripotent stem cells (iPSCs).

Supplementary Table 3 | Selection Screen 3

Screen	Compound ID	SMA (Relative to Control %)	Compound Name	Description
3	290	171,9	Icaritin	Enhances osteoblastic differentiation of mesenchymal stem cells (MSCs) while it inhibits adipogenic differentiation of MSCs by inhibiting PPAR-gamma pathway.
3	105	138,3	Acetohexamide	Stimulates insulin release
3	617	135,8	Sunitinib malate	Sunitinib malate is a receptor tyrosine kinase inhibitor, which targets VEGF-R1, VEGF-R2, VEGF-R3, PDGF-Ra, PDGF-Rβ, KIT, FLT3, CSF-1R, and RET. Sunitinib malate is an anticancer drug.
3	267	129,2	Bepridil hydrochloride	Non-selective Ca <sup>2+</sup> channel blocker which stimulates the binding of 1,4-dihydropyridine-based drugs to Ca <sup>2+</sup> channels; anti-anginal
3	430	112,5	(-)-alpha-Methylnorepinephrine	Active enantiomer; adrenoceptor agonist; vasoconstrictor; antihypertensive
3	94	106,4	2-Hydroxysaclofen	GABA-B receptor antagonist
3	460	101,0	Chlormezanone	Anxiolytic; muscle relaxant
3	278	99,1	DL-Buthionine-[S,R]-sulfoximine	Glutathione synthesis inhibitor
3	104	97,1	1-Allyl-3,7-dimethyl-8-p-sulfophenylxanthine	Weak A2 adenosine receptor antagonist; water soluble
3	1121	95,9	SB 216763	Potent, selective, cell permeable inhibitor of glycogen synthetase kinase-3 (GSK-3).
3	740	91,5	L-165,041	Peroxisome proliferator-activated receptor (PPAR) gamma agonist.
3	1172	90,4	BF-170 hydrochloride	Exhibits 3-fold greater binding affinity to tau than amyloid beta fibrils. Does not inhibit amyloid beta.

Supplementary Table 3 (Continued)

Screen	Compound ID	SMA (Relative to Control %)	Compound Name	Description
3	1458	63,5	U-74389G maleate	Free radical lipid peroxidation inhibitor
3	1409	57,5	TCPOBOP	Constitutive androstane receptor (CAR) agonist; most potent known member of the phenobarbital-like class of CYP-inducing agents
3	140	53,3	1-Amino-1-cyclohexanecarboxylic acid hydrochloride	Synthetic amino acid that crosses the blood-brain barrier by the Large Neutral Amino Acid carrier system
3	1386	50,7	Tetradecylthioacetic acid	Peroxisome proliferator-activated receptor (PPAR)-alpha agonist
3	987	49,5	H-8 dihydrochloride	Potent inhibitor of cAMP- and cGMP-dependent protein kinase
3	476	48,4	N,N,N',N'-Tetramethylazodicarboxamide	Thiol-oxidizing agent
3	247	47,5	BMY 7378 dihydrochloride	Partial 5-HT1A serotonin receptor agonist; alpha1D adrenoceptor antagonist
3	1384	46,9	SDZ-205,557 hydrochloride	Potent and selective 5-HT4 serotonin receptor antagonist
3	1240	45,8	Ammonium pyrrolidinedithiocarbamate	Prevents induction of nitric oxide synthase (NOS) by inhibiting translation of NOS mRNA
3	107	43,9	2,3-Butanedione monoxime	Blocks ATP-sensitive K+ channels
3	248	43,8	BRL 54443 maleate	Potent 5-HT1E/1F serotonin receptor agonist
3	1383	43,8	SR-95531	Specific GABA-A receptor antagonist; does not affect GABA-transaminase or glutamate-decarboxylase activities.
3	418	43,7	S(-)-Pindolol	Beta adrenergic receptor antagonist; vasodilator. Non-selective 5-HT1 serotonin receptor ligand.

Supplementary Table 3 (Continued)

Screen	Compound ID	SMA (Relative to Control %)	Compound Name	Description
3	944	42,7	Melatonin	Endogenous neurohormone which controls photo-periodic biological rhythms
3	1072	41,8	Oleic Acid	Activates protein kinase C in hepatocytes; uncouples oxidative phosphorylation
3	1181	41,7	Pergolide methanesulfonate	Dopamine receptor agonist; antiparkinsonian
3	269	41,4	Alfuzosin hydrochloride	alpha-adrenergic blocker used to treat benign prostatic hyperplasia (BPH)
3	447	40,4	(±)-CGP-12177A hydrochloride	Mixed beta adrenoceptor agonist/antagonist

Supplementary Table 4 | Selection Overlapping hits

Compound ID	SMA Screen 1 (Relative to Control %)	SMA Screen 2 (Relative to Control %)	SMA Screen 3 (Relative to Control %)	Compound Name	Description
15	57.8	9.9	38.2	PD 0325901	PD 0325901 is a potent MKK1 (MEK1) and MKK2 (MEK2) inhibitor
167	34.5	12.1	59.7	TBBz	Cell-permeable casein kinase 2 (CK2) inhibitor.
290	11.8	20.1	171.9	Icaritin	Enhances osteoblastic differentiation of mesenchymal stem cells (MSCs) while it inhibits adipogenic differentiation of MSCs by inhibiting PPAR-gamma pathway.
446	13.1	10.6	73.2	CP-91149	CP-91149 is a selective glycogen phosphorylase inhibitor.
508	51.7	10.3	16.7	3-deazaadenosine	Antiviral
676	-1.5	10	83.1	MHPG piperazine	Norepinephrine metabolite
869	35.6	17.7	1.9	PF-429242 dihydrochloride	PF-429242 is a potent inhibitor of SIP (cellular proprotein convertase sterol regulatory element-binding protein (SREBP) site 1 protease).
917	76	-2.2	35.8	8-Methoxymethyl-3-isobutyl-1-methylxanthine	Selective inhibitor of Ca <sup>2+</sup> -calmodulin-dependent phosphodiesterase (PDE I)
1121	19.6	58.2	95.9	SB 216763	Potent, selective, cell permeable inhibitor of glycogen synthetase kinase-3 (GSK-3).

Supplementary Table 4 (Continued)

Compound ID	SMA Screen 1 (Relative to Control %)	SMA Screen 2 (Relative to Control %)	SMA Screen 3 (Relative to Control %)	Compound Name	Description
1399	76.2	84.3	8.4	Oltipraz metabolite M2	Oltipraz metabolite M2 acts as a potent inhibitor of LXR $\alpha$ transcriptional activity, and also AMPK activator inducing the phosphorylation of AMPK.



# 5

## Epicardial TGF $\beta$ and BMP Signaling in Cardiac Regeneration: What Lesson Can We Learn from the Developing Heart?

Esther Dronkers<sup>1</sup>, Manon M. M. Wauters<sup>1</sup>, Marie José Goumans<sup>1</sup>,  
and Anke M. Smits<sup>1</sup>

<sup>1</sup>Department of Cell and Chemical Biology, Leiden University Medical Center,  
Leiden, The Netherlands.

*Published in Biomolecules (2020) doi: 10.3390/biom10030404*

## ABSTRACT

The epicardium, the outer layer of the heart, has been of interest in cardiac research due to its vital role in the developing and diseased heart. During development, epicardial cells are active and supply cells and paracrine cues to the myocardium. In the injured adult heart, the epicardium is re-activated and recapitulates embryonic behavior that is essential for a proper repair response. Two indispensable processes for epicardial contribution to heart tissue formation are epithelial to mesenchymal transition (EMT), and tissue invasion. One of the key groups of cytokines regulating both EMT and invasion is the transforming growth factor  $\beta$  (TGF $\beta$ ) family, including TGF $\beta$  and Bone Morphogenetic Protein (BMP). Abundant research has been performed to understand the role of TGF $\beta$  family signaling in the developing epicardium. However, less is known about signaling in the adult epicardium. This review provides an overview of the current knowledge on the role of TGF $\beta$  in epicardial behavior both in the development and in the repair of the heart. We aim to describe the presence of involved ligands and receptors to establish if and when signaling can occur. Finally, we discuss potential targets to improve the epicardial contribution to cardiac repair as a starting point for future investigation.

### Keywords

Epicardium, TGF $\beta$ , BMP, EMT, invasion, cardiac development, cardiac repair

## 1. INTRODUCTION: THE EPICARDIAL TIMELINE

The epicardium, a mesothelial layer covering the heart, has been recognized as a distinct structure for a long time, whilst its origin and function remained uncertain. Until halfway through the 20th century, the general consensus was that epicardial cells originated from the myocardium. Even though Kurkiewicz [1] discovered in 1909 that epicardial cells derive from an extra-cardiac source, we know today as the pro-epicardium (PE), this finding was neglected for several decades until it was confirmed by Manasek in 1969 [2]. In the 30 years following, the epicardium has been described by multiple observational studies in various animal species ranging from quail to hamster [3,4,5]. Nevertheless, it took until the end of the 20th century for the functional role of the epicardium to be revealed; retrovirally-labeled PE cells were traced over time and were eventually observed within the myocardium, suggesting that the epicardium contributes cells to the developing heart [6,7]. A comparable labeling approach showed that epicardial cells within the epicardium undergo epithelial to mesenchymal transition (EMT), migrate into the heart and locally become vascular smooth muscle cells and cardiac fibroblasts [8]. Over the last years, extensive research established that epicardial cells are for instance involved in stabilization of the vasculature [9], formation of the conduction system [10], and the process of myocardial compaction [11,12]. The importance of the epicardium was demonstrated when formation of the epicardium was impeded, causing severe cardiac effects such as a thin-walled myocardium and defective coronary vasculature [13,14].

In the adult mammalian heart, the epicardium as a single mesothelial cell layer displays little activation. Interestingly, this 'quiescence' is not necessarily indefinite. An important observation was made in 2006 when Lepilina et al. found that injury reactivated the epicardial layer in the zebrafish heart. This process resembled embryonic epicardial activation, and was shown to be essential for regeneration of the adult zebrafish heart [15]. To further assess the potential of the adult epicardium, *in vitro* models were established for adult mouse [16], and human [17] epicardial cells. These cell culture models revealed that adult cells retain the capacity to undergo EMT. However, *in vivo* these activation processes of EMT and subsequent migration and cell type differentiation seem to occur less efficient in the adult heart compared to the developing heart. For instance, in the adult heart there appears to be limited migration of epicardial derived cells into the injured myocardium [18,19]. This observation created a window of opportunity to boost the epicardial response to improve cardiac regeneration, which has emerged as an area of active research.

During cardiac repair in organ-regenerating animals, e.g., the newt and zebrafish, several vital processes such as cardiomyocyte proliferation [20], and blood vessel formation [21] are governed by recapitulation of developmental processes. This is in line with the general tissue regeneration paradigm that initiation of a fetal gene program is at the foundation of the endogenous regenerative response, as was also shown for e.g., mammalian axons and bone [22,23]. Therefore, to fully understand how the epicardium can be exploited to improve repair of the injured heart, it is important to comprehend its behavior during development and to unravel the signals steering this process. A signaling pathway that is involved in many processes underlying epicardial behavior is the transforming growth factor (TGF)  $\beta$  pathway. This family of growth factors, well known for its role in EMT and invasion of cells of different origins [24], is considered to be important for epicardial cell behavior during development and is therefore a potential target for rejuvenating the adult epicardium. The aim of this review is to provide one of the first comprehensive overviews of current knowledge of TGF $\beta$  family signaling in the embryonic epicardium and to discuss to what extent this response is recapitulated in the injured adult heart. We aim to achieve this in a structured approach, discussing the presence of ligands, associated receptors, and signaling for distinct components of the signaling family. Finally, we will discuss potential targets to improve the epicardial contribution to cardiac repair as a starting point for future investigation.

## 2. TGF $\beta$ FAMILY SIGNALING OVERVIEW

The TGF $\beta$  family is a large group of proteins named after the cytokine that was described first [25], the polypeptide presently known as TGF $\beta$ 1. The family has multiple members including TGF $\beta$ s, bone morphogenetic proteins (BMPs), activins/inhibins, and growth and differentiation factors (GDFs). The TGF $\beta$  family components are critical during development and disease as its proteins are involved in the regulation of essential cellular processes including proliferation, differentiation, adhesion, and apoptosis (reviewed in [26]). Signaling occurs via an intricate system of ligands, receptors, and intracellular molecules. The TGF $\beta$  family can roughly be divided into two clusters: a TGF $\beta$  cluster and a BMP cluster, which are schematically depicted in Figure 1. TGF $\beta$  and activin ligands bind to specific receptor combinations that induce the phosphorylation of SMAD2/3, while BMPs bind to receptor combinations that result in phosphorylation of SMAD1/5/8. The phosphorylated SMADs form a complex with SMAD4 and translocate to the nucleus to induce gene transcription (see Figure 1).

Multiple mechanisms ensure that the signaling cascade is highly controlled at all levels, which we will discuss separately below.

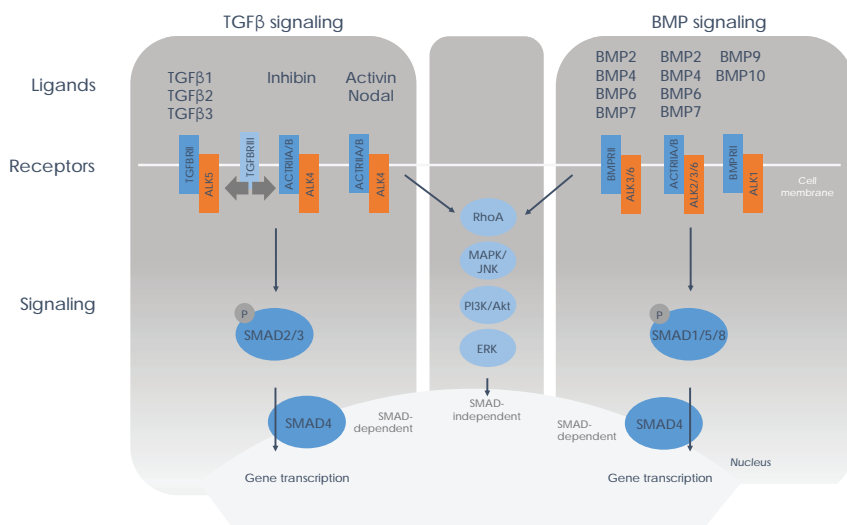


**Figure 1 | Schematic overview of TGF $\beta$  family signaling.** TGF $\beta$  family signaling can be divided into two clusters: TGF $\beta$ - (left) and BMP- (right) signaling. TGF $\beta$ 1, -2 and -3 bind the TGF $\beta$  receptor II and activate signaling via type I receptor ALK5. Activin, nodal and inhibin can bind to the activin receptor IIA or IIB and propagate signaling via ALK4. Signaling via ALK4 and ALK5 leads to phosphorylation of SMAD2/3. Upon binding to SMAD4, this SMAD complex translocates to the nucleus to initiate gene transcription. Of note is that ALK7 (not displayed) can also initiate signaling via SMAD2/3, but this type I receptor is assumed to be unimportant in epicardial behavior. On the BMP side, BMPs can bind to either the activin receptor IIA or IIB, or to the BMP type II receptor, that can activate the signaling cascade via ALK2, -3 or -6, or via ALK1. Signaling via ALK1/2/3/6 results in phosphorylation of SMAD1/5/8 which, after binding to SMAD4, translocates to the nucleus and starts gene transcription. Besides the described SMAD-dependent pathways, both TGF $\beta$  and BMP pathways can activate SMAD-independent pathways, shown in the middle panel.

TGF $\beta$  family ligands are secreted as a complex where the active growth factor is bound to a prodomain. TGF $\beta$  family members can signal in an autocrine or paracrine fashion. Upon secretion, TGF $\beta$  ligands can be stored in the extracellular matrix (ECM) by binding to heparin, or to latent TGF $\beta$  binding protein (LTBP), thereby preventing the association of the ligand with its receptor and controlling ligand bioavailability (reviewed in [27]). Activation of the latent TGF $\beta$  ligands, more specifically TGF $\beta$ 1-3, may be controlled by release of the pro-domain by the extracellular environment [28], for example by furin-mediated cleavage [29]. Additionally, as shown for BMP7,

the pro-domain can also be replaced by the type II receptor enabling the receptor to bind to the growth factor domain [30]. However, the presence of the BMP pro-domain does not compromise the biological activity of several of the BMP ligands, including BMP4, 5, 7, 9 and BMP10 [31,32,33].

After the ligands are released from the ligand binding proteins, they bind to a TGF $\beta$  family receptor complex (reviewed in [34]). These receptors are subdivided into three groups: type II receptors (TGF $\beta$ RII, BMPRII, ACTR2A or ACTR2B), type I receptors (activin receptor like kinase (ALK) 1-7) and type III receptors (endoglin and TGF $\beta$ R3). Each ligand of the TGF $\beta$  family binds to a specific combination of type I and a type II receptors, which are both essential for downstream signaling. More specifically, the ligand binds two type II receptors and two type I receptors, in order of highest affinity, to ultimately form a heterotetrameric complex. Subsequently, the type II receptor kinase activates the type I receptor. The type I receptor propagates the signal from the membrane to the nucleus by phosphorylation of receptor-mediated SMADs (R-SMADs). There are two main signal transduction cascades: either via phosphorylation of SMAD2 or -3 or via phosphorylation of SMAD1, -5 or -8. Hence, the type I receptors are subdivided into two clusters: the TGF $\beta$  cluster, in which the type I receptors ALK4 or ALK5 propagate the signal via phosphorylation of SMAD2/3, and the BMP cluster, whose type I receptors ALK2, -3 or -6 phosphorylate SMAD1/5/8 (see Figure 1). The phosphorylation of R-SMADs initiates the formation of a complex that consists of two R-SMADs and one common SMAD (co-SMAD), which is also called SMAD4 (reviewed in [35]). After translocation of the R-SMAD/SMAD4 complex into the nucleus, SMADs interact with DNA and other transcription factors to regulate gene expression. Besides receptor regulated SMADs, there are inhibitory SMADs (I-SMADs), SMAD6 and SMAD7, that negatively regulate TGF $\beta$  signaling through competing with the R-SMADs for type I receptor binding and via regulation of receptor degradation (reviewed in [36]), allowing for yet another level in signal regulation.

Of course, there are exceptions to the general division in a TGF $\beta$  and a BMP cluster; in some cases, BMPs can induce SMAD2/3 phosphorylation or TGF $\beta$  can induce SMAD1/5/8 phosphorylation [37,38]. This can be due to an aberrant composition of type I receptors in the heterotetrameric complex, e.g., TGF $\beta$  ligand can initiate SMAD1/5/8 phosphorylation when the type I receptor complex consists of a heterodimer of ALK5 and ALK1 [39]. This cross-phosphorylation can be due to the presence of TGF $\beta$  type III receptors in the receptor complex. These accessory receptors have a transmembrane domain, similar to the type II receptors, but lack the intracellular kinase domain that is essential for activation of the type I receptor. Type III receptors

are therefore not able to initiate signaling themselves, but can modulate signaling by type II receptors.

Besides signaling in a SMAD-dependent manner, TGF $\beta$  is also able to exert biological effects by activation of SMAD-independent pathways (see Figure 1). One of these pathways is Rho GTPase signaling, which is known for its role in actin reorganization, an essential part of EMT. Other pathways involved are MAPK associated, including ERK, JNK, and p38 MAPK, and the PI3K/Akt pathway (reviewed in [40]). Activation of SMAD-independent pathways can be provoked by both TGF $\beta$  and BMP ligands.

Overall, the TGF $\beta$  family of signaling components provides a broad range of responses that can be regulated on multiple levels. The highly regulated availability of ligands, and the presence of specific combinations of receptors on the cell surface determine if a cell is able to activate the signaling cascade. On top of this, type III receptors and interaction with SMAD-independent pathways can modulate the signal.

### 3. EPICARDIUM IN DEVELOPMENT AND DISEASE

As mentioned previously, the epicardium plays an essential role in the formation of the heart. Cardiac development starts with the formation of a bilayered linear heart tube consisting of a myocardial layer lined by the endocardium on the luminal side. The heart tube follows a sequence of looping events during embryonic day 9 (E9) in the mouse, which corresponds to week 3–4 of human development, ultimately resulting in the formation of a four chambered heart. From E9.5 onwards, cells from the pro-epicardium (PE), a cell cluster located at the venous inflow tract, migrate towards the heart and proliferate to cover the bare myocardium with a third cardiac layer: the epicardium [41]. By E11.5, the epicardial cells have enveloped the heart and at this point display a cuboidal epithelial phenotype [42], characterized by the expression of cell adhesion molecules such as E-cadherin and  $\beta$ -catenin, that ascertain integrity of the layer and the maintenance of an apical-basal polarity [43]. Furthermore, the epicardial cells express Wilms' tumor 1 (WT1) and retinaldehyde dehydrogenase 2 (RALDH2) [44], proteins that are often used as markers for activated epicardium. Then, a subset of the activated epicardial cells undergoes EMT [5,45] (Figure 2). During EMT, the cells lose their epithelial phenotype by disruption of their cell adhesion profile and rearrangement of their cytoskeletal organization, enabling them to detach from neighboring cells and become motile. Additionally, the cells acquire functional mesenchymal characteristics, such as the ability to secrete extracellular matrix (ECM) proteins.

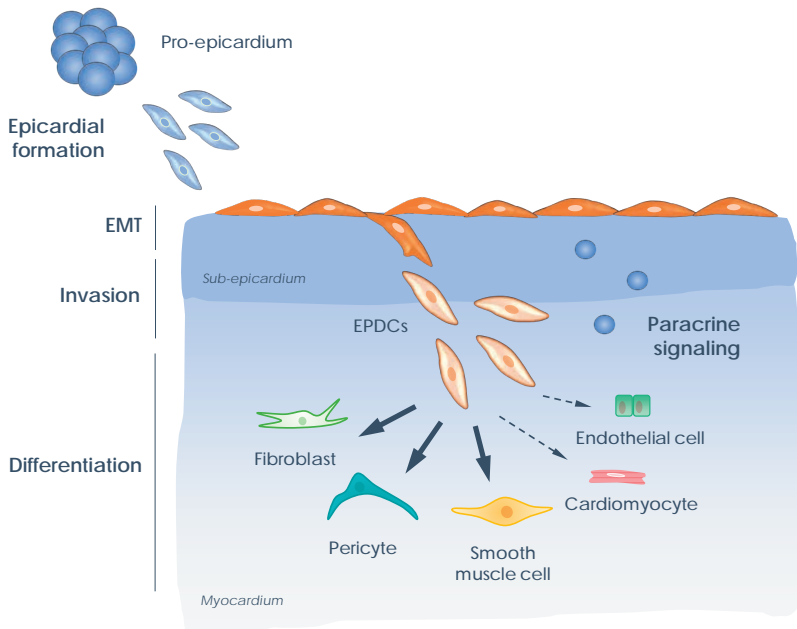


**Figure 2 | Schematic overview of epicardial behavior during development.** Pro-epicardial cells migrate towards the heart and cover it to form the epicardium. When the epicardium has enveloped the heart, cells start to undergo epithelial to mesenchymal transition (EMT). This allows the epicardial derived cells to invade into the heart and differentiate into various cell types, mainly cardiac fibroblasts, smooth muscle cells, and pericytes. In addition, epicardial cells secrete paracrine factors that contribute to the development of the heart.

The main result of epicardial EMT is that it enables the cells to invade the sub-epicardial layer and migrate into the myocardium [46] (Figure 2). After migration, the epicardial derived cells (EPDCs) can differentiate into different cell types (reviewed in [47]). They predominantly become interstitial fibroblasts and adventitial fibroblasts, which are important for proper organization of the myocardial wall [48], and smooth muscle cells (SMCs), which will cover the vessels and are crucial for vascular maturation [49]. Differentiation of EPDCs into endothelial cells and cardiomyocytes during cardiac development has been reported, but is likely to occur very rarely (reviewed in [47]). A special role for EPDCs has been postulated in the formation of the atrio-ventricular (AV) junction, the annulus fibrosus [50], and the AV valves [51] (reviewed in [52]). Besides the cellular contribution of EPDCs to the developing heart, EPDCs also have a paracrine contribution by secreting factors that are essential for the developing myocardium. For instance, epicardial derived retinoic acid [11,53] and

fibroblast growth factors (FGFs) [54] are important for cardiomyocyte proliferation, while epicardial GATA4/GATA6 signaling regulates endothelial cell recruitment that is indispensable for coronary plexus development [55].

In the adult heart, the epicardium does not display epicardial activation markers WT1 and RALDH1 and 2 [18,56], suggesting that it is a quiescent layer. However, the epicardium can be awakened by ischemic injury, resulting in thickening of the epicardial layer and sub-epicardial mesenchyme [56,57]. The post-injury epicardial activation is accompanied by recapitulation of developmental characteristics, such as the up-regulation of epicardial activation genes and EMT markers [15,18,56]. Whether adult EPDCs, like their fetal counterparts, migrate into the injured myocardium, is still under debate (reviewed in [47]) but appears to be less prominent in the adult heart [18]. Importantly, the significance of epicardial re-activation upon injury was underlined by studies demonstrating that preventing epicardial expansion and EMT resulted in a worse cardiac outcome after ischemia-reperfusion in mice [58]. Conversely, increasing epicardial EMT and migration by thymosin  $\beta$ 4 treatment resulted in improved cardiac outcome in the injured mouse heart [57].

Appreciating that the epicardium can be stimulated to improve cardiac regeneration led to a focus on pathways involved in the main features of epicardial behavior: EMT and invasion. As was introduced before, key players in regulating these processes are members of the TGF $\beta$  family. Given the distinction between TGF $\beta$  and BMP signaling, we describe their possible regulation within the epicardium separately, starting with TGF $\beta$  signaling.

## 4. TGF $\beta$ SIGNALING IN EPICARDIAL BEHAVIOR DURING CARDIAC DEVELOPMENT

### *4.1. Expression of TGF $\beta$ Members in the Epicardium during Development*

The first requirement for TGF $\beta$  signaling to occur in the epicardium is the presence of the actual proteins. There are three TGF $\beta$  ligands, TGF $\beta$ 1, -2, and -3, that are quite similar in structure and function. However, each of them has a specific spatiotemporal gene expression pattern during cardiogenesis [59] (see Figure 3).

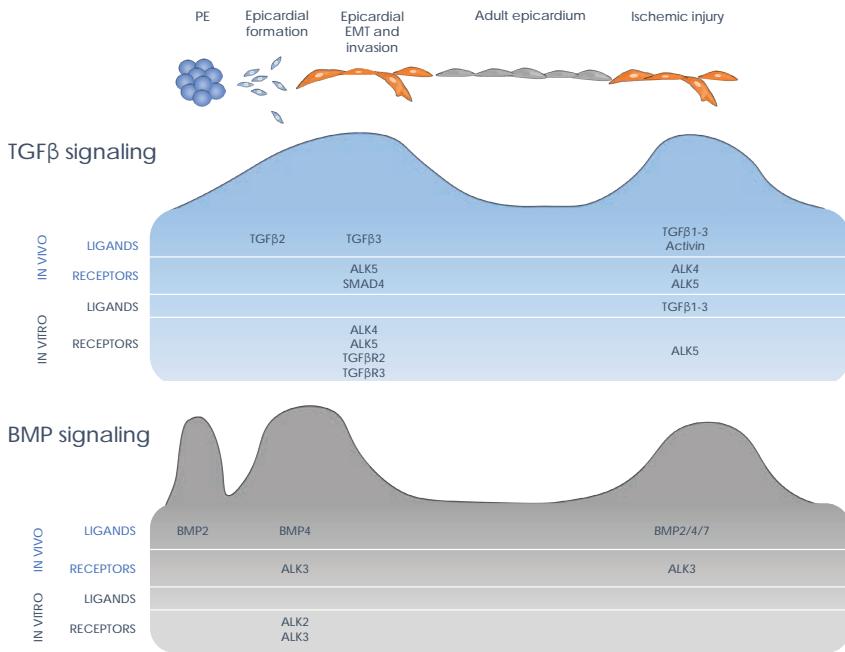


**Figure 3 | Schematic overview of TGFβ and Bone Morphogenetic Protein (BMP) signaling activity during the different stages of epicardial behavior.** At the top, a timeline of epicardial activity is indicated, starting with the pro-epicardium (PE) and pro-epicardial migration towards the heart, followed by formation of the epicardium, epicardial EMT and invasion, subsequently epicardial quiescence in the healthy adult heart and ultimately the epicardial reactivation in the injured adult heart. For every stage, the known expression levels of ligands and receptors in vivo and in vitro are specified, based on the literature described in the main text. Expression levels determined in zebrafish are noted in *italics*. Based on the expression levels, a prediction of the activity of respectively TGFβ and BMP signaling over time is displayed by the curvature.

In the mouse, the first ligand to be expressed in relation to the epicardium is TGFβ2. *Tgfb2* mRNA is present as early as E9.5 in the PE and remains detectable in the first epicardial cells that appear on the outside of the myocardium at E10.5. A clear epicardial mRNA expression pattern of *Tgfb2* is maintained until E12.5, after which it starts to decline. A similar expression pattern was observed in the epicardium of chick embryos at a comparable developmental stage [60]. *Tgfb3* is not observed anywhere in the heart at early developmental stages. However, from E11.5 onwards, when the epicardium is established and starts to participate in the formation of the heart, *Tgfb3* mRNA expression increases and is pan-epicardially expressed [59]. TGFβ3 has also been observed in the epicardium of 3 week old rat pups, suggesting

a persistent epicardial expression in the neonatal epicardium [61]. In contrast to the epicardial expression of *Tgfb2* and -3, no obvious expression for *Tgfb1* was reported in the ventricular epicardium, but *Tgfb1* mRNA was found to be localized to the epicardium of the AV sulcus [59]. Remarkably, it was found that all three TGF $\beta$  ligands are highly expressed in the epicardium lining the AV sulcus and outflow tract, suggesting they play a role in this region. In summary, TGF $\beta$ 2 is expressed during early heart development when the epicardium is formed (E9.5–E12.5); while TGF $\beta$ 3 is more likely to be involved in later phases, when the epicardium contributes to cardiogenesis (E11.5–onwards).

Since TGF $\beta$  can signal in both an autocrine and paracrine fashion, the expression observed in the epicardial region does not necessarily result in actual signaling within the epicardium. To that end, the presence of the associated receptors is required to be able to determine if a cell is susceptible for signaling. Unfortunately, literature regarding receptor expression in the epicardium is scarce, which might be related to the limited availability of specific antibodies, the very low expression levels, or simply the fact that the epicardium is often overlooked in cardiac research. Interestingly, *in vitro* studies did reveal that mouse epicardial cells in culture do not express the type I receptor *Alk7* but have high levels of *Alk4* and *Alk5* [62]. Furthermore, cultured chick epicardial cells express *TGFBR2* and *ALK5*, suggesting that TGF $\beta$  signaling in epicardial cells can occur [60]. The fact that mouse embryos with an epicardial specific knock-out of *Alk5* [63] or *Smad4* [64] display an aberrant phenotype indicates that *Alk5* and *Smad4* are present in the developing mouse heart.

TGF $\beta$  ligands are present, suggesting an important role in epicardial behavior. However, since these ligands can be stored in a latent form in the extracellular matrix of the heart, protein expression does not automatically correlate with spatiotemporal pathway activation. Therefore, determining where phosphorylated SMAD2/3 or other downstream targets are localized within the epicardium would provide better insight into which cells are involved in actual signaling.

#### **4.2. Functional Role of TGF $\beta$ in the Epicardium during Development**

To determine if the expression of TGF $\beta$  members is functionally relevant for cardiac development, multiple conventional knock-out (KO) animals have been generated which are almost all embryonically lethal. Interestingly, severe cardiac defects were only observed in *Tgfb2* deficient embryos. These embryos exhibited a spectrum of cardiac malformations including ventricular septum defects, early trabeculae formation, dual outlet of the right ventricle and dual inlet of the left ventricle [65,66]. All

other TGF $\beta$  related KO embryos did not display lethal cardiac defects. *Tgfb3* deficient mice died after birth due to cleft palate [67] and abnormal lung development [68]. Interesting to note is that in the review of Azhar et al., they describe that *Tgfb3* mutant mice displayed signs of segmentally thick epicardium and an underdeveloped myocardium, indicating that before birth an epicardial defect is present [69]. *Tgfb1* deficient embryos displayed inflammatory disease and impaired hematopoiesis, and died of compromised vasculogenesis. Any observed cardiac malformations in these embryos are likely an indirect effect of defective vasculogenesis [70,71]. *Alk5*<sup>-/-</sup> embryos [72] and *Tgfb2*<sup>-/-</sup> embryos [73] displayed phenotypes comparable to the *Tgfb1* deficient embryos, suggesting that these proteins are all involved in the same developmental processes. Since TGF $\beta$  is critical in a wide variety of developmental mechanisms, it is not surprising that KO mouse models exhibit a range of defects of which it is difficult to determine cause and consequence. However, three conclusions can be drawn. Firstly, there is a specific role for *Tgfb2* in cardiogenesis. Secondly, the distinct phenotypes of the KO models of the three ligands demonstrate that TGF $\beta$  ligands are not interchangeable in vivo, probably due to the differences in spatiotemporal expression patterns and affinity for receptor binding. And thirdly, the defects observed in *Tgfb2*<sup>-/-</sup> and *Tgfb3*<sup>-/-</sup> mice are related to developmental processes where epithelial-mesenchymal interactions occur, e.g., cochlear morphogenesis in the inner ear [65], respiratory epithelial cell differentiation, and palatal fusion [68], while malformations in *Tgfb1*<sup>-/-</sup> are more related to impaired growth and inflammation [74,75,76].

Since TGF $\beta$  is crucial for multiple cellular processes in the embryo, cell specific KO studies are essential to determine the role of TGF $\beta$  signaling specifically in the epicardium. A more specific model in this regard is a transgenic mouse line expressing *Cre*-recombinase under control of an epicardial-restricted fragment of the *Gata5* promoter [53,77]. This *Gata5-Cre* mouse was crossed with a floxed *Alk5* mouse line to specifically knock-out *Alk5* in epicardial cells as early as in the PE at E9.5 [53]. The embryos displayed a properly formed epicardium indicating that ALK5 signaling is likely dispensable for epicardium formation [63], an observation that was also done in chick pro-epicardial explants [78]. In contrast to normal formation of the epicardium, epicardial related defects were observed in these epicardial-specific *Alk5* deficient mouse embryos at E12; they displayed a detached epicardial layer, a diminished smooth muscle cell coverage of the coronary vessels, and a thinner myocardial wall due to reduced cardiomyocyte proliferation [63]. This phenotype is in agreement with disturbed epicardial function, which during normal development will contribute to vessel coverage and thickening of the myocardium [11]. Hence, this observation suggests that ALK5, although not vital for epicardial formation, is essential in epicardial

behaviour in vivo. When looking at the propagation of TGF $\beta$  and BMP signaling at the level of the SMADs, an inducible KO of *Smad4* specifically in cells expressing the epicardial marker WT1 did not induce severe cardiac malformations in the mouse embryo. Interestingly, these embryos displayed a reduced number of EPDCs and cardiac fibroblasts [64], indicating compromised epicardial EMT and invasion. The fact that the overall cardiac phenotype was not severely affected in this KO embryo, suggests that SMAD-independent signaling pathways are also involved in epicardial behavior.

The in vivo studies suggest that both ALK5 and SMAD4 are essential for epicardial behavior, yet through an unresolved mechanism. To further unravel the involvement of TGF $\beta$  signaling in the different aspects of epicardial behavior, in vitro models are important to be able to independently investigate epicardial EMT and epicardial invasion. Various in vitro models are used to study epicardial EMT. For instance, chick epicardial cells were studied by transferring hearts to a collagen gel allowing the epicardial cells to grow out as a monolayer [60]. After removal of the heart, stimulation with TGF $\beta$  ligand initiated EMT in the epicardial monolayer, demonstrated by a morphological change and an increase in EMT markers [60]. The same approach was used to show that TGF $\beta$  induces EMT in mouse epicardial cells derived from E12.5 embryonic hearts [79]. Epicardial cells were also derived from human fetal hearts [80]. Instead of epicardial outgrowth of cardiac tissue specimens, these human fetal cells were isolated by digestion of the isolated epicardial layer, followed by culture of the resulting single cell suspension in an epicardium specific culture medium. Stimulating these human fetal epicardial cells with TGF $\beta$  resulted in the induction of EMT [81]. Interestingly, the KO of *Alk5* [63] or the use of an ALK4/5/7 kinase inhibitor [60,79,81] prevents EMT of epicardial cells in chick, mouse, and human cell culture models. This finding translates to the in vivo observation that at the moment that epicardial cells should start to undergo EMT (E12), the epicardium-specific *Alk5* KO embryo presents with an aberrant epicardial phenotype. The observed detached epicardial layer could be due to the absence of a sub-epicardial mesenchyme as a result of deficient EMT. Whether the *Alk5* total KO embryo displays a detached epicardial layer and absent coronary vessel coverage remains elusive, as it has not been described. In the *Tgfb1*<sup>-/-</sup> and *Tgfb2*<sup>-/-</sup> embryos, the vascular phenotype and overall symptoms are likely to be too severe to determine an epicardial specific defect. Interestingly, in the *Tgfb3*<sup>-/-</sup> embryo an abnormal epicardial layer and immature myocardium were reported [69], which is in line with the observations in vitro.

Following EMT, epicardial cells acquire the ability to invade underlying tissue. Invasion of epicardial cells can be studied in more detail in ex vivo cultured hearts. For instance, when ex vivo E12.5 mouse embryonic hearts with YFP-labeled WT1+ cells were stimulated with TGF $\beta$ , the number of YFP+ cells invading the myocardium increased [82]. In a similar approach, this time using cultured avian hearts, TGF $\beta$  was shown to induce epicardial invasion in a dose-dependent manner [83]. Moreover, in vitro studies suggest that TGF $\beta$  signaling via ALK5 is essential in this regard. For instance, mouse embryonic epicardial cells display an increased invasion in a Boyden chamber assay when stimulated with TGF $\beta$  or transduced with constitutively active (ca)ALK5 [79]. Furthermore, viral induction of caALK5 in chick heart explant cultures also induced epicardial invasion into a collagen gel [60]. Overall, this data confirms the in vivo observation that TGF $\beta$  and its signaling is crucial for epicardial behavior, and specifically that ALK5 signaling is involved in the induction of both epicardial EMT and invasion.

There are studies reporting that TGF $\beta$  does not induce epicardial EMT and invasion, and even inhibits FGF-induced epicardial EMT and invasion in a chick heart model [84]. They describe a contraction of epicardial cells and the formation of a cell mass in response to TGF $\beta$ . However, this process of contraction was in a later publication related to loss of epithelial markers [60]. Furthermore, mesenchymal differentiation and invasion of epicardial cells might be dependent on variations in cell culture conditions. In this case, the deviant observations could be due to the absence of fetal bovine serum (FBS) and the relatively high concentration of TGF $\beta$  (10 ng/mL), which is different from other studies about epicardial EMT. Furthermore, culture conditions such as cell layer confluency can influence the EMT response [80]. Interesting to note is that in contrast to in vivo studies, where different TGF $\beta$  ligands have distinct and uninterchangeable functions, in vitro there does not seem to be a difference between the types of TGF $\beta$ ; all three TGF $\beta$  ligands elicited a similar effect on EMT and invasion in the majority of the studies [60,79,80].

To conclude, although there are some opposing findings in literature, likely due to technical differences, there is abundant evidence that in the epicardium TGF $\beta$  induced ALK5 signaling is essential for cardiac development by regulating epicardial EMT and invasion of epicardial cells.

### 4.3. Downstream Signaling Mechanisms of TGF $\beta$ in the Epicardium during Development

When the TGF $\beta$  pathway is activated, several cell biological mechanisms are set in motion. These involve orchestrating the process of EMT- including changes in cell adhesion molecules and the cytoskeleton-, and regulating invasion of transformed mesenchymal cells into the underlying tissue.

The regulation of cell adhesion molecules in epithelial cells is a well-known effect of TGF $\beta$  stimulation [85]. In the context of the epicardium, Dokic et al. demonstrated that within 30 min after addition of TGF $\beta$ , the membrane expression of the junctional proteins E-cadherin and  $\beta$ -catenin started to decline, suggesting reduced cell-cell adhesion [83]. The effect of TGF $\beta$  on intercellular strength was further demonstrated by mechanically disrupting an epicardial monolayer and determining the number of resulting fragments as a measure of the weakness or strength of cell-cell adhesions. The fragment count was much higher in TGF $\beta$ -treated epicardial monolayers, demonstrating diminished intercellular strength. The epicardial monolayers were also treated with the soluble form of the  $\alpha$ 4 $\beta$ 1 integrin ligand Vascular Cell Adhesion Molecule 1 (sVCAM1), which prevented TGF $\beta$ -induced changes in E-cadherin and  $\beta$ -catenin [83] and therefore maintained the epithelial cell adhesion profile. Indeed, incubation with soluble VCAM-1 in combination with TGF $\beta$  reduced the number of fragments compared to TGF $\beta$  alone [83]. Interestingly, incubating chick hearts with sVCAM-1 prevented TGF $\beta$  induced epicardial EMT in vitro and epicardial invasion ex vivo [83]. This experiment underlines that changes in cell adhesion molecules are essential for epicardial EMT to occur. Given the fact that TGF $\beta$  regulates the presence of cell adhesion molecules, it is likely that an important step in TGF $\beta$  initiated EMT is downregulation of cell adhesion molecules.

Concomitantly to alterations in the cell adhesion molecule profile, the cytoskeleton undergoes dramatic changes during the process of EMT. The regulation of the cytoskeleton is often related to TGF $\beta$ -induced Rho signaling [60,79,83,86,87], known for its role in actin dynamics and cytoskeletal behavior of the cell (reviewed in [88]). Indeed, Rho activity increased rapidly when rat epicardial derived cells were stimulated with TGF $\beta$  [83]. Furthermore, exposure of the cells to a p160 Rho kinase inhibitor (Y27632) prevented the TGF $\beta$ -induced formation of smooth muscle markers in chick [60] and mouse [79,86] epicardial cells. Furthermore, an activator of Rho signaling, lysophosphatidic acid (LPA), achieved a similar degree of epicardial cell invasion into chick hearts as TGF $\beta$  ligand stimulation [83]. However, one may need to take into account that LPA can also activate TGF $\beta$  signaling [89], so additional research is necessary to

confirm that Rho activation induces epicardial invasion. Together, these data imply the involvement of the Rho pathway, in TGF $\beta$  signaling initiated epicardial EMT.

Changing the cell-adhesion profile and cytoskeleton ultimately results in the transition of an epithelial to a mesenchymal cell type, after which cells are primed to become motile and invade the underlying tissue. Motility can be regulated by many factors, for example *Mylk*, *Rock1* and *Tmsb4x*. The combination of these factors has been described as an epicardial motile gene program [90]. Interestingly, it was found that TGF $\beta$  stimulation resulted in the nuclear accumulation of myocardin related transcription factors (MRTFs), essential factors in the motile gene program. In fact, viral overexpression of MRTF-A led to exaggerated epicardial invasion in an ex vivo cultured embryonic mouse heart [90], overall suggesting that TGF $\beta$  signaling can induce MRTFs which in turn are sufficient to induce epicardial invasion. Furthermore, TGF $\beta$  was shown to activate invasion via the SMAD-independent MAPK-ERK pathway. In this process, the TGF $\beta$ -dependent production of hyaluronic acid (HA) by hyaluronan synthase 2 (Has2) was essential. The produced HA binds the CD44 receptor and induces upregulation of vimentin and the initiation of invasion [91].

Overall, TGF $\beta$  signaling appears to orchestrate a range of factors that ultimately result in enhanced motility of the epicardial cell.

#### 4.4. The Role of Activin Signaling in Epicardial Behavior during Cardiac Development

So far, we mainly described epicardial TGF $\beta$  signaling through the ALK5 receptor, a process that leads to phosphorylation of SMAD2/3. Although ALK5 is predominantly described in this context, it is not the only receptor resulting in SMAD2/3 phosphorylation. As depicted in Figure 1, SMAD2/3 can also be phosphorylated via ALK4. This type I receptor dimer forms a complex with the activin receptor IIa (ACVR2A) or IIb (ACVR2B) that can initiate signaling upon binding with activins, inhibins or nodal.

Not much is known about the role of activin signaling in cardiac development or regarding the epicardial expression of activin. Most of the KO mouse models related to activin signaling do not have a clear cardiac phenotype (reviewed in [92]). An exception to this is the type II receptor ACVR2B KO mouse, which displays severe morphological cardiac malformations such as septal defects, abnormal patterning of the outflow tract, and aberrant positioning of the great arteries [93]. Furthermore, nodal has been linked to impaired left-right patterning of the heart and several anatomical defects, such as the tetralogy of Fallot [94]. Embryos devoid of the ALK4 receptor are

lethal in an early developmental stage due to disrupted primitive streak formation, and it is therefore not possible to assess its role in cardiac development in this genetic model. Some suggestion may however come from in vitro data. Firstly, *Alk4* was shown to be expressed in epicardial cells in vitro [62], implying that signaling via this receptor is a possibility. Secondly, multiple studies have shown that the ALK4/5/7 kinase inhibitor SB431542 can prevent epicardial EMT in vitro [60,79,81] pointing towards ALK4, 5 or 7 as main type I receptors, of which ALK5 is the most common. The importance of specifically ALK5 for epicardial EMT and invasion has been shown in vitro and in vivo (as described in Section 4.2) [63]. However, a potential role for ALK4 may not be neglectable, as ALK4 signaling has been implied in EMT of several cell lineages, mainly in the field of oncology [95,96,97,98,99], but also in endocardial EMT [100]. More research will be required to determine if signaling via ALK4 plays a role in epicardial behavior.

## 5. BMP SIGNALING IN EPICARDIAL BEHAVIOR CARDIAC DEVELOPMENT

5

As schematically shown in Figure 1, the other side of the TGF $\beta$  family consists of the BMP pathway that can be activated by BMPs and signals via SMAD1/5/8. While initially known for its ability to induce bone formation [101], BMP signaling emerged as a central regulator of several important processes during development and disease. In the context of cardiac development, the BMP pathway is involved in the specification of the epicardial lineage in the pro-epicardium. The ratio between BMP2 and FGF2 expression was shown to determine if the pro-epicardial cell differentiates towards the myocardial lineage, in case of high levels of BMP2, or the epicardial lineage, in case of high levels of FGF2 [102]. When directed towards the epicardial cell lineage, pro-epicardial cells migrate towards the heart. To be able to do this, pro-epicardial cells are thought to undergo EMT in order to migrate towards the heart and form the epicardium. Interestingly, pro-epicardial EMT is regulated via the type I receptor ALK2, suggesting a potentially different mechanism in pro-epicardial EMT compared to epicardial EMT which is mainly regulated via ALK5 [78].

In the developing heart, BMP ligands are mainly expressed in the myocardium [103]. They are especially highly expressed in the AV myocardium, indicating a role in the development of the AV canal [103]. Indeed, KO studies for BMP related proteins (reviewed in [104]) revealed that both the *Bmp2* deficient mouse and cardiomyocyte specific *Alk3* KO mouse displayed defects in the formation of the AV canal and also in

the formation of the AV valves [103,105,106]. This was at least in part caused by impaired endocardial EMT [103,107]. Mouse embryos with a specific KO of *Alk3* in *Wt1*<sup>+</sup> epicardial cells displayed abnormalities in the tissues of the AV junction as well [108], suggesting that in addition to the endocardium, epicardial BMP/ALK3 signaling may also be involved in the formation of the AV region. In contrast, in these embryos with epicardial specific knock-down of ALK3, neither the development of the pro-epicardium, the formation of the epicardium, nor the migration of EPDCs into the myocardium were affected [108]. Recently, BMP signaling was described to be involved in epicardial maturation [42]. Epicardial maturation is the process that starts after the epicardium has formed, during which the cells turn from a cuboidal into a squamous epithelial cell layer, characterized by flattening of the cells and elongation of the nuclei [42]. In WT1KO embryos, this process is impaired, resulting in persistence of cuboidal cells, which coincided with a higher expression of epicardial BMP4 compared to wildtype embryos. Addition of BMP inhibitor LDN-193189 rescued the phenotype of WT1KO embryos, revealing that BMP signaling needs to be absent for proper epicardial maturation [42] (see Figure 3).

The epicardial specific *Alk3*<sup>-/-</sup> embryos did not show any defects in epicardial EMT in the myocardium but revealed a potential role for BMP/ALK3 signaling in epicardial EMT in the AV region. The effect of BMP signaling on EMT was further corroborated by in vitro experiments. In murine epicardial cells, expression of both type I receptors ALK2 and ALK3 was abundant, while ALK6 levels were hardly detectable [62]. Treatment with BMP2 resulted in the loss of epithelial character in murine epicardial cells. Interestingly, contrary to TGF $\beta$ , BMP2 did not promote smooth muscle cell differentiation. An inhibitor of ALK2 and ALK3 could prevent BMP2 induced EMT. To further investigate which type I receptor is involved in EMT, epicardial cells were treated with caALK2, caALK3 or caALK5. Cells treated with caALK2 and caALK5 showed an increase in smooth muscle cell markers, while EMT induced by caALK3 did not result in SMC differentiation [62]. This finding suggests that BMP2-induced EMT signals via ALK3 and SMAD1/5/8 phosphorylation, and leads to a distinct differentiation pathway than TGF $\beta$  induced EMT via SMAD2/3 phosphorylation (see Figure 1). Given the phenotype of the epicardial specific *Alk3*<sup>-/-</sup> embryo, one could speculate that BMP/ALK3 predominantly regulates epicardial EMT in the AV junction and annulus fibrosus, giving rise to epicardial derived fibroblasts that are essential for the formation of the slow-conducting properties of this region.

Overall, developmental epicardial BMP signaling was shown to participate in pro-epicardial EMT, the maturation of the epicardium, and the formation of the AV sulcus.

Interestingly, often the absence of BMP signaling appears to be essential for proper regulation of these processes, indicating that epicardial BMP signaling is dependent on very strict spatiotemporal expression of BMP ligands and receptors (see Figure 3).

## 6. THE ROLE OF ACCESSORY RECEPTORS ENDOGLIN AND TGFBR3 IN DEVELOPMENTAL EPICARDIAL BEHAVIOR

Besides for the type II and type I receptors of the TGF $\beta$  family, an emerging role has been described for the two TGF $\beta$  type III receptors endoglin and TGF $\beta$ R3. These structurally related proteoglycans reside in the cell membrane, but cannot initiate the TGF $\beta$  signaling pathway themselves due to the lack of a kinase domain. However, they can participate in signaling by presenting ligands to type II receptors.

The accessory receptor endoglin is mainly known for its contribution to angiogenesis [109,110]. In the developing heart, endoglin is expressed in endothelial cells and in mesenchymal cells of the AV canal [111,112]. A potential role for endoglin in EMT was suggested in a study where knock-down of endoglin by siRNA in atrioventricular (AV) canal explants of the chick embryo reduced ALK5-mediated EMT during cardiac valve formation [111]. Furthermore, endoglin was shown to be essential for EMT in kidney cancer cells as reduction of endoglin levels by shRNA increased epithelial markers and reduced mesenchymal markers [113]. Similar to other mesenchymal cells, human epicardial cells increase the expression of endoglin after EMT. A direct role for endoglin in this process was shown by blocking endoglin with an antibody in epicardial cells, which increased epithelial markers E-cadherin and VCAM-1 [114]. However, it could not prevent TGF $\beta$  induced EMT, indicating that this process is not depending on endoglin. These data show that endoglin, besides its well-known function in angiogenesis, can be a driver of EMT in the heart and might be an interesting topic to investigate further in an epicardial context.

The other accessory receptor, TGF $\beta$ R3 or  $\beta$ -glycan, modulates TGF $\beta$  signaling by binding a ligand and presenting it to the type II receptors, thereby increasing the TGF $\beta$  responsiveness of the cell [115]. Although TGF $\beta$ R3 is able to bind to TGF $\beta$ 1, TGF $\beta$ 3, BMPs [116] and inhibin [117], the presence of TGF $\beta$ R3 is especially necessary to allow TGF $\beta$ 2 binding to the TGF $\beta$ RII, as this normally occurs with very low affinity [115,118,119]. Besides ligand presentation, TGF $\beta$ R3 can also modulate TGF $\beta$  signaling via its cytoplasmic domain [120].

Within the heart, TGF $\beta$ 3 is expressed in both the myocardium and epicardium [121], which is already suggestive for a role for TGF $\beta$ 3 in cardiac development. Indeed, the TGF $\beta$ 3 KO mice are embryonically lethal at E14.5 due to impaired coronary vessel formation. Interestingly, these embryos also display an aberrant epicardial phenotype, demonstrated by an excessively thick sub-epicardial layer containing blood islands, coinciding with a thin myocardial compact layer [121], while vascular smooth muscle cell recruitment to the coronary vessels appeared to be normal. This phenotype is different from the epicardium-specific *Alk5*<sup>-/-</sup> embryo, which displayed defective SMC coverage [63], indicating that TGF $\beta$ 3 has a non-redundant role next to ligand presentation to the TGF $\beta$ RII. Another explanation could be that in the absence of TGF $\beta$ 3, TGF $\beta$ 1 and -3 can still initiate signaling via ALK5, as these ligands are less dependent on the presence of TGF $\beta$ 3 compared to TGF $\beta$ 2. TGF $\beta$ 1 and -3 could therefore partially compensate for the loss of TGF $\beta$ 2 signaling, which is not possible in the *Alk5* KO.

In contrast to endoglin, the function of TGF $\beta$ 3 in the epicardium has been investigated extensively using epicardial cells isolated from murine embryonic hearts (E11.5) deficient of TGF $\beta$ 3 or their wildtype littermates [79,122]. Cultured *Tgfb3*-deficient murine epicardial cells expressed reduced levels of mesenchymal markers SM22 $\alpha$  and vimentin [123], but were able to lose their epithelial phenotype when stimulated with TGF $\beta$ 1, TGF $\beta$ 2 [122] or BMP2 [62]. Furthermore, these cells were able to acquire smooth muscle cell (SMC) characteristics when stimulated with TGF $\beta$ 1 or TGF $\beta$ 2 [122]. Therefore, TGF $\beta$ 3 does not appear to be vital for epicardial EMT *in vitro*. However, epicardial cells deficient for *Tgfb3* do display a decreased migration capacity [123] and diminished invasion potential upon stimulation with either TGF $\beta$ 1, TGF $\beta$ 2 or BMP2 in a modified Boyden chamber assay [62,122]. For epicardial invasion, the cytoplasmic domain of TGF $\beta$ 3 was found to be essential [122]. This domain is not involved in ligand presentation to the TGF $\beta$ RII [120], suggesting that TGF $\beta$ 3 regulated epicardial invasion in a different manner. Several mechanisms have been proposed to be involved in TGF $\beta$ 3 guided epicardial invasion. Firstly, the cytoplasmic domain of TGF $\beta$ 3 has a 3 C-terminal amino acids domain, STA, that can bind GIPC (GAIP-interacting protein, C terminus). While *Tgfb3*-deficient cells treated with a construct for full length *Tgfb3* demonstrated rescued invasion, *Tgfb3* lacking the 3 C-terminal acids could not restore invasion in KO cells [122]. Moreover, an siRNA against GIPC abolished TGF $\beta$ /BMP2 induced invasion in wildtype cells, demonstrating that GIPC is essential [62,122]. However, overexpression of GIPC1 in *Tgfb3*<sup>-/-</sup> cells could not rescue the *Tgfb3*<sup>-/-</sup> phenotype, indicating that the complex formation with GIPC is indispensable for TGF $\beta$ 3 to induce epicardial invasion [122]. Secondly,

TGF $\beta$ 3 was shown to be involved in TGF $\beta$ -initiated activation of the RhoA pathway, which is essential to induce epicardial invasion. Knock-down of RhoA resulted in ligand-independent epicardial invasion, demonstrating that RhoA needs to be absent for epicardial invasion to occur. The impaired invasion in TGF $\beta$ 3 $^{-/-}$  cells could partially be restored by overexpression of a dominant negative RhoA, suggesting that TGF $\beta$ 3 is involved in the reduction of RhoA that is required for epicardial invasion. This was shown to signal via Par6 and Smurf1 [87]. Lastly, a RNA sequencing experiment comparing ligand-stimulated *Tgfb3* $^{+/+}$  and *Tgfb3* $^{-/-}$  epicardial cells found that NF $\kappa$ B signaling is differently regulated in *Tgfb3* $^{-/-}$  cells compared to controls in vitro, independent of the ligand used [124]. Additional research confirmed that NF $\kappa$ B activity is reduced in ligand-stimulated *Tgfb3* $^{-/-}$  cells and that ligand-induced invasion of *Tgfb3* $^{+/+}$  cells can be prevented when NF $\kappa$ B is inhibited [124,125]. Binding of  $\beta$ -Arrestin 2 ( $\beta$ -Arr2) to the cytoplasmic domain of TGF $\beta$ 3 is suggested to be involved in this effect, for its described function in NF $\kappa$ B inhibition in breast cancer cells [126]. Indeed, preventing TGF $\beta$ 3 to bind to  $\beta$ -Arr2 promoted epicardial invasion in the absence of a ligand [125].

The exact modulation of epicardial TGF $\beta$ 3 in TGF $\beta$  and BMP signaling seems to be complex, as it is bound by an array of ligands, but can also be reduced by several inhibitors. For instance, both inhibitors of ALK4/5/7 and ALK2/3 were able to block TGF $\beta$ 3 mediated invasion in response to either TGF $\beta$ 2 or BMP2 respectively [62]. Moreover, TGF $\beta$ 3 is also essential for FGF2 [122] and high molecular weight hyaluronic acid [122] induced epicardial invasion. Therefore, the best fitting hypothesis seems to be that TGF $\beta$ 3 is an essential element in a broad spectrum of factors regulating epicardial invasion. For instance, the TGF $\beta$ 3 could bring the TGF $\beta$  and FGF receptors in spatial vicinity by binding its ligands, and subsequently initiate crosstalk between FGF and TGF $\beta$  signaling that is known to be involved in processes like EMT [127].

## 7. TGF $\beta$ FAMILY IN THE EPICARDIAL RESPONSE TO CARDIAC INJURY

### 7.1. *Epicardial TGF $\beta$ Signaling in the Injured Heart*

Thus far, we established a potential contribution of TGF $\beta$  and BMP signaling in the epicardium during heart development. However, as described previously, the epicardium is also involved in the injured heart. Cardiac injury arises when an occlusion of the coronary vasculature results in cardiac ischemia and damage of downstream tissue. The contribution of TGF $\beta$  signaling in the repair of the injured adult heart has been described extensively. Upon infarction, the protein expression of TGF $\beta$  ligands in the mouse heart increases. TGF $\beta$ 1 and TGF $\beta$ 2 expression is fast and decreases after 3–7 days, while TGF $\beta$ 3 expression is induced after a few days and remains for a longer period [128]. Concomitantly, levels of pSMAD2 increase within 24 h in the injured mouse heart [129,130], while one of the inhibitory SMADs, SMAD7, decreases [129], pointing towards increased TGF $\beta$  signaling. As the widespread availability of TGF $\beta$  ligands indicates, TGF $\beta$  is involved in multiple processes in the injured heart, such as immunoregulation, ECM regulation and fibrosis (reviewed in [131,132]). It has been shown that the epicardium is also involved in the repair program of the murine and zebrafish heart [15,58]. Hence, knowing that TGF $\beta$  and BMP signaling are of importance in the embryonic epicardium raises the question if the TGF $\beta$  family is also involved in the epicardial behavior of the injured heart.

To be able to study adult epicardial EMT and invasion, *in vitro* cell culture models using patient derived epicardial cells were developed. In these human adult cells, it was established that all three TGF $\beta$  ligands are expressed, as well as the type I receptor ALK5 [114], indicating that cells are able to respond to TGF $\beta$  ligands. When these cells were stimulated with TGF $\beta$ , protein levels of the EMT marker Snail increased, as well as the mesenchymal marker Smooth Muscle Actin. Furthermore, cells treated with TGF $\beta$  underwent a phenotypical switch from cobblestone epithelial-like cells towards spindle-shaped mesenchymal cells. This shows that adult epicardial cells in culture retain the ability to undergo EMT in response to TGF $\beta$  treatment [114], similar to the embryonic situation. In addition, TGF $\beta$ -induced EMT could be prevented by the ALK4/5/7 kinase inhibitor SB431542, indicating that EMT is initiated via ALK4 or ALK5 signaling. Interestingly, incubation of adult epicardial cells with soluble VCAM-1 prevented TGF $\beta$ -induced EMT in adult epicardial cells [114], an observation that was also done in the embryonic epicardium [83] (see Section 4.3), demonstrating that fetal mechanisms are recapitulated in the re-activated adult epicardium. On the other hand, a role for Rho signaling could not be established in adult epicardial EMT [114],

which could suggest that this pathway, although involved in fetal epicardial cells, is shut down in adult epicardial cells. Additional research is needed to confirm this observation. Interestingly, in a direct comparison between fetal and adult human epicardial cells, it was shown that adult cells are intrinsically less prone to undergo EMT than human fetal EPDCs [81]. This indicates that although the epicardium of the adult heart is still able to undergo EMT, this process might be less efficient in comparison to the fetal heart. So far, the underlying cause of this intrinsic difference is not known, but one could speculate that enhanced levels of endogenous VCAM-1 or E-cadherin, or reduced levels of TGF $\beta$  receptors can decrease the susceptibility of epicardial cells to undergo EMT.

Thus far, in vitro studies indicate that TGF $\beta$  can regulate epicardial EMT via ALK5. Limited knowledge is available on epicardial TGF $\beta$  signaling and repair in vivo. It has been shown that the activated adult epicardial cells undergo EMT and form a sub-epicardial layer [56]. From developmental studies, we know that the TGF $\beta$  family is involved in the regulation of these processes (see Section 4), suggesting that TGF $\beta$  could also be involved in epicardial behavior in the adult heart. Moreover, combining data from various studies suggest that TGF $\beta$  signaling could be relevant in the epicardium of the injured heart. For instance, one of the few studies describing expression levels of TGF $\beta$  members specifically in the epicardium showed that Raldh2<sup>+</sup> epicardial cells within the infarcted area of the zebrafish heart were positive for *tgfb1*, -2 and -3 14 days post-cryoinjury (dpci). Furthermore, strong mRNA expression of *alk5b* was present in the injured heart 4 dpci, and appeared to be specifically enhanced in the epicardium. This expression decreased over time, but was maintained up to 14 dpci. Although not described by the authors, mRNA expression of *alk4* appeared to be present in the epicardium as well at 4 dpci. The presence of relevant ligands and receptors indicates that epicardial TGF $\beta$  signaling can take place in the injured heart. Blocking TGF $\beta$  signaling with the ALK4/5/7 inhibitor SB431542 resulted in defective regeneration of the damaged tissue. This cannot be directly attributed to the epicardium because besides epicardial expression, injury induces an overall increase of pSmad3 in the zebrafish heart indicating a widespread activation of TGF $\beta$  signaling [133]. The impaired regeneration was attributed to impaired proliferation of cardiomyocytes [133]. In addition, the formation of ECM was heavily disrupted. No effect of the TGF $\beta$  inhibitor was observed on the expression pattern of Raldh<sup>+</sup> epicardial cells [133], indicating that there is no direct effect on epicardial behavior. However, one could argue that the observed defects in regeneration could be partly introduced by the absence of TGF $\beta$  signaling in the epicardium. Firstly, because cardiomyocyte proliferation in the developing heart is dependent on epicardial secretion of factors.

Secondly, because the epicardium is a contributor to the formation of the ECM in the regenerating heart, e.g., by delivering essential ECM proteins such as fibronectin [134] and ColXII [135]. Interestingly, the expression pattern of ColXII in the injured zebrafish heart changed upon treatment with the TGF $\beta$  inhibitor; while this protein was present in both the epicardium and the wounded area of the control injured heart, the ColXII protein was absent in the wounded area upon treatment with a TGF $\beta$  inhibitor, and was only present in epicardium [135]. Since epicardial derived cells secrete matrix proteins [134,135], the absence of ECM producing cells in the wound area could point to defective epicardial behavior, for instance caused by impaired EMT and migration.

Since SB431542 inhibits ALK4/5/7 signaling, its effect on the repair of the zebrafish heart can also be attributed to defective activin/ALK4 signaling. This is supported by the finding that a zebrafish KO of *inhbaa*, a subunit of Activin, results in less CM proliferation in the regenerating zebrafish heart [136], similar to treatment with SB431542. This was regulated via Alk4 and Smad3. A role for the epicardium was not implied in this study, but expression of *inhbaa* in the injured heart appeared to be mainly in the epicardial and endocardial layer [136], which could suggest that the phenotype of the *inhbaa* KO is regulated via, among others, the epicardium.

Therefore, although so far no direct link between the epicardium and the diminished regeneration of the zebrafish heart after inhibition of TGF $\beta$  signaling could be established, combination of the expression levels of TGF $\beta$  members in the epicardium (see Figure 3) with the functional effects observed in zebrafish could indicate a role for TGF $\beta$  signaling in the epicardium. Epicardial specific lineage trace models are necessary to demonstrate to what extent the defective formation of the ECM and cardiomyocyte proliferation caused by TGF $\beta$  inhibition are related to disrupted epicardial EMT and invasion in the wound area of the injured zebrafish heart. Important to note is that most of the discussed literature involves the zebrafish heart; a research model that, in contrast to the murine and human heart, has regenerative capacity. Although these results are highly valuable because they give an indication how regeneration should look like, they are not directly representative for processes in the mammalian heart.

### **7.2. Epicardial BMP Signaling in the Injured Heart**

A role for BMP signaling has also been implied in cardiovascular disease extensively [137,138,139,140], although knowledge about BMP signaling specifically after myocardial infarction remains limited (reviewed in [141]). Within 1 day after cardiac injury in mouse hearts, *bmp2* ligand expression starts to increase and reaches a maximal

level after 3 days where after expression declines. After 7 days, expression of other BMP ligands, such as *bmp4*, *bmp6* and *bmp10* appears. For the epicardium specifically, the presence of relevant signaling proteins was revealed in a spatially restricted RNA sequencing experiment [142]. Validation experiments showed that expression of BMP ligands *bmp2b* and *bmp7* were enhanced in the wound border zone and also in the epicardium covering the wound at 7 days post injury (dpi). In addition, single cell sequencing of the zebrafish epicardium identified *bmp4* as a specific epicardial marker of the adult zebrafish heart [143], suggesting that BMP4 has a role particularly in the epicardium. This epicardial *bmp4* expression in the zebrafish heart was enhanced after injury [143]. Moreover, epicardial expression of *bmpr1aa*, ortholog of BMP type I receptor ALK3, was enhanced in the viable myocardium and the epicardium 7 dpi. These expression levels indicate that BMP signaling can occur in the injured heart including the epicardium, which was confirmed by the presence of pSmad1/5/8 in the epicardial layer at 3 dpi [142]. When BMP signaling was inhibited in the zebrafish, an attenuated regeneration was observed, associated with compromised cardiomyocyte dedifferentiation and proliferation. Although no effect of BMP signaling inhibition on *wt1b* expressing epicardial cells was observed [142], a role for BMP signaling in the epicardium cannot be ruled out because in this study only re-expression of *wt1b* was assessed. Therefore, this only shows that BMP signaling does not interfere with epicardial activation, but effects on epicardial EMT and invasion were not described. Expression profiles of BMP receptors and downstream target proteins show that BMP signaling is activated in the epicardium after injury in the zebrafish heart (see Figure 3). To what extent this BMP signaling affects epicardial behavior and, as a result, cardiac regeneration is open for further research. In addition, mouse studies should reveal if epicardial BMP signaling described in the zebrafish is also present in the mammalian epicardium.

## 8. EPICARDIAL TGF $\beta$ AND BMP SIGNALING AS A TARGET FOR REGENERATIVE THERAPY?

Given the recapitulation of the fetal processes after injury, knowledge obtained in developmental research can be applied to identify pathways that could be used for regeneration. This is particularly interesting in the context of the heart, because unlike most of the other organs in the human body, the heart has limited regenerative capacity. Due to the lack of sufficient cardiomyocyte proliferation, injured muscle tissue is replaced by scar tissue. This hampers the pump function of the heart and can ultimately lead to progressive heart failure. It is therefore essential to find novel

therapeutic approaches to restore cardiac function in patients who suffered from a myocardial infarction. The epicardium could be a potential candidate for this, for its important contribution to the developing heart. It has already been shown that the epicardium becomes reactivated in the injured heart, but this response is sub-optimal compared to the contribution of the embryonic epicardium to the formation of the ventricle wall. For example, in the adult heart, epicardial cells display less migration into the injured myocardium [18], and fetal epicardial cells are more prone to undergo EMT [81]. Therefore, optimizing the epicardial response to repair could enhance cardiac function of an injured heart. This was indeed demonstrated in a mouse study where pre-treatment of the epicardium with thymosin  $\beta$ 4 resulted in an increased epicardial activation, epicardial EMT and improved cardiac function after injury [57]. Hence, the main question that remains is how we can use the knowledge about TGF $\beta$  signaling in the epicardium of the developing and diseased heart to improve the repair of the injured adult heart.

A growing body of evidence of in vitro studies indicates that increasing TGF $\beta$  and BMP signaling in the epicardium can increase the number of cells undergoing EMT. In the developing heart, promoting ALK5 signaling appears to be the most effective way to activate epicardial EMT and invasion. However, the pleiotropic and context-dependent nature of TGF $\beta$  signaling desires a more specific approach to prevent promotion of cardiac fibrosis, apoptosis and hypertrophy (reviewed in [132]). Therefore, it is preferable to look for a more specific target to kindly push ALK5 signaling in the right direction: the induction of epicardial EMT and invasion. In this regard, TGF $\beta$ R3 is a potential target since it can modulate ALK5 signaling and is essential for invasion of fetal epicardial cells. To be able to pursue this line of research, it is important to study the role of TGF $\beta$ R3 in the injured adult heart. It would be interesting to compare TGF $\beta$ R3 activity between the fetal and adult epicardium to provide potential targets for regenerative therapy. Furthermore, for a more complete and robust view on what TGF $\beta$ R3 does in the epicardium, it might be relevant to develop additional models, e.g., inducible TGF $\beta$ R3 $^{-/-}$  mouse models, to study its behavior since a lot of the current literature is depending on cell culture systems. A second way to target ALK5 signaling to repair the heart could be via TGF $\beta$ -activating proteins that are not a direct member of the TGF $\beta$  family but can regulate its activity. Of interest in the context of TGF $\beta$  and cardiac regeneration is thymosin  $\beta$ 4, a peptide that has been shown to enhance TGF $\beta$  signaling [144]. Although debated [145], one study showed that a myocardium specific KO of thymosin  $\beta$ 4 resulted in a cardiac phenotype that displays similarities to the *Alk5* KO embryonic heart, e.g., detached epicardium, non-compacted myocardium and defective smooth muscle cell coverage of coronary vessels [146]. Moreover, in the adult

heart, it has been shown that priming the epicardium with thymosin  $\beta$ 4 increases cardiac function after injury in a mouse model. This was associated with increased epicardial EMT [57]. Although indirectly, this suggests that enhancing TGF $\beta$  signaling has the potential to improve the contribution of the epicardium to repair of the heart. A third way to increase epicardial EMT and invasion could be to target downstream signaling of ALK5, e.g., VCAM-1 or Rho signaling. Both changes in cell-cell adhesion molecules and rearrangement of the cytoskeleton are essential for EMT and invasion of the embryonic epicardium (see Section 4.3). We anticipate that reducing epithelial cell-cell adhesion via VCAM-1 or E-cadherin, or enhancing cytoskeletal changes via Rho signaling could lower the threshold for a cell to undergo EMT. This would increase the number of epicardial cells that can invade into the heart, without the need for activation of the pleiotropic TGF $\beta$  pathway.

Another opportunity to activate the epicardium of the injured heart could be via BMP4 signaling. During development, BMP4 was shown to be vital for epicardial maturation [42]. Thus far, the exact nature and function of epicardial maturation is not extensively described, but the fact that two of the main epicardial specific proteins, WT1 [42] and TCF21 [147], are proposed to be involved in this process indicates that it is an essential part of epicardial development. Interestingly, *in vivo* studies in zebrafish have indicated that BMP4 is specifically upregulated in the epicardium of the injured heart, similar to cardiac development. Although not studied, this could indicate that epicardial maturation is also involved in the epicardium of the injured heart. For instance, BMP4 could be involved in the de-differentiation of the epicardium, enabling it to reactivate its fetal behavior. This is of particular interest, since this study was performed in zebrafish, a research model that, in contrast to the murine and human heart, has regenerative capacity. Although these results are not directly representative for processes in the human heart, they are highly valuable as they give an indication how regeneration could occur. Therefore, BMP4 and epicardial maturation could be an interesting research line for follow up.

To be able to investigate these mechanisms in epicardial EMT, our research group has developed an *in vitro* cell culture system that allows for a direct comparison of fetal and adult human primary epicardial cells. Interestingly, while adult cells need a trigger to undergo EMT, fetal epicardial cells are more active and need incubation with an ALK4/5/7 kinase inhibitor to prevent spontaneous EMT [81]. This observation is in line with the *in vivo* situation and therefore provides a relevant model to investigate how adult epicardial EMT and invasion can be improved, using fetal epicardial cells as a blue print.

## CONCLUSIONS

In this review we aimed to provide a structured overview of the role of multiple ligands and receptors of the TGF $\beta$  family in epicardial behavior. In our opinion, the strength of this review is the structured and detailed overview on the potential power of the TGF $\beta$  pathway. This also presents a limitation of this manuscript; there are several other signaling pathways (including Wnt [58], FGF [48] and PDGF [82]) involved in epicardial behavior which are now underrepresented, but these have been reviewed extensively elsewhere [148,149]. Regarding the TGF $\beta$  family, including TGF $\beta$  and BMP signaling, we can conclude that these signaling cascades are essential for epicardial EMT and invasion in the developing heart. Specific epicardial KO of ALK5 and ALK3 *in vivo* show an impaired development of the heart and *in vitro* studies demonstrate that this is due to the inability of epicardial cells to undergo EMT and to invade underlying tissue. The most important receptor for epicardial EMT and invasion appears to be ALK5, the main TGF $\beta$  type I receptor. In the injured heart, more research is needed to draw conclusions regarding the role of the TGF $\beta$  family in the epicardial contribution to repair, but the presence of relevant ligands and receptors in the adult epicardium indicates that TGF $\beta$  and BMP signaling occurs. For regeneration, opportunities lie within finding specific approaches to activate TGF $\beta$  signaling in a controlled manner, which could be achieved via TGF $\beta$ R3 or thymosin  $\beta$ 4.

## REFERENCES

1. Kurkiewicz T. O histogenezie mięśnia sercowego zwierząt kręgowych. *Bull. I' Acad. Sci. Cracovie*. 1909:148–191.
2. Manasek F. Embryonic development of the heart - Formation of the Epicardium. *J. Embryol. Exp. Morph.* 1969;22:333–348.
3. Virágh S., Gittenberger-de Groot A.C., Poelmann R.E., Káimán F. Early development of quail heart epicardium and associated vascular and glandular structures. *Anat. Embryol. (Berl)*. 1993;188:381–393. doi: 10.1007/BF00185947.
4. Viragh S., Challice C.E. The origin of the epicardium and the embryonic myocardial circulation in the mouse. *Anat. Rec.* 1981;201:157–168. doi: 10.1002/ar.1092010117.
5. Pérez-Pomares J.M., Macías D., García-Garrido L., Muñoz-Chápuli R. Contribution of the primitive epicardium to the subepicardial mesenchyme in hamster and chick embryos. *Dev. Dyn.* 1997;210:96–105. doi: 10.1002/(SICI)1097-0177(199710)210:2<96::AID-AJA3>3.0.CO;2-4.
6. Mikawa T., Fischman D.A. Retroviral analysis of cardiac morphogenesis: Discontinuous formation of coronary vessels. *Proc. Natl. Acad. Sci. USA*. 1992;89:9504–9508. doi: 10.1073/pnas.89.20.9504.
7. Gittenberger-de Groot A.C., Vrancken Peeters M.P., Mentink M.M., Gourdie R.G., Poelmann R.E. Epicardium-derived cells contribute a novel population to the myocardial wall and the atrioventricular cushions. *Circ. Res.* 1998;82:1043–1052. doi: 10.1161/01.RES.82.10.1043.
8. Dettman R.W., Denetclaw W., Ordahl C.P., Bristow J. Common epicardial origin of coronary vascular smooth muscle, perivascular fibroblasts, and intermyocardial fibroblasts in the avian heart. *Dev. Biol.* 1998;193:169–181. doi: 10.1006/dbio.1997.8801.
9. Gittenberger-de Groot A.C., Winter E.M., Poelmann R.E. Epicardium derived cells (EPDCs) in development, cardiac disease and repair of ischemia. *J. Cell. Mol. Med.* 2010;14:1056–1060. doi: 10.1111/j.1582-4934.2010.01077.x.
10. Kelder T.P., Duim S.N., Vicente-Steijn R., Végh A.M.D., Kruithof B.P.T., Smits A.M., van Bavel T.C., Bax N.A.M., Schalij M.J., Gittenberger-de Groot A.C., et al. The epicardium as modulator of the cardiac autonomic response during early development. *J. Mol. Cell. Cardiol.* 2015;89:251–259. doi: 10.1016/j.yjmcc.2015.10.025.
11. Chen T.H.P., Chang T.-C., Kang J.-O., Choudhary B., Makita T., Tran C.M., Burch J.B.E., Eid H., Sucov H.M. Epicardial induction of fetal cardiomyocyte proliferation via a retinoic acid-inducible trophic factor. *Dev. Biol.* 2002;250:198–207. doi: 10.1006/dbio.2002.0796.
12. Weeke-Klimp A., Bax N.A.M., Bellu A.R., Winter E.M., Vrolijk J., Plantinga J., Maas S., Brinker M., Mahtab E.A.F., Gittenberger-de Groot A.C., et al. Epicardium-derived cells enhance proliferation, cellular maturation and alignment of cardiomyocytes. *J. Mol. Cell. Cardiol.* 2010;49:606–616. doi: 10.1016/j.yjmcc.2010.07.007.
13. Männer J., Schlueter J., Brand T. Experimental analyses of the function of the proepicardium using a new microsurgical procedure to induce loss-of-proepicardial-function in chick embryos. *Dev. Dyn.* 2005;233:1454–1463. doi: 10.1002/dvdy.20487.

14. Gittenberger-de Groot A.C., Vrancken Peeters M.-P.F.M., Bergwerff M., Mentink M.M.T., Poelmann R.E. Epicardial Outgrowth Inhibition Leads to Compensatory Mesothelial Outflow Tract Collar and Abnormal Cardiac Septation and Coronary Formation. *Circ. Res.* 2000;87:969–971. doi: 10.1161/01.RES.87.11.969.
15. Lepilina A., Coon A.N., Kikuchi K., Holdway J.E., Roberts R.W., Burns C.G., Poss K.D. A Dynamic Epicardial Injury Response Supports Progenitor Cell Activity during Zebrafish Heart Regeneration. *Cell.* 2006;127:607–619. doi: 10.1016/j.cell.2006.08.052.
16. Smart N., Risebro C.A., Melville A.A.D., Moses K., Schwartz R.J., Chien K.R., Riley P.R. Thymosin  $\beta_4$  induces adult epicardial progenitor mobilization and neovascularization. *Nature.* 2007;445:177–182. doi: 10.1038/nature05383.
17. van Tuyn J., Atsma D.E., Winter E.M., van der Velde-van Dijke I., Pijnappels D.A., Bax N.A., Knaän-Shanzer S., Gittenberger-de Groot A.C., Poelmann R.E., van der Laarse A., et al. Epicardial Cells of Human Adults Can Undergo an Epithelial-to-Mesenchymal Transition and Obtain Characteristics of Smooth Muscle Cells In Vitro. *Stem Cells.* 2007;25:271–278. doi: 10.1634/stemcells.2006-0366.
18. Zhou B., Honor L.B., He H., Ma Q., Oh J.-H., Butterfield C., Lin R.-Z., Melero-Martin J.M., Dolmatova E., Duffy H.S., et al. Adult mouse epicardium modulates myocardial injury by secreting paracrine factors. *J. Clin. Investig.* 2011;121:1894–1904. doi: 10.1172/JCI45529.
19. Smits A., Riley P. Epicardium-Derived Heart Repair. *J. Dev. Biol.* 2014;2:84–100. doi: 10.3390/jdb2020084.
20. Witman N., Murtuza B., Davis B., Arner A., Morrison J.I. Recapitulation of developmental cardiogenesis governs the morphological and functional regeneration of adult newt hearts following injury. *Dev. Biol.* 2011;354:67–76. doi: 10.1016/j.ydbio.2011.03.021.
21. Kim J., Wu Q., Zhang Y., Wiens K.M., Huang Y., Rubin N., Shimada H., Handin R.I., Chao M.Y., Tuan T.-L., et al. PDGF signaling is required for epicardial function and blood vessel formation in regenerating zebrafish hearts. *Proc. Natl. Acad. Sci. USA.* 2010;107:17206–17210. doi: 10.1073/pnas.0915016107.
22. Teotia P., Van Hook M.J., Fischer D., Ahmad I. Human retinal ganglion cell axon regeneration by recapitulating developmental mechanisms: Effects of recruitment of the mTOR pathway. *Development.* 2019;146:dev178012. doi: 10.1242/dev.178012.
23. McDermott A.M., Herberg S., Mason D.E., Collins J.M., Pearson H.B., Dawahare J.H., Tang R., Patwa A.N., Grinstaff M.W., Kelly D.J., et al. Recapitulating bone development through engineered mesenchymal condensations and mechanical cues for tissue regeneration. *Sci. Transl. Med.* 2019;11:eaav7756. doi: 10.1126/scitranslmed.aav7756.
24. Kahata K., Dadras M.S., Moustakas A. TGF- $\beta$  Family Signaling in Epithelial Differentiation and Epithelial–Mesenchymal Transition. *Cold Spring Harb. Perspect. Biol.* 2018;10:a022194. doi: 10.1101/cshperspect.a022194.
25. Assoian R.K., Komoriya A., Meyers C.A., Miller D.M., Sporn M.B. Transforming growth factor- $\beta$  in human platelets. Identification of a major storage site, purification, and characterization. *J. Biol. Chem.* 1983;258:7155–7160.
26. Wu M.Y., Hill C.S. TGF- $\beta$  Superfamily Signaling in Embryonic Development and Homeostasis. *Dev. Cell.* 2009;16:329–343. doi: 10.1016/j.devcel.2009.02.012.

27. Robertson I.B., Rifkin D.B. Regulation of the Bioavailability of TGF- $\beta$  and TGF- $\beta$ -Related Proteins. *Cold Spring Harb. Perspect. Biol.* 2016;8:a021907. doi: 10.1101/cshperspect.a021907.
28. Gentry L.E., Webb N.R., Lim G.J., Brunner A.M., Ranchalis J.E., Twardzik D.R., Lioubin M.N., Marquardt H., Purchio A.F. Type 1 transforming growth factor beta: Amplified expression and secretion of mature and precursor polypeptides in Chinese hamster ovary cells. *Mol. Cell. Biol.* 1987;7:3418–3427. doi: 10.1128/MCB.7.10.3418.
29. Dubois C.M., Laprise M.H., Blanchette F., Gentry L.E., Leduc R. Processing of transforming growth factor  $\beta$ 1 precursor by human furin convertase. *J. Biol. Chem.* 1995;270:10618–10624. doi: 10.1074/jbc.270.18.10618.
30. Sengle G., Ono R.N., Lyons K.M., Bächinger H.P., Sakai L.Y. A New Model for Growth Factor Activation: Type II Receptors Compete with the Prodomain for BMP-7. *J. Mol. Biol.* 2008;381:1025–1039. doi: 10.1016/j.jmb.2008.06.074.
31. Brown M.A., Zhao Q., Baker K.A., Naik C., Chen C., Pukac L., Singh M., Tsareva T., Parice Y., Mahoney A., et al. Crystal structure of BMP-9 and functional interactions with pro-region and receptors. *J. Biol. Chem.* 2005;280:25111–25118. doi: 10.1074/jbc.M503328200.
32. Jiang H., Salmon R.M., Upton P.D., Wei Z., Lawera A., Davenport A.P., Morrell N.W., Li W. The prodomain-bound form of bone morphogenetic protein 10 is biologically active on endothelial cells. *J. Biol. Chem.* 2016;291:2954–2966. doi: 10.1074/jbc.M115.683292.
33. Sengle G., Ono R.N., Sasaki T., Sakai L.Y. Prodomains of transforming growth factor  $\beta$  (TGF $\beta$ ) Superfamily members specify different functions: Extracellular matrix interactions and growth factor bioavailability. *J. Biol. Chem.* 2011;286:5087–5099. doi: 10.1074/jbc.M110.188615.
34. Goumans M.J., ten Dijke P. TGF- $\beta$  signaling in control of cardiovascular function. *Cold Spring Harb. Perspect. Biol.* 2017;10:1–39. doi: 10.1101/cshperspect.a022210.
35. Hata A., Chen Y.G. TGF- $\beta$  signaling from receptors to smads. *Cold Spring Harb. Perspect. Biol.* 2016;8:a022061. doi: 10.1101/cshperspect.a022061.
36. Weiss A., Attisano L. The TGFbeta superfamily signaling pathway. *Wiley Interdiscip. Rev. Dev. Biol.* 2013;2:47–63. doi: 10.1002/wdev.86.
37. Zhao H.-J., Klausen C., Li Y., Zhu H., Wang Y.-L., Leung P.C.K. Bone morphogenetic protein 2 promotes human trophoblast cell invasion by upregulating N-cadherin via non-canonical SMAD2/3 signaling. *Cell Death Dis.* 2018;9:174. doi: 10.1038/s41419-017-0230-1.
38. Goumans M.-J., Valdimarsdottir G., Itoh S., Rosendahl A., Sideras P., ten Dijke P., Ananth S., Knebelmann B., Gruning W., Dhanabal M., et al. Balancing the activation state of the endothelium via two distinct TGF-beta type I receptors. *EMBO J.* 2002;21:1743–1753. doi: 10.1093/emboj/21.7.1743.
39. Goumans M.-J., Valdimarsdottir G., Itoh S., Lebrin F., Larsson J., Mummery C., Karlsson S., ten Dijke P. Activin Receptor-like Kinase (ALK)1 Is an Antagonistic Mediator of Lateral TGF $\beta$ /ALK5 Signaling. *Mol. Cell.* 2003;12:817–828. doi: 10.1016/S1097-2765(03)00386-1.
40. Zhang Y.E. Non-Smad signaling pathways of the TGF- $\beta$  family. *Cold Spring Harb. Perspect. Biol.* 2017;9:a022129. doi: 10.1101/cshperspect.a022129.

41. Männer J. Experimental study on the formation of the epicardium in chick embryos. *Anat. Embryol. (Berl)*. 1993;187:281–289. doi: 10.1007/BF00195766.
42. Velecela V., Torres-Cano A., García-Melero A., Ramiro-Pareta M., Müller-Sánchez C., Segarra-Mondejar M., Chau Y., Campos-Bonilla B., Reina M., Soriano F.X., et al. Epicardial cell shape and maturation are regulated by Wt1 via transcriptional control of Bmp4. *Development*. 2019;146:dev178723. doi: 10.1242/dev.178723.
43. Wu M., Smith C.L., Hall J.A., Lee I., Luby-Phelps K., Tallquist M.D. Epicardial Spindle Orientation Controls Cell Entry into the Myocardium. *Dev. Cell*. 2010;19:114–125. doi: 10.1016/j.devcel.2010.06.011.
44. Pérez-Pomares J.M.M., Phelps A., Sedmerova M., Carmona R., González-Iriarte M., Muñoz-Chápuli R., Wessels A., Muñoz-Chápuli R., Wessels A., Muñoz-Chápuli R., et al. Experimental Studies on the Spatiotemporal Expression of WT1 and RALDH2 in the Embryonic Avian Heart: A Model for the Regulation of Myocardial and Valvuloseptal Development by Epicardially Derived Cells (EPDCs) *Dev. Biol*. 2002;247:307–326. doi: 10.1006/dbio.2002.0706.
45. Von Gise A., Pu W.T. Endocardial and epicardial epithelial to mesenchymal transitions in heart development and disease. *Circ. Res*. 2012;110:1628–1645. doi: 10.1161/CIRCRESA-HA.111.259960.
46. von Gise A., Zhou B., Honor L.B., Ma Q., Petryk A., Pu W.T. Wt1 regulates epicardial epithelial to mesenchymal transition through beta-catenin and retinoic acid signaling pathways. *Dev. Biol*. 2011;356:421–431. doi: 10.1016/j.ydbio.2011.05.668.
47. Smits A.M., Dronkers E., Goumans M.-J.J. The epicardium as a source of multipotent adult cardiac progenitor cells: Their origin, role and fate. *Pharmacol. Res*. 2018;127:129–140. doi: 10.1016/j.phrs.2017.07.020.
48. Vega-Hernández M., Kovacs A., de Langhe S., Ornitz D.M. FGF10/FGFR2b signaling is essential for cardiac fibroblast development and growth of the myocardium. *Development*. 2011;138:3331–3340. doi: 10.1242/dev.064410.
49. Zamora M., Männer J., Ruiz-Lozano P. Epicardium-derived progenitor cells require  $\beta$ -catenin for coronary artery formation. *Proc. Natl. Acad. Sci. USA*. 2007;104:18109–18114. doi: 10.1073/pnas.0702415104.
50. Zhou B., von Gise A., Ma Q., Hu Y.W., Pu W.T. Genetic fate mapping demonstrates contribution of epicardium-derived cells to the annulus fibrosus of the mammalian heart. *Dev. Biol*. 2010;338:251–261. doi: 10.1016/j.ydbio.2009.12.007.
51. Wessels A., van den Hoff M.J.B., Adamo R.F., Phelps A.L., Lockhart M.M., Sauls K., Briggs L.E., Norris R.A., van Wijk B., Perez-Pomares J.M., et al. Epicardially derived fibroblasts preferentially contribute to the parietal leaflets of the atrioventricular valves in the murine heart. *Dev. Biol*. 2012;366:111–124. doi: 10.1016/j.ydbio.2012.04.020.
52. Lockhart M.M., Phelps A.L., van den Hoff M.J.B., Wessels A. The epicardium and the development of the atrioventricular junction in the murine heart. *J. Dev. Biol*. 2014;2:1–17. doi: 10.3390/jdb2010001.

53. Merki E., Zamora M., Raya A., Kawakami Y., Wang J., Zhang X., Burch J., Kubalak S.W., Kaliman P., Belmonte J.C.I., et al. Epicardial retinoid X receptor is required for myocardial growth and coronary artery formation. *Proc. Natl. Acad. Sci. USA.* 2005;102:18455–18460. doi: 10.1073/pnas.0504343102.
54. Lavine K.J., Yu K., White A.C., Zhang X., Smith C., Partanen J., Ornitz D.M. Endocardial and epicardial derived FGF signals regulate myocardial proliferation and differentiation in vivo. *Dev. Cell.* 2005;8:85–95. doi: 10.1016/j.devcel.2004.12.002.
55. Kolander K.D., Holtz M.L., Cossette S.M., Duncan S.A., Misra R.P. Epicardial GATA factors regulate early coronary vascular plexus formation. *Dev. Biol.* 2014;386:204–215. doi: 10.1016/j.ydbio.2013.12.033.
56. van Wijk B., Gunst Q.D., Moorman A.F.M., van den Hoff M.J.B. Cardiac regeneration from activated epicardium. *PLoS ONE.* 2012;7:e44692. doi: 10.1371/journal.pone.0044692.
57. Smart N., Bollini S., Dubé K.N., Vieira J.M., Zhou B., Davidson S., Yellon D., Riegler J., Price A.N., Lythgoe M.F., et al. De novo cardiomyocytes from within the activated adult heart after injury. *Nature.* 2011;474:640–644. doi: 10.1038/nature10188.
58. Duan J., Gherghe C., Liu D., Hamlett E., Srikantha L., Rodgers L., Regan J.N., Rojas M., Willis M., Leask A., et al. Wnt1/ $\beta$ catenin injury response activates the epicardium and cardiac fibroblasts to promote cardiac repair. *EMBO J.* 2012;31:429–442. doi: 10.1038/emboj.2011.418.
59. Molin D.G.M., Bartram U., Van der Heiden K., Van Iperen L., Speer C.P., Hierck B.P., Poelmann R.E., Gittenberger-de-Groot A.C. Expression patterns of Tgf $\beta$ 1-3 associate with myocardialisation of the outflow tract and the development of the epicardium and the fibrous heart skeleton. *Dev. Dyn.* 2003;227:431–444. doi: 10.1002/dvdy.10314.
60. Compton L.A., Potash D.A., Mundell N.A., Barnett J.V. Transforming growth factor- $\beta$  induces loss of epithelial character and smooth muscle cell differentiation in epicardial cells. *Dev. Dyn.* 2006;235:82–93. doi: 10.1002/dvdy.20629.
61. Engelmann G.L. Coordinate gene expression during neonatal rat heart development. A possible role for the myocyte in extracellular matrix biogenesis and capillary angiogenesis. *Cardiovasc. Res.* 1993;27:1598–1605. doi: 10.1093/cvr/27.9.1598.
62. Hill C.R., Sanchez N.S., Love J.D., Arrieta J.A., Hong C.C., Brown C.B., Austin A.F., Barnett J.V. BMP2 signals loss of epithelial character in epicardial cells but requires the Type III TGF $\beta$  receptor to promote invasion. *Cell. Signal.* 2012;24:1012–1022. doi: 10.1016/j.cell-sig.2011.12.022.
63. Sridurongrit S., Larsson J., Schwartz R., Ruiz-Lozano P., Kaartinen V. Signaling via the Tgf- $\beta$  type I receptor Alk5 in heart development. *Dev. Biol.* 2008;322:208–218. doi: 10.1016/j.ydbio.2008.07.038.
64. Lütke T.H., Rudat C., Kurz J., Häfner R., Greulich F., Wojahn I., Aydoğdu N., Mamo T.M., Kleppa M.-J., Trowe M.-O., et al. Mesothelial mobilization in the developing lung and heart differs in timing, quantity, and pathway dependency. *Am. J. Physiol. Cell. Mol. Physiol.* 2019;316:L767–L783. doi: 10.1152/ajplung.00212.2018.

65. Sanford L.P., Ormsby I., Gittenberger-de Groot A.C., Sariola H., Friedman R., Boivin G.P., Cardell E.L., Doetschman T. TGFbeta2 knockout mice have multiple developmental defects that are non-overlapping with other TGFbeta knockout phenotypes. *Development*. 1997;124:2659–2670.
66. Kruithof B.P.T., Kruithof-De-Julio M., Poelmann R.E., Gittenberger-De-Groot A.C., Gaussin V., Goumans M.J. Remodeling of the myocardium in early trabeculation and cardiac valve formation; a role for TGFβ2. *Int. J. Dev. Biol.* 2013;57:859–869. doi: 10.1387/ijdb.130302bk.
67. Proetzel G., Pawlowski S.A., Wiles M.V., Yin M., Boivin G.P., Howles P.N., Ding J., Ferguson M.W., Doetschman T. Transforming growth factor-beta 3 is required for secondary palate fusion. *Nat. Genet.* 1995;11:409–414. doi: 10.1038/ng1295-409.
68. Kaartinen V., Voncken J.W., Shuler C., Warburton D., Bu D., Heisterkamp N., Groffen J. Abnormal lung development and cleft palate in mice lacking TGF-β3 indicates defects of epithelial-mesenchymal interaction. *Nat. Genet.* 1995;11:415–421. doi: 10.1038/ng1295-415.
69. Azhar M., Schultz J.E.J., Grupp I., Dorn G.W., Meneton P., Molin D.G.M., Gittenberger-de Groot A.C., Doetschman T. Transforming growth factor beta in cardiovascular development and function. *Cytokine Growth Factor Rev.* 2003;14:391–407. doi: 10.1016/S1359-6101(03)00044-3.
70. Dickson M.C., Martin J.S., Cousins F.M., Kulkarni A.B., Karlsson S., Akhurst R.J. Defective haematopoiesis and vasculogenesis in transforming growth factor-beta 1 knock out mice. *Development*. 1995;121:1845–1854.
71. Shull M.M., Ormsby I., Kier A.B., Pawlowski S., Diebold R.J., Yin M., Allen R., Sidman C., Proetzel G., Calvin D. Targeted disruption of the mouse transforming growth factor-beta 1 gene results in multifocal inflammatory disease. *Nature*. 1992;359:693–699. doi: 10.1038/359693a0.
72. Larsson J., Goumans M.J., Sjöstrand L.J., Van Rooijen M.A., Ward D., Levéen P., Xu X., Ten Dijke P., Mummery C.L., Karlsson S. Abnormal angiogenesis but intact hematopoietic potential in TGF-β type I receptor-deficient mice. *EMBO J.* 2001;20:1663–1673. doi: 10.1093/emboj/20.7.1663.
73. Oshima M., Oshima H., Taketo M.M. TGF-β receptor type II deficiency results in defects of yolk sac hematopoiesis and vasculogenesis. *Dev. Biol.* 1996;179:297–302. doi: 10.1006/dbio.1996.0259.
74. Letterio J., Geiser A., Kulkarni A., Roche N., Sporn M., Roberts A. Maternal rescue of transforming growth factor-beta 1 null mice. *Science*. 1994;264:1936–1938. doi: 10.1126/science.8009224.
75. Daniel C.W., Silberstein G.B., Van Horn K., Strickland P., Robinson S. TGF-β1-induced inhibition of mouse mammary ductal growth: Developmental specificity and characterization. *Dev. Biol.* 1989;135:20–30. doi: 10.1016/0012-1606(89)90154-1.
76. Migdalska A., Molineux G., Demuyneck H., Evans G.S., Ruscettp F., Dexter T.M. Growth inhibitory effects of transforming growth factor-β1 in vivo. *Growth Factors*. 1991;4:239–245. doi: 10.3109/08977199109104820.

77. MacNeill C., French R., Evans T., Wessels A., Burch J.B.E. Modular regulation of cGATA-5 gene expression in the developing heart and gut. *Dev. Biol.* 2000;217:62–76. doi: 10.1006/dbio.1999.9539.
78. Olivey H.E., Mundell N.A., Austin A.F., Barnett J.V. Transforming growth factor- $\beta$  stimulates epithelial–mesenchymal transformation in the proepicardium. *Dev. Dyn.* 2006;235:50–59. doi: 10.1002/dvdy.20593.
79. Austin A.F., Compton L.A., Love J.D., Brown C.B., Barnett J.V. Primary and immortalized mouse epicardial cells undergo differentiation in response to TGF $\beta$ . *Dev. Dyn.* 2008;237:366–376. doi: 10.1002/dvdy.21421.
80. Dronkers E., Moerkamp A.T., van Herwaarden T., Goumans M.-J., Smits A.M. The Isolation and Culture of Primary Epicardial Cells Derived from Human Adult and Fetal Heart Specimens. *J. Vis. Exp.* 2018;134:e57370. doi: 10.3791/57370.
81. Moerkamp A.T., Lodder K., van Herwaarden T., Dronkers E., Dingenouts C.K.E., Tengström F.C., van Brakel T.J., Goumans M.-J., Smits A.M. Human fetal and adult epicardial-derived cells: A novel model to study their activation. *Stem Cell Res. Ther.* 2016;7:174. doi: 10.1186/s13287-016-0434-9.
82. Smith C.L., Baek S.T., Sung C.Y., Tallquist M.D. Epicardial-derived cell epithelial-to-mesenchymal transition and fate specification require PDGF receptor signaling. *Circ. Res.* 2011;108:e15–e26. doi: 10.1161/CIRCRESAHA.110.235531.
83. Dokic D., Dettman R.W. VCAM-1 inhibits TGF $\beta$  stimulated epithelial-mesenchymal transformation by modulating Rho activity and stabilizing intercellular adhesion in epicardial mesothelial cells. *Dev. Biol.* 2006;299:489–504. doi: 10.1016/j.ydbio.2006.08.054.
84. Morabito C.J., Dettman R.W., Kattan J., Collier J.M., Bristow J. Positive and Negative Regulation of Epicardial–Mesenchymal Transformation during Avian Heart Development. *Dev. Biol.* 2001;234:204–215. doi: 10.1006/dbio.2001.0254.
85. Xie L., Law B.K., Aakre M.E., Edgerton M., Shyr Y., Bhowmick N.A., Moses H.L. Transforming growth factor beta-regulated gene expression in a mouse mammary gland epithelial cell line. *Breast Cancer Res.* 2003;5:R187–R198. doi: 10.1186/bcr640.
86. Tao J., Barnett J., Watanabe M., Ramírez-Bergeron D. Hypoxia Supports Epicardial Cell Differentiation in Vascular Smooth Muscle Cells through the Activation of the TGF $\beta$  Pathway. *J. Cardiovasc. Dev. Dis.* 2018;5:19. doi: 10.3390/jcdd5020019.
87. Sánchez N.S., Barnett J.V. TGF $\beta$  and BMP-2 regulate epicardial cell invasion via TGF $\beta$ R3 activation of the Par6/Smurf1/RhoA pathway. *Cell. Signal.* 2012;24:539–548. doi: 10.1016/j.cellsig.2011.10.006.
88. Narumiya S., Thumkeo D. Rho signaling research: History, current status and future directions. *FEBS Lett.* 2018;592:1763–1776. doi: 10.1002/1873-3468.13087.
89. Sauer B., Vogler R., Zimmermann K., Fujii M., Anzano M.B., Schäfer-Korting M., Roberts A.B., Kleuser B. Lysophosphatidic acid interacts with transforming growth factor- $\beta$  signaling to mediate keratinocyte growth arrest and chemotaxis. *J. Investig. Dermatol.* 2004;123:840–849. doi: 10.1111/j.0022-202X.2004.23458.x.

90. Trembley M.A., Velasquez L.S., de Mesy Bentley K.L., Small E.M. Myocardin-related transcription factors control the motility of epicardium-derived cells and the maturation of coronary vessels. *Development*. 2015;142:21–30. doi: 10.1242/dev.116648.
91. Craig E.A., Austin A.F., Vaillancourt R.R., Barnett J.V., Camenisch T.D. TGF $\beta$ 2-mediated production of hyaluronan is important for the induction of epicardial cell differentiation and invasion. *Exp. Cell Res*. 2010;316:3397–3405. doi: 10.1016/j.yexcr.2010.07.006.
92. Namwanje M., Brown C.W. Activins and Inhibins: Roles in Development, Physiology, and Disease. *Cold Spring Harb. Perspect. Biol*. 2016;8:a021881. doi: 10.1101/cshperspect.a021881.
93. Oh S.P., Li E. The signaling pathway mediated by the type IIB activin receptor controls axial patterning and lateral asymmetry in the mouse. *Genes Dev*. 1997;11:1812–1826. doi: 10.1101/gad.11.14.1812.
94. Roessler E., Pei W., Ouspenskaia M.V., Karkera J.D., Veléz J.I., Banerjee-Basu S., Gibney G., Lupo P.J., Mitchell L.E., Towbin J.A., et al. Cumulative ligand activity of NODAL mutations and modifiers are linked to human heart defects and holoprosencephaly. *Mol. Genet. Metab*. 2009;98:225–234. doi: 10.1016/j.ymgme.2009.05.005.
95. Dean M., Davis D.A., Burdette J.E. Activin A stimulates migration of the fallopian tube epithelium, an origin of high-grade serous ovarian cancer, through non-canonical signaling. *Cancer Lett*. 2017;391:114–124. doi: 10.1016/j.canlet.2017.01.011.
96. Bauer J., Ozden O., Akagi N., Carroll T., Principe D.R., Staudacher J.J., Spehlmann M.E., Eckmann L., Grippo P.J., Jung B. Activin and TGF $\beta$  use diverging mitogenic signaling in advanced colon cancer. *Mol. Cancer*. 2015;14:182. doi: 10.1186/s12943-015-0456-4.
97. Valcourt U., Kowanetz M., Niimi H., Heldin C.H., Moustakas A. TGF- $\beta$  and the Smad signaling pathway support transcriptomic reprogramming during epithelial-mesenchymal cell transition. *Mol. Biol. Cell*. 2005;16:1987–2002. doi: 10.1091/mbc.e04-08-0658.
98. Murakami M., Suzuki M., Nishino Y., Funaba M. Regulatory expression of genes related to metastasis by TGF- $\beta$  and activin A in B16 murine melanoma cells. *Mol. Biol. Rep*. 2010;37:1279–1286. doi: 10.1007/s11033-009-9502-x.
99. Basu M., Bhattacharya R., Ray U., Mukhopadhyay S., Chatterjee U., Roy S.S. Invasion of ovarian cancer cells is induced byPITX2-mediated activation of TGF- $\beta$  and Activin-A. *Mol. Cancer*. 2015;14:162. doi: 10.1186/s12943-015-0433-y.
100. Moore C.S., Mjaatvedt C.H., Gearhart J.D. Expression and function of activin beta A during mouse cardiac cushion tissue formation. *Dev. Dyn*. 1998;212:548–562. doi: 10.1002/(SICI)1097-0177(199808)212:4<548::AID-AJA8>3.0.CO;2-H.
101. Urist M.R. Bone: Formation by autoinduction. *Science*. 1965;150:893–899. doi: 10.1126/science.150.3698.893.
102. Kruihof B.P.T., van Wijk B., Somi S., Kruihof-de Julio M., Pérez Pomares J.M., Weesie F., Wessels A., Moorman A.F.M., van den Hoff M.J.B. BMP and FGF regulate the differentiation of multipotential pericardial mesoderm into the myocardial or epicardial lineage. *Dev. Biol*. 2006;295:507–522. doi: 10.1016/j.ydbio.2006.03.033.

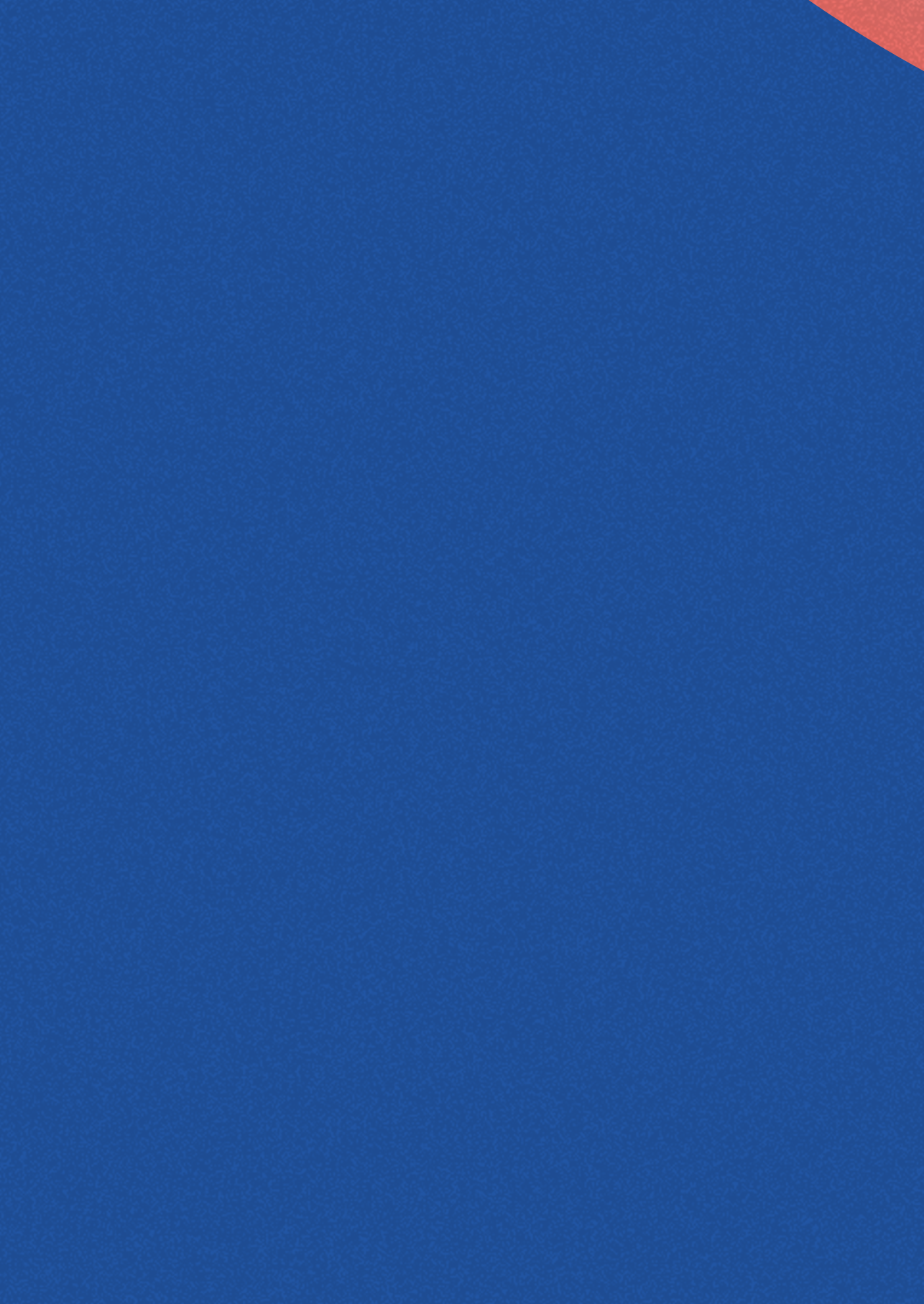
103. Ma L., Lu M.F., Schwartz R.J., Martin J.F. Bmp2 is essential for cardiac cushion epithelial-mesenchymal transition and myocardial patterning. *Development*. 2005;132:5601–5611. doi: 10.1242/dev.02156.
104. Wang R.N., Green J., Wang Z., Deng Y., Qiao M., Peabody M., Zhang Q., Ye J., Yan Z., Denduluri S., et al. Bone Morphogenetic Protein (BMP) signaling in development and human diseases. *Genes Dis*. 2014;1:87–105. doi: 10.1016/j.gendis.2014.07.005.
105. Rivera-Feliciano J., Tabin C.J. Bmp2 instructs cardiac progenitors to form the heart-valve-inducing field. *Dev. Biol*. 2006;295:580–588. doi: 10.1016/j.ydbio.2006.03.043.
106. Gaussin V., Van De Putte T., Mishina Y., Hanks M.C., Zwijsen A., Huylebroeck D., Behringer R.R., Schneider M.D. Endocardial cushion and myocardial defects after cardiac myocyte-specific conditional deletion of the bone morphogenetic protein receptor ALK3. *Proc. Natl. Acad. Sci. USA*. 2002;99:2878–2883. doi: 10.1073/pnas.042390499.
107. Song L., Fässler R., Mishina Y., Jiao K., Baldwin H.S. Essential functions of Alk3 during AV cushion morphogenesis in mouse embryonic hearts. *Dev. Biol*. 2007;301:276–286. doi: 10.1016/j.ydbio.2006.08.004.
108. Lockhart M.M., Boukens B.J.D., Phelps A.L., Brown C.-L.M., Toomer K.A., Burns T.A., Mukherjee R.D., Norris R.A., Trusk T.C., van den Hoff M.J.B., et al. Alk3 mediated Bmp signaling controls the contribution of epicardially derived cells to the tissues of the atrioventricular junction. *Dev. Biol*. 2014;396:8–18. doi: 10.1016/j.ydbio.2014.09.031.
109. Ten Dijke P., Goumans M.J., Pardali E. Endoglin in angiogenesis and vascular diseases. *Angiogenesis*. 2008;11:79–89. doi: 10.1007/s10456-008-9101-9.
110. Ollauri-Ibáñez C., López-Novoa J.M., Pericacho M. Endoglin-based biological therapy in the treatment of angiogenesis-dependent pathologies. *Expert Opin. Biol. Ther*. 2017;17:1053–1063. doi: 10.1080/14712598.2017.1346607.
111. Mercado-Pimentel M.E., Hubbard A.D., Runyan R.B. Endoglin and Alk5 regulate epithelial-mesenchymal transformation during cardiac valve formation. *Dev. Biol*. 2007;304:420–432. doi: 10.1016/j.ydbio.2006.12.038.
112. Valeria B., Maddalena G., Enrica V., Onofrio T., Gaetano B. Endoglin (CD105) Expression in the Human Heart Throughout Gestation: An Immunohistochemical Study. *Reprod. Sci*. 2008;15:1018–1026. doi: 10.1177/1933719108322429.
113. Hu J., Guan W., Yan L., Ye Z., Wu L., Xu H. Cancer Stem Cell Marker Endoglin (CD105) Induces Epithelial Mesenchymal Transition (EMT) but Not Metastasis in Clear Cell Renal Cell Carcinoma. *Stem Cells Int*. 2019;2019:1–9. doi: 10.1155/2019/9060152.
114. Bax N.A.M., Oorschot A.A.M., Maas S., Braun J., Tuyn J., Vries A.A.F., Groot A.C.G., Goumans M.-J. In vitro epithelial-to-mesenchymal transformation in human adult epicardial cells is regulated by TGF $\beta$ -signaling and WT1. *Basic Res. Cardiol*. 2011;106:829–847. doi: 10.1007/s00395-011-0181-0.
115. López-Casillas F., Wrana J.L., Massagué J. Betaglycan presents ligand to the TGF $\beta$  signaling receptor. *Cell*. 1993;73:1435–1444. doi: 10.1016/0092-8674(93)90368-Z.

116. Kirkbride K.C., Townsend T.A., Bruinsma M.W., Barnett J.V., Blobel G.C. Bone Morphogenetic Proteins Signal through the Transforming Growth Factor- $\beta$  Type III Receptor. *J. Biol. Chem.* 2008;283:7628–7637. doi: 10.1074/jbc.M704883200.
117. Wiater E., Harrison C.A., Lewis K.A., Gray P.C., Vale W.W. Identification of distinct inhibin and transforming growth factor  $\beta$ -binding sites on betaglycan: Functional separation of betaglycan co-receptor actions. *J. Biol. Chem.* 2006;281:17011–17022. doi: 10.1074/jbc.M601459200.
118. Sankar S., Mahooti-Brooks N., Centrella M., McCarthy T.L., Madri J.A. Expression of Transforming Growth Factor Type III Receptor in Vascular Endothelial Cells Increases Their Responsiveness to Transforming Growth Factor  $\beta$ 2. *J. Biol. Chem.* 1995;270:13567–13572. doi: 10.1074/jbc.270.22.13567.
119. Cheifetz S., Hernandez H., Laiho M., ten Dijke P., Iwata K.K., Massagué J. Distinct transforming growth factor-beta (TGF-beta) receptor subsets as determinants of cellular responsiveness to three TGF-beta isoforms. *J. Biol. Chem.* 1990;265:20533–20538.
120. Blobel G.C., Schiemann W.P., Pepin M.C., Beauchemin M., Moustakas A., Lodish H.F., O'Connor-McCourt M.D. Functional Roles for the Cytoplasmic Domain of the Type III Transforming Growth Factor  $\beta$  Receptor in Regulating Transforming Growth Factor  $\beta$  Signaling. *J. Biol. Chem.* 2001;276:24627–24637. doi: 10.1074/jbc.M100188200.
121. Compton L.A., Potash D.A., Brown C.B., Barnett J.V. Coronary Vessel Development Is Dependent on the Type III Transforming Growth Factor  $\beta$  Receptor. *Circ. Res.* 2007;101:784–791. doi: 10.1161/CIRCRESAHA.107.152082.
122. Sánchez N.S., Hill C.R., Love J.D., Soslow J.H., Craig E., Austin A.F., Brown C.B., Czirok A., Camenisch T.D., Barnett J.V. The cytoplasmic domain of TGF $\beta$ 3 through its interaction with the scaffolding protein, GIPC, directs epicardial cell behavior. *Dev. Biol.* 2011;358:331–343. doi: 10.1016/j.ydbio.2011.08.008.
123. Allison P., Espiritu D., Camenisch T.D. BMP2 rescues deficient cell migration in Tgfb3(-/-) epicardial cells and requires Src kinase. *Cell Adh. Migr.* 2016;10:259–268. doi: 10.1080/19336918.2015.1119362.
124. DeLaughter D.M., Clark C.R., Christodoulou D.C., Seidman C.E., Baldwin H.S., Seidman J.G., Barnett J.V. Transcriptional Profiling of Cultured, Embryonic Epicardial Cells Identifies Novel Genes and Signaling Pathways Regulated by TGF $\beta$ 3 In Vitro. *PLoS ONE.* 2016;11:e0159710. doi: 10.1371/journal.pone.0159710.
125. Clark C.R., Robinson J.Y., Sanchez N.S., Townsend T.A., Arrieta J.A., Merryman W.D., Trykall D.Z., Olivey H.E., Hong C.C., Barnett J.V. Common pathways regulate Type III TGF $\beta$  receptor-dependent cell invasion in epicardial and endocardial cells. *Cell. Signal.* 2016;28:688–698. doi: 10.1016/j.cellsig.2016.03.004.
126. You H.J., How T., Blobel G.C. The type III transforming growth factor- $\beta$  receptor negatively regulates nuclear factor kappa B signaling through its interaction with  $\beta$ -arrestin2. *Carcinogenesis.* 2009;30:1281–1287. doi: 10.1093/carcin/bgp071.
127. Miyazono K., Ehata S., Koinuma D. Tumor-promoting functions of transforming growth factor- $\beta$  in progression of cancer. *Ups. J. Med. Sci.* 2012;117:143–152. doi: 10.3109/03009734.2011.638729.

128. Dewald O., Ren G., Duerr G.D., Zoerlein M., Klemm C., Gersch C., Tincey S., Michael L.H., Entman M.L., Frangogiannis N.G. Of mice and dogs: Species-specific differences in the inflammatory response following myocardial infarction. *Am. J. Pathol.* 2004;164:665–677. doi: 10.1016/S0002-9440(10)63154-9.
129. Bujak M., Frangogiannis N. The role of TGF- $\beta$  signaling in myocardial infarction and cardiac remodeling. *Cardiovasc. Res.* 2007;74:184–195. doi: 10.1016/j.cardiores.2006.10.002.
130. Chuva De Sousa Lopes S.M., Feijen A., Korving J., Korchynskiy O., Larsson J., Karlsson S., Ten Dijke P., Lyons K.M., Goldschmeding R., Doevendans P., et al. Connective tissue growth factor expression and Smad signaling during mouse heart development and myocardial infarction. *Dev. Dyn.* 2004;231:542–550. doi: 10.1002/dvdy.20162.
131. Frangogiannis N.G. The role of transforming growth factor (TGF)- $\beta$  in the infarcted myocardium. *J. Thorac. Dis.* 2017;9:S52–S63. doi: 10.21037/jtd.2016.11.19.
132. Euler G. Good and bad sides of TGF $\beta$ -signaling in myocardial infarction. *Front. Physiol.* 2015;6:66. doi: 10.3389/fphys.2015.00066.
133. Chablais F., Jazwinska A. The regenerative capacity of the zebrafish heart is dependent on TGF signaling. *Development.* 2012;139:1921–1930. doi: 10.1242/dev.078543.
134. Wang J., Karra R., Dickson A.L., Poss K.D. Fibronectin is deposited by injury-activated epicardial cells and is necessary for zebrafish heart regeneration. *Dev. Biol.* 2013;382:427–435. doi: 10.1016/j.ydbio.2013.08.012.
135. Marro J., Pfefferli C., de Preux Charles A.-S., Bise T., Jaźwińska A. Collagen XII Contributes to Epicardial and Connective Tissues in the Zebrafish Heart during Ontogenesis and Regeneration. *PLoS ONE.* 2016;11:e0165497. doi: 10.1371/journal.pone.0165497.
136. Dogra D., Ahuja S., Kim H.-T., Rasouli S.J., Stainier D.Y.R., Reischauer S. Opposite effects of Activin type 2 receptor ligands on cardiomyocyte proliferation during development and repair. *Nat. Commun.* 2017;8:1902. doi: 10.1038/s41467-017-01950-1.
137. Morrell N.W., Bloch D.B., ten Dijke P., Goumans M.-J.T.H., Hata A., Smith J., Yu P.B., Bloch K.D. Targeting BMP signalling in cardiovascular disease and anaemia. *Nat. Rev. Cardiol.* 2016;13:106–120. doi: 10.1038/nrcardio.2015.156.
138. Lane K.B., Machado R.D., Pauciulo M.W., Thomson J.R., Phillips J.A., Loyd J.E., Nichols W.C., Trembath R.C., Aldred M., Brannon C.A., et al. Heterozygous germline mutations in BMPR2, encoding a TGF- $\beta$  receptor, cause familial primary pulmonary hypertension. *Nat. Genet.* 2000;26:81–84. doi: 10.1038/79226.
139. Urness L.D., Sorensen L.K., Li D.Y. Arteriovenous malformations in mice lacking activin receptor-like kinase-1. *Nat. Genet.* 2000;26:328–331. doi: 10.1038/81634.
140. Stahls P.F., Lightell D.J., Moss S.C., Goldman C.K., Woods T.C. Elevated serum bone morphogenetic protein 4 in patients with chronic kidney disease and coronary artery disease. *J. Cardiovasc. Transl. Res.* 2013;6:232–238. doi: 10.1007/s12265-012-9429-9.
141. Hanna A., Frangogiannis N.G. The Role of the TGF- $\beta$  Superfamily in Myocardial Infarction. *Front. Cardiovasc. Med.* 2019;6:1–15. doi: 10.3389/fcvm.2019.00140.

142. Wu C.C., Kruse F., Vasudevarao M.D., Junker J.P., Zebrowski D.C., Fischer K., Noël E.S., Grün D., Berezikov E., Engel F.B., et al. Spatially Resolved Genome-wide Transcriptional Profiling Identifies BMP Signaling as Essential Regulator of Zebrafish Cardiomyocyte Regeneration. *Dev. Cell.* 2016;36:36–49. doi: 10.1016/j.devcel.2015.12.010.
143. Cao J., Navis A., Cox B.D., Dickson A.L., Gemberling M., Karra R., Bagnat M., Poss K.D. Single epicardial cell transcriptome sequencing identifies Caveolin 1 as an essential factor in zebrafish heart regeneration. *Development.* 2016;143:232–243. doi: 10.1242/dev.130534.
144. Rossdeutsch A., Smart N., Dubé K.N., Turner M., Riley P.R. Essential Role for Thymosin  $\beta$ 4 in Regulating Vascular Smooth Muscle Cell Development and Vessel Wall Stability. *Circ. Res.* 2012;111:e89–e102. doi: 10.1161/CIRCRESAHA.111.259846.
145. Banerjee I., Zhang J., Moore-Morris T., Lange S., Shen T., Dalton N.D., Gu Y., Peterson K.L., Evans S.M., Chen J. Thymosin beta 4 is dispensable for murine cardiac development and function. *Circ. Res.* 2012;110:456–464. doi: 10.1161/CIRCRESAHA.111.258616.
146. Smart N., Risebro C.A., Melville A.A.D., Moses K., Schwartz R.J., Chien K.R., Riley P.R. Thymosin  $\beta$ -4 is essential for coronary vessel development and promotes neovascularization via adult epicardium. *Ann. N. Y. Acad. Sci.* 2007;1112:171–188. doi: 10.1196/annals.1415.000.
147. Tandon P., Miteva Y.V., Kuchenbrod L.M., Cristea I.M., Conlon F.L. Tcf21 regulates the specification and maturation of proepicardial cells. *Development.* 2012;140:2409–2421. doi: 10.1242/dev.093385.
148. Smart N., Riley P.R. The epicardium as a candidate for heart regeneration. *Future Cardiol.* 2012;8:53–69. doi: 10.2217/fca.11.87.
149. Quijada P., Trembley M.A., Small E.M. The Role of the Epicardium During Heart Development and Repair. *Circ. Res.* 2020;126:377–394. doi: 10.1161/CIRCRESAHA.119.315857.





# 6

## Activin A and ALK4 Identified as Novel Regulators of Epithelial to Mesenchymal Transition (EMT) in Human Epicardial Cells

Esther Dronkers<sup>1</sup>, Tessa van Herwaarden<sup>1</sup>, Thomas J van Brakel<sup>2</sup>, Gonzalo Sanchez-Duffhues<sup>1</sup>, Marie-José Goumans<sup>1</sup>, and Anke M Smits<sup>1</sup>

<sup>1</sup>Department of Cell and Chemical Biology, Leiden University Medical Center, Leiden, The Netherlands.

<sup>2</sup>Department of Cardiothoracic Surgery, Leiden University Medical Center, Leiden, The Netherlands.

*Published in Frontiers in Cell and Developmental Biology (2021)*  
*doi: 10.3389/fcell.2021.765007*

## ABSTRACT

The epicardium, the mesothelial layer covering the heart, is a crucial cell source for cardiac development and repair. It provides cells and biochemical signals to the heart to facilitate vascularization and myocardial growth. An essential element of epicardial behavior is epicardial epithelial to mesenchymal transition (epiMT), which is the initial step for epicardial cells to become motile and invade the myocardium. To identify targets to optimize epicardium-driven repair of the heart, it is vital to understand which pathways are involved in the regulation of epiMT. Therefore, we established a cell culture model for human primary adult and fetal epiMT, which allows for parallel testing of inhibitors and stimulants of specific pathways. Using this approach, we reveal Activin A and ALK4 signaling as novel regulators of epiMT, independent of the commonly accepted EMT inducer TGF $\beta$ . Importantly, Activin A was able to induce epicardial invasion in cultured embryonic mouse hearts. Our results identify Activin A/ALK4 signaling as a modulator of epicardial plasticity which may be exploitable in cardiac regenerative medicine.

### Keywords

epicardium, EMT—epithelial to mesenchymal transition, ALK4, activin A, cardiac repair and regeneration, heart, primary cell culture

## INTRODUCTION

The epicardium, a mesothelial cell layer enveloping the heart, is increasingly recognized as a crucial contributor to heart development and repair. During cardiac development, the epicardium supplies the myocardium with cardiogenic biochemical signals and with cells such as fibroblasts, smooth muscle cells and pericytes (Dettman et al., 1998; Smits et al., 2018). Studies preventing the formation of the epicardium reported severe defects in vascularization and in myocardial compaction (Gittenberger-de Groot et al., 2000; Männer et al., 2005) demonstrating the physiological significance of the epicardium in cardiogenesis. Furthermore, disruption of epicardial behavior, for example due to genetic mutations, can contribute to congenital heart disease (Ruiz-Villalba and Pérez-Pomares, 2012).

To partake in heart development, epicardial cells undergo epithelial to mesenchymal transition (epiMT) (Dettman et al., 1998). This process is characterized by exchanging epicardial markers such as WT1, for mesenchymal proteins such as  $\alpha$ SMA, POSTN and N-cadherin, thereby modulating their cytoskeleton and cell-cell adhesive properties. These dramatic phenotypical changes allow the cell to degrade the basal membrane and migrate into the underlying tissue.

In the healthy adult heart, the epicardium is a quiescent cell-layer. However, ischemic injury induces recapitulation of fetal epicardial processes (Zhou et al., 2011), including the upregulation of epiMT related genes (van Wijk et al., 2012). Similar to its function in development, the epicardium participates in tissue formation in the cardiac post-injury response (Duan et al., 2012; Wang et al., 2015). Importantly, it has been shown that increased epicardial activity is associated with an improved reparative response of the mammalian heart (Smart et al., 2011; Balbi et al., 2019), thereby suggesting that activation of this cell layer can be an attractive therapeutic target to improve cardiac repair. A recent finding by Mantri et al. using pseudotime analysis of chick heart single cell RNA sequencing data suggested that epiMT occurs prior to fate specification (Mantri et al., 2021), emphasizing that regulation of epiMT is an essential first step in the epicardial contribution to tissue formation. This is further substantiated by embryonal mouse models where epicardial EMT was hampered, resulting in severe defects in smooth muscle cell coverage of the vessels and in myocardial invasion (Zamora et al., 2007; Sridurongrit et al., 2008; Liu et al., 2018; Jackson-Weaver et al., 2020). Therefore, regulating epiMT is the key step to control the epicardium-driven repair response post-injury.

In order to study epiMT we have previously developed a cell culture system using human primary fetal and adult epicardial cells (Moerkamp et al., 2016). In this model, we have shown that adult epicardial cells efficiently undergo epiMT upon stimulation with Transforming growth factor (TGF) $\beta$ , whereas fetal epicardial cells undergo epiMT spontaneously which is counteracted by SB431542, a TGF $\beta$  type I receptor kinase inhibitor (Moerkamp et al., 2016). TGF $\beta$  is an extensively described regulator of epithelial to mesenchymal differentiation (Kahata et al., 2018). TGF $\beta$  family ligands induce intracellular signaling responses upon activation of a transmembrane receptor complex consisting of type I and type II receptors with enzymatic serine threonine kinase activity. In the case of TGF $\beta$ 1/2/3, they act by binding to TGF $\beta$  type II receptor (TGF $\beta$ RII) that forms a complex with, and transphosphorylates the TGF $\beta$  type I receptor activin receptor-like kinase 5 (ALK5). Once activated, ALK5 kinase in turn phosphorylates SMAD2 and SMAD3 that partners with SMAD4 and translocates into the nucleus in order to modulate the expression of a specific subset of genes, several of them involved in EMT (Goumans and ten Dijke, 2018). However, the TGF $\beta$  pathway can also interact with other pathways, such as nuclear factor kappa B (NF- $\kappa$ B) (López-Rovira et al., 2000). Furthermore, the TGF $\beta$  family does not solely consist of TGF $\beta$  signaling, but also includes signaling via BMP and Activins which can signal via other type I and type II receptor complexes. The role of these related pathways in epiMT is yet unexplored (Dronkers et al., 2020).

In order to study epiMT regulating pathways in more detail, we have further exploited our primary cell culture system. The unique feature of having both highly active fetal epicardial cells and inducible adult cells allows for studying pathway inhibitors and stimulants of epiMT. When interrogating this model, we identified Activin A and its receptor ALK4 signaling as novel regulators of epicardial plasticity *in vitro*. Additionally we show that Activin A can indeed induce epicardial invasion in *ex vivo* cultured mouse hearts.

## METHODS

### Collection of Human Cardiac Tissue

Human adult heart auricles were collected anonymously as surgical waste from patients undergoing cardiac surgery under general informed consent. Human fetal cardiac tissue was collected with informed consent and anonymously from elective abortion material of fetuses with a gestational age between 10 and 20 weeks. This research was carried out according to the official guidelines of the Leiden University Medical

Center and approved by the local Medical Ethics Committee (number P08.087). This research conforms to the Declaration of Helsinki.

## Cell Culture and Experiments

### *Cell Culture*

Epicardial tissue was isolated as described (Dronkers et al., 2018). Briefly, the epicardial layer was stripped from the cardiac tissue and minced followed by several rounds of incubation with 0.25% trypsin/EDTA. The suspension was passed through a syringe and filtered to obtain a single cell suspension. Cells were seeded on 0.1% gelatin (Sigma Aldrich) coated plates and cultured in EPDC medium which consists of Dulbecco's modified Eagle's medium (DMEM low- glucose, Gibco) and Medium 199 (M199, Gibco) mixed in a 1:1 ratio, supplemented with 10% fetal bovine serum (heat inactivated for 25 min at 56°C, Biowest), and 100 U/mL penicillin (Roth) and 100 mg/ml streptomycin (Roth). Cells were cultured in the presence of 10  $\mu$ M SB431542 (Tocris) at 37°C in 5% CO<sub>2</sub>.

### *Ligand and Inhibitor Stimulation*

To reduce patient variation, only those cell isolations were included that upon isolation displayed a clear epithelial phenotype shown by a cobblestone morphology. For experiments, fetal or adult EPDCs were trypsinized and seeded in a ~30–50% confluency. The next day, cells were stimulated for five days with either TGF $\beta$ 3 (1 ng/ml, R and D systems), BMP6 (50 ng/ml, Peprotech), TNF $\alpha$  (10 ng/ml, Peprotech), Activin A (50 ng/ml, Peprotech), SB431542 (10  $\mu$ M, Tocris), LY2157299 (20  $\mu$ M, Calbiochem), TGF $\beta$ 1/2/3 monoclonal capture antibody (1D11) (1  $\mu$ g/ml, ThermoFisher), control capture antibody (13C4) (1  $\mu$ g/ml, Genzyme), LDN212854 (100 nM, Axon Medchem), Bay 11-7085 (5  $\mu$ M, Sigma-Aldrich) or Follistatin 288 (5  $\mu$ g/ml, homemade). Working concentrations of ligands and inhibitors were determined based on concentrations series experiments, selecting the lowest concentration that exerted epiMT. For the factors that did not elicit an effect, we used the concentration that is commonly described in literature.

### *Staining and Imaging*

Cells were fixed in 4% PFA, washed and blocked in 1%BSA/0.1% Tween 20/PBS and incubated with a primary antibody against human  $\alpha$ SMA (Human alpha-Smooth Muscle Actin Alexa Fluor® 488-conjugated Antibody, R&D systems), HA (12CA5, Roche) or ALK4 (Activin A Receptor Type IB/ALK-4, Abcam). Then, cells were incubated with a secondary antibody (Alexa Fluor 488, 555 or 647, Thermo Scientific) combined with

phalloidin conjugated antibody (Rhodamine Phalloidin, Invitrogen). Lastly, cells were stained with DAPI (Thermo Scientific). Imaging was performed using the Leica AF6000.

### ***Isolation of mRNA and qPCR***

mRNA was isolated using ReliaPrep™ RNA Miniprep Systems (Promega). The mRNA concentration and purity were measured using NanoDrop 1000 Spectrophotometer (Thermo Fisher Scientific) followed by cDNA synthesis using the RevertAid H Minus First Strand cDNA Synthesis Kit (Thermo Fisher Scientific). qPCR was performed in a 384 wells format using SYBR Green (Promega) and run on a CFX384 Touch™ Real-Time PCR Detection System (Bio-Rad). Expression levels were normalized for two reference genes (*HPRT1* and *TBP*) which were designed and tested for robust expression in adult and fetal EPDCs and in epithelial and mesenchymal samples using geNorm (VandeSompele 2002). Primers sequences are provided in Supplementary Table S1.

### ***Adenoviral Transduction***

For transduction with constitutively active ALK4 (Ad-caALK4), or wild type ALK4 (Ad-ALK4-OE), adenovirus was generated as described (Fujii et al., 1999), and produced using ViraPower adenoviral expression system (Life technologies). To determine the effect on cellular phenotype and epiMT markers, adult EPDCs were transduced with Ad-caALK4, Ad-ALK4-OE or control Ad-LacZ virus for 24 h and subsequently cultured for four days. To establish expression of EMT transcription factors, mRNA of adult EPDCs was isolated 20 h after transduction.

### ***Baseline Gene Expression Profiles***

To eliminate the potential effect of SB431542 on baseline levels, it was first established that the effect of ALK4/5/7 kinase inhibition expired 3 h after removal of SB. Therefore, adult and fetal cobble EPDCs with a confluency of 60–80% were cultured for 3 h in the absence of SB431542 whereafter RNA was isolated.

### ***Ex vivo Invasion Assay***

All animal experiments were performed according to protocols approved by the animal welfare committee of the Leiden University Medical Center and conform the guidelines from Directive 2010/63/EU of the European Parliament on the protection of animals used for scientific purposes. Female Rosa26<sup>mTmG/mTmG</sup> mice were set-up for timed matings with male Wt1<sup>creERT2/+</sup>. The presence of a plug in the morning was denoted as embryonic day (E)0.5. At E9.5, the mother was injected with tamoxifen (2 mg) to label the pro-epicardial cells. After three days, when the epicardium has covered the heart, embryos were isolated from which the embryonic heart was dissected

and cultured based on a previously published protocol (Jackson-Weaver et al., 2020). Embryonic tissue was cultured in DMEM high glucose and M199 mixed in a 1:1 ratio supplemented with 0.1% FBS and 100 U/mL penicillin and 100 mg/ml streptomycin at 37°C in 5% CO<sub>2</sub>. After 24 h, the culture medium of the embryos carrying the Cre + genotype was supplemented with 2 ng/ml FGF with or without 200 ng/ml Activin A and incubated for another 48 h. The tissue was fixed in 4% PFA, embedded in paraffin, sectioned, and stained as described (Kruithof et al., 2020) using the following antibodies: α-GFP(Abcam, ab13970), α-Tropomyosin (Sigma-Aldrich, T9283) and α-Wt1 (Abcam, ab89901).

### Quantification and Statistics

αSMA surface area was quantified by taking four blinded pictures per condition per cell isolation, which subsequently were analyzed in an unbiased fashion using Fiji software and corrected for the number of DAPI + nuclei per picture. For every experiment, the n number is indicated, referring to the number of individual cell isolations that have been used. Displayed pictures are representative for multiple observations. Statistics were performed using Graphpad 9.0.1 software. Only relevant comparisons, which are indicated in the figures by a stripe, were statistically tested. For every experiment, the performed statistical test is indicated in the figure legend. Significance was considered when  $p < 0.05$ .

## RESULTS

To study EMT in epicardial cells (epiMT), we established a model consisting of primary epicardial derived cells (EPDCs) isolated from human adult and fetal cardiac specimens. In agreement with our previous results, EPDCs cultured in the presence of the ALK4/5/7 kinase inhibitor SB431542 (SB) maintained an epithelial phenotype characterized by a round cobblestone morphology (Supplementary Figures S1A,B, orange arrows) (Moerkamp et al., 2016). After exposure to exogenous TGFβ, EPDCs underwent epiMT, demonstrated by a change towards a spindle-shaped, mesenchymal cell morphology (Supplementary Figures S1A,B, bright field). This was accompanied by a high expression α Smooth Muscle Actin (αSMA).

Importantly, removing SB from the culture medium (CTRL) did not affect the morphology of adult EPDCs (Supplementary Figure S1B), while in fetal EPDCs the absence of SB was sufficient to initiate epiMT (Supplementary Figure S1A). The ability to spontaneously undergo epiMT makes the human fetal cell culture system an attractive

model to identify inhibitors of epiMT (Figure 1A). Conversely, adult EPDC can be used to detect inducers of epiMT (Figure 1B).

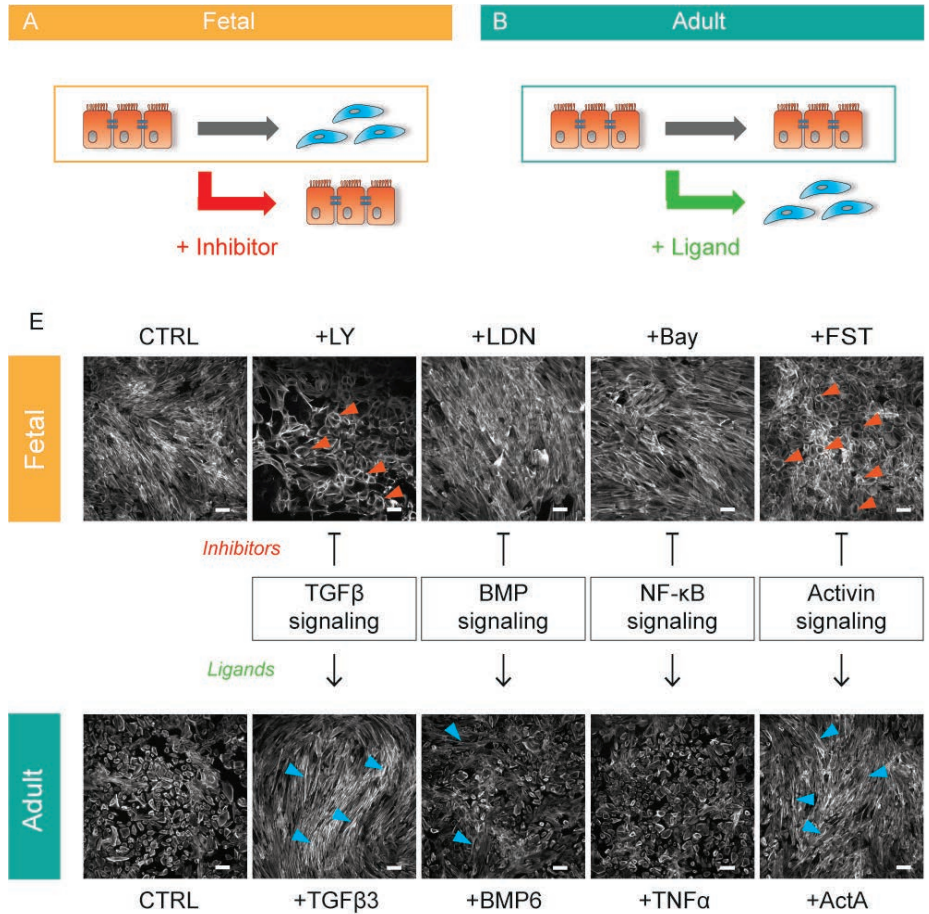
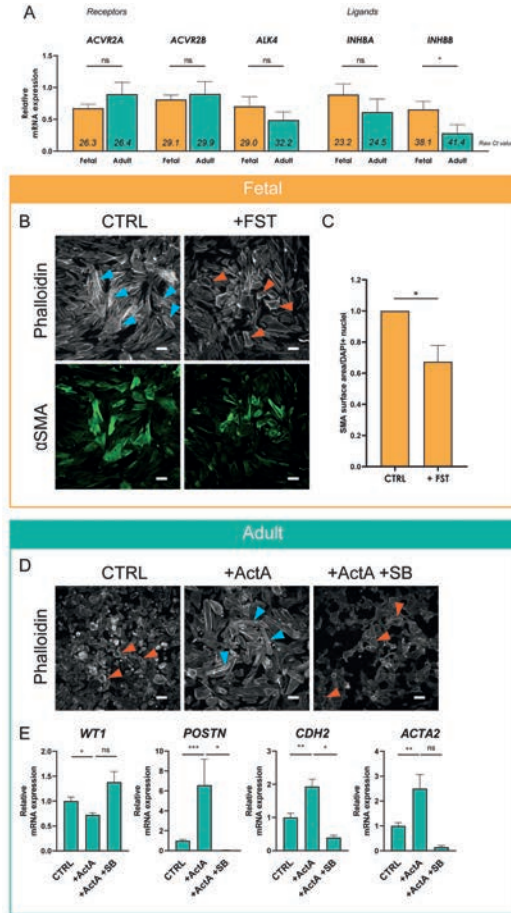


Figure 1 | Bi-directional cell culture model to unravel epiMT regulating pathways.

(A) Schematic representation of spontaneous fetal epiMT as a platform to identify inhibitors of epiMT. (B) Schematic representation of adult EPDCs as a model to identify inducers of epiMT. (C) Combined bi-directional model of human fetal (top) and adult (bottom) EPDCs cultured for 5 days with multiple inhibitor-ligand combinations to assess pathway involvement in epiMT. Phalloidin staining shows the epithelial (orange arrows) and mesenchymal (blue arrows) phenotype. Inhibitors: LY-2157299 (LY), LDN212854 (LDN), Bay 11-7085 (Bay), Follistatin (FST), Ligands: Transforming growth factor beta 3 (TGFβ 3), bone morphogenetic protein 6 (BMP6), tumor necrosis factor alpha (TNFα), Activin A (ActA). Representative for  $n = 3$ . Scale bar: 100 μM.

Therefore, to identify novel pathways involved in human epiMT, we applied our *in vitro* model as a bi-directional cell culture system, allowing parallel analysis of pathway inhibitors in fetal EPDCs and their affiliated ligands in adult EPDCs. The fact that SB blocks spontaneous epiMT in fetal cells suggests that this process is governed via an ALK4/5/7 mediated pathway. First, we confirmed the role of TGF $\beta$  signaling in epiMT using an alternative ALK4/5/7 kinase inhibitor LY2157299 (LY). While TGF $\beta$  induced an obvious morphological change compared to adult epicardial control conditions -as shown by the appearance of F-Actin stress fibers (Figure 1C, blue arrows)- LY prevented spontaneous fetal epiMT. Cells maintained a cobblestone morphology, with a cortical organization of F-Actin fibers as revealed by phalloidin staining at the inner cell surface (Figure 1C, orange arrows), which was distinctly different from the fetal control condition, thereby confirming our previous finding. Next, we explored TGF $\beta$ -related signaling pathways which have been associated with EMT, namely BMP signaling (Dituri et al., 2019) and nuclear factor kappa B (NF- $\kappa$ B) signaling (López-Rovira et al., 2000). After stimulation with BMP6, adult EPDCs displayed some patches of spindle shaped cells, but no gross morphological switch was observed compared to control cells. Moreover, since the BMP type I receptor kinase inhibitor LDN-212854 (LDN) was unable to block epiMT we disregarded BMP signaling as a major player in this process. Modulation of the NF- $\kappa$ B pathway did not morphologically alter either the fetal or the adult epicardial cells. However, exogenous Activin A stimulation of adult EPDCs led to a clear transition towards a spindle shaped morphology (Figure 1C, blue arrows). Moreover, fetal EPDCs incubated with the Activin natural antagonist Follistatin (FST) maintained an epithelial phenotype (Figure 1C, orange arrows). The combination of these two observations points towards a role for a previously unknown ability of Activin A signaling to regulate epiMT.

We continued to explore the role of Activin A signaling in epiMT. First, we determined the expression levels of relevant signaling components related to Activin. Activin homo- or heterodimeric ligands are composed by combinations of two subunits encoded by *INHBA* and/or *INHBB*, which signal by binding to the type II receptors ACVR2A or ACR2B, and type I receptor ALK4. The presence of all components could be established in both adult and fetal EPDCs (Figure 2A, raw Ct values in italics indicate presence of mRNA transcripts). Furthermore, ALK4, *INHBA* and *INHBB* mRNA showed a trend towards higher expression in fetal EPDCs.



**Figure 2 | Activin A signaling regulates epiMT. (A)** mRNA expression levels for Activin receptor type 2A (*ACVR2A*), Activin receptor type 2B (*ACVR2B*), Activin receptor type 1B (*ALK4*), Inhibin subunit beta A (*INHBA*) and Inhibin subunit beta B (*INHBB*) determined in cobble fetal and adult EPDCs cultured for 3 h after removal of SB ( $n = 6$ ). Raw Ct values per condition are shown in italics. \* =  $p < 0.05$ , ns = not significant (unpaired Student's  $t$ -test). Data are displayed as mean + SEM. **(B)** Immunofluorescent staining for phalloidin and  $\alpha$ SMA in fetal EPDCs cultured for 5 days in control (CTRL) or FST containing medium. Orange arrows indicate examples of epithelial cobblestone-shaped cells, blue arrows of mesenchymal spindle-shaped cells. Scale bar: 100  $\mu$ m. **(C)** Quantification of  $\alpha$ SMA positive surface area of FST treated cells relative to CTRL ( $n = 7$ ). \* =  $p < 0.05$  (paired Student's T-Test). **(D)** Phalloidin staining in adult EPDCs cultured for 5 days in control medium (CTRL), medium containing Activin A, or Activin A in combination with SB431542. Scale bar: 100  $\mu$ m. **(E)** mRNA expression levels of *WT1*, *POSTN*, *CDH2* and *ACTA 2* of adult EPDCs cultured for 5 days in the presence of ActA ( $n = 7$ ) or ActA + SB ( $n = 3$ ), relative to CTRL. \* =  $p < 0.05$ , \*\* =  $p < 0.01$ , ns = not significant (mixed-effects analysis, Sidak's multiple comparisons test).

Next, we validated the effect of Activin A signaling on epiMT markers in more detail. Fetal EPDCs treated with FST displayed a significant reduction of  $\alpha$ SMA expression compared to control cells, confirming the prevention of epiMT (Figures 2B,C and Supplementary Figure S2 for DAPI). In adult EPDCs, the Activin A-induced phenotypical change towards a mesenchymal cell type was accompanied by a significant decrease of epicardial marker WT1, and an increase of mRNA expression of mesenchymal markers *ACTA2* (encoding  $\alpha$ SMA), *POSTN* and *CDH2* confirming the occurrence of epiMT (Figures 2D,E). However, this did not result in a large change in  $\alpha$ SMA protein levels (Supplementary Figure S3).

To study the Activin A signaling pathway in more detail, we focused on the type I receptor ALK4. Noteworthy, besides inhibition of ALK5 kinase activity, SB and LY also inhibit the Activin type I receptor kinase ALK4. As expected based on its signaling via ALK4, Activin A initiated epiMT could be blocked by SB (Figures 2D,E).

To further confirm that ALK4 signaling is relevant for epiMT, adult EPDCs were transduced with an adenovirus expressing constitutively active ALK4 (Ad-caALK4) bound to an HA-tag. Successful viral transduction was confirmed by HA-tag protein expression (Supplementary Figure S4), and co-localisation of HA and ALK4 protein (Figure 3A). Within five days, Ad-caALK4 transduced adult EPDCs robustly displayed a mesenchymal phenotype, and an increased expression of *POSTN* and N-cadherin (Figures 3B,C). Furthermore, Ad-caALK4 transduction elicited an extensive upregulation of EMT transcription factors (Figure 3D). In addition, adenoviral overexpression of wild type ALK4 in adult EPDCs (Ad-ALK4-OE) provoked a quick and profound induction of epiMT (Figures 3B,C), which could suggest that ALK4 receptor availability impedes adult EPDCs to undergo epiMT *in vitro*.

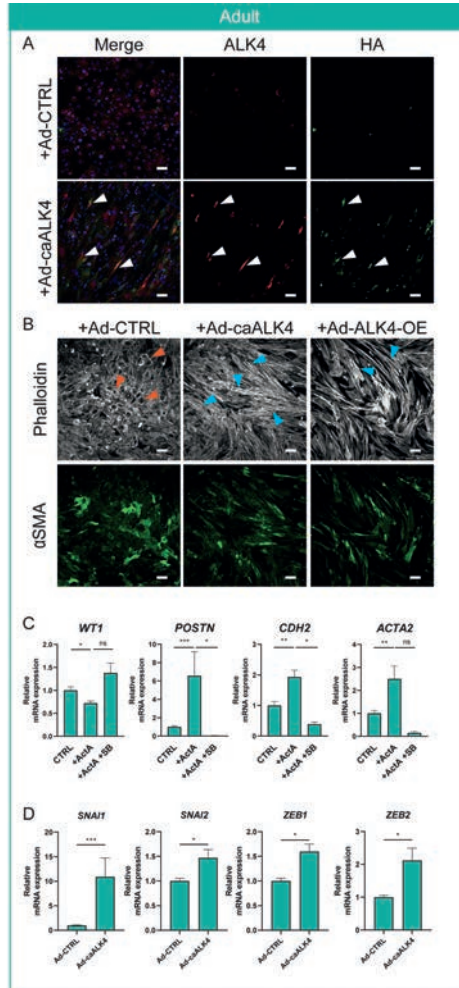


**Figure 3 | Activin receptor ALK4 overexpression induces epiMT in adult EPDCs.** (A) Representative example of ALK4 and HA staining in Ad-CTRL and Ad-caALK4 transduced adult EPDCs. Arrows indicate co-localization of ALK4 and HA in Ad-caALK4 treated cells. (B) Phalloidin and  $\alpha$ SMA staining of adult EPDCs transduced with Ad-CTRL, Ad-caALK4 or Ad-ALK4-OE ( $n = 3$ ). Scale bar: 100  $\mu$ m. Orange arrows indicate examples of epithelial cobblestone-shaped cells, blue arrows of mesenchymal spindle-shaped cells. (C) mRNA expression levels of *WT1*, *POSTN*, *CDH2* and *ACTA2* ( $n = 3$ ) of adult EPDCs cultured for 5 days after transduction with Ad-caALK4 or Ad-ALK4-OE, relative to Ad-CTRL. \* =  $p < 0.05$ , ns = not significant (mixed-effects analysis, Sidak's multiple comparisons test). (D) mRNA expression levels of EMT transcription factors *SNAI1*, *SNAI2*, *ZEB1*, *ZEB2* ( $n = 3$ ) of adult EPDCs cultured for 20 h after transduction with Ad-caALK4 or Ad-ALK4-OE, relative to Ad-CTRL. \* =  $p < 0.05$ , \*\* =  $p < 0.01$ , \*\*\* =  $p < 0.001$ , ns = not significant (mixed-effects analysis, Sidak's multiple comparisons test).

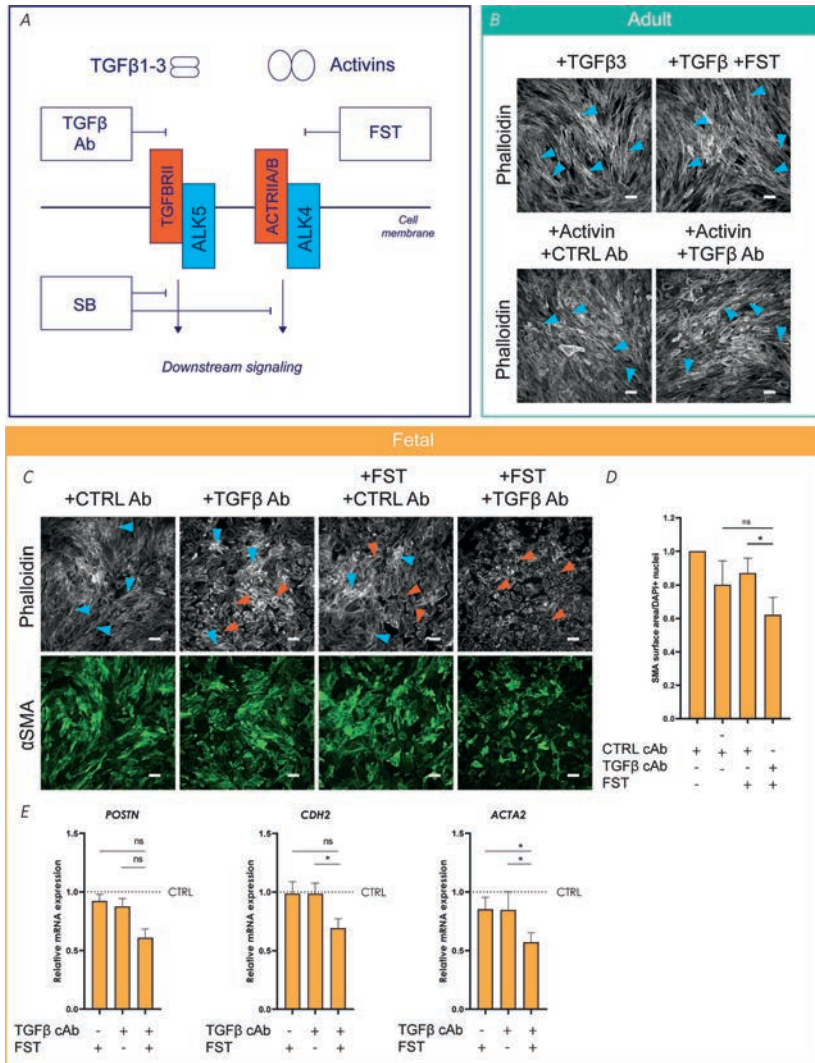


**Figure 4 | Activin A-induced epIMT is independent of TGFβ signaling.** (A) Schematic overview of TGFβ and Activin signaling and their concomitant inhibitors. (B) Phalloidin staining of adult EPDCs cultured for 5 days in the presence of TGFβ3, TGFβ3+FST, ActA + CTRL capture Ab (cAb), or Activin A + TGFβ cAb ( $n = 3$ ). Scale bar: 100 μm. (C) Phalloidin and αSMA staining ( $n = 5$ ) of fetal EPDCs cultured for 5 days in the presence of Activin A or TGFβ inhibitors. Scale bar: 100 μm. Orange arrows indicate examples of epithelial cobblestone-shaped cells, blue arrows of mesenchymal spindle-shaped cells. (D) Quantification of αSMA area ( $n = 4$ ), \* =  $p < 0.05$  (mixed-effects analysis, Sidak's multiple comparisons test). Data are displayed as mean + SEM. (E) mRNA expression levels of *POSTN*, *ACTA2*, *CDH2* ( $n = 4$ ) of fetal EPDCs cultured for 5 days. \* =  $p < 0.05$ , ns = not significant (mixed-effects analysis, Sidak's multiple comparisons test). Data are displayed as mean + SEM.

Thus far, we established that Activin A and ALK4 can regulate epiMT *in vitro*. Next, we explored potential synergistic effects between TGF $\beta$  and Activins by stimulating with one ligand and simultaneously blocking the alternate ligand-receptor interaction with a ligand neutralizing antibody, as schematically depicted in Figure 4A. As such, adult EPDCs were treated with TGF $\beta$  in combination with FST, or Activin A in combination with a TGF $\beta$  capture antibody (cAb) (for cAb effectivity tests, see Supplementary Figures S5,S6). EpiMT induction by TGF $\beta$  could not be blocked by the Activin inhibitor FST. Likewise, Activin A-induced epiMT was not prevented by the TGF $\beta$  cAb (Figure 4B and Supplementary Figures S5, S6 for controls). This suggests that both ALK5 and ALK4 mediated signaling independently have the ability to induce epiMT. Next, we assessed the effect of combined TGF $\beta$  and Activin blockade on fetal epicardial cells. Importantly, combined treatment with TGF $\beta$  cAb and FST exhibited an additive effect compared to FST treatment alone in fetal cells, as assessed by  $\alpha$ SMA protein expression levels, and on mRNA levels of mesenchymal genes (Figures 4C-E and Supplementary Figure S7 for DAPI). Taken together, our results demonstrate that Activin A and TGF $\beta$  can drive epiMT independently.

Finally, we validated our *in vitro* findings in a physiologically relevant setting of *ex vivo* murine embryonic heart cultures with an epicardial specific lineage trace system to study epicardial invasion (Figure 5A). Wt1<sup>creERT2/+</sup> Rosa26<sup>mTmG</sup> embryos were exposed *in utero* to tamoxifen at embryonic day E (9.5) to label Wt1<sup>+</sup> epicardial cells with GFP. At E12.5, hearts were isolated and cultured *ex vivo* as depicted in Figure 5, and invasion of epicardial cells into the myocardium was analyzed by fluorescent microscopy. Under control conditions, GFP<sup>+</sup> epicardial cells remained mostly at the surface of the heart. Interestingly, stimulation with Activin A induced a profound induction of epicardial invasion (Figure 5B), confirming that the Activin pathway is relevant for epiMT in a whole organ setting.

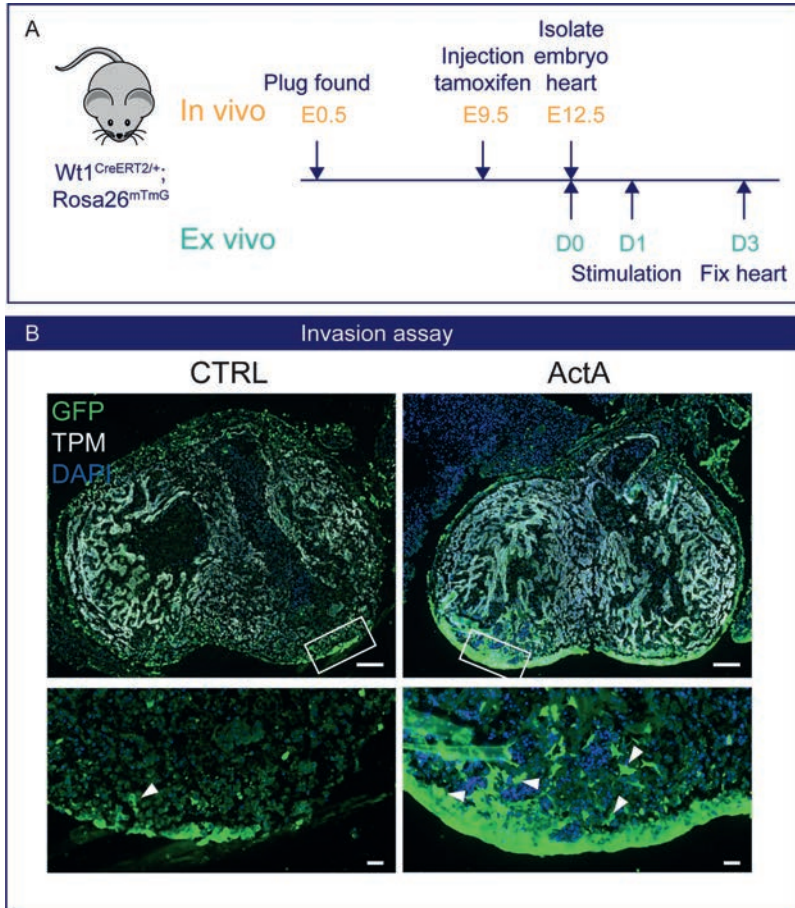


**Figure 5 | Activin A signaling initiates epicardial invasion in mouse heart. (A)** Experimental design: Pregnant dams are injected with tamoxifen at E9.5 and embryos are isolated on E12.5. Wt1<sup>CreERT2/+</sup>;Rosa26<sup>mTmG/+</sup> embryos were cultured *ex vivo* for 24 h and then stimulated with either 200 ng/ml Activin A ( $n = 3$ ) or control medium for 48 h. **(B)** Immunofluorescent staining for GFP (green), tropomyosin (TPM, white), and DAPI (blue). White arrows indicate Wt1-Cre-GFP+ epicardial cells that have invaded the myocardium. Scale bar: 100  $\mu$ m for overview and 20  $\mu$ m for zoom-in.

## DISCUSSION

The external layer of the heart, so called epicardium, has been implicated in key developmental processes and regenerative episodes. However, approaches to regulate epicardial plasticity remain elusive. Using a unique screening model consisting of human adult and fetal EPDCs, here we demonstrate that 1) epiMT can be regulated by Activin A (ActA) and ALK4 receptor activation, which 2) occurs in a TGF $\beta$ -signaling independent manner. As validation of these findings, we showed that 3) Activin A can initiate epicardial invasion in *ex vivo* heart tissue.

We have previously shown that primary fetal epicardial cells display an augmented epithelial-mesenchymal plasticity and readily undergo epiMT, while adult epicardial cells are relatively quiescent and only undergo epiMT when stimulated (Moerkamp et al., 2016). Combining these two models into a bidirectional cell culture system revealed Activin signaling as a novel regulator of epiMT. A role for Activin A and its receptor ALK4 in epicardial cells has not been described to date, but this signaling pathway is known to be able to promote EMT in multiple cancer cell lines (Valcourt et al., 2005; Murakami et al., 2010; Basu et al., 2015; Bauer et al., 2015; Dean et al., 2017). In our study, we established epiMT based on morphological changes, gene expression profiles of both EMT transcription factors and epicardial and mesenchymal markers, F-actin localization,  $\alpha$ SMA protein expression, and invasion capacity, as recommended by Yang et al. (2020). Interestingly, we observed a trend towards higher expression of ALK4, INHBA, and INHBB mRNA in fetal compared to adult EPDCs. Moreover, increasing ALK4 receptor availability on the surface of adult epicardial cells using adenoviral overexpression was sufficient to induce spontaneous epiMT in adult cells. Combined with the observation that fetal epiMT can partially be prevented by removal of Activin ligand with FST suggests a higher sensitivity of fetal EPDCs for Activin signaling, which may be one of the reasons why these cells are more prone to undergo EMT compared to adult EPDCs.

We demonstrated that both TGF $\beta$  and Activin A induce human epiMT independently. Interestingly, although TGF $\beta$  has been recognized as a central regulator of epiMT (Dronkers et al., 2020), the TGF $\beta$  cAb by itself was not able to prevent spontaneous epiMT in fetal epicardial cells. This suggests that other factors, such as Activin A, may compensate for the inactivation of TGF $\beta$  signaling. Activin A and ALK4 appear to induce less SMA expression compared to TGF $\beta$  which suggest that Activin signaling follows a separate differentiation path. In addition, our observation that incubation with recombinant FST in addition to the TGF $\beta$  cAb, prevents spontaneous epiMT also

points at Activin A/ALK4 signaling as an independent regulator of epiMT. The same principle has been shown in colon cancer cells, where the joint effect of TGF $\beta$  and Activin was vital for pro-metastatic function (Staudacher et al., 2017), which is related to EMT and invasion. In hindsight, the shared effects of TGF $\beta$ /ALK5 and Activin A/ALK4 signaling might have been overlooked in other studies since SB is often regarded as an ALK5 kinase inhibitor, while it actually targets ALK4, 5 and, 7 activity. Therefore, while the importance of TGF $\beta$  in epiMT has been established multiple times using SB, this approach likely masked the involvement of Activin signaling via ALK4.

To confirm our *in vitro* findings, we took advantage of an *ex vivo* cultured embryonic mouse heart model. In this system, Activin A endows the cells with more migratory and invasion properties, suggesting the presence of the ALK4 receptor and implicating that Activin A signaling could be of importance in cardiac development and regeneration. The necessity of epicardial Activin signaling during the development of the heart has not been studied, mainly because most of the Activin-related KO mice do not show a cardiac phenotype (Namwanje and Brown, 2016) or die at an early developmental stage before heart formation is initiated. However, the availability of Activin A in (sub)epicardial tissue has been reported (Feijen et al., 1994; Lupu et al., 2020), and therefore the secreted protein should be able to reach epicardial cells and initiate signaling. The presence of ALK4 is difficult to assess because most antibodies are not suitable for immunostainings. Nevertheless, a single cell RNA sequencing dataset of embryonic mouse epicardium indicates mRNA expression of ALK4 in a subset of epicardial cells (Lupu et al., 2020).

To conclude, with this study we add a novel pathway to epiMT regulation. As the epicardium has been proposed as an endogenous source for increased repair of injured cardiac tissue, our findings can serve as a starting point for further investigation into the therapeutic role of epicardial Activin A and ALK4 signaling in development and cardiac injury.

## ACKNOWLEDGMENTS

FST was a kind gift from Olli Ritvos. We thank Maarten van Dinther, Martijn Rabelink and Rob Hoeben for their help with virus production.

## **ETHICS STATEMENT**

The studies involving human participants were reviewed and approved by Medical Ethics Committee of the Leiden University Medical Center. The patients/participants provided their written informed consent to participate in this study. The animal study was reviewed and approved by Animal welfare committee of the Leiden University Medical Center.

## REFERENCES

- Balbi, C., Lodder, K., Costa, A., Moimas, S., Moccia, F., van Herwaarden, T., et al. (2019). Re-activating Endogenous Mechanisms of Cardiac Regeneration via Paracrine Boosting Using the Human Amniotic Fluid Stem Cell Secretome. *Int. J. Cardiol.* 287, 87–95. doi:10.1016/j.ijcard.2019.04.011
- Basu, M., Bhattacharya, R., Ray, U., Mukhopadhyay, S., Chatterjee, U., and Roy, S. S. (2015). Invasion of Ovarian Cancer Cells Is Induced byPITX2-Mediated Activation of TGF- $\beta$  and Activin-A. *Mol. Cancer* 14 (1), 162. doi:10.1186/s12943-015-0433-y
- Bauer, J., Ozden, O., Akagi, N., Carroll, T., Principe, D. R., Staudacher, J. J., et al. (2015). Activin and TGF $\beta$  Use Diverging Mitogenic Signaling in Advanced colon Cancer. *Mol. Cancer* 14 (1), 1–14. doi:10.1186/s12943-015-0456-4
- Dean, M., Davis, D. A., and Burdette, J. E. (2017). Activin A Stimulates Migration of the Fallopian Tube Epithelium, an Origin of High-Grade Serous Ovarian Cancer, through Non-canonical Signaling. *Cancer Lett.* 391, 114–124. doi:10.1016/j.canlet.2017.01.011
- Dettman, R. W., Denetclaw, W., Ordahl, C. P., and Bristow, J. (1998). Common Epicardial Origin of Coronary Vascular Smooth Muscle, Perivascular Fibroblasts, and Intermycardial Fibroblasts in the Avian Heart. *Develop. Biol.* 193, 169–181. doi:10.1006/dbio.1997.8801
- Dituri, F., Cossu, C., Mancarella, S., and Giannelli, G. (2019). The Interactivity between TGF $\beta$  and BMP Signaling in Organogenesis, Fibrosis, and Cancer. *Cells* 8 (10), 1130. doi:10.3390/cells8101130
- Dronkers, E., Moerkamp, A. T., van Herwaarden, T., Goumans, M.-J., and Smits, A. M. (2018). The Isolation and Culture of Primary Epicardial Cells Derived from Human Adult and Fetal Heart Specimens. *JoVE* 134, e57370. doi:10.3791/57370
- Dronkers, E., Wauters, M. M. M., Goumans, M. J., and Smits, A. M. (2020). Epicardial TGF $\beta$  and BMP Signaling in Cardiac Regeneration: What Lesson Can We Learn from the Developing Heart? *Biomolecules* 10 (3), 404. doi:10.3390/biom10030404
- Duan, J., Gherghe, C., Liu, D., Hamlett, E., Srikantha, L., Rodgers, L., et al. (2012). Wnt1/ $\beta$ catenin Injury Response Activates the Epicardium and Cardiac Fibroblasts to Promote Cardiac Repair. *EMBO J.* 31 (2), 429–442. doi:10.1038/emboj.2011.418
- Feijen, A., Goumans, M. J., van den, A. J., and Raaij, E.-v. (1994). Expression of Activin Subunits, Activin Receptors and Follistatin in Postimplantation Mouse Embryos Suggests Specific Developmental Functions for Different Activins. *Development* 120 (12), 3621–3637. doi:10.1242/dev.120.12.3621
- Fujii, M., Takeda, K., Imamura, T., Aoki, H., Sampath, T. K., Enomoto, S., et al. (1999). Roles of Bone Morphogenetic Protein Type I Receptors and Smad Proteins in Osteoblast and Chondroblast Differentiation. *MBoC* 10 (11), 3801–3813. doi:10.1091/mbc.10.11.3801
- Gittenberger-de Groot, A. C., Vrancken Peeters, M.-P. F. M., Bergwerff, M., Mentink, M. M. T., and Poelmann, R. E. (2000). Epicardial Outgrowth Inhibition Leads to Compensatory Mesothelial Outflow Tract Collar and Abnormal Cardiac Septation and Coronary Formation. *Circ. Res.* 87 (11), 969–971. doi:10.1161/01.RES.87.11.969Circ Res [Internet]

- Goumans, M.-J., and ten Dijke, P. (2018). TGF- $\beta$  Signaling in Control of Cardiovascular Function. *Cold Spring Harb Perspect. Biol.* 10 (2), a022210–39. doi:10.1101/cshperspect.a022210
- Jackson-Weaver, O., Ungvijanpunya, N., Yuan, Y., Qian, J., Gou, Y., Wu, J., et al. (2020). PRMT1-p53 Pathway Controls Epicardial EMT and Invasion. *Cel Rep.* 31 (10), 107739. doi:10.1016/j.celrep.2020.107739
- Kahata, K., Dadras, M. S., and Moustakas, A. (2018). TGF- $\beta$  Family Signaling in Epithelial Differentiation and Epithelial-Mesenchymal Transition. *Cold Spring Harb Perspect. Biol.* 10 (1), a022194. doi:10.1101/cshperspect.a022194
- Kruihof, B. P. T., Paardekooper, L., Hiemstra, Y. L., Goumans, M.-J., Palmén, M., Delgado, V., et al. (2020). Stress-induced Remodelling of the Mitral Valve: a Model for Leaflet Thickening and Superimposed Tissue Formation in Mitral Valve Disease. *Cardiovasc. Res.* 116, 931–943. doi:10.1093/cvr/cvz204
- Liu, X., Wang, Y., Liu, F., Zhang, M., Song, H., Zhou, B., et al. (2018). Wdpcp Promotes Epicardial EMT and Epicardium-Derived Cell Migration to Facilitate Coronary Artery Remodeling. *Sci. Signal.* 11 (27), eaah5770. doi:10.1126/scisignal.aah5770
- López-Rovira, T., Chalaux, E., Rosa, J. L., Bartrons, R., and Ventura, F. (2000). Interaction and Functional Cooperation of NF- $\kappa$ B with Smads. *J. Biol. Chem.* 275 (37), 28937–28946. doi:10.1074/jbc.M909923199
- Lupu, I.-E., Redpath, A. N., and Smart, N. (2020). Spatiotemporal Analysis Reveals Overlap of Key Proepicardial Markers in the Developing Murine Heart. *Stem Cell Rep.* 14 (5), 770–787. doi:10.1016/j.stemcr.2020.04.002
- Männer, J., Schlueter, J., and Brand, T. (2005). Experimental Analyses of the Function of the Proepicardium Using a New Microsurgical Procedure to Induce Loss-Of-Proepicardial-Function in Chick Embryos. *Dev. Dyn.* 233 (4), 1454–1463. doi:10.1002/dvdy.20487
- Mantri, M., Scuderi, G. J., Abedini-Nassab, R., Wang, M. F. Z., McKellar, D., Shi, H., et al. (2021). Spatiotemporal Single-Cell RNA Sequencing of Developing Chicken Hearts Identifies Interplay between Cellular Differentiation and Morphogenesis. *Nat. Commun.* 12 (1), 1771. doi:10.1038/s41467-021-21892-z
- Moerkamp, A. T., Lodder, K., van Herwaarden, T., Dronkers, E., Dingenouts, C. K. E., Tengström, F. C., et al. (2016). Human Fetal and Adult Epicardial-Derived Cells: a Novel Model to Study Their Activation. *Stem Cell Res Ther* 7 (1), 174. doi:10.1186/s13287-016-0434-9
- Murakami, M., Suzuki, M., Nishino, Y., and Funaba, M. (2010). Regulatory Expression of Genes Related to Metastasis by TGF- $\beta$  and Activin A in B16 Murine Melanoma Cells. *Mol. Biol. Rep.* 37 (3), 1279–1286. doi:10.1007/s11033-009-9502-x
- Namwanje, M., and Brown, C. W. (2016). Activins and Inhibins: Roles in Development, Physiology, and Disease. *Cold Spring Harb Perspect. Biol.* 8 (7), a021881. doi:10.1101/cshperspect.a021881
- Ruiz-Villalba, A., and Pérez-Pomares, J. M. (2012). The Expanding Role of the Epicardium and Epicardial-Derived Cells in Cardiac Development and Disease. *Curr. Opin. Pediatr.* 24 (5), 569–576. doi:10.1097/MOP.0b013e328357a532

- Smart, N., Bollini, S., Dubé, K. N., Vieira, J. M., Zhou, B., Davidson, S., et al. (2011). De Novo cardiomyocytes from within the Activated Adult Heart after Injury. *Nature* 474 (7353), 640–644. doi:10.1038/nature10188
- Smits, A. M., Dronkers, E., and Goumans, M.-J. (2018). The Epicardium as a Source of Multipotent Adult Cardiac Progenitor Cells: Their Origin, Role and Fate. *Pharmacol. Res.* 127, 129–140. doi:10.1016/j.phrs.2017.07.020
- Sridurongrit, S., Larsson, J., Schwartz, R., Ruiz-Lozano, P., and Kaartinen, V. (2008). Signaling via the Tgf- $\beta$  Type I Receptor Alk5 in Heart Development. *Develop. Biol.* 322 (1), 208–218. doi:10.1016/j.ydbio.2008.07.038
- Staudacher, J. J., Bauer, J., Jana, A., Tian, J., Carroll, T., Mancinelli, G., et al. (2017). Activin Signaling Is an Essential Component of the TGF- $\beta$  Induced Prometastatic Phenotype in Colorectal Cancer. *Sci. Rep.* 7 (1), 1–9. doi:10.1038/s41598-017-05907-8
- Valcourt, U., Kowanetz, M., Niimi, H., Heldin, C.-H., and Moustakas, A. (2005). TGF- $\beta$  and the Smad Signaling Pathway Support Transcriptomic Reprogramming during Epithelial-Mesenchymal Cell Transition. *MBoC* 16 (4), 1987–2002. doi:10.1091/mbc.E04-08-0658
- van Wijk, B., Gunst, Q. D., Moorman, A. F. M., and van den Hoff, M. J. B. (2012). Cardiac Regeneration from Activated Epicardium. *PLoS One* 7 (9), e44692. doi:10.1371/journal.pone.0044692
- Wang, J., Cao, J., Dickson, A. L., and Poss, K. D. (2015). Epicardial Regeneration Is Guided by Cardiac Outflow Tract and Hedgehog Signalling. *Nature* 522, 226–230. doi:10.1038/nature14325
- Yang, J., Antin, P., Berx, G., Blanpain, C., Brabletz, T., Bronner, M., et al. (2020). Guidelines and Definitions for Research on Epithelial-Mesenchymal Transition. *Nat. Rev. Mol. Cell Biol* 21 (6), 341–352. doi:10.1038/s41580-020-0237-9
- Zamora, M., Männer, J., and Ruiz-Lozano, P. (2007). Epicardium-derived Progenitor Cells Require  $\beta$ -catenin for Coronary Artery Formation. *Proc. Natl. Acad. Sci.* 104 (46), 18109–18114. doi:10.1073/pnas.0702415104
- Zhou, B., Honor, L. B., He, H., Ma, Q., Oh, J.-H., Butterfield, C., et al. (2011). Adult Mouse Epicardium Modulates Myocardial Injury by Secreting Paracrine Factors. *J. Clin. Invest.* 121 (5), 1894–1904. doi:10.1172/JCI45529

SUPPLEMENTARY FIGURES AND TABLES

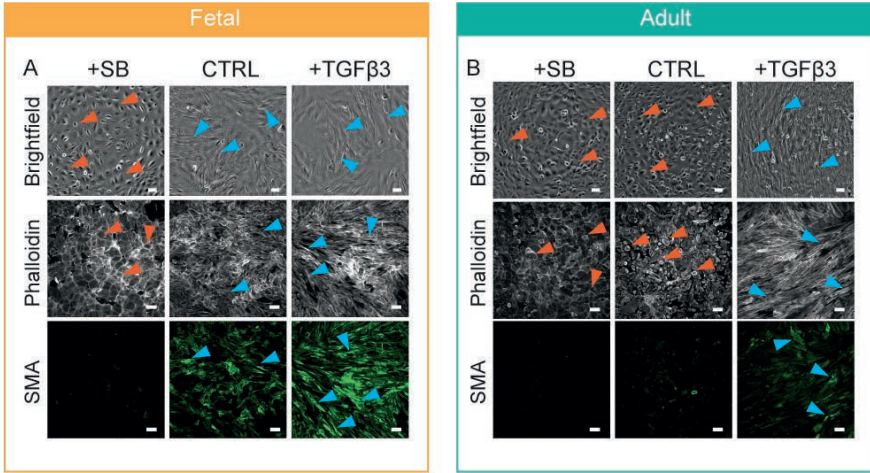


Fig. S1 | EpiMT in adult and fetal EPDCs. Representative brightfield pictures and phalloidin and  $\alpha$ SMA immunostaining of human fetal (A), and adult (B) epicardial derived cells (EPDCs) cultured for 5 days in the presence of SB431542 (SB), empty culture medium (CTRL) or TGFβ3 (representative images for n=5). Orange arrows indicate examples of epithelial cobblestone-shaped cells, blue arrows of mesenchymal spindle-shaped cells. Scale bar: 100  $\mu$ m.

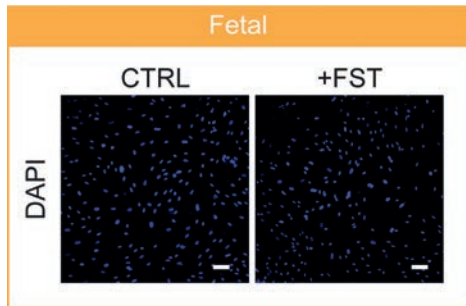


Fig. S2 | DAPI staining of CTRL and FST treated fetal EPDCs. DAPI staining corresponding to images in Fig.2B. Scale bar: 100  $\mu$ m.

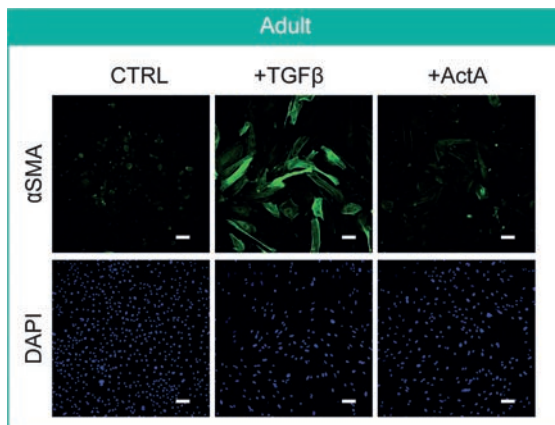


Fig. S3 | ActA does not enhance αSMA protein expression in adult EPDCs. αSMA and DAPI staining corresponding to images in Fig.2D complemented with αSMA and DAPI staining of TGFβ3 treated cells from the same experiment. Scale bar: 100 μm.

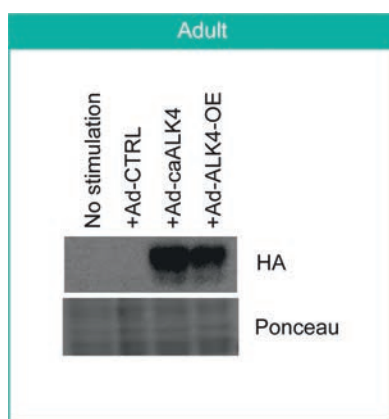
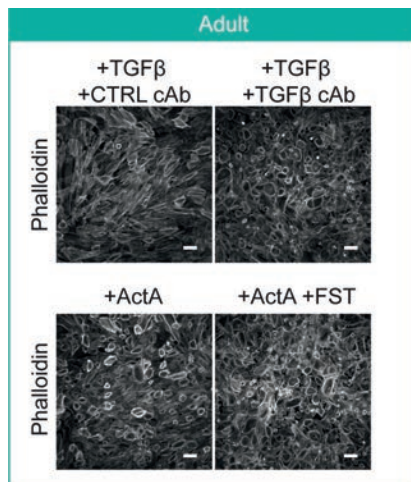
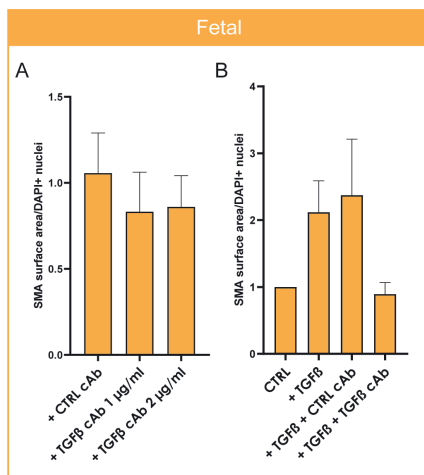


Fig. S4 | Western blot confirms viral transduction of Ad-caALK4 in adult EPDCs. Representative example of western blot of HA-tag presence in adult EPDCs stimulated with empty culture medium (CTRL), adenoviral LacZ (Ad-CTRL), adenoviral constitutively active ALK4 (Ad-caALK4) or adenoviral overexpression of wild type ALK4 (Ad-ALK4-OE) (n=2). Presence of protein in all lanes was confirmed using ponceau staining.



**Fig. S5 | Effectivity of TGFβ and Activin signaling inhibitors.** Phalloidin staining of adult EPDCs cultured for 5 days in the presence of ligand and inhibitor to proof effectivity of inhibitors. Scale bar: 100 μm.



**Fig. S6 | Effectivity of TGFβ cAb.** (A) Five-day treatment of fetal EPDCs with TGFβ cAb shows that 1 μg/mL is sufficient to block TGFβ as a higher concentration does not enhance the effect (n=5). (B) Five-day treatment with TGFβ cAb can completely block the SMA-induction of exogenous TGFβ in fetal EPDCs, demonstrating its effectivity (n=4).

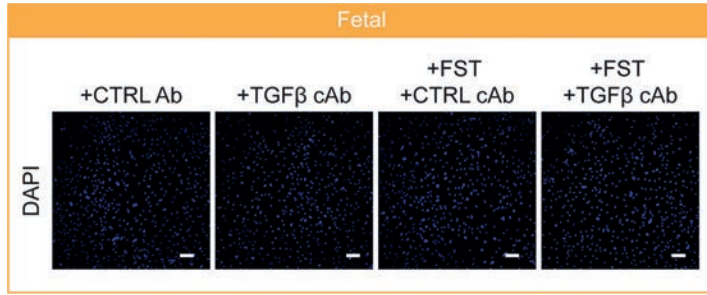
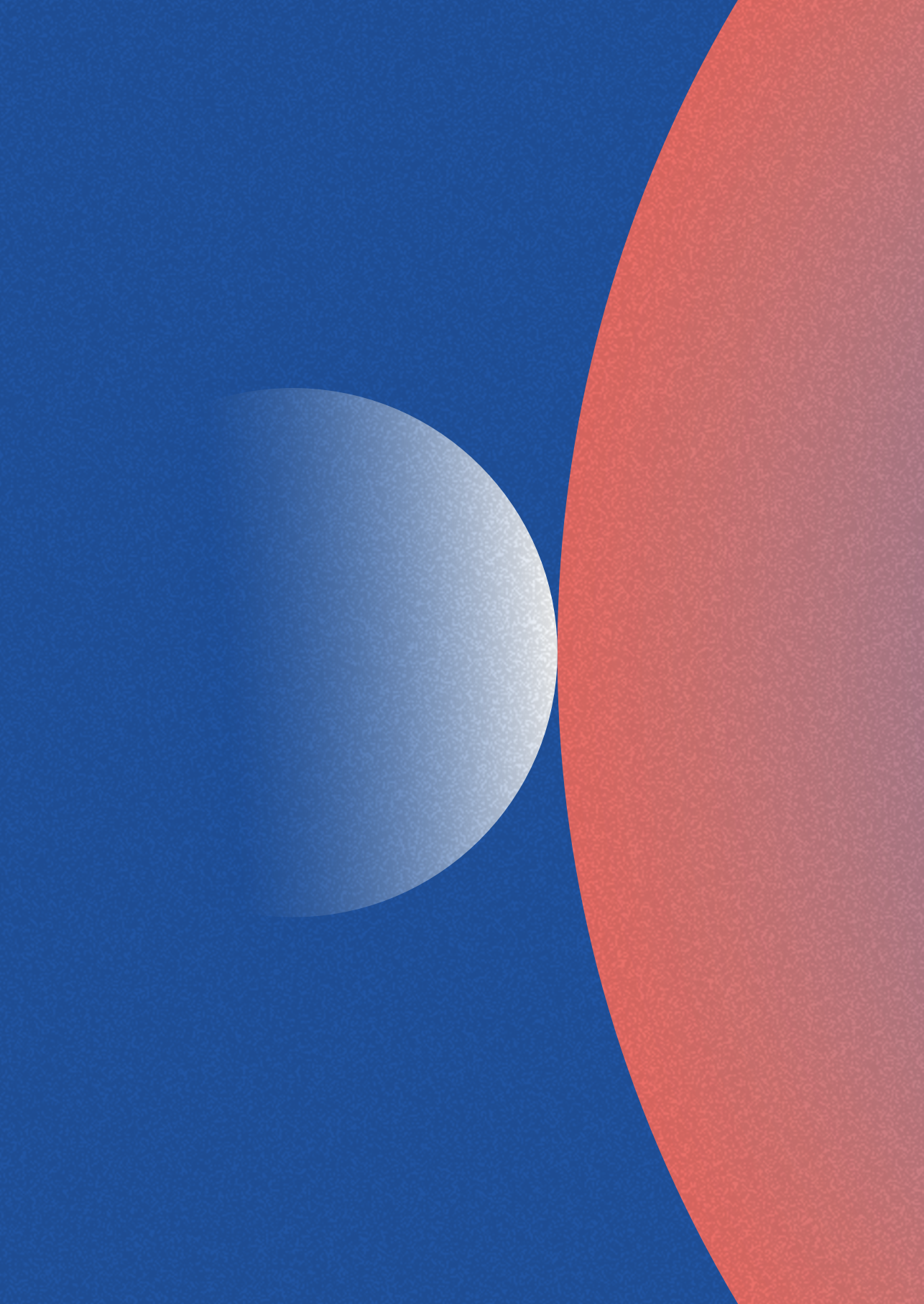


Fig. S7 | DAPI staining of TGFβ cAb and FST treated fetal EPDCs. DAPI staining corresponding to images in Fig.4C. Scale bar: 100 μm.

Supplemental table 1 | Primer sequences for qPCR

	Forward	Reverse
<i>ALK4</i>	GCTCGAAGATGCAATTCTGG	TTGGCATACCAACACTCTCG
<i>ACVR2A</i>	GCATCACAAAGATGGCTACC	CCAGGCAAACGTAGACTTC
<i>ACVR2B</i>	ATGTGGACATCCATGAGGAC	TGAAGATCTCCCGTTCACTC
<i>INHBA</i>	ATAGCCCCTTTGCCAACCTC	GCTGGGCAACTCTATGAGC
<i>INHBB</i>	ATGATTGTGGAGGAGTGCGG	TGTCAGTTGAGGGTTCTCGC
<i>WT1</i>	CAG CTT GAA TGC ATG ACC TG	TAT TCT GTA TTG GGC TCC GC
<i>POSTN</i>	GGAGGCAAACAGCTCAGAGT	GGCTGAGGAAGGTGCTAAAG
<i>CDH2</i>	CAGACCGACCCAAACAGCAAC	GCAGCAACAGTAAGGACAAACATC
<i>ACTA2</i>	CCGGGAGAAAATGACTCAA	GAAGGAATAGCCACGCTCAG
<i>SNAI1</i>	CCAGTGCCTCGACCACTATG	CTGCTGGAAGGTAAACTCTGGA
<i>SNAI2</i>	CGGACCCACACATTACCTTGT	TTCTCCCCGTGTGAGTTCTA
<i>ZEB1</i>	AGCAGTGAAAGAGAAGGGAATGC	GGTCCTTTCAGGTGCCTCA
<i>ZEB2</i>	CAC AAG CCA GGG ACA GAT CA	TTG CCA CAC TCT GTG CAT TTG
<i>HPRT1</i>	CTCATGGACTGATTATGGACAGGAC	GCAGGTCAGCAAAGAACTTATAGCC
<i>TBP</i>	TGGA AAAAGTTGTATTAACAGGTGCT	GCAAGGGTACATGAGAGCCA



# 7

## Epicardial Prrx1b restricts fibrosis and promotes Nrg1-dependent cardiomyocyte proliferation during zebrafish heart regeneration

Dennis E. M. de Bakker<sup>1\*</sup>, Mara Bouwman<sup>1\*</sup>, Esther Dronkers<sup>2</sup>, Filipa C. Simões<sup>3</sup>, Paul R. Riley<sup>3</sup>, Marie-José Goumans<sup>2</sup>, Anke M. Smits<sup>2</sup>, Jeroen Bakkers<sup>1,4</sup>

<sup>1</sup>Hubrecht Institute-KNAW and University Medical Center Utrecht, Utrecht, The Netherlands.

<sup>2</sup>Department of Cell and Chemical Biology, Leiden University Medical Centre, Leiden, The Netherlands.

<sup>3</sup>Department of Physiology, Anatomy and Genetics, University of Oxford, Oxford, UK.

<sup>4</sup>Department of Pediatric Cardiology, University Medical Centre Utrecht, Utrecht, The Netherlands.

*Adapted from:* Prrx1b restricts fibrosis and promotes Nrg1-dependent cardiomyocyte proliferation during zebrafish heart regeneration

*Dennis E. M. de Bakker\*, Mara Bouwman\*, Esther Dronkers, Filipa C. Simões, Paul R. Riley, Marie-José Goumans, Anke M. Smits, Jeroen Bakkers*

*\* These authors contributed equally to this work*

*Published in Development (2021)*

## ABSTRACT

Fibroblasts are activated to repair the heart following injury. Fibroblast activation in the mammalian heart leads to a permanent fibrotic scar that impairs cardiac function. In other organisms, such as zebrafish, cardiac injury is followed by transient fibrosis and scar-free regeneration. The mechanisms that drive scarring versus scar-free regeneration are not well understood. Here, we show that the homeobox-containing transcription factor *Prrx1b* is required for scar-free regeneration of the zebrafish heart as the loss of *Prrx1b* results in excessive fibrosis and impaired cardiomyocyte proliferation. Through lineage tracing and single-cell RNA sequencing, we find that *Prrx1b* is activated in epicardial-derived cells where it restricts TGF $\beta$  ligand expression and collagen production. Furthermore, through combined *in vitro* experiments in human fetal epicardial-derived cells and *in vivo* rescue experiments in zebrafish, we conclude that *Prrx1* stimulates *Nrg1* expression and promotes cardiomyocyte proliferation. Interestingly, *Prrx1* is nearly absent in the injured human heart. Collectively, these results indicate that *Prrx1* is a key transcription factor that balances fibrosis and regeneration in the injured zebrafish heart.

## INTRODUCTION

The regenerative capacity of damaged organs and body parts differs widely within the animal kingdom, which is particularly true for the heart (Nguyen et al., 2021; Poss, 2010). Indeed, whereas zebrafish display robust regeneration after heart injury, the wound response in mammalian hearts does not include replenishment of the lost myocardium. Instead, the affected myocardium is permanently lost and replaced by a fibrotic scar, which does not contribute to cardiac contraction resulting in reduced cardiac output.

The fibrotic scar is formed by cardiac fibroblasts that become activated to produce large amounts of extracellular matrix (ECM) components, such as collagens. Cardiac fibroblasts mainly originate from the embryonic epicardium, which consists of a heterogeneous population of epithelial cells that cover the heart (Acharya et al., 2012; Cao et al., 2016; Gittenberger-de Groot et al., 1998; Hortells et al., 2020; Travers et al., 2016; Weinberger et al., 2020). During embryonic heart development, a subset of epicardial cells undergoes an epithelial-to-mesenchymal transition (EMT) and migrates into the cardiac wall to give rise to a variety of cell types, which are commonly referred to as epicardial-derived cells (EPDCs) and include predominantly cardiac fibroblasts and vascular support cells (Cao and Poss, 2018).

In contrast to mammals, adult zebrafish can fully regenerate their heart after resection or cryoinjury of 20-30% of the ventricle (Chablais et al., 2011; González-Rosa et al., 2011; Poss et al., 2002; Schnabel et al., 2011), as a result of reactivation of proliferation in border zone cardiomyocytes (Jopling et al., 2010; Kikuchi et al., 2010; Wu et al., 2015). One of the first responses upon injury is the activation of a developmental gene expression programme in the epicardium, at 1-2 days after the injury (Lepilina et al., 2006). This response becomes confined to the injury area as the epicardium is regenerated, which completely surrounds the injury area between 3 and 7 days post-injury (dpi) (Kikuchi et al., 2011; Lepilina et al., 2006). The epicardium is essential for the regeneration process as ablating *tcf21*-expressing epicardial cells from the injured zebrafish heart impairs cardiomyocyte proliferation and regeneration (Wang et al., 2015). Similar to observations in the mammalian heart, lineage tracing of *wt1b*- and *tcf21*-expressing cells in zebrafish revealed that the embryonic epicardium gives rise to EPDCs, such as cardiac fibroblasts and vascular support cells (González-Rosa et al., 2012; Kikuchi et al., 2011; Sánchez-iranzo et al., 2018). Upon injury, EPDCs secrete signals guiding regeneration such as TGF $\beta$  ligands, platelet derived growth factor, cytokines, such as Cxcl12, and mitogenic factors, such as *Nrg1*

(Chablais and Jaźwińska, 2012; Gemberling et al., 2015; Itou et al., 2012; Kim et al., 2010). In addition, EPDCs also contribute to fibrosis by producing ECM components, such as collagen (Sánchez-iranzo et al., 2018). Fibrosis in the zebrafish heart is transient and regresses as regeneration proceeds, which coincides with the inactivation of cardiac fibroblasts, ultimately resulting in a scar-free heart (Chablais et al., 2011; Sánchez-iranzo et al., 2018). Although EPDCs play important roles during fibrosis and pro-regenerative signalling, the molecular mechanism regulating these processes remains largely unknown.

The paired related homeobox 1 (*Prrx1*) gene encodes a transcription factor and its expression correlates with scar-free wound healing and limb regeneration (Satoh et al., 2010; Stelnicki et al., 1998; Yokoyama et al., 2011). Although its function has been studied during embryonic development, its role during wound healing or regeneration remains largely unknown. Here, we find that *Prrx1b* expression is induced in the epicardium and EPDCs during zebrafish heart regeneration and we show that *Prrx1b* is required for scar-free regeneration. By single-cell RNA sequencing of EPDCs, we identified that loss of *prrx1b* results in an excess of pro-fibrotic fibroblasts and fibrosis. Furthermore, we find that *Prrx1b* is necessary for the induction of *nrg1* signalling, which we confirmed in an *in vitro* system of human fetal EPDCs. Altogether, our data indicate that *Prrx1b* regulates zebrafish heart regeneration by maintaining the balance between the fibrotic and regenerative responses after heart injury.

## RESULTS

### ***prrx1b* is required for zebrafish cardiomyocyte proliferation and heart regeneration**

In order to address a potential role for *Prrx1* in heart regeneration, we utilized *prrx1a*<sup>-/-</sup> and *prrx1b*<sup>-/-</sup> adult fish, which harbour nonsense mutations upstream of the conserved DNA-binding domain (Barske et al., 2016). Both *prrx1a*<sup>-/-</sup> and *prrx1b*<sup>-/-</sup> display no developmental defects owing to redundant gene functions and only *prrx1a*<sup>-/-</sup>;*prrx1b*<sup>-/-</sup> embryos display craniofacial defects (Barske et al., 2016). We subjected adult *prrx1a*<sup>-/-</sup> and *prrx1b*<sup>-/-</sup> fish to cardiac cryoinjury and analysed scar sizes at 30 dpi. Although we observed comparable scar sizes in wild-type and *prrx1a*<sup>-/-</sup> hearts, scar sizes were significantly larger in *prrx1b*<sup>-/-</sup> hearts compared with their control siblings (Fig. 1A,B, Fig. S1A). This difference in scar size was still apparent at 90 dpi, when wild-type hearts had completely resolved their scars (12/12) whereas the majority of *prrx1b*<sup>-/-</sup> hearts (4/7) had not (Fig. 1C).

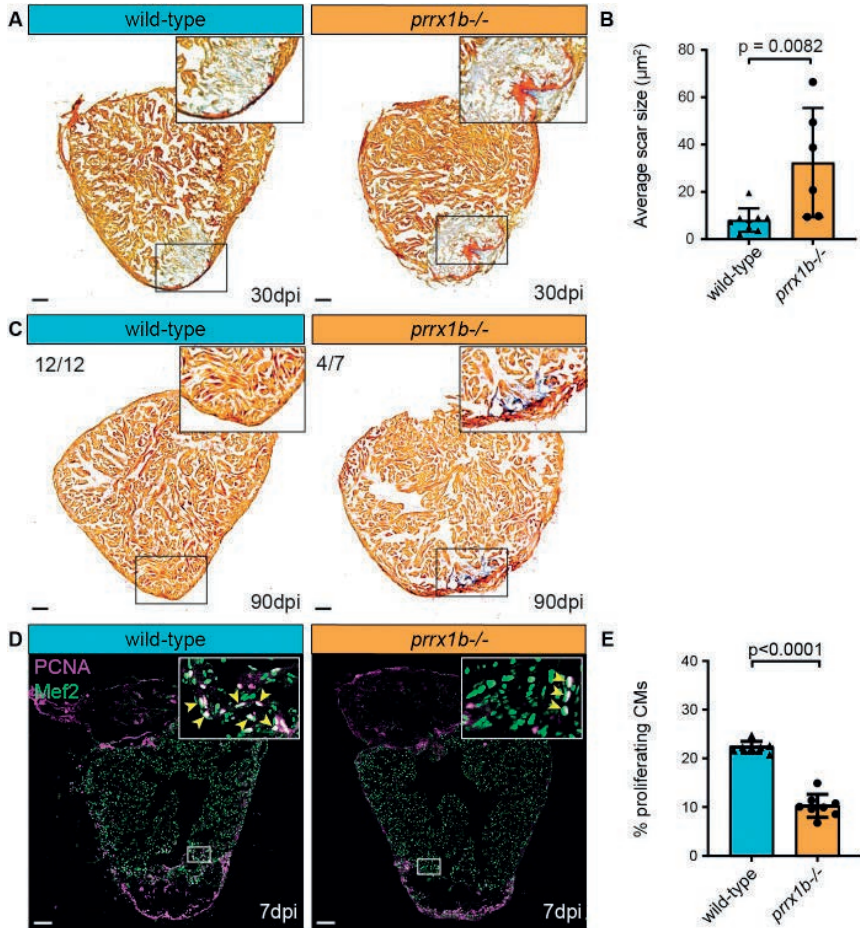


**Fig. 1 | Heart regeneration and border zone cardiomyocyte proliferation is impaired in *prrx1b*<sup>-/-</sup> zebrafish.** (A) AFOG staining on 30 dpi wild-type and *prrx1b*<sup>-/-</sup> heart sections showing fibrin in red, collagen in blue and remaining muscle tissue in orange. Scale bars: 100 μm. (B) Quantification of the remaining scar size at 30 dpi in *prrx1b*<sup>-/-</sup> hearts (*n*=6) and wild-type sibling hearts (*n*=9) (mean±s.d., *P*=0.0082, unpaired *t*-test). (C) AFOG staining on sections of 90 dpi hearts. Scars were completely resolved in wild-type hearts (*n*=12), whereas incomplete scar resolution was observed in *prrx1b*<sup>-/-</sup> four out of seven hearts. Scale bars: 100 μm. (D) Immunofluorescence staining on 7 dpi wild-type and *prrx1b*<sup>-/-</sup> heart sections using an anti-Mef2 antibody as a marker for cardiomyocyte nuclei, and an anti-PCNA antibody as a nuclear proliferation marker. Insets show higher magnifications of the boxed areas. Arrowheads indicate proliferating cardiomyocytes. Scale bars: 100 μm (main panels); 10 μm (insets). (E) Quantification of the percentage of proliferating (PCNA<sup>+</sup>) border zone cardiomyocytes in *prrx1b*<sup>-/-</sup> hearts (*n*=8) and wild-type sibling hearts (*n*=7) (mean±s.d., *P*<0.0001, unpaired *t*-test).

Because myocardial regeneration is achieved through proliferation of the surviving cardiomyocytes at the injury border zone, we investigated cardiomyocyte proliferation in the *prrx1a*<sup>-/-</sup> and *prrx1b*<sup>-/-</sup> hearts. Indeed, *prrx1b*<sup>-/-</sup> hearts showed a significant reduction in border zone cardiomyocyte proliferation at 7 dpi whereas no significant differences were observed in *prrx1a*<sup>-/-</sup> hearts (Fig. 1D,E, Fig. S1B,C). From these results, we conclude that *prrx1b*, but not *prrx1a*, is required for zebrafish cardiomyocyte proliferation and heart regeneration.

### **Prrx1 is expressed in epicardial and epicardial-derived cells**

To address how Prrx1b could function during zebrafish heart regeneration, we investigated the spatial distribution of Prrx1b expression. By mRNA *in situ* hybridization (ISH) we observed only a very weak signal for *prrx1b* on sections of 7 dpi hearts with some signal in the (sub)epicardium close to the border zone and some signal in the injury area (Fig. S2A). As these weak signals were difficult to interpret, we instead used an antibody raised against the N terminus of the axolotl Prrx1 protein that recognizes zebrafish Prrx1 (Gerber et al., 2018; Ocaña et al., 2017). Prrx1 protein was mainly detected in (sub)epicardial cells covering the injury area and some sparse cells within the injury (Fig. S2B). Importantly, we could validate that the Prrx1 antibody recognizes the zebrafish Prrx1b protein as injured *prrx1b*<sup>-/-</sup> hearts showed a near lack of the signal (Fig. S2B,C). In addition, Prrx1 protein was nearly undetectable in uninjured zebrafish hearts (Fig. S2D), together indicating that Prrx1 protein expression is induced upon heart injury and at 7 dpi localizes in cells covering and within the injury area.

As this localization of Prrx1 suggested a possible expression in EPDCs, we used the *Tg(tcf21:CreERT2)* line, which marks a subset of EPDCs when crossed with the ubiquitous reporter *Tg(ubi:loxP-EGFP-loxP-mCherry)* and recombined during embryonic heart development (Kikuchi et al., 2011). Hearts from embryonic recombined *Tg(tcf21:CreERT2; ubi:loxP-EGFP-loxP-mCherry)* fish were cryo-injured, extracted at different time points and analysed for Prrx1 and mCherry expression (Fig. 2A-F). At 1 dpi, we observed a strong expression of Prrx1 in the entire intact epicardium (Fig. 2B), coinciding with the previously reported ventricle-wide injury response of the epicardium (Lepilina et al., 2006). At 3 dpi and 7 dpi, we started to observe double-labelled mCherry<sup>+</sup> and Prrx1<sup>+</sup> cells around and in the injury area whereas Prrx1 expression became less dense in the remote ventricle (Fig. 2C,D,H). Interestingly, from 1 to 7 dpi we observed an accumulation of mCherry/Prrx1<sup>+</sup> cells in the regions where the (sub)epicardium is close to the border between injured and uninjured myocardium (the so-called border zone, BZ), which we refer to as the BZ epicardium (Fig. 2B-D,H).

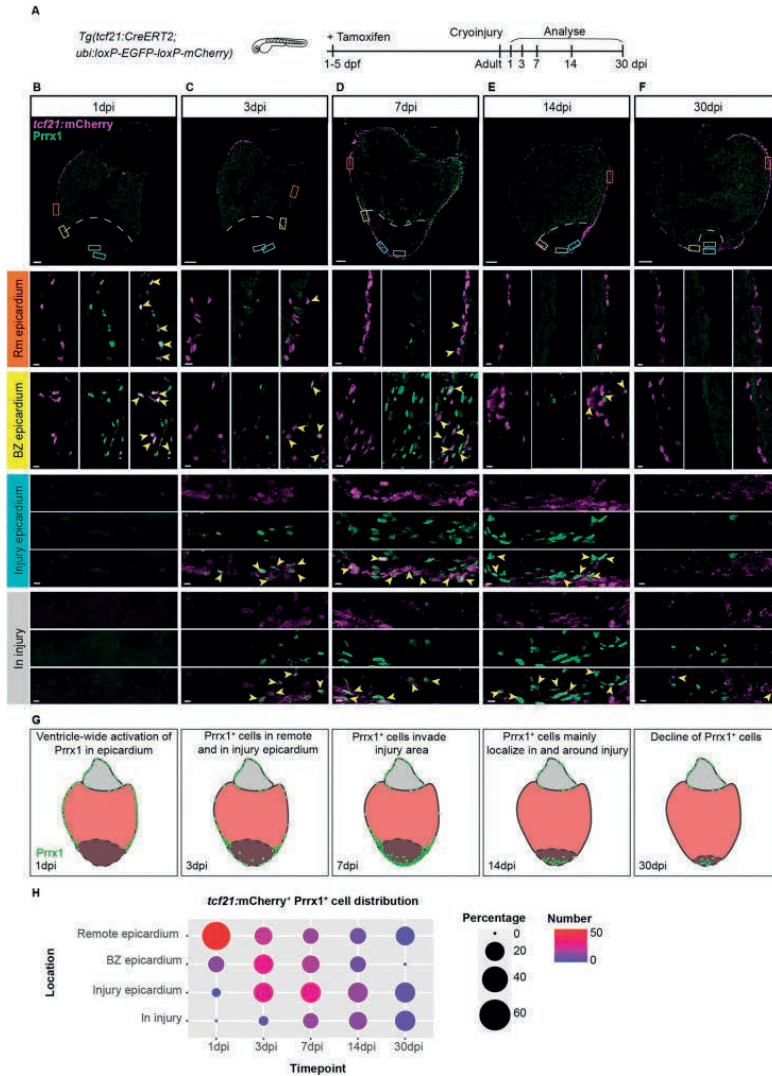


**Fig. 2 | Prrx1 is expressed in the epicardium/EPDCs and follows epicardial dynamics post-injury.** (A) Schematic illustrating the experimental procedures. (B-F) Immunofluorescence staining on 1, 3, 7, 14 and 30 dpi *tcf21:mCherry*<sup>+</sup> wild-type heart sections staining Prrx1 (green) and mCherry (magenta). Areas in the coloured boxes are shown at higher magnification below. Arrowheads indicate *tcf21:mCherry*<sup>+</sup>/Prrx1<sup>+</sup> cells. Scale bars: 100  $\mu$ m (low-magnification images); 10  $\mu$ m (high-magnification images). BZ epicardium, border zone epicardium; Rm epicardium, remote epicardium. Six hearts analysed per condition. Dashed line indicates the border between myocardium and injury area. (G) Schematic of Prrx1 dynamics upon injury. Prrx1<sup>+</sup> cells are in green. Dark colour at the apex represents the injury area. (H) Quantification of the distribution of *tcf21:mCherry*<sup>+</sup>/Prrx1<sup>+</sup> cells per time point. Size of the dots represents the percentage of *tcf21:mCherry*<sup>+</sup>/Prrx1<sup>+</sup> cells and absolute count number is visualized by a colour gradient.

At 14 dpi, we observed the majority of *Prrx1* expression in and around the injury area (Fig. 2E,H). At 30 dpi, only a few mCherry/*Prrx1*<sup>+</sup> cells were detected, of which the majority was located at the apex and inside the remaining injury area (Fig. 2F,H). Importantly, although at all time points *Prrx1* was mostly found in mCherry<sup>+</sup> cells, not all mCherry<sup>+</sup> cells were *Prrx1*<sup>+</sup> and vice versa, confirming the previously reported heterogeneity of the epicardium and EPDCs (González-Rosa et al., 2012). To address whether other epicardial subpopulations express *Prrx1*, we analysed *Prrx1* expression in *Tg(tbx18:myr-eGFP)* and *Tg(wt1b:H2B-Dendra2)* hearts. Indeed, we observed that *Prrx1* is co-expressed with *tbx18* and *wt1b* (Fig. S3). Taken together, these results indicate that upon cardiac injury *Prrx1* expression is induced in *tcf21*<sup>+</sup>, *tbx18*<sup>+</sup> and *wt1*<sup>+</sup> epicardial subpopulations. *Prrx1* expression starts in the epicardium covering the remote myocardium, after which it becomes more restricted to the injury epicardium followed by expression in EPDCs localized in the injury area at later stages.

#### **Proliferation and invasion of epicardial cells is unaffected in *prrx1b*<sup>-/-</sup> hearts**

Because cardiac injury induces the proliferation of epicardial cells (Lepilina et al., 2006) and *Prrx1b* is expressed in this cell type, we decided to investigate whether *prrx1b* plays a role in epicardial cell proliferation. To do so, we used the *Tg(tcf21:CreERT2; ubi:loxP-EGFP-loxP-mCherry)* line to identify epicardial cells in wild-type and *prrx1b*<sup>-/-</sup> hearts and used PCNA expression to identify proliferating cells (Fig. S4A,B). We observed that the number of PCNA-expressing epicardial cells was highest at 1 and 3 dpi, after which their number dropped to significantly lower amounts at 30 dpi, which is in line with previous reports (Lepilina et al., 2006). We found no indication of an epicardial proliferation defect in *prrx1b*<sup>-/-</sup> hearts, as no significant differences were observed in the number of PCNA-expressing epicardial cells at any of the examined time points (Fig. S4B).

Furthermore, we wondered whether *prrx1b* could play a role during the invasion of EPDCs into the injury area. To quantify this, we determined the contribution of *tcf21*:mCherry<sup>+</sup> surface area found within the injury area as a proportion of the total *tcf21*:mCherry<sup>+</sup> surface area found in and around the injury area (Fig. S4C). We used this percentage as a measure of invasion efficiency of the EPDCs. At all time points, except for 3 dpi, there was no significant difference in the percentage of mCherry<sup>+</sup> cells inside the injury between the wild-type and *prrx1b*<sup>-/-</sup> hearts. At 3 dpi, the percentage of mCherry<sup>+</sup> cells invading the injury area was significantly lower in the *prrx1b*<sup>-/-</sup> hearts, but this was mitigated from 7 dpi onwards.

Taken together, we did not find evidence suggesting a profound role for *Prrx1* in epicardial proliferation or EMT. Although the incomplete labelling of *tcf21*<sup>+</sup> cells resulted in substantial variation in the collected data, potentially masking a subtle difference between wild-type and *prrx1b*<sup>-/-</sup> hearts, we conclude that *Prrx1* is largely dispensable for proliferation and invasion into the injury area of epicardial and epicardial-derived cells.

### Characterization of EPDCs in the regenerating heart by single-cell sequencing

Next, we wanted to identify which processes are regulated by *Prrx1b* in EPDCs that could explain the impaired regenerative response observed in the *prrx1b*<sup>-/-</sup> hearts. Given that the epicardium and EPDCs are formed by heterogenous cell populations, we decided to take a single-cell RNA sequencing (scRNAseq) approach to characterize these cells within the context of heart regeneration. First, we isolated ventricles from recombinant *Tg(tcf21:CreERT2; ubi:loxP-EGFP-loxP-mCherry)* wild-type sibling or *prrx1b*<sup>-/-</sup> fish at 7 dpi and identified the mCherry<sup>+</sup> cells by fluorescence-activated cell sorting (FACS) (Fig. S5A-C). Next, we performed scRNAseq using the SORT-seq (Sorting and Robot-assisted Transcriptome Sequencing) platform on the isolated single cells (Muraro et al., 2016) (Fig. 3A,B). We analysed over 1400 cells with >1000 reads per cell using the RaceID3 algorithm, which resulted in the identification of ten cell clusters grouped based on their transcriptomic features (Fig. 3C,D, Table S1).

To confirm that the sorting strategy worked, we plotted the expression of the epicardial markers *tcf21*, *tbx18*, *aldh1a2* and *wt1b* and observed that most cells express at least one of these albeit in different patterns (Fig. 3E). These differences in *tcf21*, *tbx18*, *aldh1a2* and *wt1b* expression confirm the previously observed heterogeneity of epicardial cells and EPDCs (Cao et al., 2016; Weinberger et al., 2020). Unfortunately, *prrx1b* expression was too low to correlate it to any of the clusters (Fig. S6). To identify different cell types, we selected marker genes for known cell types and analysed their expression in the various clusters. The cells from clusters 4, 7 and 10 expressed *tcf21* and *tbx18* but lacked expression of *aldh1a2* and *wt1b*, suggesting that these represent epicardial cells covering the remote myocardium. Indeed, ISH for additional genes with high expression in these clusters labelled epicardial cells covering the uninjured part of the heart (Fig. 3F). By contrast, *wt1b* and *aldh1a2* were expressed in most of the remaining clusters, with highest expression in cluster 1. ISH for additional genes marking cluster 1 revealed that their expression was mostly located in the epicardial region covering the injury area but not the remote myocardium (Fig. 3G).

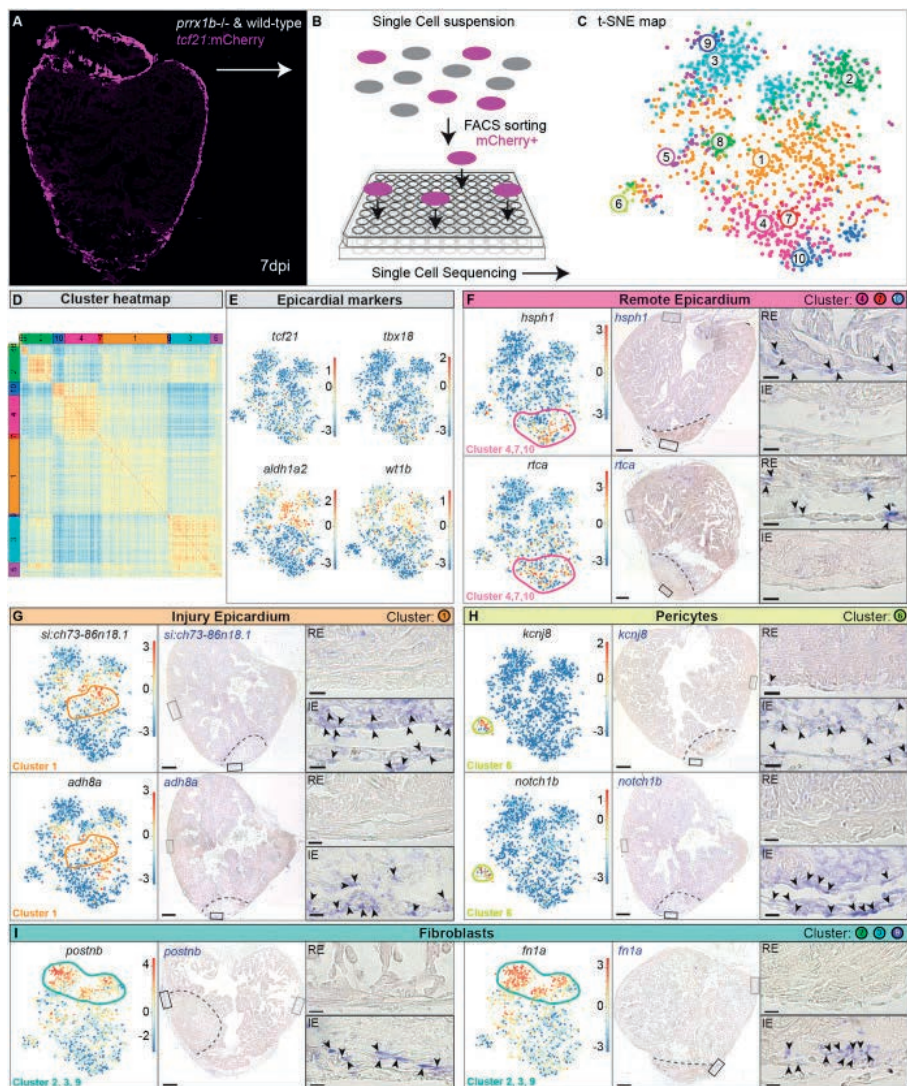


**Fig. 3 | Single-cell sequencing identifies epicardial-derived cell populations in the injured zebrafish heart.** (A,B) Workflow of the isolation (A) and sorting (B) of *tcf21:mCherry*<sup>+</sup> cells in wild-type and *prrx1b*<sup>-/-</sup> hearts at 7 dpi. (C,D) tSNE plotting of the data results in ten transcriptionally distinct clusters (C), as also indicated by the heatmap (D). (E) tSNE maps visualizing log<sub>2</sub>-transformed read-counts for *tcf21*, *tbx18*, *aldh1a2* and *wt1b*. (F-I) Characterization of the different cell clusters. Left: Panels show tSNE maps visualizing log<sub>2</sub>-transformed read-counts for genes with high expression in the indicated cluster (circled). Middle: *In situ* hybridization for the cluster-enriched genes in wild-type hearts at 7 dpi. Dashed line indicates injury border. Scale bars: 100  $\mu$ m. Right: Magnifications of the boxed regions in remote (RE) and injury epicardium (IE) with arrowheads pointing to cells with high expression. Scale bars: 10  $\mu$ m. Three hearts analysed per condition. Gene lists are provided in Table S1.

As the epicardium gives rise to fibroblasts and pericytes, we plotted known marker genes for these cell types. Pericytes express genes such as the potassium channel *kcnj8* and the Notch receptor *notch1b* (Guichet et al., 2015; Vanlandewijck et al., 2018). The expression of these genes was most abundant in cluster 6 and Gene Ontology analysis revealed that cluster 6 has an enrichment in genes linked to smooth muscle contraction and cell junction organization. These findings suggest that cells in cluster 6 represent pericytes (Fig. 3H). Periostin (*postnb*) and fibronectin (*fn1a*) are expressed in fibroblasts and both genes showed highest expression in clusters 2, 3 and 9 (Fig. 3I). In addition, we observed that these clusters are enriched for various other genes reported to be expressed in fibroblasts in the context of tissue injury (e.g. *dkk3b*, *fstl1b*, *ptx3a*) (Table S2), suggesting that these clusters are formed by injury-responsive cardiac fibroblasts (Sánchez-iranzo et al., 2018). Gene Ontology analyses with genes enriched in clusters 2, 3 and 9 indeed indicated processes such as ‘extracellular matrix organization’, ‘dissolution of fibrin clot’ and ‘collagen biosynthesis and modifying enzymes’ (Table S3).

From these results, we conclude that the scRNAseq data represent different populations of epicardial and epicardial-derived cells from the regenerating heart. Based on our analysis, we divided the cells into four general groups: remote epicardium (clusters 4, 7 and 10), injury epicardium (cluster 1), epicardial-derived fibroblasts (clusters 2, 3 and 9) and epicardial-derived pericytes (cluster 6).

### **Prrx1 restricts fibrosis**

Next, we mapped the wild-type and *prrx1b*<sup>-/-</sup> cells separately on the t-distributed stochastic neighbour embedding (tSNE) map to reveal differences in contribution to the various cell clusters (Fig. 4A,B). Interestingly, we found a clear difference in the contribution of wild-type and *prrx1b*<sup>-/-</sup> cells to the fibroblast clusters 2 and 3. Whereas cluster 2 consisted of mostly wild-type cells (89%) and few *prrx1b*<sup>-/-</sup> cells (11%), cluster 3 was enriched in *prrx1b*<sup>-/-</sup> cells (71%) compared with wild-type cells (29%) (Fig. 4B-D). Although both cluster 2 and cluster 3 cells expressed markers for activated fibroblasts, such as *postnb*, differential gene analysis between cluster 2 and 3 revealed that cluster 3 cells are enriched for genes involved in TGFβ signalling (*tgfb1a*, *tgfb2*, *tgfb3*;  $P=7.1E-4$ ), extracellular matrix proteins ( $P=3.3E-4$ ) and collagen fibril organization ( $P=1.2E-4$ ) (Fig. 4E). Instead, cluster 2 cells lacked robust expression of fibrosis-related genes, therefore representing a more quiescent cell type that instead expresses genes linked to chordate embryonic development ( $P=3.8E-10$ ) and stress response ( $P=7.9E-6$ ). Together, the scRNAseq data suggest that injured *prrx1b*<sup>-/-</sup> hearts contain more activated, pro-fibrotic fibroblasts.

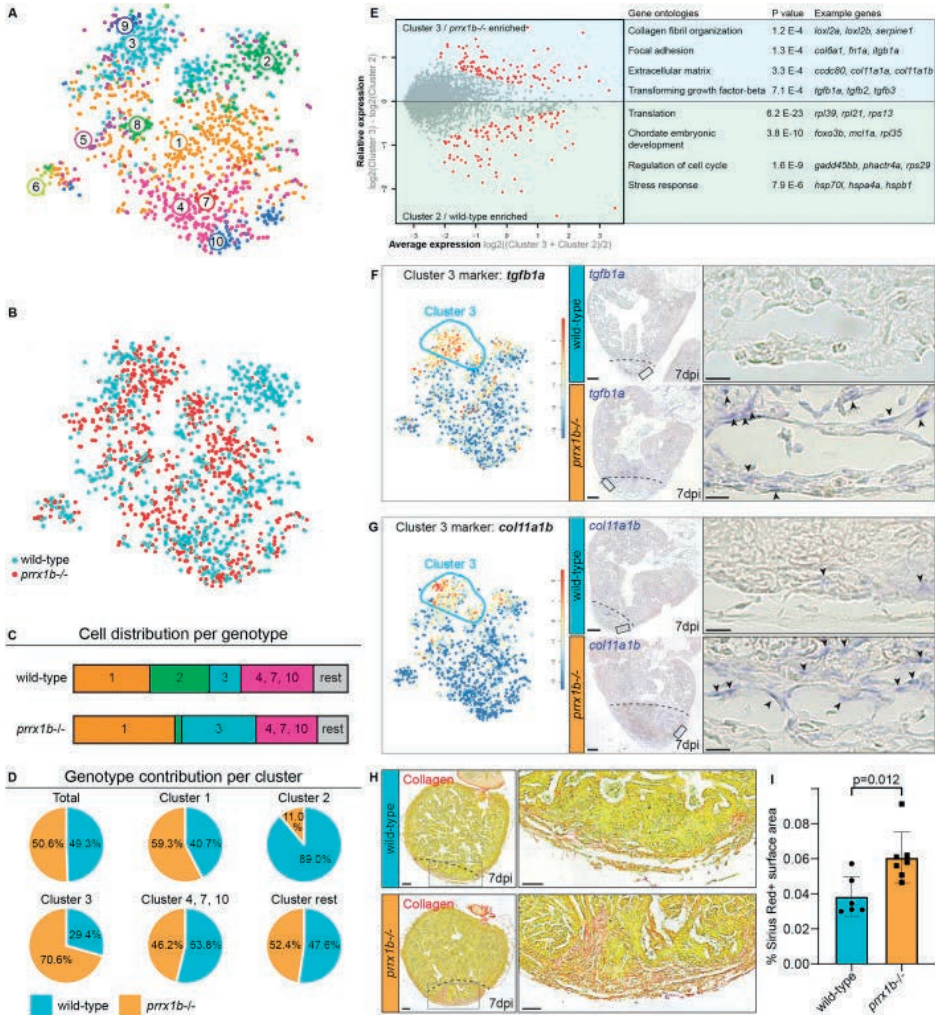


**Fig. 4 | *prrx1b*<sup>-/-</sup> hearts contain excessive amounts of pro-fibrotic fibroblasts.** (A) tSNE map of the single-cell sequencing data as shown in Fig. 3C, indicating ten transcriptionally distinct cell populations. (B) tSNE map showing the contribution of wild-type cells (cyan) and *prrx1b*<sup>-/-</sup> cells (red). (C) Stacked bar graph showing the relative cell contribution to major clusters in wild-type and *prrx1b*<sup>-/-</sup> hearts. (D) Pie charts showing the contribution of wild-type and *prrx1b*<sup>-/-</sup> cells per cluster. (E) Differential gene expression analysis using the DESeq algorithm between fibroblast clusters 2 and 3. Enriched genes were selected for either cluster 2 or 3 with a *P*-value cut-off of <0.05 (red). Gene Ontology analysis was performed using the online tool DAVID. Gene and full Gene Ontology lists are provided in Tables S2 and S3. (F,G) Characterization of cluster 3. Left: tSNE maps visualizing log<sub>2</sub>-transformed read-counts for genes with high expression in the indicated cluster (circled). Middle: *In situ* hybridization for the cluster 3-enriched genes in wild-type and *prrx1b*<sup>-/-</sup> hearts at 7 dpi. Dashed line indicates injury border. Scale bars: 100  $\mu$ m. Right: Magnifications of the boxed regions in the injury area with arrowheads pointing to cells with

high expression. Scale bars: 25  $\mu\text{m}$ . Three hearts analysed per condition. (H) Sirius Red staining showing collagen in red on sections of wild-type and *prrx1b*<sup>-/-</sup> hearts at 7 dpi. Right-hand panels show magnifications of the boxed regions in the sub-epicardial layer and further inside the injury area. Scale bars: 100  $\mu\text{m}$  (left); 50  $\mu\text{m}$  (right). (I) Quantification of Sirius Red (collagen) staining in wild-type ( $n=6$ ) and *prrx1b*<sup>-/-</sup> ( $n=7$ ) hearts showing significantly more fibrosis in *prrx1b*<sup>-/-</sup> hearts inside and around the injury area (mean $\pm$ s.d.,  $P=0.012$ , unpaired  $t$ -test).

To validate these findings, we performed ISH for genes with high expression in cluster 2 or 3 cells. Indeed, we observed increased expression of *tgfb1a* and *col11a1b* in injured *prrx1b*<sup>-/-</sup> hearts compared with their wild-type siblings (Fig. 4F,G), whereas we identified a strong reduction in expression of the cluster 2 marker *si:dkeyp-1h4.9* (Fig. S7). In addition, we performed Sirius Red staining to visualize collagen, which showed an excess of collagen fibres in the *prrx1b*<sup>-/-</sup> hearts in and around the injury area (Fig. 4H,I). From these results, we conclude that in injured *prrx1b*<sup>-/-</sup> hearts an excess of TGF $\beta$  ligand and ECM-producing fibroblasts is formed, resulting in an enhanced fibrotic response to the injury.

### **NRG1 administration rescues the cardiomyocyte proliferation defect of *prrx1b*<sup>-/-</sup> hearts**

Fibroblasts are not only required for fibrosis in the injured zebrafish heart; they also exhibit pro-regenerative activity by stimulating cardiomyocyte proliferation (Sánchez-iranzo et al., 2018). Because EPDCs secrete Nrg1, a growth factor necessary to induce cardiomyocyte proliferation (Gemberling et al., 2015; Ieda et al., 2009; Wang et al., 2015), we hypothesized that *nrg1* expression may be impaired in *prrx1b*<sup>-/-</sup> hearts and responsible for the observed reduction in cardiomyocyte proliferation. Considering that *nrg1* expression was nearly absent in the scRNAseq data (<100 combined reads from 1438 cells), we investigated expression of *nrg1* through RNAscope ISH. We observed expression of *nrg1* in the epicardial and sub-epicardial region in wild-type hearts at 7 dpi (Fig. 5A,B). The BZ epicardium regions showed profound *nrg1* expression, which is in line with previously reported *nrg1* localization upon injury (Gemberling et al., 2015). Importantly, we observed co-expression of *nrg1* and *Prrx1* in BZ epicardial cells at 7 dpi (Fig. 5A). Next, we wanted to investigate whether *nrg1* expression is impaired in *prrx1b*<sup>-/-</sup> hearts. Corroborating our hypothesis, we found a significant reduction of *nrg1* expression in the BZ epicardium of injured *prrx1b*<sup>-/-</sup> hearts compared with wild-type sibling hearts (Fig. 5B,C). To address whether the impaired *nrg1* expression in *prrx1b*<sup>-/-</sup> hearts could explain the observed reduction in cardiomyocyte proliferation, we injected injured wild-type and *prrx1b*<sup>-/-</sup> fish daily with recombinant NRG1 protein or DMSO as a control from 3 dpi to 7 dpi and quantified cardiomyocyte proliferation in the border zone. Importantly, injecting *prrx1b*<sup>-/-</sup> zebrafish with recombinant

NRG1 protein did indeed rescue cardiomyocyte proliferation in the border zone to wild-type levels (Fig. 5D,E). Together, these results demonstrate that *nrg1* and Prrx1 are co-expressed and that Prrx1 promotes *nrg1* expression in EPDCs. Furthermore, the results suggest that the reduction in Nrg1 is responsible for the reduced cardiomyocyte proliferation observed in the border zones of *prrx1b* mutant hearts.

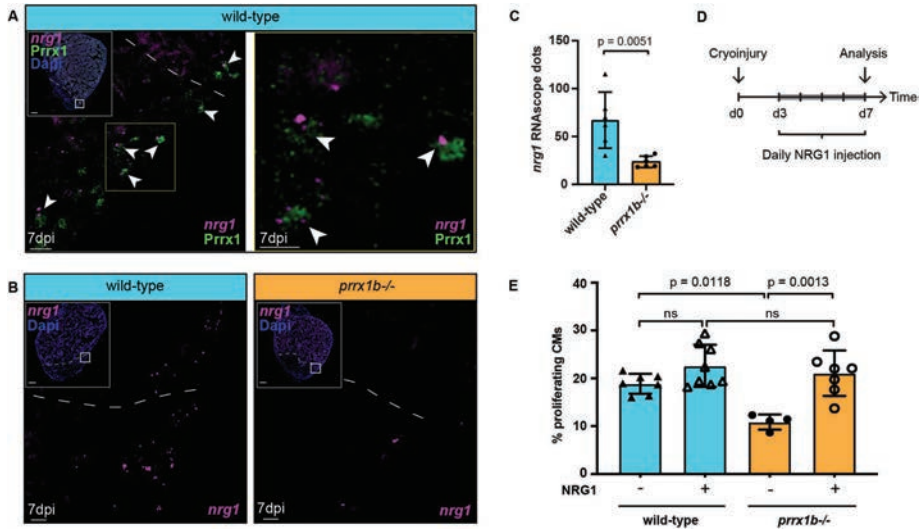


**Fig. 5 | Prrx1b stimulates Nrg1 expression.** (A) RNAscope *in situ* hybridization for *nrg1* co-detected with Prrx1 antibody on 7 dpi wild-type hearts. Arrowheads indicate colocalization of *nrg1* and Prrx1. Dashed line marks edge of the border zone. Insets show higher magnifications of the boxed areas. Scale bars: 100  $\mu$ m (main panels); 10  $\mu$ m (insets). Four hearts analysed. (B) RNAscope *in situ* hybridization for *nrg1* on 7 dpi wild-type and *prrx1b*<sup>-/-</sup> hearts. Dashed line marks edge of the border zone. Insets show higher magnifications of the boxed areas. Scale bars: 100  $\mu$ m (main panels); 10  $\mu$ m (insets). (C) Quantification of *nrg1* RNAscope dots in the BZ epicardium in 7 dpi wild-type ( $n=6$ ) and *prrx1b*<sup>-/-</sup> ( $n=5$ ) hearts. BZ epicardium is defined as a 100- $\mu$ m-wide strip, 100  $\mu$ m up and 100  $\mu$ m down from where the edge of intact myocardium meets the epicardium (mean $\pm$ s.d.,  $P=0.0051$ , unpaired *t*-test). (D) Schematic of the workflow used for NRG1 injection experiments shown in E. (E) Quantification of the percentage of proliferating (PCNA<sup>+</sup>) BZ cardiomyocytes (mean $\pm$ s.d., wild-type -NRG1  $n=7$ ; wild-type+NRG1  $n=8$ ; *prrx1b*<sup>-/-</sup> -NRG1  $n=4$ ; *prrx1b*<sup>-/-</sup> +NRG1  $n=7$ ; wild-type -NRG1 versus *prrx1b*<sup>-/-</sup>-NRG1  $P=0.0118$ ; *prrx1b*<sup>-/-</sup>-NRG1 versus *prrx1b*<sup>-/-</sup>+NRG1  $P=0.0013$ ; ns, not significant; one-way ANOVA followed by multiple comparisons analysis using Tukey's test).

### PRRX1 promotes NRG1 expression in human EPDCs

Next, we wanted to address whether *nrg1* expression in EPDCs is regulated by *Prrx1*. As the *prrx1b*<sup>-/-</sup> fish lack *Prrx1* in all cells, we exploited a previously established *in vitro* model (Dronkers et al., 2018) in which human fetal epicardial cells can be cultured in an epithelial phenotype in the presence of the ALK4/5/7 kinase inhibitor SB-431542. Removal of the inhibitor for at least 5 days results in the induction of EMT, which can be appreciated by the transition of cobblestone epithelial-like cells towards spindle-shaped mesenchymal cells and upregulation of the mesenchymal genes *POSTN* and *FN1* (Fig. 6A-C) (Moerkamp et al., 2016).

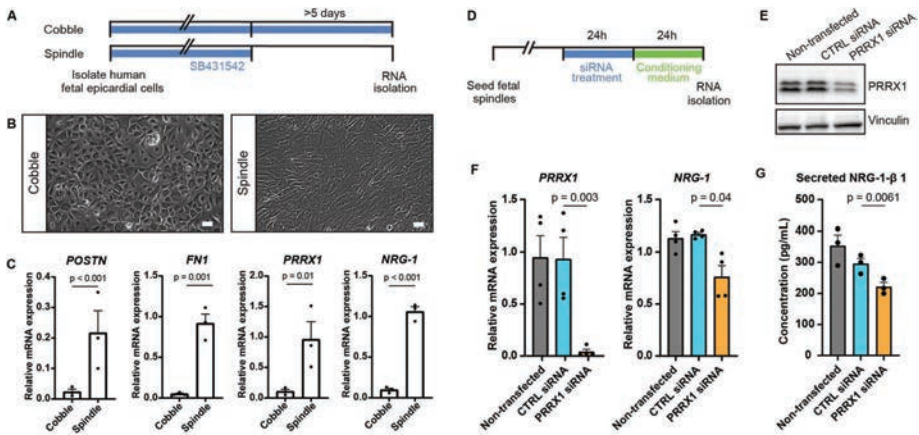


**Fig. 6 | PRRX1 promotes NRG1 expression in human EPDCs.** (A) Schematic of the workflow for the experiments shown in B and C. After isolation, human fetal epicardial cells are cultured in the presence of the ALK4/5/7 kinase inhibitor SB-431542. Cells transform from cobble- to spindle-shape upon removal of SB-431542. (B) Representative brightfield pictures of cobble- and spindle-shaped human fetal epicardial cells. Scale bars: 100 μm. (C) qPCR results for *POSTN*, *FN1*, *PRRX1* and *NRG-1* in human fetal cobble (*n*=3) and spindle (*n*=3) epicardial cells (mean±s.d.; *POSTN* *P*<0.001, *FN1* *P*=0.001, *PRRX1* *P*=0.01, *NRG-1* *P*<0.001, unpaired *t*-tests). (D) Schematic of the workflow for the experiments shown in E and F. (E) Western blot for *PRRX1* in U87 cells. Vinculin was used as a loading control. (F) qPCR results for *PRRX1* and *NRG-1* in human fetal spindle epicardial cells after *PRRX1* siRNA treatment (non-transfected cells *n*=4, CTRL siRNA *n*=4, *PRRX1* siRNA *n*=4) (mean±s.d., *PRRX1* CTRL siRNA versus *PRRX1* siRNA *P*=0.003, *NRG-1* CTRL siRNA versus *PRRX1* siRNA *P*=0.04, unpaired *t*-tests) (G) ELISA results for secreted NRG1-β1 in the conditioned cell culture medium of human fetal spindle epicardial cells between 24 and 48 h after *PRRX1* siRNA treatment (non-transfected cells *n*=3, CTRL siRNA *n*=3, *PRRX1* siRNA *n*=3) (mean±s.d., CTRL siRNA versus *PRRX1* siRNA *P*=0.0061, unpaired *t*-tests).

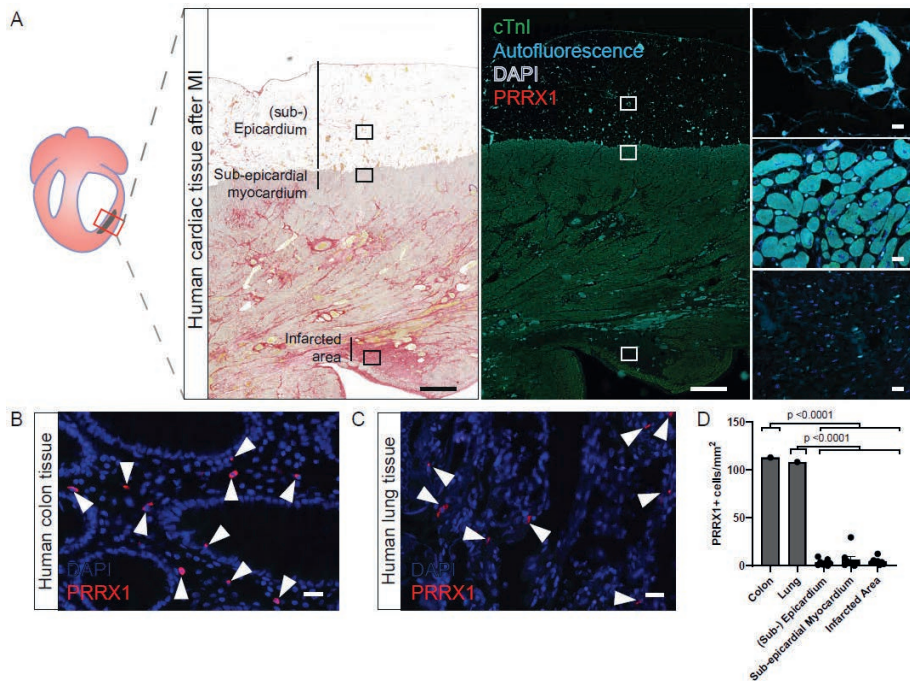


**Fig. 7 | PRRX1 is nearly undetectable in adult injured human hearts.** (A) Sirius red and immunofluorescent staining on consecutive human tissue samples of patients with a recent myocardial infarction for PRRX1 (red), cTnI (green) as marker for the myocardium and autofluorescence (light blue) to indicate the extracellular matrix and DAPI (dark blue). Scale bars represent 1000  $\mu\text{m}$  in overview pictures and 20  $\mu\text{m}$  in zoom-ins. (B-C) Positive control for PRRX1 staining in human colon and lung tissue. Arrowheads indicate PRRX1+ cells. Scale bars represent 20  $\mu\text{m}$ . (D) Quantification of PRRX1+ cells in human tissue at different locations. For D, a one-way ANOVA with Dunnett's multiple comparisons test was used to determine statistical significance. SE = sub-epicardial.

Although some *PRRX1* expression was detected in cobblestone epithelial-like cells, its expression was increased 8-fold in spindle-shaped mesenchymal cells (Fig. 6C). Importantly, *NRG1* expression followed the same pattern as *PRRX1* expression, as they were both increased in spindle-shaped cells. To determine whether *PRRX1* can regulate *NRG1* expression, spindle-shaped mesenchymal cells were subjected to *PRRX1* knockdown (KD) using siRNAs (Fig. 6D). The effect of *PRRX1* KD was confirmed using western blot (Fig. 6E). Indeed, *PRRX1* KD led to a significant decrease in *NRG1* mRNA, as well as a significant decrease of secreted *NRG1*- $\beta$ 1 protein (Fig. 6F,G). From these results, we conclude that in EPDCs after EMT induction, *PRRX1* and *NRG1* are co-expressed and that *PRRX1* is required for efficient *NRG1* expression. This suggests that the role of *PRRX1* in EPDCs is conserved between zebrafish and

human. Therefore, we aimed to investigate the relevance of PRRX1 during human heart repair and analyzed PRRX1 expression in human tissue from eight patients that suffered a recent myocardial infarction, showing beginning scar formation and fibroblasts infiltration (Fig. 7A). Positive staining could be observed in human colon and lung tissue, which indicates that the immunostaining protocol is able to detect PRRX1 in human tissue (Fig. 7B,C). However, only very few PRRX1+ cells could be identified in human injured heart tissue, either in the (sub-)epicardium, sub-epicardial myocardium or in the infarcted area (Fig.7D). Taken together, these findings indicate that the efficient induction of *NRG1* is dependent on PRRX1. Furthermore, while PRRX1 is abundantly present in the regenerative zebrafish heart, it is nearly absent in the non-regenerative injured adult human heart.

## DISCUSSION

The results described here demonstrate that *prrx1b* is required for the scar-free regeneration of the injured zebrafish heart. The zebrafish genome contains a *prrx1a* and a *prrx1b* gene, which are likely the result of an ancient genome duplication that occurred in teleosts (Howe et al., 2013). Our results demonstrate that whereas *prrx1b* is required for heart regeneration, *prrx1a* is dispensable, which suggests these paralogues have non-redundant roles. This is different from their role during cartilage formation in the embryo where *prrx1a* and *prrx1b* are redundant (Barske et al., 2016).

*Prrx1* expression is rapidly induced in the epicardium upon injury. This is reminiscent of the induction of other genes in the epicardium, such as *tbx18* and *aldh1a2* (also known as *raldh2*), and implies that *Prrx1* induction is part of the early activation that occurs in the entire epicardium (Cao and Poss, 2018; Lepilina et al., 2006). Importantly, all three previously identified subpopulations (*tcf21*<sup>+</sup>, *tbx18*<sup>+</sup> and *wt1*<sup>+</sup>) of epicardial cells and EPDCs express *Prrx1* (Cao et al., 2016; Weinberger et al., 2020).

It has been well established that EPDCs differentiate into various cell types (reviewed by Cao and Poss, 2018). Retroviral labelling and Cre-mediated recombination studies in chick, mouse and zebrafish have demonstrated that EPDCs differentiate into fibroblasts and vascular support cells (e.g. pericytes) (Acharya et al., 2012; Gittenberger-de Groot et al., 1998; González-Rosa et al., 2012; Kikuchi et al., 2011; Männer, 1999; Mikawa and Gourdie, 1996), which is in good agreement with our scRNAseq data. There are also numerous reported observations suggesting that EPDCs can differentiate into endothelial cells and cardiomyocytes (Cai et al., 2008; Guadix et

al., 2006; Katz et al., 2012; Männer, 1999; Mikawa and Gourdie, 1996; Smart et al., 2011; Zangi et al., 2013), although some of these observations have been questioned by others (Christoffels et al., 2009; Rudat and Kispert, 2012). In our scRNAseq analysis of EPDCs recovered from the regenerating zebrafish heart, we did not find a cell type representing endothelial cells or cardiomyocytes, which is in agreement with earlier observations that *tcf21*-derived EPDCs in the zebrafish do not contribute to either endothelial or myocardial cell lineages (González-Rosa et al., 2012; Kikuchi et al., 2011).

Fibroblasts are one of the main contributors to ECM deposition in response to cardiac injury and are therefore an important cell type in maintaining the balance between the fibrotic and regenerative injury response (Chablais and Jaźwińska, 2012; Gemberling et al., 2015; Sánchez-iranzo et al., 2018). In addition, subpopulations of cardiac fibroblasts can have distinct roles in cardiomyocyte maturation and innervation (Hortells et al., 2020). By scRNAseq analysis, we identified two distinct fibroblast cell states in the regenerating heart. The pro-fibrotic fibroblast cluster (cluster 3) expresses all three TGF $\beta$  ligands, supporting earlier findings that these ligands are expressed in the injury area to activate a pro-fibrotic response (Chablais and Jaźwińska, 2012). Pro-fibrotic fibroblasts express fibronectin-1 (*fn1a*) and various collagens (Sánchez-iranzo et al., 2018), which we found to be upregulated in the cluster 3 fibroblasts, corroborating their pro-fibrotic nature. In *prrx1b*<sup>-/-</sup> hearts, these pro-fibrotic fibroblasts were more abundant, which is consistent with the observed excess of collagen deposition. Whereas cardiac fibrosis is permanent in the injured mammalian heart, it is resolved in the zebrafish heart. The mechanism for this regression in the zebrafish heart is not well understood. It could be related to the observation that activated fibroblasts partially return to a quiescent state (Sánchez-iranzo et al., 2018). Our results showing that an increase in activated (pro-fibrotic) fibroblast cell numbers can lead to an excessive fibrotic response supports the theory that the de-activation of injury-responsive pro-fibrotic fibroblasts is detrimental to successful scar regression.

Cluster 2 cells have only limited expression of pro-fibrotic genes and might therefore represent de-activated, quiescent fibroblasts. Many factors secreted by activated fibroblasts have been implicated in cardiac development and regeneration, suggesting that the pro-regenerative function of fibroblasts might be accomplished through their secretory role. In addition, experiments co-culturing fibroblasts with cardiomyocytes show that fibroblasts can induce cardiomyocyte proliferation (Ieda et al., 2009). Our results demonstrate Prrx1-dependent *nrg1* expression in EPDCs near the proliferating cardiomyocytes in the border zone. Nrg1 is a potent inducer of cardiomyocyte proliferation by activation of the ErbB2 signalling pathway (Bersell et al., 2009; D'Uva et

al., 2015; Gemberling et al., 2015), which is consistent with our observation that the cardiomyocyte proliferation defect in *prrx1b*<sup>-/-</sup> hearts can be rescued by exogenous Nrg1. Both the *in vitro* experiments in human fetal EPDCs and the *in vivo* experiments in zebrafish demonstrate that *Nrg1* expression depends on Prrx1. Whether this is through binding of Prrx1 to regulatory sequences in the *nrg1* locus or whether is through a more indirect mechanism needs to be further investigated for example by chromatin immunoprecipitation experiments.

In conclusion, we have shown that during zebrafish heart regeneration Prrx1b expression in EPDCs restricts the amount of pro-fibrotic fibroblasts and stimulates cardiomyocyte proliferation. In doing so, Prrx1b establishes a balance between fibrotic repair and the regeneration of lost myocardium during zebrafish heart regeneration.

## MATERIALS AND METHODS

### Animal experiments

Animal care and experiments conformed to the Directive 2010/63/EU of the European Parliament. All animal work was approved by the Animal Experimental Committee of the Instantie voor Dierenwelzijn Utrecht (IvD) and was performed in compliance with the Dutch government guidelines. Zebrafish were housed under standard conditions (Aleström et al., 2019).

### Zebrafish lines

The following zebrafish lines were used: TL, *prrx1a*, *prrx1a*<sup>el558</sup>, *prrx1b*<sup>el491</sup> (Barske et al., 2016), *Tg(tcf21:CreERT2)* (Kikuchi et al., 2011) and *Tg(ubi:loxP-EGFP-loxP-mCherry)* (Mossimann et al., 2011).

### Cryoinjuries in zebrafish

To address experiments in a regeneration context, cardiac cryo-injuries were performed on TL and *prrx1b*<sup>el491</sup> [with and without *Tg(tcf21:CreERT2; ubi:loxP-EGFP-loxP-mCherry)*] fish of both sexes that were ~4-18 months of age. The cryoinjuries were performed as described by Schnabel et al. (2011), with the exception of the use of a copper filament (0.3 mm) cooled in liquid nitrogen instead of dry ice. Animals were excluded from the study if they exhibited signs of aberrant behaviour, sickness or infection, according to animal care guidelines.

## Histology and enzyme histochemistry

Acid Fuchsin Orange G (AFOG) staining was performed on paraffin sections of zebrafish ventricles as previously described (Poss et al., 2002). Paraffin sections of 7, 30 and 90 dpi hearts were prepared as described below (see '*In situ* hybridization' section). Sirius Red staining was performed on similar paraffin sections as previously described (Junqueira et al., 1979), excluding the Haematoxylin step.

## Immunofluorescence

Adult zebrafish ventricles were isolated and fixed in 4% paraformaldehyde (4°C overnight on shaker). The next day, the hearts were washed three times, 10 min each wash, in 4% sucrose phosphate buffer, after which they were incubated at room temperature for at least 5 h in 30% sucrose phosphate buffer until the hearts sank. Then, they were embedded in cryo-medium (OCT). The hearts were cryosectioned at 10 µm thickness using a Thermo Scientific Cryostar NX70 cryostat. Primary antibodies used were: anti-PCNA (Dako, M0879; 1:800), anti-Mef2c (Santa Cruz Biotechnology, SC313 or Biorbyt, orb256682; both 1:1000), anti-tropomyosin (Sigma-Aldrich, 122M4822; 1:400), Living Colors anti-DsRed (Clontech, 632496; 1:100), anti-RFP (Novus Biologicals, 42649; 1:100), anti-Prrx1 (gift from the Tenaka lab; Gerber et al., 2018; Oliveira et al., 2017; 1:200), mouse IgG2b anti-Dendra2 [Origene, TA180094, clone OT11G6 (for Wt1b H2B dendra); 1:400], chicken polyclonal anti-GFP [Abcam, ab13970 (for Tbx18 myr GFP); 1:200]. Secondary antibodies were: anti-chicken Alexa 488 (Thermo Fisher, A21133; 1:500), anti-rabbit Alexa 555 (Thermo Fisher, A21127; 1:500), anti-mouse Cy5 (Jackson ImmunoResearch, 118090; 1:500), anti-mouse IgG2b Alexa 647 (Jackson ImmunoResearch, 102371; 1:100). Nuclei were stained using 4',6-diamidino-2-phenylindole (DAPI) or Hoechst 405 staining. Images of immunofluorescence staining are single optical planes acquired with a Leica SP8 confocal microscope. Human tissue was used for immunofluorescent staining as described (Kruithof et al. 2020, CVR) using the following antibodies: anti-cTnl (Hytest, #4T21, 1:1000), anti-Prrx1 (1:200). As a control, sections without primary antibody were taken along. Nuclei were shown by DAPI staining. Tissue sections were imaged using Panoramic 250 slide scanner (3DHISTECH).

## Quantitative analyses

All quantifications were performed blind. Unless stated otherwise, three individual sections with the largest injuries per heart were analysed including data obtained through *in situ* hybridization, immunohistochemistry and Sirius Red staining. Imaris x64 V3.2.1 software (Oxford Instruments) was used to analyse immunofluorescence images made with a Leica SP8 confocal microscope. Proliferation percentages of border zone cardiomyocytes were determined using the spots selection tool in Imaris.

A region of interest (200  $\mu\text{m}$ ) consisting of the border zone was chosen and cardiomyocytes (identified by *Mef2* expression) were selected by classifying them as 5  $\mu\text{m}$  diameter or bigger. Proliferating cardiomyocytes were selected by hand using the PCNA channel. To quantify the distribution of *tcf21*<sup>+</sup> *Prrx1*<sup>+</sup> cells over different locations and different time points, the spot selection tool in Imaris was used to select all *Prrx1*<sup>+</sup> cells in the ventricle, after which a subselection of all *tcf21*:mCherry<sup>+</sup> *Prrx1*<sup>+</sup> cells was made by hand. Distinguished regions were remote epicardium, BZ epicardium (100  $\mu\text{m}$  up and 100  $\mu\text{m}$  down from the edge of intact myocardium), injury epicardium and within the injury. Double-positive cells in each of these regions were counted and presented as a percentage of the total double-positive cells in the ventricle. To quantify the percentage of *tcf21*:mCherry<sup>+</sup> cell invasion into the injury, the surface selection tool was used to mark the total *tcf21*:mCherry<sup>+</sup> area in the ventricle. The measurement we used was the average value of the volume. Then, the total injury area plus 100  $\mu\text{m}$  border zone was chosen as a region of interest designated as the 'whole injury area'. Then, *tcf21*:mCherry<sup>+</sup> surfaces within the injury were selected manually to create a subset of the whole injury area surface. Proliferation of *tcf21*:mCherry<sup>+</sup> cells was defined as the number of PCNA<sup>+</sup> cells per  $\mu\text{m}^2$  of *tcf21*:mCherry<sup>+</sup> tissue surface, as the cytoplasmic mCherry signal does not allow for the distinction between individual cells. *tcf21*:mCherry<sup>+</sup> PCNA<sup>+</sup> cells were counted manually. *Nrg1* RNAscope signal was quantified by using the spots selection tool in Imaris to count the absolute number of *nrg1* transcripts in the BZ epicardium regions. ImageJ software (NIH) was used to quantify the remaining scar size of 30 and 90 dpi heart sections following AFOG staining. All sections of each heart were stained, imaged and quantified for scar tissue area using ImageJ. Sirius Red staining in wild-type and *prrx1b*<sup>-/-</sup> hearts was analysed using the ImageJ-macros MRI Fibrosis Tool ([http://dev.mri.cnrs.fr/projects/imagej-macros/wiki/Fibrosis\\_Tool](http://dev.mri.cnrs.fr/projects/imagej-macros/wiki/Fibrosis_Tool)). Caseviewer (3DHISTECH) was used to analyse PRRX1<sup>+</sup> cells in human cardiac tissue. Positive cells were manually counted in 10 areas of 0.1 mm<sup>2</sup> in the (sub-) epicardial layer, sub-epicardial myocardium and infarcted area, that were blindly selected. As a technical positive control, 10 areas of 0.1 mm<sup>2</sup> were similarly quantified in human colon and lung tissue.

### Lineage tracing of zebrafish epicardial cells

To lineage trace epicardial and epicardial-derived cells, we combined *Tg(tcf21:CreERT2)* with *Tg(ubi:loxP-EGFP-loxP-mCherry)*. Both wild-type and *prrx1b*<sup>-/-</sup> embryos with a single copy of both transgenes [*Tg(tcf21:CreERT2*; *ubi:loxP-EGFP-loxP-mCherry)*] were incubated in 4-hydroxytamoxifen (4-OHT) as described by Kikuchi et al. (2011) and Mosimann et al. (2011) from 1 dpf until 5 dpf at

a concentration of 5  $\mu$ M. At 5 dpf, embryos were selected that were positive for epicardial mCherry signal and grown to adulthood.

### Isolation of single cells from cryoinjured hearts

Cryoinjured hearts of either *prrx1b* wild-type siblings ( $n=20$ ) or *prrx1b* homozygous mutants ( $n=20$ ) previously recombined as embryos [*Tg(tc21:CreERT2; ubi:loxP-EGFP-loxP-mCherry*)] were extracted at 7 dpi. Cells were dissociated according to Tessadori et al. (2012). For cell sorting, viable cells were gated by negative DAPI staining and positive YFP fluorescence. In brief, the FACS gating was adjusted to sort cells positive for mCherry (recombined epicardial-derived cells) and negative for EGFP (unrecombined cells). In total, 1536 cells (768 *prrx1b* wild-type sibling cells and 768 *prrx1b* homozygous mutant cells) were sorted into 384-well plates and processed for scRNAseq as described below.

### scRNAseq

Single-cell sequencing libraries were prepared using SORT-seq (Muraro et al., 2016). Live cells were sorted into 384-well plates with Vapor-Lock oil containing a droplet with barcoded primers, spike-in RNA and dNTPs, followed by heat-induced cell lysis and cDNA syntheses using a robotic liquid handler. Primers consisted of a 24 bp polyT stretch, a 4 bp random molecular barcode (UMI), a cell-specific 8 bp barcode, the 5' Illumina TruSeq small RNA kit adapter and a T7 promoter. After cell lysis for 5 min at 65°C, RT and second strand mixes were distributed with the Nanodrop II liquid handling platform (Inovadyne). After pooling all cells in one library, the aqueous phase was separated from the oil phase, followed by IVT transcription. The CEL-Seq2 protocol was used for library prep (Hashimshony et al., 2016). Illumina sequencing libraries were prepared with the TruSeq small RNA primers (Illumina) and paired-end sequenced at 75 bp read length on the Illumina NextSeq platform. Mapping was performed against the zebrafish reference assembly version 9 (Zv9).

### Bioinformatic analysis

To analyse the scRNAseq data, we used an updated version (RaceID3) of the previously published RaceID algorithm (Grün et al., 2015). For the adult hearts, we obtained a dataset consisting of two different libraries of 384 cells per genotype (wild type or *prrx1b* homozygous mutants) each for a combined dataset of 768 cells, in which we detected a total of 20,995 genes. We detected an average of 7022 reads per cell. Based on the distribution of the log<sub>10</sub> total reads plotted against the frequency, we introduced a cutoff at minimally 1000 reads per cell before further analysis. This reduced the number of cells used in the analysis to 711 wild-type and 727 mutant cells.

The top 20 noisy genes were identified by the StemID algorithm, which we excluded from the downstream analysis to increase clustering robustness. Batch-effects were analysed and showed no plate-specific clustering of certain clusters. The StemID algorithm were used as previously described (Grün et al., 2016). In short, StemID is an approach developed for inferring the existence of stem cell populations from single-cell transcriptomics data. StemID calculates all pairwise cell-to-cell distances ( $1 - \text{Pearson correlation}$ ) and uses this to group similar cells into clusters that correspond to the cell types present in the tissue. The StemID algorithm calculates the number of links between clusters. This is based on the assumption that cell types with fewer links are more canalized whereas cell types with a higher number of links have a higher diversity of cell states. Besides the number of links, the StemID algorithm also calculates the change in transcriptome entropy. Differentiated cells usually express a small number of genes at high levels in order to perform cell-specific functions, which is reflected by a low entropy. Stem cells and progenitor cells display a more diverse transcriptome reflected by high entropy (Banerji et al., 2013). By calculating the number of links from one cluster to other clusters and multiplying this with the change in entropy, it generates a StemID score, which is representative of the 'stemness' of a cell population. Differential gene expression analysis was performed using the 'diffexpnb', which makes use of the DESeq algorithm. *P*-values were Benjamini-Hochberg corrected for false discovery rate to make the cutoff.

### Statistical analysis of data

Statistical analyses were performed using GraphPad Prism8 software. Unless stated otherwise, unpaired *t*-tests were used for all statistical testing. For the NRG1 rescue experiment (Fig. 5E) one-way ANOVA followed by multiple comparisons analysis using the Tukey's test was performed.

### *In situ* hybridization

*In situ* hybridization was performed on paraffin sections. After overnight fixation in 4% paraformaldehyde, hearts were washed in PBS twice, dehydrated in ethanol, and embedded in paraffin. Serial sections were made at 8  $\mu\text{m}$  thickness. *In situ* hybridization was performed as previously described (Moorman et al., 2001) except that the hybridization buffer used did not contain heparin and yeast total RNA. When *in situ* hybridization was carried out for multiple probes, INT-BCIP staining solution (red/brown staining) was used for the additional probe instead of NBT-BCIP (blue staining).

### **RNAscope**

RNAscope *in situ* hybridization was performed on fixed frozen sections following the Advanced Cell Diagnostics company protocol for RNAscope Multiplex Fluorescent Reagent Kit v2 with the following modification: target retrieval was not performed as this was not required for the *nrg1* probe. The probe used for *nrg1* detection was RNAscope Probe- Dr-nrg1-CDS (414131). For co-detection with Prrx1 antibody, the RNA-Protein Co-detection Ancillary Kit was used following the Advanced Cell Diagnostics company protocol. Prrx1 antibody was used at 1:200.

### **Intraperitoneal injections in zebrafish**

Intraperitoneal injections of human recombinant NRG1 (recombinant human heregulin-b1, Peprotech, 100-03) were performed as described by Kinkel et al. (2010). Fish were sedated using MS222 (0.032% wt/vol). Injections were performed using a Hamilton syringe (Gauge 30), cleaned before use by washing in 70% ethanol followed by two washes in PBS. Injection volumes were adjusted to the weight of the fish (30  $\mu$ l/g) and a single injection contained 60  $\mu$ g/kg (diluted in 0.1% bovine serum albumin in PBS).

### **Human epicardial cell culture**

Human fetal hearts of a gestational age between 12 and 18 weeks were collected anonymously and under informed consent from abortion material after elective abortion. Epicardial cells were isolated as described by Dronkers et al. (2018). Cells were cultured in Dulbecco's modified Eagle's medium (DMEM low-glucose, Gibco) and Medium 199 (M199, Gibco) mixed in a 1:1 ratio, supplemented with 10% fetal bovine serum (heat-inactivated for 25 min at 56°C, Gibco), 100 U/ml penicillin (Roth), 100 mg/ml streptomycin (Roth) and 10  $\mu$ M ALK4/5/7 kinase inhibitor SB-431542 (Tocris) at 37°C in 5% CO<sub>2</sub>. EMT was induced by removal of SB-431542 from the medium. This research was carried out according to the official guidelines of the Leiden University Medical Center and approved by the local Medical Ethics Committee. This research conforms to the Declaration of Helsinki. Cells were tested for contamination every 3 months.

### **Cell culture U87 cells**

U87 cells were cultured in Dulbecco's modified Eagle's medium (DMEM high-glucose, Gibco), supplemented with 10% fetal bovine serum (Gibco), 100 U/ml penicillin (Roth) and 100 mg/ml streptomycin (Roth). Cells were tested for contamination every 3 months.

### **PRRX1 KD in human epicardial cells**

Cells were treated with SMARTpool ON-TARGETplus PRRX1 or a non-targeting control siRNA according to the manufacturer's protocol at a concentration of 25 nM (Dharmacon). After 48 h, cells were collected for qPCR or western blot. All experiments in human fetal epicardial cells were performed with three or four individual cell isolations.

### **qPCR**

ReliaPrep RNA Miniprep Systems (Promega) was used to isolate mRNA, of which the concentration and purity were determined using a NanoDrop 1000 Spectrophotometer (Thermo Fisher Scientific). cDNA synthesis was performed using the RevertAid H Minus First Strand cDNA Synthesis Kit (Thermo Fisher Scientific). Next, qPCR was performed using SYBR Green (Promega) and run on a C1000 Touch thermal cycler (Bio-Rad). All samples were run in triplicate; expression levels were corrected for primer efficiency and normalized for two reference genes (*TBP* and *HPRT1*).

Primer sequences were: *POSTN* forward, GGAGGCAAACAGCTCAGAGT; *POSTN* reverse, GGCTGAGGAAGGTGCTAAAG; *FN1* forward, CGTCATAGTGGAGGCACTGA; *FN1* reverse, CAGACATTCGTTCCCACTCA; *PRRX1a* forward, CGCAGGAATGAGAGAGCCAT; *PRRX1a* reverse, AACATCTGGGAGGGACGAG; *NRG1* forward, CACATGATGCCGACCACAAG; *NRG1* reverse, GGTGATCGCTGCCAAACTA; *TBP* forward, TGGAAAAGTTGTATTAACAGGTGCT; *TBP* reverse, GCAAGGGTACATGAGAGCCA; *HPRT1* forward, CTCATGGACTGATTATGGACAGGAC; *HPRT1* reverse, GCAGGTCAGCAAAGAACTTATAGCC.

### **Western blot**

Cells were lysed in radioimmunoprecipitation assay (RIPA) buffer containing protease and phosphatase inhibitors (cComplete Protease Inhibitor Cocktail tablets, Roche Diagnostics). Protein concentration was determined using the Pierce BCA Protein Assay Kit (Thermo Fisher Scientific). For every sample, 50 µg of protein was loaded onto a 10% SDS-polyacrylamide gel. Subsequently, protein was transferred onto Immobilon-P PVDF Membrane (Millipore). Blots were blocked in 5% bovine serum albumin in Tris-buffered saline with 0.1% Tween 20 (TBST) for 1 h and incubated overnight with primary antibody (anti-PRRX1, 1:500, gift from the Tenaka lab; Gerber et al., 2018; Oliveira et al., 2017; anti-Vinculin, 1:5000, Sigma-Aldrich, V9131, 1:5000). Blots were incubated for 1 h with horseradish peroxidase anti-rabbit secondary antibody (Abcam, ab98493), which was detected by WesternBright Quantum (Advansta).

## ELISA

Conditioned medium was collected for 24 h after 24 h of siRNA treatment, centrifuged at 200 *g* for 2 min and immediately frozen at  $-20^{\circ}$ . Cell culture medium was taken as a control sample. An NRG1- $\beta$ 1 ELISA assay was performed according to the manufacturer's protocol (Human NRG1- $\beta$ 1 DuoSet ELISA, R&D Systems). Absolute NRG1- $\beta$ 1 concentration was calculated based on the standard curve.

We would like to thank all members of the Bakkers lab for their input during this study, Jens Puschhof for technical help with the RNAscope analysis, Jeroen Korving for his help with histology, and the Hubrecht Institute FACS facility and Single Cell Discoveries for their expertise with sorting and sequencing.

## REFERENCES

- Acharya, A., Baek, S. T., Huang, G., Eskiocak, B., Goetsch, S., Sung, C. Y., Banfi, S., Sauer, M. F., Olsen, G. S., Duffield, J. S. et al. (2012). The bHLH transcription factor Tcf21 is required for lineage-specific EMT of cardiac fibroblast progenitors. *Development* 139, 2139-2149. <https://doi.org/10.1242/dev.079970>
- Aleström, P., D'Angelo, L., Midtlyng, P. J., Schorderet, D. F., Schulte-Merker, S., Sohm, F. and Warner, S. (2019). Zebrafish: Housing and husbandry recommendations. *Lab. Anim.* 54, 213-224. <https://doi.org/10.1177/0023677219869037>
- Banerji, C. R. S., Miranda-Saavedra, D., Severini, S., Widschwendter, M., Enver, T., Zhou, J. X. and Teschendorff, A. E. (2013). Cellular network entropy as the energy potential in Waddington's differentiation landscape. *Sci. Rep.* 3, 3039. <https://doi.org/10.1038/srep03039>
- Barske, L., Askary, A., Zuniga, E., Balczerski, B., Bump, P., Nichols, J. T. and Crump, J. G. (2016). Competition between Jagged-Notch and endothelin1 signaling selectively restricts cartilage formation in the zebrafish upper face. *PLoS Genet.* 12, e1005967. <https://doi.org/10.1371/journal.pgen.1005967>
- Bersell, K., Arab, S., Haring, B. and Kühn, B. (2009). Neuregulin1/ErbB4 signaling induces cardiomyocyte proliferation and repair of heart injury. *Cell* 138, 257-270. <https://doi.org/10.1016/j.cell.2009.04.060>
- Cai, C.-L., Martin, J. C., Sun, Y., Cui, L., Wang, L., Ouyang, K., Yang, L., Bu, L., Liang, X., Zhang, X. et al. (2008). A myocardial lineage derives from Tbx18 epicardial cells. *Nature* 454, 104-108. <https://doi.org/10.1038/nature06969>
- Cao, J. and Poss, K. D. (2018). The epicardium as a hub for heart regeneration. *Nat. Rev. Cardiol.* 15, 631-647. <https://doi.org/10.1038/s41569-018-0046-4>
- Cao, J., Navis, A., Cox, B. D., Dickson, A. L., Gemberling, M., Karra, R., Bagnat, M. and Poss, K. D. (2016). Single epicardial cell transcriptome sequencing identifies caveolin 1 as an essential factor in zebrafish heart regeneration. *Development (Camb.)* 143, 232-243. <https://doi.org/10.1242/dev.130534>
- Chablais, F. and Jaźwińska, A. (2012). The regenerative capacity of the zebrafish heart is dependent on TGFβ signaling. *Development (Camb.)* 139, 1921-1930. <https://doi.org/10.1242/dev.078543>
- Chablais, F., Veit, J., Rainer, G. and Jaźwińska, A. (2011). The zebrafish heart regenerates after cryoinjury-induced myocardial infarction. *BMC Dev. Biol.* 11, 21. <https://doi.org/10.1186/1471-213X-11-21>
- Christoffels, V. M., Grieskamp, T., Norden, J., Mommersteeg, M. T. M., Rudat, C. and Kispert, A. (2009). Tbx18 and the fate of epicardial progenitors. *Nature* 458, E8-E9. <https://doi.org/10.1038/nature07916>
- Dronkers, E., Moerkamp, A. T., van Herwaarden, T., Goumans, M.-J. and Smits, A. M. (2018). The isolation and culture of primary epicardial cells derived from human adult and fetal heart specimens. *J. Vis. Exp.* 134, e57370. <https://doi.org/10.3791/57370>

- D'Uva, G., Aharonov, A., Lauriola, M., Kain, D., Yahalom-Ronen, Y., Carvalho, S., Weisinger, K., Bassat, E., Rajchman, D., Yifa, O. et al. (2015). ERBB2 triggers mammalian heart regeneration by promoting cardiomyocyte dedifferentiation and proliferation. *Nat. Cell Biol.* 17, 627-638. <https://doi.org/10.1038/ncb3149>
- Gemberling, M., Karra, R., Dickson, A. L. and Poss, K. D. (2015). Nrg1 is an injury-induced cardiomyocyte mitogen for the endogenous heart regeneration program in zebrafish. *eLife* 4, 1-17. <https://doi.org/10.7554/eLife.05871>
- Gerber, T., Murawala, P., Knapp, D., Masselink, W., Schuez, M., Hermann, S., Gac-Santel, M., Nowoshilow, S., Kageyama, J., Khattak, S. et al. (2018). Single-cell analysis uncovers convergence of cell identities during axolotl limb regeneration. *Science* 362, eaaq0681. <https://doi.org/10.1126/science.aaq0681>
- Gittenberger-de Groot, A. C., Vrancken Peeters, M.-P. F. M., Mentink, M. M. T., Gourdie, R. G. and Poelmann, R. E. (1998). Epicardium-derived cells contribute a novel population to the myocardial wall and the atrioventricular cushions. *Circ. Res.* 82, 1043-1052. <https://doi.org/10.1161/01.RES.82.10.1043>
- González-Rosa, J. M., Martín, V., Peralta, M., Torres, M. and Mercader, N. (2011). Extensive scar formation and regression during heart regeneration after cryoinjury in zebrafish. *Development (Camb.)* 138, 1663-1674. <https://doi.org/10.1242/dev.060897>
- González-Rosa, J. M., Peralta, M. and Mercader, N. (2012). Pan-epicardial lineage tracing reveals that epicardium derived cells give rise to myofibroblasts and perivascular cells during zebrafish heart regeneration. *Dev. Biol.* 370, 173-186. <https://doi.org/10.1016/j.ydbio.2012.07.007>
- Grün, D., Lyubimova, A., Kester, L., Wiebrands, K., Basak, O., Sasaki, N., Clevers, H. and van Oudenaarden, A. (2015). Single-cell messenger RNA sequencing reveals rare intestinal cell types. *Nature* 525, 251-255. <https://doi.org/10.1038/nature14966>
- Grün, D., Muraro, M. J., Boisset, J.-C., Wiebrands, K., Lyubimova, A., Dharmadhikari, G., van den Born, M., van Es, J., Jansen, E., Clevers, H. et al. (2016). De novo prediction of stem cell identity using single-cell transcriptome data. *Cell Stem Cell* 19, 266-277. <https://doi.org/10.1016/j.stem.2016.05.010>
- Guadix, J. A., Carmona, R., Muñoz-Chápuli, R. and Pérez-Pomares, J. M. (2006). In vivo and in vitro analysis of the vasculogenic potential of avian proepicardial and epicardial cells. *Dev. Dyn.* 235, 1014-1026. <https://doi.org/10.1002/dvdy.20685>
- Guichet, P.-O., Guelfi, S., Teigell, M., Hoppe, L., Bakalara, N., Bauchet, L., Duffau, H., Lamszus, K., Rothhut, B. and Hugnot, J. P. (2015). Notch1 stimulation induces a vascularization switch with pericyte-like cell differentiation of glioblastoma stem cells. *Stem Cells* 33, 21-34. <https://doi.org/10.1002/stem.1767>
- Hashimshony, T., Senderovich, N., Avital, G., Klochendler, A., de Leeuw, Y., Anavy, L., Genert, D., Li, S., Livak, K. J., Rozenblatt-Rosen, O. et al. (2016). CEL-Seq2: Sensitive highly-multiplexed single-cell RNA-Seq. *Genome Biol.* 17, 77. <https://doi.org/10.1186/s13059-016-0938-8>

- Hortells, L., Valiente-Alandi, I., Thomas, Z. M., Agnew, E. J., Schnell, D. J., York, A. J., Vagnozzi, R. J., Meyer, E. C., Molkentin, J. D. and Yutzey, K. E. (2020). A specialized population of Periostin-expressing cardiac fibroblasts contributes to postnatal cardiomyocyte maturation and innervation. *Proc. Natl. Acad. Sci. USA* 117, 21469-21479. <https://doi.org/10.1073/pnas.2009119117>
- Howe, K., Clark, M. D., Torroja, C. F., Tarrant, J., Berthelot, C., Muffato, M., Collins, J. E., Humphray, S., McLaren, K., Matthews, L. et al. (2013). The zebrafish reference genome sequence and its relationship to the human genome. *Nature* 496, 498-503. <https://doi.org/10.1038/nature12111>
- Ieda, M., Tsuchihashi, T., Ivey, K. N., Ross, R. S., Hong, T.-T., Shaw, R. M. and Srivastava, D. (2009). Cardiac fibroblasts regulate myocardial proliferation through  $\beta$ 1 integrin signaling. *Dev. Cell* 16, 233-244. <https://doi.org/10.1016/j.devcel.2008.12.007>
- Itou, J., Oishi, I., Kawakami, H., Glass, T. J., Richter, J., Johnson, A., Lund, T. C. and Kawakami, Y. (2012). Migration of cardiomyocytes is essential for heart regeneration in zebrafish. *Development* 139, 4133-4142. <https://doi.org/10.1242/dev.079756>
- Jopling, C., Sleep, E., Raya, M., Martí, M., Raya, A. and Belmonte, J. C. I. (2010). Zebrafish heart regeneration occurs by cardiomyocyte dedifferentiation and proliferation. *Nature* 464, 606-609. <https://doi.org/10.1038/nature08899>
- Junqueira, L. C. U., Bignolas, G. and Bretani, R. R. (1979). Picrosirius red staining plus polarization microscopy, a specific method for collagen detection in tissue sections. *Histochem. J.* 11, 447-455. <https://doi.org/10.1007/BF01002772>
- Katz, T. C., Singh, M. K., Degenhardt, K., Rivera-Feliciano, J., Johnson, R. L., Epstein, J. A. and Tabin, C. J. (2012). Distinct compartments of the proepicardial organ give rise to coronary vascular endothelial cells. *Dev. Cell* 22, 639-650. <https://doi.org/10.1016/j.devcel.2012.01.012>
- Kikuchi, K., Holdway, J. E., Werdich, A. A., Anderson, R. M., Fang, Y., Egnaczyk, G. F., Evans, T., Macrae, C. A., Stainier, D. Y. R. and Poss, K. D. (2010). Primary contribution to zebrafish heart regeneration by *gata4*(+) cardiomyocytes. *Nature* 464, 601-605. <https://doi.org/10.1038/nature08804>
- Kikuchi, K., Gupta, V., Wang, J., Holdway, J. E., Wills, A. A., Fang, Y. and Poss, K. D. (2011). *Tcf21*<sup>+</sup> epicardial cells adopt non-myocardial fates during zebrafish heart development and regeneration. *Development* 138, 2895-2902. <https://doi.org/10.1242/dev.067041>
- Kim, J., Wu, Q., Zhang, Y., Wiens, K. M., Huang, Y., Rubin, N., Shimada, H., Handin, R. I., Chao, M. Y., Tuan, T.-L. et al. (2010). PDGF signaling is required for epicardial function and blood vessel formation in regenerating zebra fish hearts. *Proc. Natl. Acad. Sci. USA* 107, 17206-17210. <https://doi.org/10.1073/pnas.0915016107>
- Kinkel, M. D., Eames, S. C., Philipson, L. H. and Prince, V. E. (2010). Intraperitoneal injection into adult zebrafish. *J. Vis. Exp.* 42, e2126. <https://doi.org/10.3791/2126>
- Kruithof, B.P.T., Paardekooper, L., Hiemstra, Y.L., Goumans, M.J. Palmén, M., Delgado, V., Klautz, R.J.M., Ajmone Marsan, N. (2020). Stress-induced remodelling of the mitral valve: a model for leaflet thickening and superimposed tissue formation in mitral valve disease. *Cardiovascular Research* 116, 931-943. <https://doi.org/10.1093/cvr/cvz204>

- Lepilina, A., Coon, A. N., Kikuchi, K., Holdway, J. E., Roberts, R. W., Burns, C. G. and Poss, K. D. (2006). A dynamic epicardial injury response supports progenitor cell activity during zebrafish heart regeneration. *Cell* 127, 607-619. <https://doi.org/10.1016/j.cell.2006.08.052>
- Männer, J. (1999). Does the subepicardial mesenchyme contribute myocardioblasts to the myocardium of the chick embryo heart? A quail-chick chimera study tracing the fate of the epicardial primordium. *Anat. Rec.* 255, 212-226. [https://doi.org/10.1002/\(SICI\)1097-0185\(19990601\)255:2<212::AID-AR11>3.0.CO;2-X](https://doi.org/10.1002/(SICI)1097-0185(19990601)255:2<212::AID-AR11>3.0.CO;2-X)
- Mikawa, T. and Gourdie, R. G. (1996). Pericardial mesoderm generates a population of coronary smooth muscle cells migrating into the heart along with ingrowth of the epicardial organ. *Dev. Biol.* 174, 221-232. <https://doi.org/10.1006/dbio.1996.0068>
- Moerkamp, A. T., Lodder, K., Van Herwaarden, T., Dronkers, E., Dingenouts, C. K. E., Tengström, F. C., Van Brakel, T. J., Goumans, M.-J. and Smits, A. M. (2016). Human fetal and adult epicardial-derived cells: A novel model to study their activation. *Stem Cell Res. Ther.* 7, 174. <https://doi.org/10.1186/s13287-016-0434-9>
- Moorman, A. F., Houweling, A. C., de Boer, P. A. and Christoffels, V. M. (2001). Sensitive nonradioactive detection of mRNA in tissue sections: novel application of the whole-mount in situ hybridization protocol. *J. Histochem. Cytochem.* 49, 1-8. <https://doi.org/10.1177/002215540104900101>
- Mosimann, C., Kaufman, C. K., Li, P., Pugach, E. K., Tamplin, O. J. and Zon, L. I. (2011). Ubiquitous transgene expression and Cre-based recombination driven by the ubiquitin promoter in zebrafish. *Development (Camb.)* 138, 169-177. <https://doi.org/10.1242/dev.059345>
- Muraro, M. J., Dharmadhikari, G., Grün, D., Groen, N., Dielen, T., Jansen, E., van Gurp, L., Engelse, M. A., Carlotti, F., de Koning, E. J. P. and et al. (2016). A single-cell transcriptome atlas of the human pancreas. *Cell Systems* 3, 385-394.e3. <https://doi.org/10.1016/j.cels.2016.09.002>
- Nguyen, P. D., de Bakker, D. E. M. and Bakkers, J. (2021). Cardiac regenerative capacity: an evolutionary afterthought? *Cell. Mol. Life Sci.* 78, 5107-5122. <https://doi.org/10.1007/s00018-021-03831-9> Epub ahead of print.
- Ocaña, O. H., Coskun, H., Minguillón, C., Murawala, P., Tanaka, E. M., Galcerán, J., Muñoz-Chápuli, R. and Nieto, M. A. (2017). A right-handed signalling pathway drives heart looping in vertebrates. *Nature* 549, 86-90. <https://doi.org/10.1038/nature23454>
- Oliveira, C. R., Lemaitre, R., Murawala, P., Tazaki, A., Drechsel, D. N. and Tanaka, E. M. (2017). Pseudotyped baculovirus is an effective gene expression tool for studying molecular function during axolotl limb regeneration. *Dev. Biol.* 433, 1-14. <https://doi.org/10.1016/j.ydbio.2017.10.008>
- Poss, K. D. (2010). Advances in understanding tissue regenerative capacity and mechanisms in animals. *Nat. Rev. Genet.* 11, 710-722. <https://doi.org/10.1038/nrg2879>
- Poss, K. D., Wilson, L. G. and Keating, M. T. (2002). Heart regeneration in zebrafish. *Science* 298, 2188-2190. <https://doi.org/10.1126/science.1077857>
- Rudat, C. and Kispert, A. (2012). Wt1 and epicardial fate mapping. *Circ. Res.* 111, 165-169. <https://doi.org/10.1161/CIRCRESAHA.112.273946>

- Sánchez-Iranzo, H., Galardi-Castilla, M., Sanz-Morejón, A., González-Rosa, J. M., Costa, R., Ernst, A., de Aja, J. S., Langa, X. and Mercader, N. (2018). Transient fibrosis resolves via fibroblast inactivation in the regenerating zebrafish heart. *Proc. Natl. Acad. Sci. USA* 115, 4188-4193. <https://doi.org/10.1073/pnas.1716713115>
- Satoh, A., Cummings, G. M. C., Bryant, S. V. and Gardiner, D. M. (2010). Neurotrophic regulation of fibroblast dedifferentiation during limb skeletal regeneration in the axolotl (*Ambystoma mexicanum*). *Dev. Biol.* 337, 444-457. <https://doi.org/10.1016/j.ydbio.2009.11.023>
- Schnabel, K., Wu, C.-C., Kurth, T. and Weidinger, G. (2011). Regeneration of cryoinjury induced necrotic heart lesions in zebrafish is associated with epicardial activation and cardiomyocyte proliferation. *PLoS ONE* 6, e18503. <https://doi.org/10.1371/journal.pone.0018503>
- Smart, N., Bollini, S., Dubé, K. N., Vieira, J. M., Zhou, B., Davidson, S., Yellon, D., Riegler, J., Price, A. N., Lythgoe, M. F. et al. (2011). De novo cardiomyocytes from within the activated adult heart after injury. *Nature* 474, 640-644. <https://doi.org/10.1038/nature10188>
- Stelnicki, E. J., Arbeit, J., Cass, D. L., Saner, C., Harrison, M. and Largman, C. (1998). Modulation of the human homeobox genes PRX-2 and HOXB13 in scarless fetal wounds. *J. Investig. Dermatol.* 111, 57-63. <https://doi.org/10.1046/j.1523-1747.1998.00238.x>
- Tessadori, F., van Weerd, J. H., Burkhard, S. B., Verkerk, A. O., de Pater, E., Boukens, B. J., Vink, A., Christoffels, V. M. and Bakkers, J. (2012). Identification and functional characterization of cardiac pacemaker cells in zebrafish. *PLoS ONE* 7, e47644. <https://doi.org/10.1371/journal.pone.0047644>
- Travers, J. G., Kamal, F. A., Robbins, J., Yutzey, K. E. and Blaxall, B. C. (2016). Cardiac fibrosis: the fibroblast awakens. *Circ. Res.* 118, 1021-1040. <https://doi.org/10.1161/CIRCRESA-HA.115.306565>
- Vanlandewijck, M., He, L., Mäe, M. A., Andrae, J., Ando, K., Del Gaudio, F., Nahar, K., Lebouvier, T., Laviña, B., Gouveia, L. et al. (2018). A molecular atlas of cell types and zonation in the brain vasculature. *Nature* 554, 475-480. <https://doi.org/10.1038/nature25739>
- Wang, J., Cao, J., Dickson, A. L. and Poss, K. D. (2015). Epicardial regeneration is guided by cardiac outflow tract and Hedgehog signalling. *Nature* 522, 226-230. <https://doi.org/10.1038/nature14325>
- Weinberger, M., Simões, F. C., Patient, R., Sauka-Spengler, T. and Riley, P. R. (2020). Functional heterogeneity within the developing zebrafish epicardium. *Dev. Cell* 52, 574-590. e6. <https://doi.org/10.1016/j.devcel.2020.01.023>
- Wu, C.-C., Kruse, F., Vasudevarao, M. D., Junker, J. P., Zebrowski, D. C., Fischer, K., Noël, E. S., Grün, D., Berezikov, E., Engel, F. B. et al. (2015). Spatially resolved genome-wide transcriptional profiling identifies BMP signaling as essential regulator of zebrafish cardiomyocyte regeneration. *Dev. Cell* 36, 36-49. <https://doi.org/10.1016/j.devcel.2015.12.010>
- Yokoyama, H., Maruoka, T., Aruga, A., Amano, T., Ohgo, S., Shiroishi, T. and Tamura, K. (2011). *Prx-1* expression in *xenopus laevis* scarless skin-wound healing and its resemblance to epimorphic regeneration. *J. Investig. Dermatol.* 131, 2477-2485. <https://doi.org/10.1038/jid.2011.223>

- Zangi, L., Lui, K. O., Von Gise, A., Ma, Q., Ebina, W., Ptaszek, L. M., Später, D., Xu, H., Tabebordbar, M., Gorbатов, R. et al. (2013). Modified mRNA directs the fate of heart progenitor cells and induces vascular regeneration after myocardial infarction. *Nat. Biotechnol.* 31, 898-907. <https://doi.org/10.1038/nbt.2682>

## SUPPLEMENTARY INFORMATION

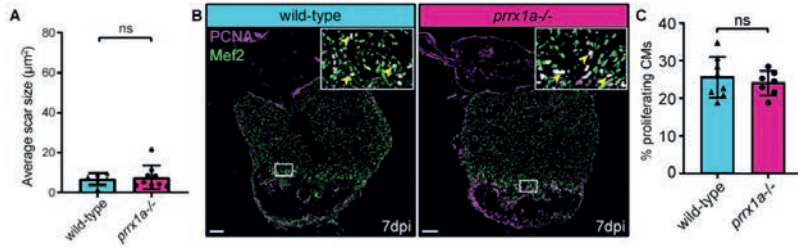


**Fig. S1 | *prrx1a* is dispensable for zebrafish border zone cardiomyocyte proliferation and heart regeneration.** (A) Quantification of the remaining scar size at 30dpi shows no significant difference between *prrx1a*<sup>-/-</sup> hearts (n=9) and wild-type siblings (n=6). (mean $\pm$ s.d., ns= not significant, unpaired t-test). (B) Immunofluorescent staining on 7dpi wildtype and *prrx1a*<sup>-/-</sup> heart sections using an anti-Mef2 antibody as a marker for cardiomyocyte nuclei, and an anti-PCNA antibody as a nuclear proliferation marker. Arrowheads in zoom-ins indicate proliferating cardiomyocytes. Scale bars represent 100 $\mu\text{m}$  in the overview images and 10 $\mu\text{m}$  in the zoom-ins. (C) Quantification of the percentage of (PCNA+) proliferating border zone cardiomyocytes shows no significant difference between *prrx1a*<sup>-/-</sup> hearts (n=7) and their wildtype siblings (n=8). (mean $\pm$ s.d., ns= not significant, unpaired t-test)

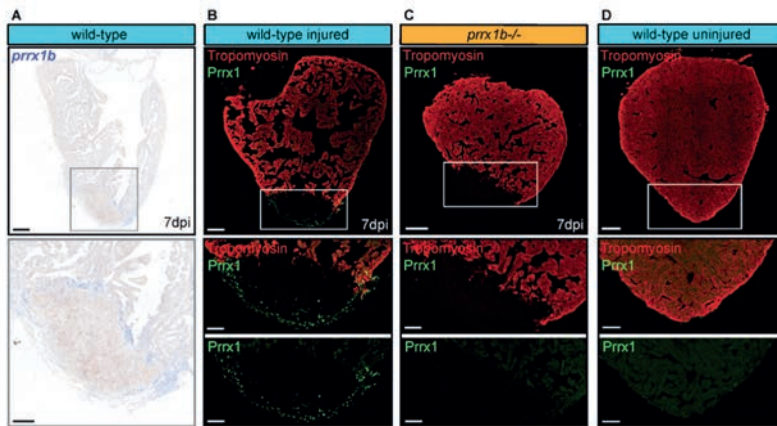


**Fig. S2 | Injured zebrafish hearts express Prrx1 in cells surrounding the injury area, which is severely reduced in the *prrx1b*<sup>-/-</sup> hearts.** (A) in situ hybridization for *prrx1b* on 7dpi wild-type hearts shows *prrx1b* mRNA surrounding and within the injury area. (B-D) Immunofluorescent staining of tropomyosin staining CM nuclei (red) and Prrx1 protein (green) in (B) injured wild-type hearts at 7dpi, (C) injured *prrx1b*<sup>-/-</sup> hearts at 7 dpi and (D) uninjured wildtype hearts. Scale bars represent 100 $\mu\text{m}$  in the overview images and 50 $\mu\text{m}$  in the zoom-ins. Hearts analyzed per condition: 3.

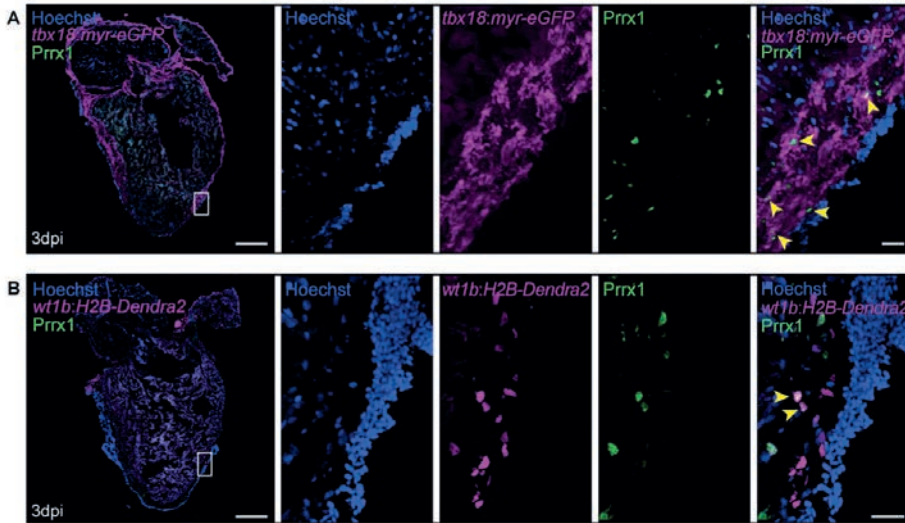


**Fig. S3 | Prrx1 is expressed in *tbx18*<sup>+</sup> and *wt1b*<sup>+</sup> epicardial cells.** (A) Immunofluorescent staining on a 3dpi Tg(*tbx18:myr-eGFP*) heart, staining Hoechst, *tbx18:myr eGFP* (membrane) and Prrx1 (nuclei). Arrowheads indicate double positive cells. (B) Immunofluorescent staining on a 3dpi Tg(*wt1b:H2B-Dendra2*) heart, staining Hoechst, *wt1b:H2BDendra2* (nuclei) and Prrx1 (nuclei). Arrowheads indicate double positive cells. Scale bars in the overview images represent 100um and in the zoom ins 20um.

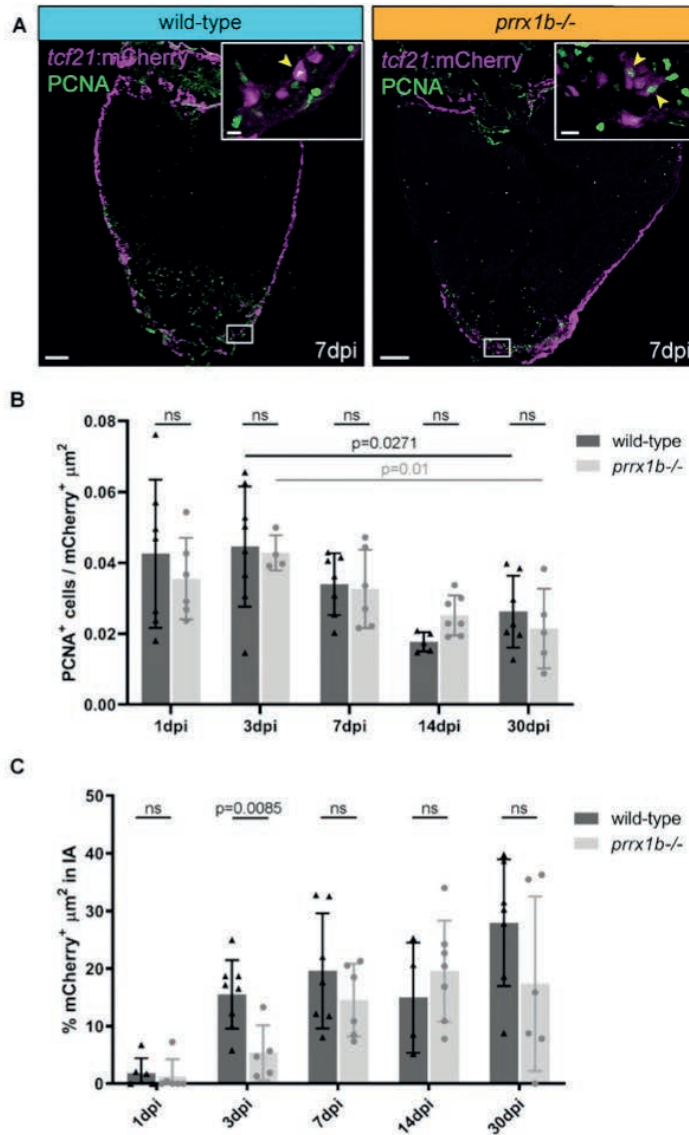


Fig. S4 | Quantification of invasion and proliferation of *tcf21:mCherry*<sup>+</sup> cells at 1, 3, 7, 14 and 30dpi in wild-type and *prrx1b*<sup>-/-</sup> hearts. (A) Immunofluorescent staining showing PCNA (green) and *tcf21:mCherry* (magenta) in wild-type sibling and *prrx1b*<sup>-/-</sup> hearts at 7dpi. Scalebar = 100μm, scale bar in zoom in = 10μm. (B) Proliferation of *tcf21:mCherry*<sup>+</sup> cells quantified as amount of PCNA<sup>+</sup> cells per total μm<sup>2</sup> of *tcf21:mCherry*<sup>+</sup> tissue surface in the ventricle at 1, 3, 7, 14 and 30dpi. (mean±s.d., wild-type 3dpi vs wild-type 30dpi p=0.0271, *prrx1b*<sup>-/-</sup> 3dpi vs *prrx1b*<sup>-/-</sup> 30dpi p=0.01, ns= not significant, unpaired t-test). (C) Percentage of the total injury *tcf21:mCherry*<sup>+</sup> μm<sup>2</sup> found inside the injury area at 1, 3, 7, 14 and 30dpi. (mean±s.d., wild-type 3dpi vs *prrx1b*<sup>-/-</sup> 3dpi p=0.0085, ns=not significant, unpaired t-test). IA = injury area.

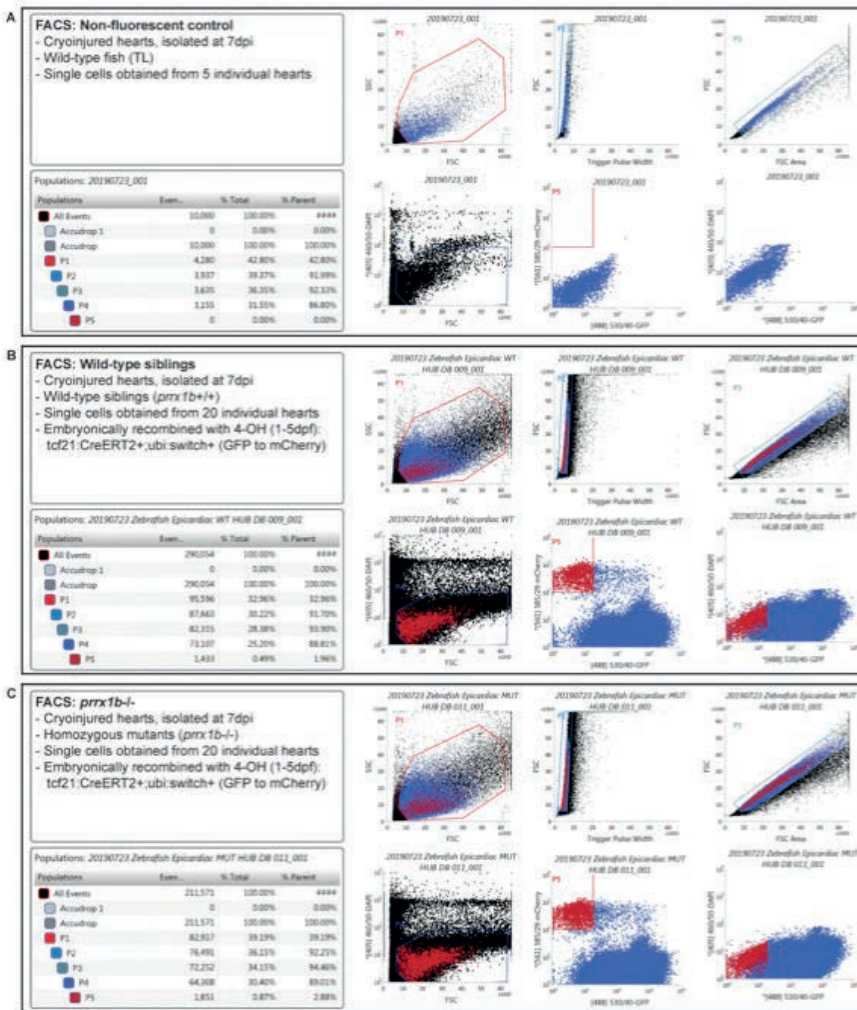


Fig. S5 | Gating details for FACS. (A-C) Gates (P1-P5) used to sort out mCherry<sup>+</sup>/GFP<sup>-</sup> cells used for single cell sequencing analysis.

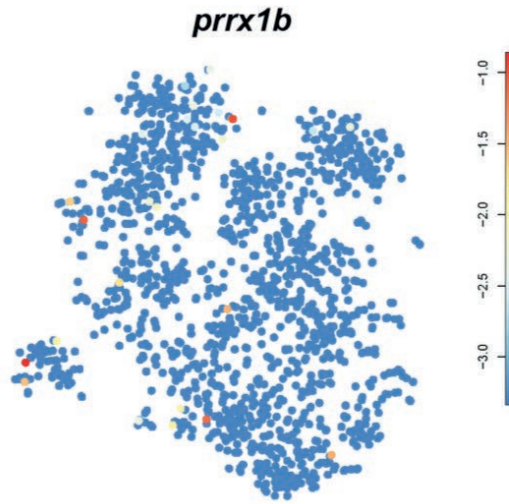


Fig. S6 | *prrx1b* read counts. tSNE map visualizing log<sub>2</sub>-transformed read-counts for *prrx1b* based on our scRNA sequencing of *tcf21:mCherry*<sup>+</sup> cells.

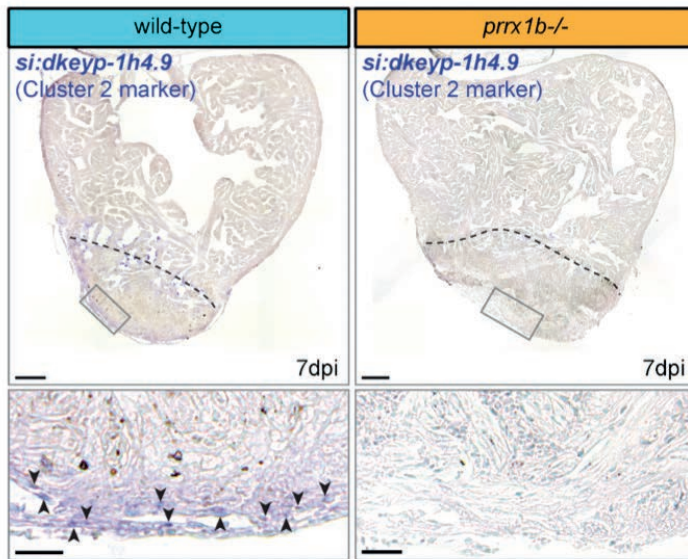
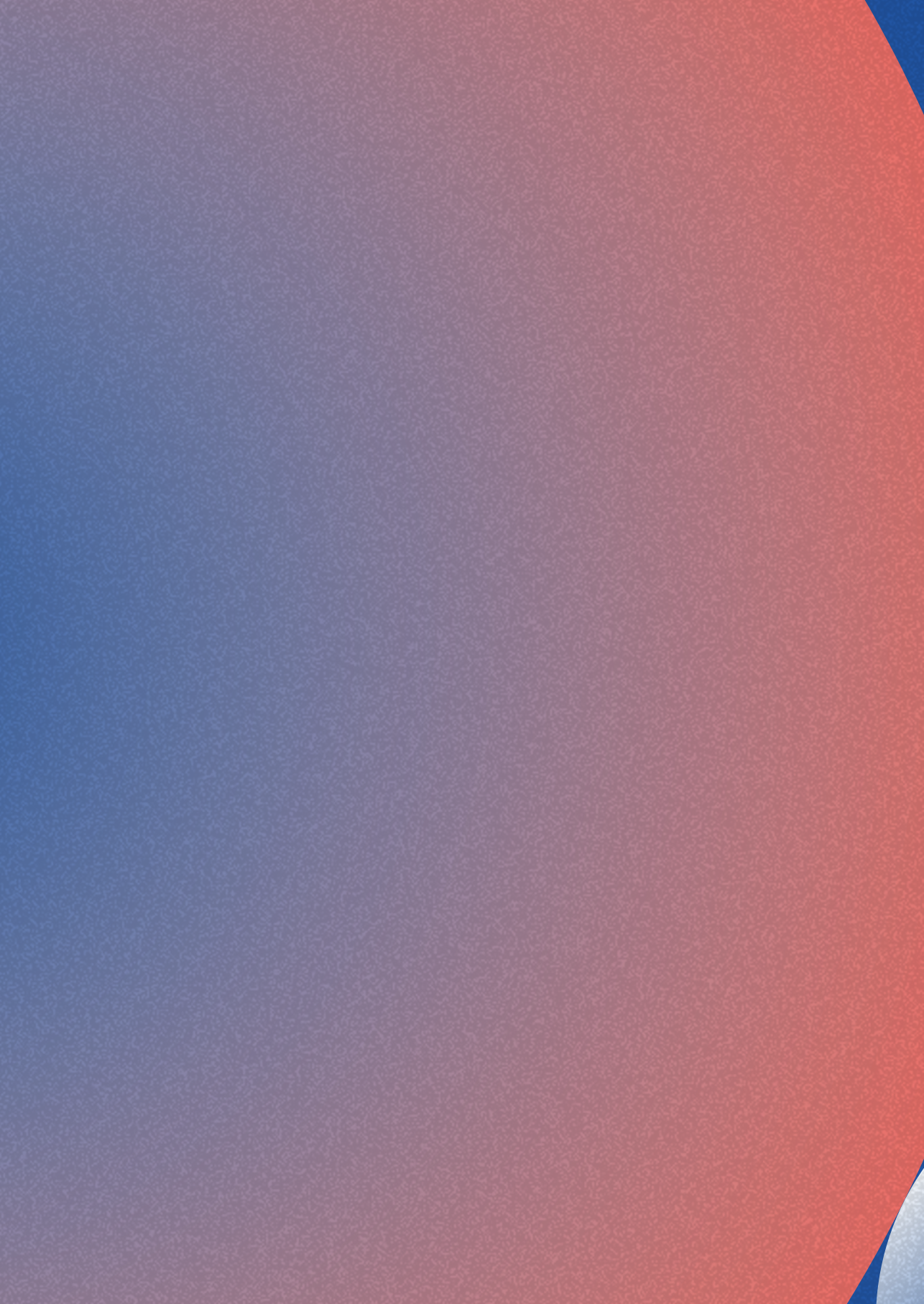


Fig. S7 | *prrx1b*<sup>-/-</sup> hearts show a strong reduction of *si:dkeyp-1h4.9* expression. (A,B) In situ hybridization for the cluster 2 gene *si:dkeyp-1h4.9* in either wild-type or *prrx1b*<sup>-/-</sup> hearts at 7dpi. Arrowheads point to cells with high expression. Scale bars represent 100µm in the overview images and 25µm in the zoom-in. Hearts analysed per condition: 3

**Table S1** (Differentially expressed genes for scRNAseq cluster identification), **Table S2** (Differentially expressed genes in multiple scRNAseq clusters) and **Table S3** (Gene Ontologies for differentially expressed genes in multiple scRNAseq clusters) are available online at <https://doi.org/10.1242/dev.198937>.







## Optimization of two self-adhering drug delivery patches to target the epicardium of the injured heart

Esther Dronkers<sup>1</sup>, Tessa van Herwaarden<sup>1</sup>, Maaïke JG Schotman<sup>2</sup>, Esmee Groeneveld<sup>1</sup>, Francesca Lauta<sup>1</sup>, Patricia YW Dankers<sup>2</sup>, Marie-Jose Goumans<sup>1</sup>, Anke M Smits<sup>1</sup>

<sup>1</sup>Department of Cell and Chemical Biology, Leiden University Medical Centre, Leiden, The Netherlands.

<sup>2</sup>Department of Biomedical Engineering, Eindhoven University of Technology, Eindhoven, The Netherlands.

## ABSTRACT

The heart has limited capacity to repair itself. The epicardium, the outer layer of the heart, is an interesting therapeutic target for restoring cardiac tissue. Compounds that activate epicardial cells have been identified. However, a biomaterial is required to secure temporal exposure of the epicardium to these compounds. Therefore, the aim of this study was to optimize a drug delivery patch to target the epicardium of the infarcted heart. We tested six potential epicardial patches. Of these six biomaterials, two hydrogel patches were selected based on the simplicity of the preparation procedure, the ability to provide sustained release for at least one week and the capacity of the patch to adhere to cardiac tissue. When testing these two epicardial patches in a mouse model for myocardial infarction, both patches demonstrated high adherence to cardiac tissue. In conclusion, we have optimized two epicardial patches that are feasible to use in *in vivo* mice experiments to target the epicardium.

## INTRODUCTION

As the heart has a limited potential to repair itself, the loss of myocardial tissue due to a myocardial infarction causes irreversible damage. Currently, a major goal in cardiac research is to identify therapeutic targets to restore cardiac tissue. One of these targets is the epicardium, the outer layer of the heart, which is a source for progenitor cells during cardiac development and repair. In order to participate in the cardiac tissue formation, epicardial epithelial to mesenchymal transition (epiMT) is an essential step. It is a process which allows cells to detach from the epicardial layer, invade underlying tissue, and contribute to multiple cardiac cell lineages (1). Therefore, epiMT has been studied extensively to identify targets to further enhance the contribution of the cell population to cardiac repair. Over time, multiple factors have been identified *in vitro* that activate epiMT, such as Activin (2) and TBBz (unpublished, chapter 4 of this thesis). Investigating the effect of these compounds on epiMT in *in vivo* models for myocardial infarction requires a method to administer the factor to the epicardium. Previous studies have shown that simply injecting a fluid into the myocardium leads to wash out of the fluid within a few contractions of the heart muscle (3). Given that epithelial to mesenchymal transition is also related to pathological conditions such as cancer and fibrosis, it is vital that an epiMT stimulating factor is locally applied and does not spread throughout the body. Furthermore, in mice, the epicardium is most active between 3-7 days after MI (4) and therefore the epiMT inducing factor should be available for at least one week to be fully effective. Because of the convenient location of the epicardium at the outside of the heart, it is possible to target these cells directly by applying a drug-loaded patch on top of the epicardial cells.

The aim of this study was to generate and optimize a drug releasing patch that can be applied on the outside of the injured heart to deliver factors to the epicardium. Ideally, the patch should meet the following demands. Firstly, the patch should adhere to the cardiac tissue, but not to the surrounding (lung) tissue, preferably through self-adhesive properties instead of previously described sutures. Secondly, the patch should release the factor over at least a week and both the patch and its derivatives should not be toxic to the surrounding tissue. Thirdly, to obtain feasible and reproducible results, it is essential that the patch can easily be prepared and that it is compatible with multiple factors (e.g. proteins, small molecules, viruses) and solvents (e.g. PBS and DMSO).

In this study, we describe the optimization of two epicardial patches that are easy to prepare, release a drug over time, adhere to cardiac tissue and are feasible to use in vivo studies in the infarcted mouse heart.

## MATERIALS AND METHODS

### *Cell culture*

Human primary epicardial cells were isolated and cultured as described (5). Briefly, cells were isolated from human heart auricles and cultured in a medium consisting of a mix of Dulbecco's modified Eagle's medium (DMEM low-glucose, Gibco) and Medium 199 (M199, Gibco) mixed in a 1:1 ratio, supplemented with 10% fetal bovine serum (heat inactivated for 25 minutes at 56 °C, Biowest), 100 U/mL penicillin (Roth) and 100 mg/mL streptomycin (Roth). Cells were cultured in the presence of 10 µM SB431542 (SB, Tocris) at 37 °C in 5% CO<sub>2</sub>. Experiments were performed in cell culture medium without SB.

HT1080 cells, stably transfected with a CAGA-luciferase reporter construct (6), were used as TGFβ reporter cell line. Cells were maintained in Dulbecco's modified Eagle's medium (DMEM high-glucose, Gibco) supplemented with 10% fetal bovine serum (Biowest), 100 U/mL penicillin (Roth) and 100 mg/mL streptomycin (Roth) at 37 °C in 5% CO<sub>2</sub>.

### *Preparation of UPy-catechol patch*

UPy-catechol was synthesized as described (7). The polymer was dissolved in 100 µl PBS and pH was adjusted with 1.25 µl 1N NaOH up to a pH of 8, while stirring at 50 °C for 15 minutes. When completely dissolved, 5 µl of TBBz (stock concentration of 10 mM in DMSO), or 5 µl of DMSO was added and mixed for 5 minutes at 50 °C. Subsequently, 15 µl of the hydrogel mixture was applied onto an electrospun supra-molecular mesh with a 5 mm diameter (as described (8)). Gelation was initiated by 2 drops of 0.75 µl sodium periodate, one directly applied onto the mesh and one on top of the hydrogel. The mesh and hydrogel were immediately applied onto the heart.

### *Preparation of TISSEEL patch*

For the TISSEEL patch, TBBz (10 mM in DMSO) was mixed with PBS in a 1:1 ratio. Subsequently, the TBBz/PBS solution was mixed with Thrombin solution (TISSEEL, Baxter) in a 1:1 ratio. To form the patch, 15 µl adhesion solution was pipetted on a piece of parafilm and 15 µl of the thrombin/compound mixture was pipetted into the droplet

of adhesion solution. The TISSEEL patch was cured for 5 minutes before application onto the heart. To secure proper adherence to the tissue, 4  $\mu$ l of adhesion solution was applied onto the heart and 4  $\mu$ l of thrombin solution was applied on the patch before administration.

### ***Release studies in vitro***

To study drug release from patches, patches were prepared and applied onto the upper side of a transwell insert (6.5 mm, 8.0  $\mu$ m Pore Polycarbonate Membrane Insert, Transwell, Corning). The insert was placed in a 24 wells plate well containing 500  $\mu$ l releasing medium. For experiments with epicardial cells, epicardial cell medium was used. For experiments with HT1080-CAGA cells, DMEM without FBS was used, which was supplemented with 1%BSA. BSA was added to prevent binding of TGF $\beta$  to the plate surface. After the indicated duration of 1 hour or 1 day, the transwell was moved to the next well containing 500  $\mu$ l fresh medium. This process was repeated every day up to the end of the experiment. Because of practical reasons, occasionally the medium was not refreshed daily which is indicated in the figure (e.g. 5-7 days). Releasing medium was collected and stored at -20 °C.

### ***TGF $\beta$ reporter assay***

Ht1080-CAGA cells were seeded in 24 wells plate with a density of 50.000 cells/well. After two days, cells were washed with PBS and exposed to releasing medium samples which were supplemented with TGF $\beta$  (1 ng/mL). After 6 hours incubation, cells were lysed in 50  $\mu$ l passive lysis buffer (Promega) and luciferase activity was measured using the Luciferase Assay System (Promega). Luciferase activity was normalized by total protein concentration of the samples, which was determined using the Pierce BCA Protein Assay Kit (Thermo Scientific).

### ***EpiMT assay***

Epicardial cells were seeded. When confluency reached 50%, cells were stimulated with releasing medium samples for 5 days.

### ***Mice pilot study and immunostaining***

All animal experiments were performed according to protocols approved by the animal welfare committee of the Leiden University Medical Center and conform the guidelines from Directive 2010/63/EU of the European Parliament on the protection of animals used for scientific purposes. Wt1CreERT2/+;R26RmTmG/+ mice, both male and female of 12-15 weeks old, were injected with 4x2 mg tamoxifen, two days before and two days after MI. MI was induced by permanent ligation of the left anterior

descending artery (LAD ligation) under isoflurane anesthesia, as described previously (9). Immediately after MI, the patch was applied onto the heart. All surgical procedures were performed by a blinded investigator. After 7 days, mice were sacrificed by cervical dislocation. Hearts were flushed by injecting 3 mL of PBS in the right ventricle and subsequently isolated and fixed in 4% PFA for 24 hours. Tissue was embedded in paraffin and sectioned in 6  $\mu$ m slices. Immunostaining was performed as described (10) using the following antibodies:  $\alpha$ -GFP (Abcam, ab13970),  $\alpha$ -Tropomyosin (Sigma-Aldrich, T9283) and  $\alpha$ -Wt1 (Abcam, ab89901)

## RESULTS

We defined a list of potential patch materials based on literature and on collaborative efforts (Table 1). We identified six materials that we considered to fulfill our criteria. We prepared the patches and established for each patch 1) the feasibility of the protocol, 2) the coherence of the patch, 3) their compatibility with multiple factors and solvents, such as DMSO and PBS, and 4) their adhesive abilities. We started by preparing the collagen patch described by Wei et al. (11) but due to technical issues we were not able to fully repeat their protocol and produce a proper biomaterial to be used as a patch. Next, we tested Pluronic F-127 polymer, which can form a gel-like structure and is very easy to work with. Unfortunately, it did not result in a coherent patch that can be handled with forceps. Then, we tested an electrospun mesh developed by Putti et al. (8) which consists of a sheet of electrospun fibers generating a layer of randomly aligned thin threads appearing like soft woven cloth. The core of this thread contains the factor of interest, which is encapsulated in a hydrophilic shell of ureido-pyrimidinones poly(ethylene glycol) (UPy-PEG) that regulates its release. The mesh is very easy to handle, and because of its flexible characteristics it can cover the heart without interfering with contraction. One disadvantage of the spinning procedure is that only small molecules can be incorporated in this patch. In addition, the patch is not adhesive and will need a suture or glue to apply it to the outside of the heart. The TachoSil patch is a bilayered sponge that is used in surgeries to stop local bleeding. This material has been exploited as an epicardial patch before (12). The TachoSil patch is ordered as a dry material, consisting of a collagen layer at the outside that serves as a mechanical carrier for the inner lining of thrombin and fibrinogen that requires activation with fluid (e.g. blood or PBS). In theory, the application of a solution containing the factor of interest will cause the thrombin and fibrinogen to form an adhesive layer thereby incorporating the compound. This approach is highly robust and very easy to execute. Moreover, the collagen layer,

on the outside of the patch protects the thoracic organs. We combined the excellent release capacities of the supramolecular UPy-PEG hydrogel with that of the TachoSil. Unfortunately, the application of the UPy-PEG hydrogel massively impaired the adhesive capabilities of the patch and using this combined patch in an in vivo experiment therefore would require stitches or glue. TISSEEL is a tissue glue which is routinely used in the clinic. It has previously been described for atrial epicardial application for encapsulating viruses (13) and cells (14). TISSEEL is a two-compound glue consisting of an adhesion solution and a thrombin solution that require mixing, after which solidification occurs resulting in a patch that can easily be picked up using forceps. To add releasing properties to this glue, the factor of interest can be mixed in either the adhesion solution or the thrombin solution which subsequently forms a hydrogel patch upon combining the solutions. The patch can be prepared ex vivo, according to a straight-forward protocol and produces a coherent patch. We were able to mix the TISSEEL with adenoviruses, conditioned medium, PBS and DMSO, although the latter did have some effect on the structure of the patch. Because the ex vivo prepared TISSEEL patch once gelified is not adherent, it will not stick to the surrounding tissue, but also not to the heart. To facilitate this, a fresh drop of liquid TISSEEL was applied directly on to the heart and on the basis of the drug-loaded patch which allowed firm adhesion onto the outside of the heart. Lastly, we tested a UPy-catechol patch, which is based on a synthetic UPy-PEG hydrogel which has been functionalized with a catechol group that provides strong binding in wet environments (7). To be able to apply the hydrogel to the heart and to protect surrounding tissue, the hydrogel was prepared on an electrospun mesh made of UPy fibers. The mesh allows for application of the patch onto the heart, and provides a shield between the patch and surrounding tissue and allows for unidirectional release, e.g. towards the heart. The preparation of the patch is more elaborate than the TISSEEL patch, but still straightforward. The UPy-catechol preparation includes a final step where the hydrogel mixture requires to be maintained at 50 °C to prevent premature gelification. This means that the factor of interest that is mixed into the biomaterial should keep its functionality at this temperature. Furthermore, the catechol groups can bind to the included factor (e.g. to TGF $\beta$ ) thereby preventing its release and limiting wide use of this patch. However, the adhesiveness of this patch is outstanding and the best that we have observed in this study. In summary, all patches we have tested in this study have strong and weak points summarized in Table 1. We continued our experiments with the two most promising patches, the TISSEEL patch and the UPy-Catechol patch.

**Table 1 Overview of tested patches**

	Feasibility protocol	Coherent patch	Compatibility with factors/solvents	Adherence to heart tissue	Timed release	Biocompatible	Unidirectional release
Collagen (Wei et al.)	-	-	NA	NA	NA	NA	NA
Pluronic gel	-	-	NA	NA	NA	NA	NA
Electrospun patch	+	+++	+/-	-	NA	+	+/-
Tachosil (+UPy-PEG hydrogel)	++	+++	+	+/-	NA	+	+/-
TISSEEL patch	++	++	++	++	++	++	-
UPy-catechol patch	++	+++	+	+++	++	+/-	+

Next we determined if these two patches were effective drug release materials by performing *in vitro* experiments to assess the release profile. We prepared patches containing DMSO (control) or the ALK4/5/7 kinase inhibitor SB431542 (SB), placed them in transwells and determined the release of compound over time into the cell culture medium (Fig. 1A). The medium was collected after 1 hour, refreshed and subsequently collected daily. To establish the release of SB, TGF $\beta$  reporter cells (HT1080-CAGA luciferase cells) were stimulated with TGF $\beta$  combined with the collected medium. Release of SB from the material into the medium would inhibit the TGF $\beta$  induced CAGA reporter activity. Quantification of the luciferase activity demonstrated the release of SB for at least 8 days (Fig. 1B) for both the TISSEEL and the UPy-catechol patch since patches containing SB demonstrate a lower luciferase response along the total timeline compared to the DMSO patches. Interestingly we also prepared a TISSEEL patch containing TGF $\beta$ , and using the same assay demonstrated release of this growth factor at a similar level of luciferase activity as the positive control (ctrl medium + TGF $\beta$ ). The UPy-catechol patch is not compatible with TGF $\beta$  and was therefore not tested. In summary, both patches serve as a drug releasing system for at least a week *in vitro*.

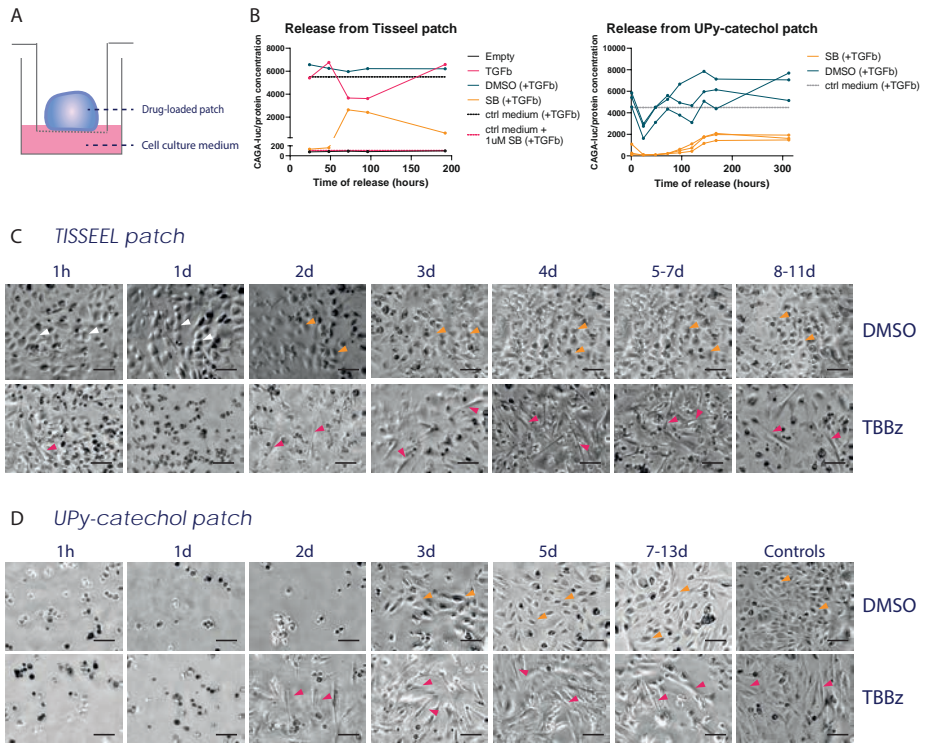


**Fig. 1 | TISSEEL and UPy-catechol patch release SB and TBBz for at least 7 days in vitro.** (A) Schematic overview of set-up to obtain releasing medium. (B) Temporal release of TGF $\beta$  and SB from patches measured by CAGA-activity. Release was evaluated by the ability of the released TGF $\beta$  to initiate CAGA-luciferase response (only for the TISSEEL patch (n=1)) compared to the response of an empty patch and the ability of the released SB to inhibit the TGF $\beta$  induced CAGA-luciferase response (TISSEEL (n=1), UPy-catechol (n=3)) compared to a DMSO loaded patch. As controls for the luciferase assay, medium supplemented with TGF $\beta$  and medium supplemented with TGF $\beta$ +SB were included. (C) and (D) Temporal release of TBBz from the patches measured by an epiMT assay. Release was evaluated by the morphology of epicardial cells, indicating epiMT. Orange arrows indicate examples of epithelial cells while pink arrows indicate examples of mesenchymal cells. Scale bar: 100  $\mu$ m.

The next step was to determine if there was release of an epiMT inducing compound, TBBz (unpublished, chapter 4 of this thesis), and if it retained its activity. Therefore, we generated TBBz-containing patches and used the same transwell set-up to collect media of DMSO (control) and TBBz patches. To study epiMT, human primary epicardial cells were exposed to the collected media. For both the TISSEEL and the UPy-catechol TBBz patches, the collected medium of the first hour and day were toxic to the cells (Fig. 1C and 1D) indicating a burst of release of TBBz resulting in toxic levels. The

medium collected from the control UPy-catechol DMSO patch was also toxic during the first two days. However, after this initial toxic burst, the TBBz medium derived from both patches clearly induced a morphological change in the epicardial cells that indicated epiMT at all measured time points (Fig. 1C and 1D). Interestingly, for both patches, this effect lasted for more than 7 days.

To test the feasibility of preparing and handling these patches for *in vivo* application in experimentally induced myocardial infarction (MI), we performed a pilot experiment using *Wt1CreERT2/+;Rosa26mTmG* mice that express GFP in epicardial (*Wt1+*) cells once tamoxifen is administered (Fig. 2A). This lineage tracing approach allows for studying epicardial behavior. To induce MI, mice were subjected to a left anterior descending coronary artery (LAD) ligation, causing major cell death in downstream tissue. Directly after the LAD ligation, the patches containing DMSO or TBBz were applied to the outside of the heart (Fig. 2B and 2D).

While performing these *in vivo* mouse experiments, we observed that the time needed to prepare the TISSEEL patch is very short and the protocol is robust, as temperature management and timing are flexible. However, the TISSEEL patch leaves behind some of the fluid after preparation indicating that not all the compound may be incorporated. The procedure to prepare the UPy-catechol patch is a little more sensitive to error but once applied, this patch is highly adhesive. Furthermore, the hydrogel sometimes got scraped from the electrospun patch when moving the patch along the ribs to apply it to the outside of the heart.

Seven days after application of the patch, the mice were sacrificed, hearts were collected and embedded in paraffin for further analysis. Immunofluorescent analysis demonstrated that both patches could be easily identified and were located on top of the infarcted area (Fig. 2C and 2E). We observed that the GFP-labeled epicardial cells were still present underneath the patches, and found mainly around the edges of the patch (Fig. 2C''' and 2E'''). For the TISSEEL patch, we did not observe any sign of toxicity, e.g. disintegrated nuclei or a large influx of immune cells. Underneath the UPy-catechol patch, some unidentified structures were observed in 2 out of 4 hearts (Fig. S1A). To conclude, the TISSEEL and UPy-catechol patch can readily be prepared and subsequently applied *in vivo*. Moreover, both patches demonstrated sufficient adherence and were easily located afterwards.

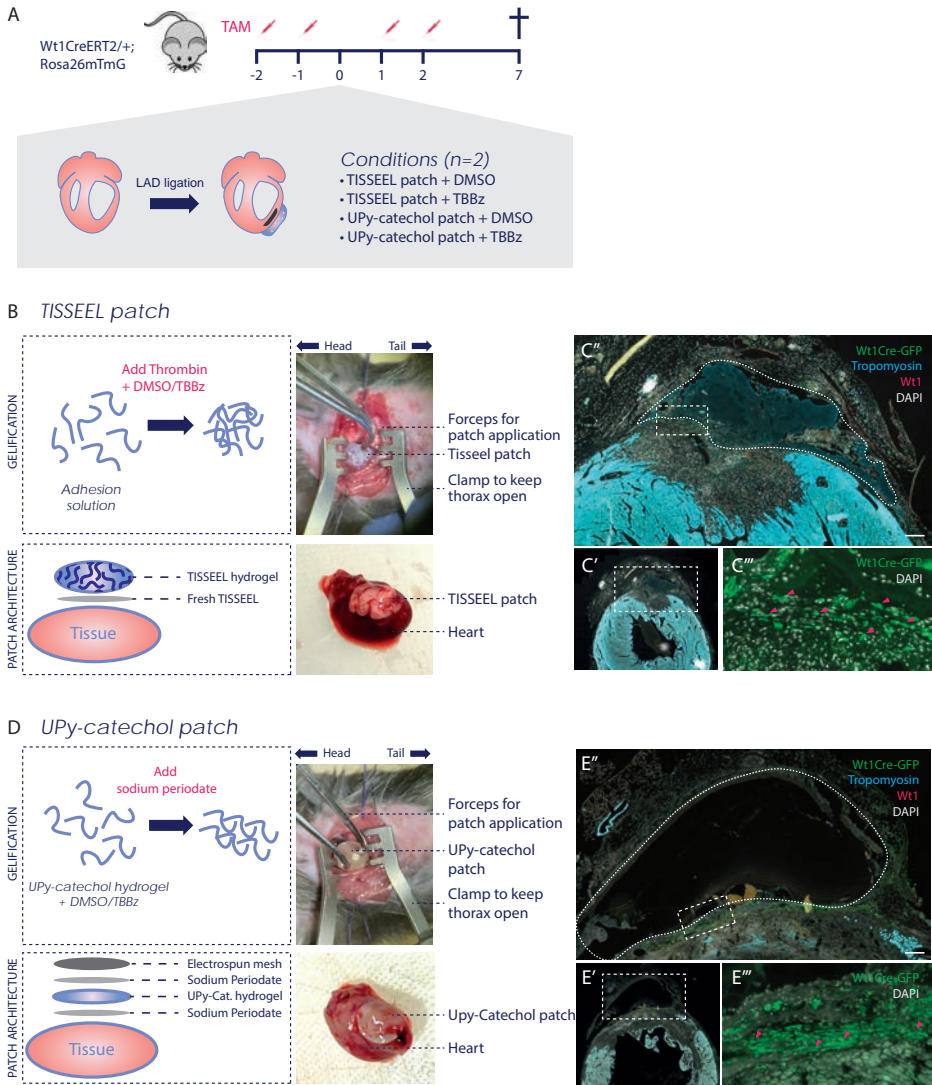


**Fig. 2 | TISSEEL and UPy-catechol patch are feasible to use in vivo study.** (A) Schematic overview of study design of mouse study. (B) Schematic overview of preparation of the TISSEEL patch. Thrombin solution was mixed with the compound and combined with adhesion solution to form a patch. The patch was applied onto the heart with a drop of fresh TISSEEL. (C) Immunostaining with antibodies against Wt1Cre-GFP, Tropomyosin and Wt1 in the infarcted mouse heart treated with a TISSEEL patch. C' shows a magnification of the TISSEEL patch on top of the infarcted area, highlighted by a dotted line. Scale bar: 200  $\mu$ m. C'' demonstrates the epicardial Wt1Cre-GFP cells underneath the patch. (D) Schematic overview of preparation of the UPy-catechol patch. UPy-catechol hydrogel was mixed with the compound. A droplet of sodium

periodate was applied onto a 5 mm electrospun mesh. Subsequently, the hydrogel was applied and another droplet of sodium periodate to initiate gelification. The total of mesh and hydrogel was directly applied onto the heart. (E) Immunostaining with antibodies against Wt1Cre-GFP, Tropomyosin and Wt1 in the infarcted mouse heart treated with a UPy-catechol patch. E' shows a magnification of the UPy-catechol patch on top of the infarcted area, highlighted by a dotted line. Scale bar: 200  $\mu\text{m}$ . E'' demonstrates the epicardial Wt1Cre-GFP cells underneath the patch.

## DISCUSSION

In this study, we identified and optimized two self-adhering drug-eluting hydrogel patches and demonstrated 1) easy and robust protocols that gave rise to patches with 2) a sustained release of compounds *in vitro* for at least 7 days, and 3) adherence to the beating mouse heart *in vivo*.

Using biomaterials to repair the heart is a fast-emerging research field aiming to support the heart in its reparative response, and to deliver drugs or cells to the myocardium (15). In this study, we aimed to place a patch to the outside of the heart to target the epicardium. For this, it is essential that the epicardium itself is not harmed during the procedure, which is more likely when using stitches or aggressive glue. Therefore we explored different self-adhering patch materials. Although several epicardial patches have been described (15), we were aiming for a simple procedure that would not require complicated methods or specific equipment which is undesirable during a mouse experiment. After compiling a list of patch materials to deliver drugs to the epicardium, we identified two highly promising patches in which we observed gradual release over time of the incorporated factor *in vitro* and a strong adherence to mouse hearts *in vivo*.

The main difference between the two patches is their nature, the TISSEEL being a natural hydrogel and UPy-catechol being a synthetic one. TISSEEL is based on the coagulation system and consists of a mixture of sealer protein solution (fibrinogen and aprotinin) and thrombin solution (human thrombin and calcium chloride dihydrate). Upon mixing these two solutions, a sealant is formed that is used in patients to stop internal bleeding. Besides its clinical use, this hydrogel has been used before to deliver AAVs to the atria in rats (13), and as engineered tissue construct to support the infarcted mouse heart with cardiac adipose tissue-derived progenitor cells (14). This shows the all-round applicability of this hydrogel and it also demonstrates that the protocol is robust in multiple laboratories. Similarly, we observed that the TISSEEL protocol is highly straight forward. The main disadvantage of the TISSEEL patch is its

poor tolerance for DMSO, demonstrated by fluid that was left after picking up the patch, showing that not all the liquid was incorporated in the patch. In general, we found that all hydrogels displayed significant structural changes upon mixing with DMSO. We therefore aimed to keep the DMSO concentrations as low as possible and attempt to use other solvents when applicable.

Ureido-pyrimidinone (UPy) is a synthetic supramolecular hydrogel: a group of materials that consists of polymers that are cross linked by non-covalent interactions. Supramolecular materials are tunable and considered to mimic the biological environment. The UPy hydrogel used in this study was functionalized with catechol groups to introduce adhesiveness, inspired by mussels that demonstrate exceptional adhesiveness under wet conditions (7). In our current set-up we used an electrospun mesh as a carrier of the gel, allowing for easy handling. This electrospun mesh can also be modified. This creates a window of opportunity, e.g. when applying an impermeable mesh that allows for unidirectional release of the hydrogel towards the epicardium. Similar to the TISSEEL patch, a small difference was observed between the addition of DMSO or PBS to the hydrogel. We observed that the structure of the hydrogel is different on a microscopic level in PBS patches compared to DMSO patches (Fig. S1B-C), validating our observation that DMSO intervenes with the patch structure during the formulation. However, except for the fact that the gelification appeared to be a little weaker with DMSO compared to PBS patches, we did not find any functional differences, both patches adhered well onto the heart *in vivo*.

In this study, the data regarding the biocompatibility of this patch was inconclusive. *In vitro*, release during the first 48 hours was highly toxic to the cells, indicating either a burst release of DMSO (we expect this amount of cell death in a concentration higher than 2%) or a toxic effect of the degraded hydrogel. Comparing an empty UPy-catechol patch with a DMSO loaded patch will provide insight in the origin of the toxicity. *In vivo*, we observed some unidentified structures beneath the patch. Further examination of the structures should reveal if this is a sign of any harmful events (e.g. excessive immune influx or toxicity). Potential toxicity may be reduced by using a replacement for sodium periodate to initiate gelification of the hydrogel.

In conclusion, the TISSEEL patch is most widely applicable for epicardial application due to its tolerance for all types of compounds, and its robust and easy preparation. The UPy-catechol patch requires a more elaborate protocol but can be fully adjusted to one's needs and shows the best adhesiveness. Which patch should be used depends on the requirements of the specific application. Here, we have used both

patches to study the effect of small molecules on epiMT. The numbers in this study are not sufficient to compare the effect of the two patches. However, we demonstrated the feasibility of the experiment. In addition to this, one could think of other applications such as viral knock down or overexpression to study a specific pathway or mix cell specific conditioned medium into the patch.

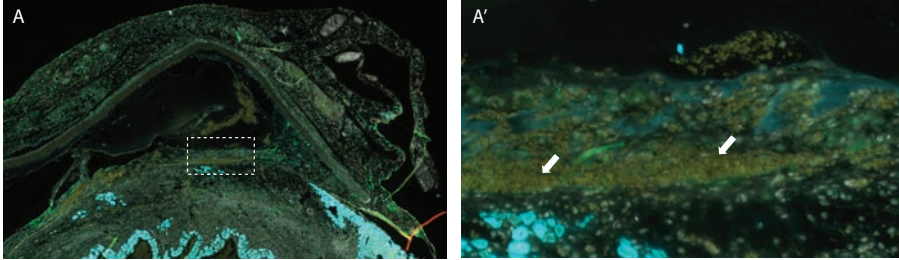
## REFERENCES

1. Smits AM, Dronkers E, Goumans M-JJ. The epicardium as a source of multipotent adult cardiac progenitor cells: Their origin, role and fate. *Pharmacol Res.* 2018 Jan 24 [cited 2017 Sep 4];127:129–40.
2. Dronkers E, van Herwaarden T, van Brakel TJ, Sanchez-Duffhues G, Goumans M-J, Smits AM. Activin A and ALK4 Identified as Novel Regulators of Epithelial to Mesenchymal Transition (EMT) in Human Epicardial Cells. *Front Cell Dev Biol.* 2021 Dec 16;9.
3. van den Akker F, Feyen DAM, van den Hoogen P, van Laake LW, van Eeuwijk ECM, Hoefler I, et al. Intramyocardial stem cell injection: go(ne) with the flow. *Eur Heart J.* 2016 Feb 24;ehw056.
4. van Wijk B, Gunst QD, Moorman AFM, van den Hoff MJB. Cardiac regeneration from activated epicardium. *PLoS One.* 2012;7(9):e44692.
5. Dronkers E, Moerkamp AT, van Herwaarden T, Goumans M-J, Smits AM. The Isolation and Culture of Primary Epicardial Cells Derived from Human Adult and Fetal Heart Specimens. *J Vis Exp.* 2018 Apr 24;134:e57370.
6. Dennler S. Direct binding of Smad3 and Smad4 to critical TGFbeta<sup>-</sup>inducible elements in the promoter of human plasminogen activator inhibitor-type 1 gene. *EMBO J.* 1998 Jun 1;17(11):3091–100.
7. Spaans S, Fransens PPKH, Ippel BD, de Bont DFA, Keizer HM, Bax NAM, et al. Supramolecular surface functionalization via catechols for the improvement of cell–material interactions. *Biomater Sci.* 2017;5(8):1541–8.
8. Putti M, Mes T, Huang J, Bosman AW, Dankers PYW. Multi-component supramolecular fibers with elastomeric properties and controlled drug release. *Biomater Sci.* 2020;8(1):163–73.
9. van Laake LW, Passier R, Monshouwer-Kloots J, Nederhoff MG, Ward-van Oostwaard D, Field LJ, et al. Monitoring of cell therapy and assessment of cardiac function using magnetic resonance imaging in a mouse model of myocardial infarction. *Nat Protoc.* 2007 Oct 11;2(10):2551–67.
10. Kruithof BPT, Paardekooper L, Hiemstra YL, Goumans M-J, Palmén M, Delgado V, et al. Stress-induced remodelling of the mitral valve: a model for leaflet thickening and superimposed tissue formation in mitral valve disease. *Cardiovasc Res.* 2020 Sep 8 [cited 2020 Jun 24];116:931–43.
11. Wei K, Serpooshan V, Hurtado C, Diez-Cuñado M, Zhao M, Maruyama S, et al. Epicardial FSTL1 reconstitution regenerates the adult mammalian heart. *Nature.* 2015 Sep 16 [cited 2016 Oct 7];525(7570):479–85.
12. Kobayashi K, Ichihara Y, Sato N, Umeda N, Fields L, Fukumitsu M, et al. On-site fabrication of Bi-layered adhesive mesenchymal stromal cell-dressings for the treatment of heart failure. *Biomaterials.* 2019 Jul;209:41–53.
13. Nyns ECA, Poelma RH, Volkers L, Plomp JJ, Bart CI, Kip AM, et al. An automated hybrid bioelectronic system for autogenous restoration of sinus rhythm in atrial fibrillation. *Sci Transl Med.* 2019 Feb 27;11(481).

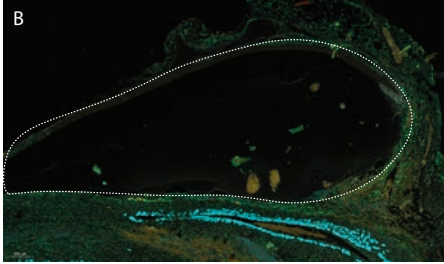
14. Lluçia-Valldeperas A, Soler-Botija C, Gálvez-Montón C, Roura S, Prat-Vidal C, Perea-Gil I, et al. Electromechanical Conditioning of Adult Progenitor Cells Improves Recovery of Cardiac Function After Myocardial Infarction. *Stem Cells Transl Med.* 2017 Mar 1;6(3):970–81.
15. Chang T, Liu C, Lu K, Wu Y, Xu M, Yu Q, et al. Biomaterials based cardiac patches for the treatment of myocardial infarction. *J Mater Sci Technol.* 2021 Dec;94:77–89.

## SUPPLEMENTAL FIGURES

*UPy-catechol + DMSO*



*UPy-catechol + DMSO (n=2)*



*UPy-catechol + PBS (n=1)*

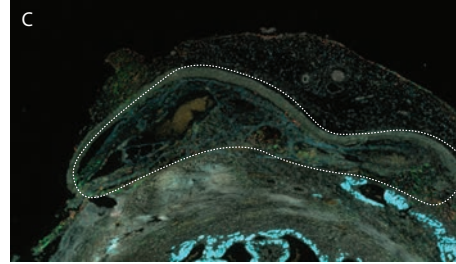
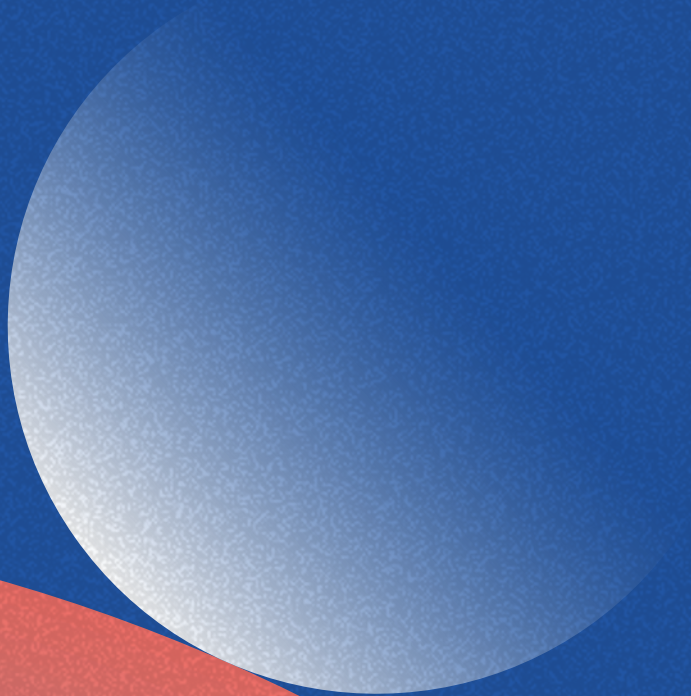


**Fig. S1 | Observations of UPy-catechol patch in infarcted mouse heart.** (A) Infarcted mouse heart treated with a UPy-catechol patch with DMSO. In the magnification in A', arrows point to unidentified structures below the patch, that may indicate toxicity. (B) Infarcted mouse heart treated with a UPy-catechol patch with DMSO. The patch is highlighted by a dotted line. (C) Infarcted mouse heart treated with a UPy-catechol patch with PBS. The patch is highlighted by a dotted line.



# 9

Discussion





## REGENERATION IS NOT AN EASY TASK

Each year 34.000 patients are hospitalized in the Netherlands because of a myocardial infarction (1). The inability of cardiac tissue to regenerate causes these patients to suffer from a dysfunctional heart which can ultimately progress into fatal heart failure. Regenerating the mammalian heart has therefore been a dynamic research area over the past decades, characterized by trial and error. The first decade of this century was dominated by research into adult stem cells, that reside in the bone marrow or in the heart itself. The ultimate goal was to show that these cells are capable of differentiating into cardiomyocytes after transplanting the cells into the heart. After 20 years of research, we now know that although it may be possible to generate cardiac cells out of adult stem cells, the numbers are most likely not clinically relevant (2). The initial success of stem cell injections has been attributed to stem cell derived paracrine factors but may be predominantly due to activation of the innate immune response, as transplantation of dead cells generates comparable beneficial effects to living cells (3). The extensive research into adult stem cells revealed the main hick ups of cardiac regeneration: 1) there is no adult cardiac stem cell that can replenish cardiomyocytes in the injured heart (4), 2) also failing angiogenesis (5) and dysregulated inflammatory responses (6) play an essential role in the limited regenerative response of the heart, and 3) it is particularly difficult to administer any solution containing cells into a heart without it being flushed out in one heartbeat (7). Although we now realize that simply delivering stem cells into the heart does not regenerate the tissue, the research did provide a lot of knowledge where to start. The focus of the research field steered towards stimulation of endogenous mechanisms to initiate cardiac tissue formation, and biomaterials to deliver cells and factors to the heart without washout. The epicardium is such an endogenous source of progenitor cells that can participate in myocardial growth and the formation of proper vasculature.

## IMPORTANCE OF EPIMT

In all regenerative processes there is a similar sequence of events. It starts with an inflammatory phase, aiming at clearing all dead cells by macrophages and neutrophils. This is followed by a proliferative phase, in which fibroblasts provide support by producing matrix. Finally, remodelling of the scar region takes place. In the mammalian heart, this remodelling results in cardiac fibrosis. However, in some animal species, such as the zebrafish, remodelling can lead to regeneration. This final regenerative process often mimics the development of the organ (8). In this regard, the epicardium

is of interest as it plays a major role in cardiac development (reviewed in Chapter 2). As such, enhancing recapitulation of embryonic epicardial behaviour could be a target for therapeutic intervention for the injured heart. One of the main features of epicardial cells is their plastic phenotype, allowing them to switch from being an epithelial cell on the outside of the heart to becoming a motile mesenchymal cell – a process called epithelial to mesenchymal transition (epiMT). We hypothesized that epiMT is an essential step for induction of the beneficial effects that the epicardium exerts on the developing myocardium. This is based on the fact that the foetal epicardial cells, which are actively involved in tissue formation, are much more prone to undergo epiMT *in vitro* than the less active adult cells (9). In addition, recent papers exploited single cell sequencing to describe the trajectory of epiMT in the developing heart (10–12), showing that epiMT must be completed before cells can start to differentiate and fate specification can take place. This suggests that epiMT is an essential first step in the epicardial contribution to the heart. Moreover, one of the rare studies comparing pre- and post-EMT epicardial cells performed by Quijada et al. found that epiMT is vital for maturation of the vasculature and fate specification of the endothelial cells during development (13). These studies all point to a vital role for epiMT in tissue development which may serve as a blueprint for enhancing tissue formation in the injured adult heart. Besides a potential role in repair, dysregulated epiMT has been described as a driving factor in fibrosis and fibro-fatty remodelling of the myocardium leading to atrial fibrillation (14–16) and arrhythmogenic cardiomyopathy (17). The fact that epiMT is a fundamental process in epicardial behaviour in disease and repair demonstrates that understanding its regulation is essential in the identification of cardiac therapies.

## REGULATION OF EPIMT

The regulation of epiMT has been studied extensively, revealing that the main regulatory pathways are TGF $\beta$ , PDGF, FGF and Wnt signalling. Over the years, more detailed studies have shown that Retinoic acid, WT1, and TCF21 are important downstream players of epiMT regulation (reviewed in (18)). Additionally, an array of factors has been identified that intervene with these pathways, for example, the extracellular matrix (ECM) component Agrin was identified as an epiMT regulator that signals via  $\beta$ -catenin and WT1 (19), and hypoxia was demonstrated to stimulate epiMT by increasing TGF $\beta$  expression levels (20). All epiMT inducers have in common that they activate at least one of the so called EMT-transcription factors (EMT-TFs), which are SNAIL, SLUG, ZEB1, ZEB2, or TWIST. These factors are essential in the orchestration of

epiMT by repressing epithelial characteristics, such as the downregulation of E-cadherin, and inducing mesenchymal features.

In our cell culture model, we have shown multiple times that TGF $\beta$  robustly induces epiMT. However, the pleiotropic nature of this signalling pathway, including its role in the development of severe fibrosis, makes it a less desirable target for therapeutic purposes. Therefore, we aimed at finding other epiMT inducers. In this thesis we describe the identification of three novel inducers of epiMT: Activin/ALK4 signalling, TBBz, and Oltipraz Metabolite M2 (M2). Activin/ALK4 was identified based on analysis of TGF $\beta$  related pathways in our bi-directional cell culture system allowing us to identify both stimulators and inhibitors of epiMT. TBBz and M2 were identified in a phenotypic small molecule screen using the human adult epicardial cells. Of all the epiMT inducers that passed by during the course of these experiments, we could not identify one common pathway that would explain the induction of epiMT for all of them. Only Activin/ALK4 is related to a well-known epiMT inducer, which is TGF $\beta$ . Because of this, we expected Activin to induce epiMT via TGF $\beta$  or TGF $\beta$ -associated signalling. However, although we found that ALK4-induced epiMT results in activation of SNAIL, similar to the downstream effect of TGF $\beta$ , the effects of Activin/ALK4 are TGF $\beta$  independent. The question that remains is how the downstream signalling is conveyed after ALK4 activation. Because of the lack of  $\alpha$ SMA upregulation, it is to be expected that Activin/ALK4 induced epiMT follows a path different from TGF $\beta$ . Therefore, we assume that a SMAD-independent pathway is activated, resulting in the activation of SNAIL, leading to epiMT. For the other epiMT inducers, TBBz and M2, it was less clear via which pathway they induce epiMT. TBBz is labelled as a CK2 inhibitor and M2 as LXR $\alpha$  inhibitor. Based on our sequencing data, we anticipate that M2 induces epiMT via expression of FOXQ1 which is a TGF $\beta$ -related transcription factor (21) and may therefore be indirectly involved in TGF $\beta$  signalling. This was difficult to assess since a combination of M2 and SB was toxic to the cells. Regarding TBBz, although it is labelled as specific inhibitor of CK2, we could not find any effect on CK2 activity in our cell culture model. We revealed that TBBz induces epiMT most likely indirectly via epigenetic changes, which lead to histone methylation modifications that ultimately result in induction of SLUG. This is in line with a recent publication that the epicardial cells undergo major changes in the chromatin accessibility upon activation in zebrafish hearts (22). Interestingly, Activin and TGF $\beta$  both induce SNAIL, while TBBz and M2 act via SLUG which demonstrates that a distinct set of transcription factors is involved. This shows that TBBz and M2 do not elicit epiMT by indirect activation of TGF $\beta$  signalling but suggest that different pathways are involved. Future research into the exact epigenetic mechanisms should reveal the detailed mechanisms and

may also provide options to use other histone modifiers that may be less toxic to cells than TBBz.

A general remark that can be made regarding research using stimulants and inhibitors is that it is very tricky to claim that a molecule has a specific target. Often, it is known what the intended target of a molecule is, but it is difficult to exclude any off-target effects. To deal with these inconsistencies, we used multiple approaches to identify the actual targets of our compounds. In case of TBBz, labelled as a specific CK2 inhibitor that is elaborately studied, we found no clear effect on the predicted target. We measured the effect of TBBz on CK2 activity and compared its effect with other CK2 inhibitors. Additionally, we performed RNA sequencing as an unbiased attempt to identify its direct target, pointing to a role for TBBz in histone modification. Although a specific targets of TBBz have been described (23), to our knowledge, the role of TBBz in histone methylation has not been described before warranting further investigations into the mechanism. Regarding SB431542 (SB), it is known that it blocks the kinase activity of ALK4, 5, and 7 but it is most often referred to as a TGF $\beta$  blocker or an ALK5 inhibitor. This 'mislabelling' of the inhibitor in scientific literature probably caused the role of ALK4 in epiMT to be neglected. For SB, we have tried to selectively demonstrate the role of ALK5 and ALK4 in epicardial cells using siRNAs, but these experiments were hampered by technical difficulties. Therefore, we chose to use specific ligand-receptor inhibitors, FST for ALK4 and TGF $\beta$  capture antibody for ALK5, to study the specific role of ALK4 in epiMT. To conclude, the described mode of action of a compound can only serve as a starting point for studying its mechanism. Accurate and thorough reporting of compound effects could help to smoothen this search.

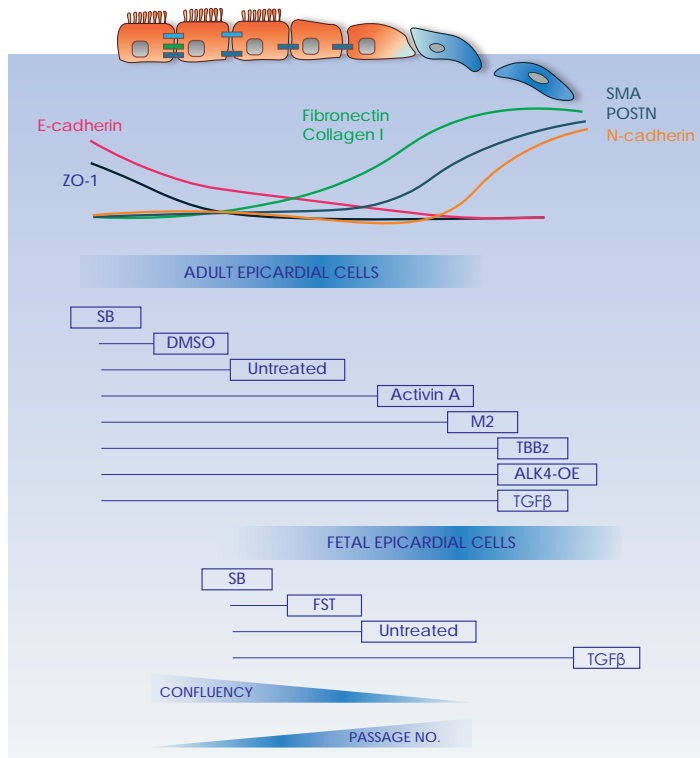


**Fig. 1 | Factors that influence the plasticity of epicardial cells.** A schematic overview of the epiMT axis and how factors influence the epiMT status of adult and foetal epicardial cells. The epiMT markers are an interpretation of differences in expression that we have observed in our studies. We find that there is a gradient of marker expression along the epiMT axis that allows us to discriminate between intermediate epiMT stages. Importantly, it also shows that some markers are already differentially expressed in untreated cells. The markers represent a schematic interpretation of multiple experiments and are not intended to be fully accurate for every individual cell stimulation.

## EPIMT CELL CULTURE MODEL

Studying the regulation of epiMT is often performed *in vitro*. Using the right cell culture model, understanding it, and recognising its strong points and limitations is essential to obtain useful and translational data. In chapter 3 we describe a detailed protocol for the isolation and culture of human adult and foetal primary epicardial cells that have been used extensively to study epiMT. Although epiMT is often presented as a binary process where cells are either epithelial or mesenchymal (also in this thesis), in reality epiMT resembles a much more plastic process with several

intermediate states between the epithelial and mesenchymal phenotype (24)(Fig. 1). When performing epiMT experiments, we observed that a range of factors push the epicardial cells leftward or rightward on this epiMT axis (Fig. 1). An example of this is the effect of SB, which is routinely added to our epicardial cell culture. Removal of SB from the cell culture medium of adult cells already morphologically changes the cells, as the cells lose some adhesion molecules and downregulate Zonula occludens-1 (ZO-1) at the cell border (data not shown), indicating a shift to the right on the epiMT axis (Fig. 1). Remarkably, removing SB from foetal cells pushes the cells much further to the right, towards a mesenchymal phenotype. The fact that foetal cells are more prone to epiMT suggests that they are intrinsically already further on the epiMT gradient compared to adult cells (Fig. 1). This is supported by the fact that foetal epicardial cells in the presence of SB already express lower levels of E-cadherin, and higher levels of mesenchymal markers Vimentin and TCF21 compared to adult cells (9). We have not been able to identify the molecular explanation of this disparity between foetal and adult epicardial cells. However, our recent finding that TBBz induces histone modifications implies that epiMT induction also depends on the epigenetic landscape of the cell, which is supported by literature (24). A divergent epigenetic status in foetal cells may well explain its position on the epiMT axis. A first step towards proving this concept is shown in Figure 2, where TBBz stimulation pushes adult cells towards an epigenetic status that is comparable to foetal cells.

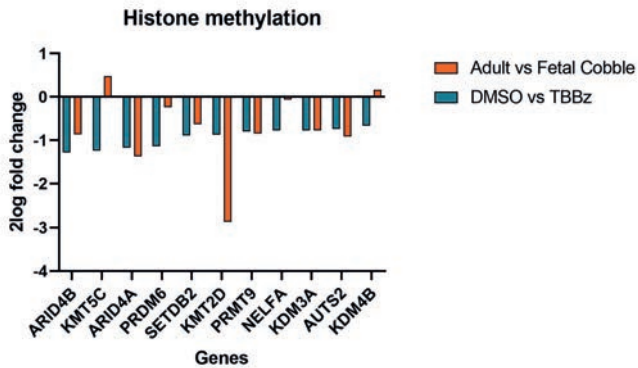


**Fig. 2 | TBBz pushes adult epicardial cells towards a foetal histone methylation gene profile.** Genes involved in histone methylation that were differentially expressed in TBBz vs DMSO treated adult epicardial cells (3 hours stimulation, see chapter 4 for details) were listed. The expression of these genes was established in a dataset of adult and foetal cobblestone epicardial cells cultured in SB431542. The fact that 9 out of 11 genes follow the same pattern (gene expression is decreased in both TBBz treated adult cells and in foetal cells) points to a mesenchymal histone methylation status.

We exploited these difference in epiMT status between foetal and adult epicardial cells in our in vitro experiments. For example, the different status of adult and foetal cells allowed us to simultaneously study the effects of stimulants and inhibitors of pathways potentially involved in epiMT. The addition of SB, which helps to maintain an epithelial state, as a control condition provided a reliable negative control. In addition, the concept of intermediate stages of epiMT also helps to explain some of the results, e.g. the fact that we find only partial inhibition of FST on foetal epiMT. Interestingly, we also found that DMSO, a solvent for almost all our stimulants (including SB), seems to push the cells leftwards on the epiMT scale. This has been found by others before (25) and suggests that a low concentration of DMSO could be preferable in all epiMT experiments. But despite the presence of it, TBBz and M2 (both dissolved in DMSO) were able to induce epiMT. In practice, there are also other factors that influence the position on this epiMT-gradient. An example of this is that the occurrence of epiMT is highly dependent on the confluency of the cell culture plate, and the cell passage (Fig. 1). We postulate that also the status of the heart where we isolate the epicardium from (diseased or healthy, age, gender) is relevant in this setting. It is therefore essential to resemble this complexity in the in vitro study design, by using primary cells derived from multiple cell isolations to make sure that we observe a robust and translational result.

### Differentiation of EPDCs

Besides the regulation of epiMT itself, it is also relevant to consider the differentiation capacity of the generated mesenchymal cells and their potential contribution to tissue formation. Differentiation capacity is in general influenced by a combination of the cell itself and by the biochemical and mechanistic input from the local environment (26). As described in chapter 2, in the developing heart epicardial derived cells (EPDCs) mainly differentiate into smooth muscle cells, (myo-) fibroblasts and pericytes. While epiMT in the mammalian adult hearts has been described to be beneficial for repair (see Chapter 2), the actual contribution of epiMT derived cells remains uncertain. Noteworthy in this context is that in the mammalian heart epiMT has been linked to the induction of fibrosis in the atria (15). Interestingly, the process of atrial fibrosis was related to increased levels of Activin A secreted by epicardial adipose tissue (EAT) (27). It suggests that Activin pushes induces epicardial cells into epiMT whereafter the EPDCs differentiate towards a fibroblast phenotype involved in atrial fibrosis. Moreover, in an environment of stress, such as an infarct, EPDCs can also become adipogenic (28–30). These findings raise the question whether stimulating epiMT in the adult mammalian heart will ultimately be beneficial for the patient. There are a few things to consider in this context. Firstly, epiMT has

been related to cardiac generation in mammals and regeneration in zebrafish. An example of this is NRG-1 secretion by post-epiMT cells that is essential for zebrafish regeneration, as described by us (chapter 7) and others (31,32). We have shown that NRG-1 secretion is PRRX1 dependent in zebrafish and in human cells. PRRX1 was almost absent in patient cardiac tissue samples, which could indicate that the lack of PRRX1-dependent NRG-1 expression hampers mammalian cardiac repair resulting in a fibrotic response. It would be interesting to investigate whether overexpression of PRRX1 in diseased mammalian hearts could affect fibrosis. Secondly, although differentiation towards fibroblasts is mainly considered a bad thing because it is often related to the development of fibrosis and arrhythmogenic substrate, in many organs fibroblasts and their secreted ECM lie at the base of repair and regeneration (33). Thirdly, it is likely that EPDCs will sense their environment, whereby the cues derived from the ECM as well as the stiffness of underlying tissue will influence their differentiation. Pathological remodelling is by itself not a disease but a reaction to a diseased environment. Therefore, targeting the microenvironment in order to steer the EPDC towards the desired cell type will be of relevance for epiMT to be beneficial to cardiac repair.

## **APPLICATION OF IDENTIFIED FACTORS IN A MOUSE MODEL – TOWARDS A THERAPEUTIC APPROACH**

The next step towards an epicardial based regenerative therapy is the application of epiMT stimulating factors to the infarcted heart. The simplest method for this is systemic application, via injection or orally. However, given that induction of EMT is undesirable in most organs due to development of fibroses and metastatic cancer, local application is preferred. Local therapy in the heart is often injected into the heart muscle. But the difficulty with injecting something into the heart is that it is expelled within a few contractions (7). Therefore, a biomaterial is essential to keep the factor in the heart for a certain time-period. The additional benefit of a biomaterial is the possibility of timed release, thereby prolonging the therapy with a single intervention. Interestingly, because of the convenient location of the epicardium at the outside of the heart, it is relatively easy to apply a drug-releasing patch directly on top of the epicardium instead of a potential harmful injection into the heart muscle. This would mainly be beneficial when the patch is self-adhesive and does not require stiches or glue, and moreover when the release is uni-directional to secure specific release to the epicardium. Although quite extensive research has been performed to develop epicardial patches (reviewed in (34)), most of them aim to target the underlying myocardium or have the goal to deliver additional contractile units by generating patches

containing cardiac cells. In our research, we wanted to hit the epicardium itself. We aimed for a robust protocol to prepare a patch that can easily be reproduced and a highly adhesive patch that does not require stitches or glue. Therefore, we have optimized two drug releasing patches that could be applied onto the epicardium. The TISSEEL method relies on the gellification of fibrinogen upon mixing with thrombin, which provides a hydrogel that can be picked up and placed on the heart. The TISSEEL constituents can be mixed with many different types of factors prior to solidification and provides a robust protocol that is easily applicable during *in vivo* experiments. The supramolecular UPy-catechol patch consists of a UPy-PEG molecule that has been functionalized with a catechol group that provides outstanding binding to tissue. The hydrogel is mixed with the compound of interest and subsequently solidified on top of a UPy-PEG electrospun layer. We use this layer to easily pick up the patch and to protect the lungs. However, this layer could easily be adjusted to an impermeable layer, allowing for unidirectional release from the patch.

In the research described in this thesis, we aimed for identifying factors that interfere with epiMT *in vitro* whereafter we intended to test this *in vivo* in the injured mouse heart using a patch. One of the identified pathways was Activin/ALK4 signaling. Given the fact that Activin is broadly expressed in the infarcted heart (35), viral overexpression of ALK4 specifically in the epicardium could be a potential solution to induce epiMT. We executed a study in a mouse model for myocardial infarction to compare a TISSEEL patch containing control virus to a TISSEEL patch containing a constitutively active ALK4 adenovirus. Unfortunately, we encountered difficulties with inefficient viral transduction and therefore we were not able to draw any conclusions. In a second mouse study, we aimed to determine the effect of epiMT-inducing small molecules that were identified in chapter 4. We applied TISSEEL patches containing TBBz and M2 onto the injured mouse heart and we used DMSO and SB eluting patches as controls. Unfortunately, no differences were found in heart function or infarct size between DMSO and TBBz/M2 stimulated hearts after 4 weeks. To determine if the release of compounds from the patch was sufficient, we established the release of SB after 7 days which should be detectable by measuring SMA and pSMAD2 in the underlying infarcted area. However, we did not find a difference between SB and DMSO. There are three possible explanations for the fact that we were not able to observe an effect of epiMT-inducing factors *in vivo*. The first is that the compounds simply do not exert any effect on the heart. Although this is a realistic option for our newly identified compounds, it is less plausible for SB, given the fact that blocking of TGF $\beta$  signalling in the heart has been demonstrated to have major effects on SMA expression, ECM production and fibrosis (reviewed in (36)). The second possibility is

that there is a flaw in the design of the mouse studies, e.g. the timing of the experiment, the release properties of the patch in vivo, the concentration of the factors that was used, or the methods applied for functional analysis. These reasons warrant further investigation before any conclusions can be drawn about the usefulness of these patches to target the epicardium. The third explanation is that the epicardium does not easily take up certain compounds from the outside. Given its barrier function, it would not be surprising that the epicardium displays a reduced permeability, resulting in a suboptimal targeting efficiency. Targeting the epicardium from the inside of the heart by injecting a hydrogel containing the factor of interest would be an alternative approach to cope with this. Interesting to mention in this case is that a peptide has been identified that actively targets the epicardium and could serve as a cargo to deliver small molecules (37). Although injection into the heart muscle is less optimal compared to an epicardial applied patch, delivery of this peptide in the heart should specifically hit the epicardium and therefore will be local and circumvent the current issues.

## THE FUTURE OF EPICARDIAL RESEARCH

In animals that display regenerative capacity, such as newts who can fully regrow amputated limbs, an essential element of regeneration is the blastema, a mass of progenitor cells able to grow and differentiate into new tissue. A blastema coordinates the transition from the initial wound healing response, consisting of the inflammatory and proliferative phase, to regeneration. The blastema consists of a group of fibroblast derived progenitor cells, among others PRRX1+ cells (38), which is surrounded by ECM and covered by an epithelium. Regenerative processes within the blastema are coordinated by paracrine signalling, among others CXCR4-CXCL12 signalling (39) and ECM cues such as Tenascin-C and hyaluronic acid (40). Although a one-to-one comparison with a cardiac blastema may not be applicable due to the lack of pluripotent stem cells in the heart, blastema formation may shed light on the actual role of the epicardium in the developing and diseased heart, which is to secure a micro-environment where regeneration can take place. There are phenotypic similarities between epicardial reactivation and blastema formation, such as the epithelial layer (the epicardium) with subepicardial ECM production, Tenascin-C and hyaluronic acid expression (14,41), CXCR4-CXCL12 signalling (18), and the presence of PRRX1+ mesenchymal cells (this thesis).

The concept that the epicardium functions as a blastema is in line with the dynamics in the epicardial research field. For several years the general idea was that epicardial cells would contribute to cardiac repair by increasing the number of epicardial derived cardiomyocytes and endothelial cells, either by endogenous stimulation towards these cell lineages or via cell transplantation of isolated epicardial cells (42–46). However, although these studies show beneficial effects of epicardial cells on cardiac repair, the absolute numbers of cells that differentiate towards cardiomyocytes or endothelial cells turned out to be non-existent or minimal at best and could not explain the observed improvement in cardiac function. The cellular epicardial contribution to fibroblast and SMCs has been demonstrated multiple times (see chapter 3), but most cardiac fibroblasts in the infarcted myocardium seem to derive from pre-existing fibroblasts instead of the epicardial layer (47). The past few years, the focus of epicardium-driven repair research has switched from cellular contribution towards a regulatory role for the epicardium during disease and repair. This regulatory role was demonstrated when the beneficial effects of epicardial cell injection (46) were attributed to epicardial cell derived secretome instead of a cellular contribution (48). Interestingly, in this study mesenchymal EPDC-derived secretome was injected, indicating that the beneficial effects derive from post-epiMT cells. There is a wide array of observations pointing towards the regulatory role of these mesenchymal EPDCs as opposed to pre-epiMT epithelial epicardial cells. Firstly, multiple studies have shown that epicardial cells secrete factors that promote cardiomyocyte proliferation and maturation (49,50), e.g. Follistatin-like 1 (51). In this manuscript we describe a similar finding, namely the secretion of NRG-1 by post-epiMT epicardial cells. Secondly, EPDCs are essential for vessel maturation, both by a cellular contribution (pericytes) and a regulatory contribution (13). And thirdly, epicardial derived spindles secrete ECM components, which are essential for a proper repair response, such as periostin (52) and fibronectin (53). Together, this shows that the epicardium, and particularly the mesenchymal epicardial cells, are central players in the tissue generating response of the heart, not solely by providing cells but mainly by regulating the processes necessary to generate a fully functioning tissue. Therefore, in my opinion, epicardial research should focus on increasing epiMT, as we describe in this thesis, and on studying how EPDCs orchestrate the post-injury response. Finetuning this response by investigating both the developing heart and the regenerating zebrafish heart may be the key to optimize the epicardial response to repair.

A specific therapeutic approach to benefit from the regulatory role of the epicardium is the use of engineered heart tissue (EHT). EHTs consist of beating cardiomyocytes which are produced in vitro and subsequently applied to the outside of the injured

heart for cardiac support (54). Pre-clinical experiments have been exceptionally convincing, and the engineered tissues are now being tested in patients (55). Interestingly, numerous studies have come to the conclusion that epicardial cells highly improve the maturation of such engineered tissues (50,56–58), demonstrating once more the significance of the epicardium as regulator of cardiac tissue generation. There is also an indirect value in the optimization of EHTs, since development of highly matured cardiac microtissues can be used for research purposes, such as high throughput screening, toxicity tests, and, in combination with patient derived induced pluripotent stem cells (iPSCs), for disease modelling (56).

The bottleneck of epicardial research is the translation of preclinical findings towards a therapeutic approach in patients, mainly due to the size of the human heart and the ratio between the number of epicardial cells and the amount of myocardial tissue. Size issues become more pronounced when taking into the account that patients often have massive epicardial fat deposition and thickening of the sub-epicardium. It is difficult to envision how epicardial cells or epicardial derived factors should reach the infarcted heart. Mouse models are often used for this type of research, but mice barely develop EAT (59), and are young and healthy while patients often suffer from additional comorbidities. Currently there is very little information available about the endogenous role of the epicardium in the human repair response to injury, let alone if the epicardial layer is deployable for cardiac repair. The main challenge for the coming years is to translate findings from cell and animal research to the human heart. As a first step we used primary human cells for our studies instead of animal cells or cell lines. Using epicardial cells derived from multiple patients includes the biological variability present in patients. A rapidly upcoming approach to study patient characteristics is the use of iPSC derived epicardial cells. The benefit of this is the option to specifically study a patient derived genotype combined with their isogenic control. In contrast, the value of patient derived primary epicardial cells is that these represent cells of the patient in its current situation, e.g. exposed to adipose tissue, medication, etc. This will presumably be more representative for the end-user of developed therapy compared to a more development-like iPSC.

Using this cell culture model we were able to easily study signalling pathways because almost all parameters could be controlled and read-outs were relatively strict and clear. This allowed us to investigate the regulation of epiMT in detail. Another significant benefit of in vitro models is the low costs per sample compared to organoids or animal models, and as a result, the possibility of high throughput screening, as we did in chapter 4. The next step in translational research is to study the behaviour

of the cell in its natural context, as it has been shown numerous times that cell-cell interactions and cell-ECM interactions are essential for cell behaviour (60). Therefore, validation in tissue makes the *in vitro* finding much stronger. However, findings in tissue often reflect a single timepoint, making it difficult to determine the processes that occur, and the cell types that are involved. Therefore, the combination of *in/ex vivo* and *in vitro* results will provide the most robust data. In our studies, we aimed for validation of our findings in mouse and human tissue. We used embryonic mouse hearts to validate Activin induced epicardial invasion and we determined PRRX1 expression in human hearts to translate findings from zebrafish studies to the human heart.

Potential opportunities to study the epicardium in the human heart lie within the culture of human tissue. One example of this is tissue culture of specimens from diseased human hearts (61) or human heart auricles (15). These approaches are high throughput and could include semi-healthy versus diseased tissue. Because it is difficult to obtain fresh healthy adult ventricular tissue, the use of healthy and diseased pig hearts may be a good alternative since one heart can provide a large number of slices to study *ex vivo*, and porcine hearts resemble human hearts in size. Interestingly, a recent paper describes a method to specifically study the epicardium in heart slices (62), which is a highly promising approach to bridge the gap between cell culture models, small animal models, and the patient. In addition, the ongoing progress in omics such as single cell sequencing, spatially-resolved proteomics and Tomo-seq will provide a wide potential to study processes over time in single cells derived from tissue.

## CONCLUSION

In this thesis, we describe the isolation and culture of human primary epicardial cells and we demonstrate an extensive list of experiments to better understand the process of epiMT. While studying the signalling cascade of epiMT, we found that other factors than the pleiotropic TGF $\beta$  ligand can be used for the induction of epiMT. Furthermore, we showed that it is feasible to set up a screen using primary epicardial cells to reveal novel regulatory mechanisms of epiMT. In addition, we used the epiMT cell culture model to translate zebrafish findings to the human setting. Finally, we have explored the use of epicardial, compound eluting patches which may serve as a first step for further investigation into how factors identified based on their potential to stimulate the epicardium can be exploited to repair the injured heart.

Overall, we have described that the epicardium is an attractive therapeutic target for the injured heart, we have shown how to study it and we have provided novel approaches for stimulating this cell population to enhance cardiac repair.

## REFERENCES

1. Koop Y, Wimmers RH, Vaartjes I, Bots ML. Hart- en vaatziekten in Nederland 2021. 2021.
2. Li J, Hu S, Zhu D, Huang K, Mei X, López de Juan Abad B, et al. All Roads Lead to Rome (the Heart): Cell Retention and Outcomes From Various Delivery Routes of Cell Therapy Products to the Heart. *J Am Heart Assoc*. 2021 Apr 20;10(8).
3. Vagnozzi RJ, Mailliet M, Sargent MA, Khalil H, Johansen AKZ, Schwanekamp JA, et al. An acute immune response underlies the benefit of cardiac stem cell therapy. *Nature*. 2020;577(7790):405–9.
4. Maliken BD, Molkentin JD. Undeniable Evidence That the Adult Mammalian Heart Lacks an Endogenous Regenerative Stem Cell. *Circulation*. 2018 Aug 21;138(8):806–8.
5. Kocijan T, Rehman M, Colliva A, Groppa E, Leban M, Vodret S, et al. Genetic lineage tracing reveals poor angiogenic potential of cardiac endothelial cells. *Cardiovasc Res*. 2021 Jan 1;117(1):256–70.
6. Prabhu SD, Frangogiannis NG. The Biological Basis for Cardiac Repair After Myocardial Infarction. *Circ Res*. 2016 Jun 24;119(1):91–112.
7. van den Akker F, Feyen DAM, van den Hoogen P, van Laake LW, van Eeuwijk ECM, Hoefler I, et al. Intramyocardial stem cell injection: go(ne) with the flow. *Eur Heart J*. 2016 Feb 24;ehw056.
8. Simkin J, Sammarco MC, Dawson LA, Schanes PP, Yu L, Muneoka K. The mammalian blastema: regeneration at our fingertips. *Regeneration*. 2015 Jun;2(3):93–105.
9. Moerkamp AT, Lodder K, van Herwaarden T, Dronkers E, Dingenouts CKE, Tengström FC, et al. Human fetal and adult epicardial-derived cells: a novel model to study their activation. *Stem Cell Res Ther*. 2016 Dec 29 [cited 2017 Sep 7];7(1):174.
10. Mantri M, Scuderi GJ, Abedini-Nassab R, Wang MFZ, McKellar D, Shi H, et al. Spatiotemporal single-cell RNA sequencing of developing chicken hearts identifies interplay between cellular differentiation and morphogenesis. *Nat Commun*. 2021 Dec 19;12(1):1771. Available from: <http://dx.doi.org/10.1038/s41467-021-21892-z>
11. Lupu IE, Redpath AN, Smart N. Spatiotemporal Analysis Reveals Overlap of Key Proepicardial Markers in the Developing Murine Heart. *Stem Cell Reports*. 2020;14(5):770–87.
12. Xiao Y, Hill MC, Zhang M, Martin TJ, Morikawa Y, Wang S, et al. Hippo Signaling Plays an Essential Role in Cell State Transitions during Cardiac Fibroblast Development. *Dev Cell*. 2018 Apr;45(2):153–169.e6.
13. Quijada P, Trembley MA, Misra A, Myers JA, Baker CD, Pérez-Hernández M, et al. Coordination of endothelial cell positioning and fate specification by the epicardium. *Nat Commun*. 2021 Dec 6;12(1):4155. A
14. van den Berg NWE, Neefs J, Kawasaki M, Nariswari FA, Wesselink R, Fabrizi B, et al. Extracellular matrix remodeling precedes atrial fibrillation: Results of the PREDICT-AF trial. *Hear Rhythm*. 2021 Dec;18(12):2115–25.

15. van den Berg NWE, Kawasaki M, Fabrizi B, Nariswari FA, Verduijn AC, Neefs J, et al. Epicardial and endothelial cell activation concurs with extracellular matrix remodeling in atrial fibrillation. *Clin Transl Med.* 2021 Nov 4;11(11).
16. Suffee N, Moore-Morris T, Jagla B, Mougenot N, Dilanian G, Berthet M, et al. Reactivation of the Epicardium at the Origin of Myocardial Fibro-Fatty Infiltration during the Atrial Cardiomyopathy. *Circ Res.* 2020;1330–42.
17. Kohela A, van Kampen SJ, Moens T, Wehrens M, Molenaar B, Boogerd CJ, et al. Epicardial differentiation drives fibro-fatty remodeling in arrhythmogenic cardiomyopathy. *Sci Transl Med.* 2021 Sep 22;13(612).
18. Quijada P, Trembley MA, Small EM. The Role of the Epicardium During Heart Development and Repair. *Circ Res.* 2020 Jan;126(3):377–94.
19. Sun X, Malandraki-Miller S, Kennedy T, Bassat E, Klaourakis K, Zhao J, et al. The extracellular matrix protein agrin is essential for epicardial epithelial-to-mesenchymal transition during heart development. *Development.* 2021 May 1;148(9).
20. Tao J, Barnett J, Watanabe M, Ramírez-Bergeron D. Hypoxia Supports Epicardial Cell Differentiation in Vascular Smooth Muscle Cells through the Activation of the TGF $\beta$  Pathway. *J Cardiovasc Dev Dis.* 2018 Apr 13;5(2):19.
21. Zhang H, Meng F, Liu G, Zhang B, Zhu J, Wu F, et al. Forkhead Transcription Factor Foxq1 Promotes Epithelial–Mesenchymal Transition and Breast Cancer Metastasis. *Cancer Res.* 2011 Feb 15;71(4):1292–301.
22. Cao Y, Xia Y, Balowski JJ, Ou J, Song L, Safi A, et al. Identification of enhancer regulatory elements that direct epicardial gene expression during zebrafish heart regeneration. *Development.* 2022 Feb 15;149(4).
23. Duncan JS, Gyenis L, Lenehan J, Bretner M, Graves LM, Haystead TA, et al. An Unbiased Evaluation of CK2 Inhibitors by Chemoproteomics. *Mol Cell Proteomics.* 2008 Jun;7(6):1077–88.
24. Nieto MA, Huang RY-J, Jackson RA, Thiery JP. Emt: 2016. *Cell.* 2016;166(1):21–45.
25. Pagan R, Martin I, Llobera M, Vilaro S. Epithelial-mesenchymal transition of cultured rat neonatal hepatocytes is differentially regulated in response to epidermal growth factor and dimethyl sulfoxide. *Hepatology.* 1997 Mar;25(3):598–606.
26. Sullivan KE, Quinn KP, Tang KM, Georgakoudi I, Black LD. Extracellular matrix remodeling following myocardial infarction influences the therapeutic potential of mesenchymal stem cells. *Stem Cell Res Ther.* 2014 Mar 24;5(1):14.
27. Venteclef N, Guglielmi V, Balse E, Gaborit B, Cotillard A, Atassi F, et al. Human epicardial adipose tissue induces fibrosis of the atrial myocardium through the secretion of adipo-fibrokinases. *Eur Heart J.* 2015 Apr 1;36(13):795–805.
28. Liu Q, Huang X, Oh J-H, Lin R-Z, Duan S, Yu Y, et al. Epicardium-to-fat transition in injured heart. *Cell Res.* 2014 Nov 26;24(11):1367–9.
29. Qureshi R, Kindo M, Boulberdaa M, von Hunolstein J-J, Steenman M, Nebigil CG. A prokineticin-driven epigenetic switch regulates human epicardial cell stemness and fate. *Stem Cells.* 2018 Jun 6;(Umr 7242).

30. Suffee N, Moore-Morris T, Jagla B, Mougnot N, Dilanian G, Berthet M, et al. Reactivation of the Epicardium at the Origin of Myocardial Fibro-Fatty Infiltration During the Atrial Cardiomyopathy. *Circ Res.* 2020 May 8;126(10):1330–42.
31. D'Uva G, Aharonov A, Lauriola M, Kain D, Yahalom-Ronen Y, Carvalho S, et al. ERBB2 triggers mammalian heart regeneration by promoting cardiomyocyte dedifferentiation and proliferation. *Nat Cell Biol.* 2015 May 6;17(5):627–38.
32. Gemberling M, Karra R, Dickson AL, Poss KD. Nrg1 is an injury-induced cardiomyocyte mitogen for the endogenous heart regeneration program in zebrafish. *Elife.* 2015;2015(4):1–17.
33. Gomes RN, Manuel F, Nascimento DS. The bright side of fibroblasts: molecular signature and regenerative cues in major organs. *npj Regen Med.* 2021 Dec 10;6(1):43.
34. Chang T, Liu C, Lu K, Wu Y, Xu M, Yu Q, et al. Biomaterials based cardiac patches for the treatment of myocardial infarction. *J Mater Sci Technol.* 2021 Dec;94:77–89.
35. Hu J, Wang X, Tang Y, Shan Y, Zou Q, Wang Z, et al. Activin A inhibition attenuates sympathetic neural remodeling following myocardial infarction in rats. *Mol Med Rep.* 2018 Jan 25.
36. Parichatikanond W, Luangmonkong T, Mangmool S, Kurose H. Therapeutic Targets for the Treatment of Cardiac Fibrosis and Cancer: Focusing on TGF- $\beta$  Signaling. *Front Cardiovasc Med.* 2020 Mar 10;7.
37. Straub T, Nave J, Bouvain P, Akbarzadeh M, Dasa SSK, Kistner J, et al. MRI-based molecular imaging of epicardium-derived stromal cells (EpiSC) by peptide-mediated active targeting. *Sci Rep.* 2020 Dec 10;10(1):21669.
38. Suzuki M, Satoh A, Ide H, Tamura K. Transgenic *Xenopus* with *prx1* limb enhancer reveals crucial contribution of MEK/ERK and PI3K/AKT pathways in blastema formation during limb regeneration. *Dev Biol.* 2007 Apr;304(2):675–86.
39. Dufourcq P, Vriza S. The chemokine SDF-1 regulates blastema formation during zebrafish fin regeneration. *Dev Genes Evol.* 2006 Oct 4;216(10):635–9.
40. Calve S, Odelberg SJ, Simon H-G. A transitional extracellular matrix instructs cell behavior during muscle regeneration. *Dev Biol.* 2010 Aug;344(1):259–71.
41. Mercer SE, Odelberg SJ, Simon HG. A dynamic spatiotemporal extracellular matrix facilitates epicardial-mediated vertebrate heart regeneration. *Dev Biol.* 2013;382(2):457–69.
42. Smart N, Bollini S, Dubé KN, Vieira JM, Zhou B, Davidson S, et al. De novo cardiomyocytes from within the activated adult heart after injury. *Nature.* 2011;474(7353):640–4.
43. van Wijk B, Gunst QD, Moorman AFM, van den Hoff MJB. Cardiac regeneration from activated epicardium. *PLoS One.* 2012;7(9):e44692.
44. Zangi L, Lui KO, von Gise A, Ma Q, Ebina W, Ptaszek LM, et al. Modified mRNA directs the fate of heart progenitor cells and induces vascular regeneration after myocardial infarction. *Nat Biotechnol.* 2013;31(10):898–907.
45. Limana F, Zacheo A, Mocini D, Mangoni A, Borsellino G, Diamantini A, et al. Identification of myocardial and vascular precursor cells in human and mouse epicardium. *Circ Res.* 2007;

46. Winter EM, Grauss RW, Hogers B, Van Tuyn J, Van Der Geest R, Lie-Venema H, et al. Preservation of left ventricular function and attenuation of remodeling after transplantation of human epicardium-derived cells into the infarcted mouse heart. *Circulation*. 2007;116(8):917–27.
47. Kanisicak O, Khalil H, Ivey MJ, Karch J, Maliken BD, Correll RN, et al. Genetic lineage tracing defines myofibroblast origin and function in the injured heart. *Nat Commun*. 2016 Jul 22 [cited 2017 May 19];7:12260.
48. Zhou B, Honor LB, He H, Ma Q, Oh J-H, Butterfield C, et al. Adult mouse epicardium modulates myocardial injury by secreting paracrine factors. *J Clin Invest*. 2011 May 2 [cited 2016 Mar 9];121(5):1894–904.
49. Eid H, Larson DM, Springhorn JP, Attawia MA, Nayak RC, Smith TW, et al. Role of epicardial mesothelial cells in the modification of phenotype and function of adult rat ventricular myocytes in primary coculture. *Circ Res*. 1992 Jul;71(1):40–50.
50. Weeke-Klump A, Bax NAM, Bellu AR, Winter EM, Vrolijk J, Plantinga J, et al. Epicardium-derived cells enhance proliferation, cellular maturation and alignment of cardiomyocytes. *J Mol Cell Cardiol*. 2010 Oct [cited 2017 Sep 4];49(4):606–16.
51. Wei K, Serpooshan V, Hurtado C, Diez-Cuñado M, Zhao M, Maruyama S, et al. Epicardial FSTL1 reconstitution regenerates the adult mammalian heart. *Nature*. 2015 Sep 16 [cited 2016 Oct 7];525(7570):479–85.
52. Kühn B, del Monte F, Hajjar RJ, Chang Y-S, Lebeche D, Arab S, et al. Periostin induces proliferation of differentiated cardiomyocytes and promotes cardiac repair. *Nat Med*. 2007 Aug 15;13(8):962–9.
53. Wang J, Karra R, Dickson AL, Poss KD. Fibronectin is deposited by injury-activated epicardial cells and is necessary for zebrafish heart regeneration. *Dev Biol*. 2013 Oct;382(2):427–35.
54. Zimmermann W-H, Melnychenko I, Wasmeier G, Didié M, Naito H, Nixdorff U, et al. Engineered heart tissue grafts improve systolic and diastolic function in infarcted rat hearts. *Nat Med*. 2006 Apr 2;12(4):452–8.
55. DZHK. Start of First Clinical Trial on Tissue Engineered Heart Repair (Study BioVAT-DZ-HK20). 2021.
56. Giacomelli E, Meraviglia V, Campostrini G, Cochrane A, Cao X, van Helden RWJ, et al. Human-iPSC-Derived Cardiac Stromal Cells Enhance Maturation in 3D Cardiac Microtissues and Reveal Non-cardiomyocyte Contributions to Heart Disease. *Cell Stem Cell*. 2020 Jun;26(6):862-879.e11.
57. Bargehr J, Ong LP, Colzani M, Davaapil H, Hofsteen P, Bhandari S, et al. Epicardial cells derived from human embryonic stem cells augment cardiomyocyte-driven heart regeneration. *Nat Biotechnol*. 2019;37(8):895–906.
58. Tan JJ, Guyette JP, Miki K, Xiao L, Kaur G, Wu T, et al. Human iPSC-derived pre-epicardial cells direct cardiomyocyte aggregation expansion and organization in vitro. *Nat Commun*. 2021 Dec 17;12(1):4997.

59. Yamaguchi Y, Cavallero S, Patterson M, Shen H, Xu J, Kumar SR, et al. Adipogenesis and epicardial adipose tissue: A novel fate of the epicardium induced by mesenchymal transformation and PPAR $\gamma$  activation. *Proc Natl Acad Sci*. 2015 Feb 17;112(7):2070–5.
60. Pampaloni F, Reynaud EG, Stelzer EHK. The third dimension bridges the gap between cell culture and live tissue. *Nat Rev Mol Cell Biol*. 2007 Oct;8(10):839–45.
61. Korteweg N. Flinterdunne plakjes mensenhart leven door in het laboratorium. NRC. 2021;
62. Maselli D, Matos RS, Johnson RD, Chiappini C, Camelliti P, Campagnolo P. Epicardial slices: an innovative 3D organotypic model to study epicardial cell physiology and activation. *npj Regen Med*. 2022 Dec 17;7(1):7.



## LIST OF PUBLICATIONS

- **Dronkers E**, van Herwaarden T, van Brakel TJ, Sanchez-Duffhues G, Goumans MJ, Smits AM. Activin A and ALK4 Identified as Novel Regulators of Epithelial to Mesenchymal Transition (EMT) in Human Epicardial Cells. *Front Cell Dev Biol.* 2021 Dec 16;9:765007. doi: 10.3389/fcell.2021.765007. PMID: 34977017; PMCID: PMC8716764.
- de Bakker DEM, Bouwman M, **Dronkers E**, Simões FC, Riley PR, Goumans MJ, Smits AM, Bakkers J. Prrx1b restricts fibrosis and promotes Nrg1-dependent cardiomyocyte proliferation during zebrafish heart regeneration. *Development.* 2021 Oct 1;148(19):dev198937. doi: 10.1242/dev.198937. Epub 2021 Oct 4. PMID: 34486669; PMCID: PMC8513610.
- **Dronkers E**, Wauters MMM, Goumans MJ, Smits AM. Epicardial TGF $\beta$  and BMP Signaling in Cardiac Regeneration: What Lesson Can We Learn from the Developing Heart? *Biomolecules.* 2020 Mar 5;10(3):404. doi: 10.3390/biom10030404. PMID: 32150964; PMCID: PMC7175296.
- **Dronkers E**, Moerkamp AT, van Herwaarden T, Goumans MJ, Smits AM. The Isolation and Culture of Primary Epicardial Cells Derived from Human Adult and Fetal Heart Specimens. *J Vis Exp.* 2018 Apr 24;(134):57370. doi: 10.3791/57370. PMID: 29757271; PMCID: PMC6100756.
- Smits AM, **Dronkers E**, Goumans MJ. The epicardium as a source of multipotent adult cardiac progenitor cells: Their origin, role and fate. *Pharmacol Res.* 2018 Jan;127:129-140. doi: 10.1016/j.phrs.2017.07.020. Epub 2017 Jul 24. PMID: 28751220.
- Amatngalim GD, Schrupf JA, Henic A, **Dronkers E**, Verhoosel RM, Ordonez SR, Haagsman HP, Fuentes ME, Sridhar S, Aarbiou J, Janssen RAJ, Lekkerkerker AN, Hiemstra PS. Antibacterial Defense of Human Airway Epithelial Cells from Chronic Obstructive Pulmonary Disease Patients Induced by Acute Exposure to Nontypeable *Haemophilus influenzae*: Modulation by Cigarette Smoke. *J Innate Immun.* 2017;9(4):359-374. doi: 10.1159/000455193. Epub 2017 Feb 8. PMID: 28171878; PMCID: PMC5569706.
- Moerkamp AT, Lodder K, van Herwaarden T, **Dronkers E**, Dingenouts CK, Tengström FC, van Brakel TJ, Goumans MJ, Smits AM. Human fetal and adult epicardial-derived cells: a novel model to study their activation. *Stem Cell Res Ther.* 2016 Nov 29;7(1):174. doi: 10.1186/s13287-016-0434-9. PMID: 27899163; PMCID: PMC5129650.



## CURRICULUM VITAE

Esther Dronkers werd geboren op 6 februari 1992 in Wageningen. Na het behalen van haar VWO diploma aan het Ichthus College in Veenendaal startte ze in 2011 met de bachelor Biomedische Wetenschappen aan de Universiteit van Leiden. Hierbij volgde ze de minor "Filosofie" aan de Erasmus Universiteit en voltooide ze een stage over de rol van vitamine D in de antibacteriële activiteit van het longepitheel. Hier maakte ze kennis met primaire humane celkweek. Hierna vervolgde ze de opleiding aan de Universiteit Leiden met de onderzoeksmaster Biomedical Sciences, waarin ze koos voor vakken en stages die betrekking hebben op hart- en vaatziekten. Tijdens de eerste stage deed ze onderzoek naar het effect van temperatuur op vaatverwijding aan de Erasmus Universiteit. Tijdens de tweede stage onderzocht zij het verschil tussen adulte en foetale epicardiale EMT en de rol van de endoglin receptor hierin. Als vervolg op de laatste stage startte zij in 2016 haar promotieonderzoek naar de rol van epicardiale EMT in het beschadigde hart. Dit onderzoek voerde Esther uit in de Cardiovasculaire Celbiologie groep onder Marie José Goumans. Tijdens haar promotietraject specialiseerde Esther zich in primaire celkweek, werkte ze met muismodellen en verdiepte ze zich in methodes en technieken voor data-analyses.

In 2022 is Esther gestart als programmaleider bij LOGEX BV in Amsterdam waar ze door middel van data-analyses zich inzet voor het verbeteren van doelmatige gebruik van geneesmiddelen.



## DANKWOORD

Dank aan Marie José, promotor, en oneindige kennisbron als het gaat om TGF $\beta$  signaling en ontwikkeling van het hart. Je hebt me geleerd dat netwerk cruciaal is, maar dat onderzoek uiteindelijk de passie is die ons hele werkveld drijft.

Anke, ik waardeer dat je niet alleen oog hebt voor het onderzoek maar minstens zoveel voor de mens erachter. Samenwerking binnen ons 'EPDC-team' was altijd plezierig en voor mij een sterke motivatie om elke dag met plezier naar het lab te komen.

Mijn PhD tijd kan makkelijk worden ingedeeld in twee periodes: de start met Annemarie en de afronding met Tom. Annemarie, je hebt me binnengehaald, geleerd hoe het werkt en laten zien waar je verantwoordelijkheid ligt (en waar niet). Bovendien sleepte je me overal mee naartoe, dit heeft ervoor gezorgd dat ik elke dag met veel plezier heb gewerkt. Deze functie heeft Tom daarna met verve overgenomen: nooit wars van gezelligheid, een felle discussie of een inspirerende quote.

Tessa je was van onschatbare waarde voor de totstandkoming van dit proefschrift. Dank voor je kundigheid, oneindige behulpzaamheid en leuke en serieuze gesprekken tijdens de vele uren in de celkweek. Veel dank aan het CVCB team: Aida, Asja, Alessandra, Babu, Boudewijn, Calinda, Clarissa, Gonzalo, Kirsten, Marian, Marius, Monika, Robert, Tiago, Valérie en Vera voor de altijd goede en inhoudelijke discussies, het eindeloos doorbomen over signaling pathways en voor de gezelligheid in het lab. Esmee, dank voor je vele hulp; eerst als student en later als collega. *Many thanks to the other two intelligent and skilled students I had the pleasure to supervise: Francesca and Manon.*

Ik bedank ook graag iedereen binnen de MCB, later de CCB. Specifiek de vaste gezichten Peter, Maarten en Midory waar ik terecht kon voor alle vragen rondom TGF $\beta$  liganden, remmers en virussen. Daarnaast ook Martijn Rabelink en Rob Hoeben voor hulp bij de ALK4 virus productie. Voor de mooiste microscopie plaatjes kon ik altijd terecht bij Lennard, Karien en Annelies. Geen vraag was niet binnen enkele momenten opgelost door Julia of Willem. Dank voor jullie bijdrage aan mijn goede tijd in het LUMC!

Dennis de Bakker, dank voor de bijzonder goede samenwerking! Het was altijd gebaseerd op een gedeelde nieuwsgierigheid naar hoe het echt zit. In dezelfde categorie noem ik ook graag Renee Maas, voor de samenwerking rondom toxiciteitstesten in IPSCs en Frank van Steenbeek voor de unieke kans om epicardiale cellen van een hond te isoleren en te bestuderen; dank voor de fijne en soepele samenwerking. De

MGC commissie van 2018 verdient daarnaast een speciale vermelding; zoveel pro-activiteit heb ik zelden meegemaakt in een commissie. Verder wil ik nog de samenwerking met de anatomie afdeling benoemen: Monique, Marco, Bert, Conny, Yang, voor wie geen enkele vraag over ontwikkelingsbiologie te ingewikkeld is. Dank ook aan de Quax groep voor goede samenwerking en gezellige congressen. Van de Technische Universiteit Eindhoven bedank ik graag Patricia Dankers, Sergio, Matilde, Maaïke; ik zal nooit meer op dezelfde manier naar een stukje kipfilet kijken.

Pap en mam, de inspiratie voor het hele traject is gestart bij het goede voorbeeld van papa's promotie in 2013. De nieuwsgierigheid is altijd door jullie gestimuleerd (overigens geldt hetzelfde voor 's nachts werken). Gelukkig is mama er om een rem te zetten op de oeverloze discussies die daar soms uit voortkomen. Dank voor jullie onvoorwaardelijke support en coaching.

Rick, celbiologie is niet jouw ding, maar ik kan altijd bij je terecht voor de nodige support en excel-, layout- en carrière-advies. Dankjewel voor het fijne leven samen.





